VOLUME 26 (1961) No. 1

NUCLEAR PHYSICS

JOURNAL DEVOTED TO THE EXPERIMENTAL AND THEORETICAL STUDY OF THE FUNDAMENTAL CONSTITUENTS OF MATTER AND THEIR INTERACTIONS

EDITOR: L. ROSENFELD - COPENHAGEN

SYUREI IWAO, Double hyperfragments and relative parity of Λ and Σ hyperons 1
J. VERVIER, Circular polarization of γ-rays following the capture of polarized neutrons 10
A. UEDA and C. B. A. MCCUSKER, Characteristics of high-energy nuclear interactions at and above 10^{14} eV 35
ALLADI RAMAKRISHNAN, A. P. BALACHANDRAN, N. R. RANGANATHAN and N. G. DESHPANDE, On an isobaric spin scheme for leptons and the leptonic decays of strange particles 52
T. L. TRUEMAN, Energy level shifts in atomic states of strongly-interacting particles 57
PAUL BENIOFF, Nuclear rearrangement and simple nuclear reactions. . . . 68
P. O. LIPAS and J. P. DAVIDSON, Octupole vibrations of deformed even nuclei 80
WOJCIECH KRÓLIKOWSKI, Some remarks on global symmetry 91
JAMES E. YOUNG and PAUL R. STEIN, A cluster model representation for the 3-body ground state. 97
H. VIGNAU and S. J. NASSIFF, Yield ratios of the isomeric pair $Ce^{137m/137}$ formed by $La^{139}(d,4n)Ce^{137}$ reaction 108
O. DIETZSCH, R. A. DOUGLAS and VIOLETA GOMES, A search for an isomeric state in Mn^{54}. 113
K. BAUMANN and R. SEXL, A one-dimensional field theory with degenerate vacuum 117
R. VAN WAGENINGEN, Elementary derivation of the Minami phase shift ambiguity 126
AMNON KATZ, On the treatment of a perturbation in a system of paired fermions 129
L. M. DELVES, Elastic and inelastic scattering of neutrons by deuterons near the inelastic threshold 136
H. J. LIPKIN, Pairing and quadrupole forces in a two-dimensional soluble model 147
J. B. FRENCH, Isobaric spin relationship between nuclear spectra 161
J. B. FRENCH and M. H. MACFARLANE, Isobaric-spin splitting of single-particle resonances 168

July 1961

NORTH-HOLLAND PUBLISHING COMPANY-AMSTERDAM

EDITORIAL BOARD

AUSTRALIA & NEW ZEALAND:	H. Messel (Sydney), M. L. Oliphant (Canberra)
AUSTRIA:	B. Karlik (Vienna), H. Thirring (Vienna)
BELGIUM:	M. de Hemptinne (Louvain), J. Verhaeghe (Ghent)
CANADA:	G. Volkoff (Vancouver)
DENMARK:	C. Møller (Copenhagen), S. Rozental (Copenhagen), G. E. Brown (Copenhagen)
FINLAND:	L. Simons (Helsinki)
FRANCE:	A. Berthelot (Saclay), S. Gorodetzky (Strasbourg)
GERMANY (DEM. REP.):	G. Hertz (Leipzig)
GERMANY (FED. REP.):	W. Gentner (Freiburg i. B.), J. H. D. Jensen (Heidelberg)
GREAT BRITAIN:	W. E. Burcham (Birmingham), T. H. R. Skyrme (Harwell)
HUNGARY:	L. Janossy (Budapest)
INDIA:	H. Bhabha (Bombay), R. Ramanna (Trombay)
IRISH REPUBLIC:	J. McConnell (Maynooth)
ISRAEL:	G. Racah (Jerusalem)
ITALY:	E. Amaldi (Rome)
JAPAN:	S. Kikuchi (Tokay), S. Tomonaga (Tokyo)
MEXICO:	M. Moshinsky (Mexico)
NETHERLANDS:	H. Brinkman (Groningen), S. R. de Groot (Leiden)
NORWAY:	E. Hylleraas (Oslo), A. Lundby (Oslo), H. Wergeland (Trondheim)
POLAND:	L. Infeld (Warsaw), J. Werle (Warsaw)
PORTUGAL:	J. M. Araújo (Porto), J. R. de Almeida Santos (Coimbra)
SOUTH AMERICA:	G. Beck (São Paulo), J. Leite Lopes (Rio de Janeiro)
SPAIN:	J. M. Otero (Madrid), C. Sanchez del Rio (Madrid)
SWEDEN:	O. Klein (Stockholm), K. Siegbahn (Uppsala), I. Waller (Uppsala)
SWITZERLAND:	P. Huber (Basel), P. Scherrer (Zürich)
U.A.R. & ARAB COUNTRIES:	F. El Bedewi (Cairo), M. G. Nooh (Cairo)
U.S.A.:	H. H. Barschall (Madison, Wisconsin), S. Devons (New York), V. F. Weisskopf (Cambridge, Mass.)
U.S.S.R.:	M. A. Markov (Moscow), I. S. Shapiro (Moscow), D. V. Skobeltzyn (Moscow)
YUGOSLAVIA:	I. Supek (Zagreb)

CONTRIBUTIONS may be sent to the Editor, Professor L. Rosenfeld, NORDITA, Blegdamsvej 17, Copenhagen Ø, either directly, or preferably through the intermediary of one of the members of the Editorial Board of the country or region in which the author is working. They may be written in English, French or German.

NUCLEAR PHYSICS is published in fortnightly issues. The subscription price per volume of 700 pages is fl 57.00; 114s; $ 15.00. Post-free.

SUBSCRIPTIONS should be sent to the publishers, NORTH-HOLLAND PUBLISHING COMPANY P.O. Box 103, Amsterdam or to any subscription-agent.

BOOKS FOR REVIEW should be sent to Professor Rosenfeld.

No part of this issue may be reproduced in any form, by print, photoprint, microfilm or any other means without permission from the publisher.

Printed in the Netherlands

8.B

Nuclear Physics **26** (1961) 1—9; © *North-Holland Publishing Co., Amsterdam*

Not to be reproduced by photoprint or microfilm without written permission from the publisher

DOUBLE HYPERFRAGMENTS AND RELATIVE PARITY OF Λ AND Σ HYPERONS

SYUREI IWAO †

Department of Physics, Syracuse University, Syracuse 10, New York

Received 16 February 1961

Abstract: A method for the determination of the relative parity of Λ and Σ hyperon is proposed. The possible bound states of the double hyperfragments are predicted from the parameters obtained before. If the $\Lambda-\Lambda$ interaction is attractive in the singlet S state, Λ and Σ will have the same parity, otherwise the opposite parity.

1. Introduction

In a previous paper [1]), a theory of hyperfragments involving two-body N$-\Lambda$ forces and shell model configuration for nucleons has been developed. The parameters of the two-body N$-\Lambda$ interaction were determined from the observed binding energies of the Λ hyperon. They explained well the present experimental data on hyperfragments.

We here apply this method to the so-called "double hyperfragments" making use of the parameters determined from the Λ hyperfragments. The double hyperfragments are bound states of two Λ particles and ordinary nuclei. While no such systems have been observed, one might expect that they could be produced by the absorption of high energy K^- mesons or Σ^- by complex nuclei. According to the Pauli principle, the two Λ hyperons in an s-state couple in a singlet spin state. This makes the expression for the binding energies of the double hyperfragments simpler than those of the usual Λ hyperfragments essentially because the two Λ hyperons form a closed shell. One has only one additional parameter in the $^1S_0$ state not previously determined by the single hyperfragment analysis.

Considerations based on the two-pion exchange $\Lambda-\Lambda$ potential lead one to expect that double hyperfragments should exist for $A \gtrapprox 5$. The binding energies of the double hyperfragments are of interest because the sign of the $^1S_0$ potential for the $\Lambda-\Lambda$ interaction is closely related to the relative parity of the Λ and Σ particles. The two-pion exchange force is attractive if Λ and Σ have the same parity; it is repulsive if they have opposite parity, and bound states may then be formed for $A \gtrapprox 6$.

† Work supported in part by the National Science Foundation and Air Force Office of Scientific Research.

We further discuss the evaporation probability of the double hyperfragments from heavy nuclei and compare it with the evaporation probability of the usual nuclear fragments. The Ξ-hyperfragments with low mass number are also discussed.

2. Binding Energies of Double Hyperfragments

In a previous paper we developed a formalism for the determination of the binding energy applicable for any number of Λ hyperons bound to the nucleus[1]). In order to calculate the binding energies of two Λ hyperons, we have to add to the Hamiltonian given in formula (3) of ref. [1]) the two-body $\Lambda-\Lambda$ potential and the single particle kinetic energy operators of two Λ hyperons.

The general form of the binding energy of the two Λ hyperons $B_{\Lambda\Lambda}$ $(A-2)$ is given for $14 \gtrsim A \gtrsim 2$ by

$$-B_{\Lambda\Lambda}(A-2) = 2T_{\Lambda}+a\sum_{x}[x]S_{x}+b\sum_{y}[y]P'_{y}+{}^{1}S_{0}. \tag{1}$$

Here, T_{Λ} is the kinetic energy of the Λ hyperons; the S_x and P'_y are the expectation values of the two-body N$-\Lambda$ interaction potentials between an s-state nucleon and between the hyperon and a $p_{\frac{3}{2}}$-state nucleon: hence there appear four parameters, S_0, S_1, P'_1 and P'_2, which are given numerically in ref. [1]) together with T_{Λ}; the parameter ${}^{1}S_0$ is the expectation value of the $\Lambda-\Lambda$ interaction potential in the singlet S state; the coefficients a and b depend on the mass numbers and configuration of the system. Since two Λ hyperons always couple in a singlet S state, the spin of the system of nucleons will give the spin of the double hyperfragments. We assume that the total spin of the system of nucleons is the same as that it would have without the two hyperons. Thus we expect a unique value for the spin in the ground state of a double hyperfragment.

The derivation of a and b is very simple and we just list the calculated results in table 1. One sees that the numerical parameters a and b are increasing linearly with the mass number A except for ${}^{6}H_{\Lambda\Lambda}$ and ${}^{6}\mathrm{Li}_{\Lambda\Lambda}$, where we have three s-nucleons and one $p_{\frac{3}{2}}$ nucleon. If the configuration of the composite nucleons of the double hyperfragments is the same, the two Λ binding energies are independent of the spins of the double hyperfragments. For instance, ${}^{8}\mathrm{He}_{\Lambda\Lambda}$, ${}^{8}\mathrm{Li}_{\Lambda\Lambda}$ and ${}^{8}\mathrm{Be}_{\Lambda\Lambda}$ have the same binding energy for the two Λ hyperons whereas their expected spins are 0, 1 and 0, respectively, which are the spins of the nucleon systems in their ground states without the two Λ hyperons. This is caused by the completely symmetric state (the singlet S-state) of the two Λ hyperons. In table 1, we tabulated the values of the binding energies determined from the N$-\Lambda$ parameters for anti-parallel spins assuming ${}^{1}S_0 = 0$; those for the case of the parallel spins differ at most by 0.13 MeV even for

$^{14}C_{\Lambda\Lambda}$. The parameters T_Λ, S_0 and S_1 are taken as the means of two sets of values in ref. [1]), $T_\Lambda = 8.28$ MeV, $S_0 = -4.87$ MeV and $S_1 = -2.17$ MeV. The P'_1 and P'_2 for anti-parallel spins are -1.41 and -0.551 MeV, respectively.

TABLE 1

The binding energy $B_{\Lambda\Lambda}(A-2)$

A	Double hyperfragment	J	a	b	Calculated $B_{\Lambda\Lambda}(A-2)$ for $^1S_0 = 0$ in MeV
2	$\Lambda\Lambda$	0	0	0	-17
3	n$\Lambda\Lambda$ and $^3H_{\Lambda\Lambda}$	$\frac{1}{2}$	$\frac{1}{2}$	0	-11
4	$^4H_{\Lambda\Lambda}$	1	1	0	-5.2
	nn$\Lambda\Lambda$ and $^4He_{\Lambda\Lambda}$	0	1	0	-5.2
5	$^5H_{\Lambda\Lambda}$ and $^5He_{\Lambda\Lambda}$	$\frac{1}{2}$	$\frac{3}{2}$	0	0.51
6	$^6He_{\Lambda\Lambda}$	0	2	0	6.2
	$^6H_{\Lambda\Lambda}$ and $^6Li_{\Lambda\Lambda}$	1 or 2	$\frac{3}{2}$	$\frac{1}{4}$	2.26
7	$^7He_{\Lambda\Lambda}$ and $^7Li_{\Lambda\Lambda}$	$\frac{3}{2}$	2	$\frac{1}{4}$	7.95
8	$^8Li_{\Lambda\Lambda}$	1	2	$\frac{1}{2}$	9.69
	$^8He_{\Lambda\Lambda}$ and $^8Be_{\Lambda\Lambda}$	0	2	$\frac{1}{2}$	9.69
9	$^9Li_{\Lambda\Lambda}$ and $^9Be_{\Lambda\Lambda}$	$\frac{3}{2}$	2	$\frac{3}{4}$	11.4
10	$^{10}Be_{\Lambda\Lambda}$	0	2	1	13.2
	$^{10}Li_{\Lambda\Lambda}$ and $^{10}B_{\Lambda\Lambda}$	2	2	1	13.2
11	$^{11}Be_{\Lambda\Lambda}$ and $^{11}B_{\Lambda\Lambda}$	$\frac{1}{2}$	2	$\frac{5}{4}$	14.9
12	$^{12}B_{\Lambda\Lambda}$	3	2	$\frac{3}{2}$	16.7
	$^{12}Be_{\Lambda\Lambda}$ and $^{12}C_{\Lambda\Lambda}$	0	2	$\frac{3}{2}$	16.7
13	$^{13}B_{\Lambda\Lambda}$ and $^{13}C_{\Lambda\Lambda}$	$\frac{1}{2}$	2	$\frac{7}{4}$	18.4
14	$^{14}C_{\Lambda\Lambda}$	0	2	2	20.2

As seen from table 1 the binding energies for the $A = 5$ double hyperfragment is about 0.5 MeV with $^1S_0 = 0$, hence it will be a bound state if the $\Lambda-\Lambda$ potential $^1S_0$ is < 0.5 MeV.

If we plot $B_{\Lambda\Lambda}$ $(A-2)$ as a function of A for $^1S_0 = 0$, we have two straight lines connected at $A = 6$ (fig. 1). For an attractive or repulsive $\Lambda-\Lambda$ potential in the singlet S state, the lines in fig. 1 are displaced parallel to themselves upwards or downwards, respectively. It is interesting to compare this result with the calculated and the observed binding energies of the single hyperfragments [2]), which have no such simple features (fig. 2).

The validity of a calculation of this type was checked by applying our method to the binding energies of nuclei with the corresponding mass number. The agreement with the experimental values are of the order of a few percent †.

† The result of our calculation will be reported elsewhere.

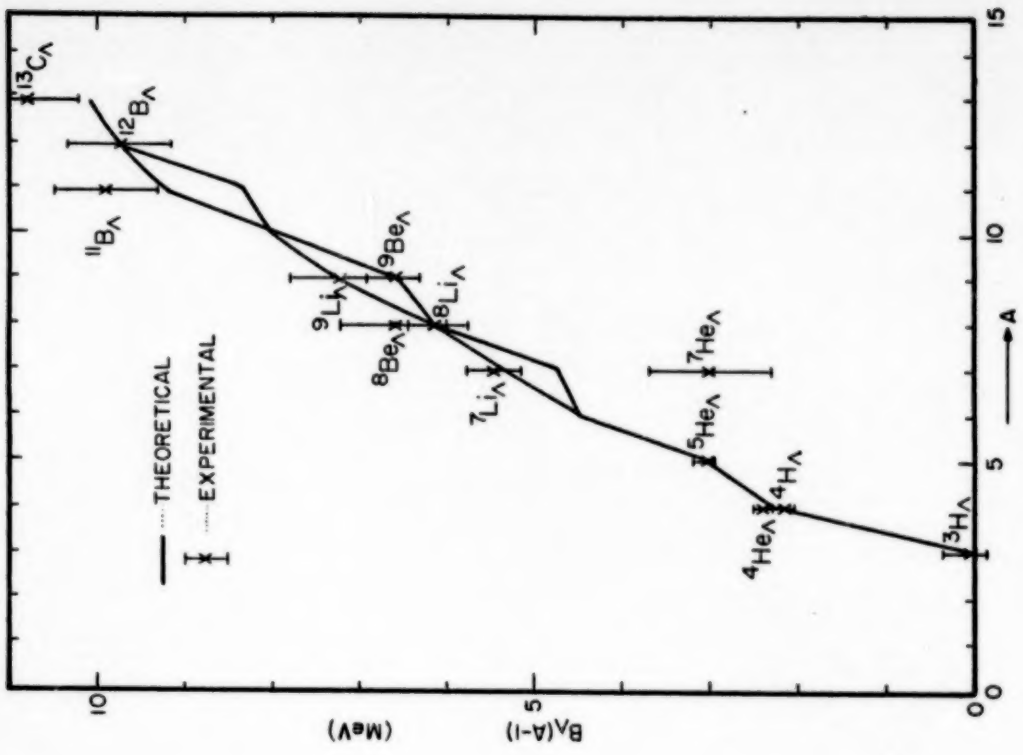

Fig. 2. Binding energy $B_\Lambda(A-1)$ of the Λ hyperon.

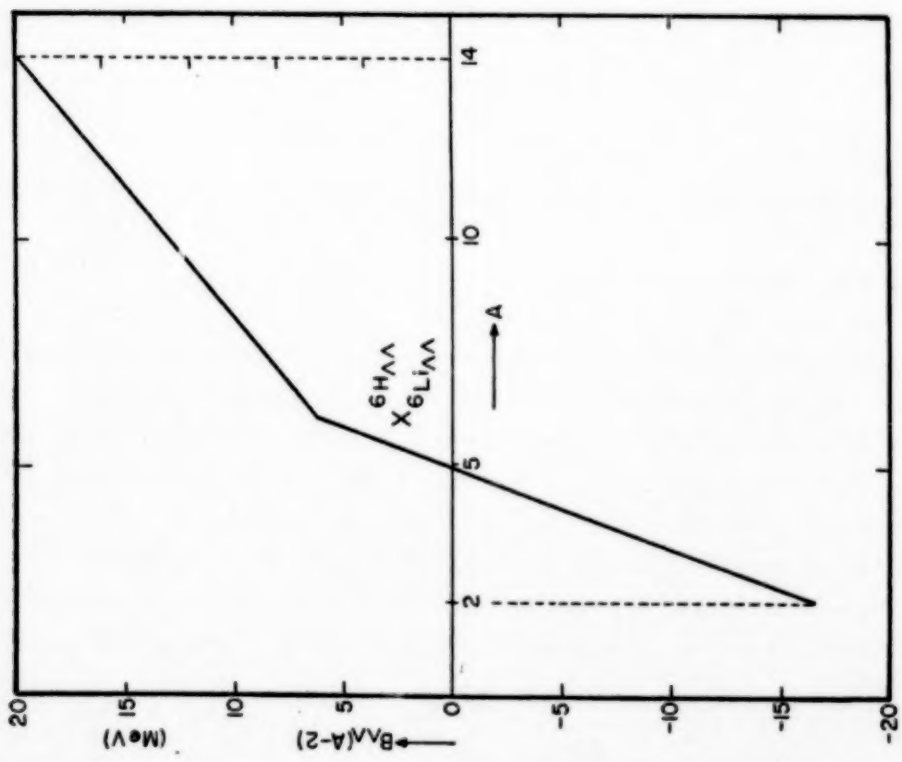

Fig. 1. Binding energy of double hyperfragments for $^1S_0 = 0$.

3. The Λ—Λ Potential and the Relative Parity of Λ and Σ

Because of the charge independence, the lowest order $\Lambda-\Lambda$ potential is due to two-pion exchange. For the same reason, the K-exchange potential also starts from two K-mesons, hence it can be neglected compared to the two-pion contribution (because the largeness of the energy denominator of the K-propagator and perhaps also because of the weakness of the coupling).

We are mostly interested in the effect of the relative parity of Λ and Σ hyperons upon the sign and the size of the $\Lambda-\Lambda$ potential in the singlet S state. Let us confine ourselves to the fourth order potential due to the two-pion exchange in which two Σ hyperons appear as intermediate baryons. The static Hamiltonian of our problem is given for even relative parity of Λ and Σ in the form

$$H_{\Lambda\Sigma\pi} = (4\pi)^{\frac{1}{2}}(f/\mu)\sum_{\lambda}\eta_{\lambda}\int\rho(\mathbf{r})\,\boldsymbol{\sigma}\cdot\boldsymbol{\nabla}\varphi_{\lambda}(\mathbf{r})\mathrm{d}\mathbf{r}, \tag{2}$$

where f is a rationalized and unrenormalized coupling constant, η_{λ} an Hermitian operator defined by Wick [3]), $\rho(\mathbf{r})$ a density function and μ is a pion mass. For odd relative parity it is

$$H_{\Lambda\Sigma\pi} = (4\pi)^{\frac{1}{2}}g\sum_{\lambda}\eta_{\lambda}\int\rho(\mathbf{r})\,\varphi_{\lambda}(\mathbf{r})\mathrm{d}\mathbf{r}. \tag{3}$$

Neglecting the mass difference of baryons, we obtain the $\Lambda-\Lambda$ potential in the following forms:

(i) In the case that Λ and Σ hyperons have the same parity, we get

$$V_{\Lambda\Lambda} = \mu f^4\{-\tfrac{1}{2}U_{\tau}(x)+\tfrac{2}{3}(\boldsymbol{\sigma}^{(1)}\cdot\boldsymbol{\sigma}^{(2)})\;U_{\sigma}(x)+\tfrac{2}{3}S_{12}U_{T}(x), \tag{4}$$

where

$$U_{\tau}(x) = \frac{-8}{\pi}\left\{\left(\frac{1}{x}+\frac{23}{4x^3}\right)K_0(2x)+\left(\frac{3}{x^2}+\frac{23}{4x^4}\right)K_1(2x)\right\}, \tag{4.a}$$

$$U_{\sigma}(x) = \frac{8}{\pi}\left\{\frac{3}{x^3}K_0(2x)+\left(\frac{2}{x^2}+\frac{3}{x^4}\right)K_1(2x)\right\}, \tag{4.b}$$

$$U_{T}(x) = \frac{-8}{\pi}\left\{\frac{3}{x^3}K_0(2x)+\left(\frac{1}{x^2}+\frac{15}{4x^4}\right)K_1(2x)\right\}. \tag{4.c}$$

Here we use $x=\mu r$ and K_0 and K_1 are modified Bessel functions.

(ii) In the case that Λ and Σ hyperons have the opposite parity, we have

$$V_{\Lambda\Lambda} = \mu g^4\frac{2}{\pi}\frac{K_0(2x)}{x}. \tag{5}$$

If we put $x=1$ and $f^2=0.08$ in (4) and make use of (4.a)—(4.c) we get ${}^1S_0=-2.6$ MeV, which is large enough to be detected experimentally and

gives bound states for $A \gtrsim 5$ double hyperfragments (see table 1). On the other hand the potential (5) gives ${}^1S_0 = 10g^4$ MeV, which gives bound states for $A \gtrsim 6$ if $g^2 \approx 0.3$. Although the estimates made here are very rough, they may be checked experimentally.

We remark that the "global symmetry" proposed by Gell-Mann [5]) gives the Λ—Λ potential (for even $\Lambda\Sigma$ parity) in terms of the N—N potential in the following form (see Appendix):

$$V_{\Lambda\Lambda} = \tfrac{1}{4}V_{\mathrm{NN}}(I=0)+\tfrac{3}{4}V_{\mathrm{NN}}(I=1). \tag{6}$$

Combining eq. (6) with a static N—N potential [5]) the spin dependent part is given by $-2\,U_\sigma(x)$ in the ${}^1S_0$ state but no $U_\tau(x)$ part appears. Hence the potential obtained by G. S. gives a contribution about twice as large as that of eq. (4).

4. Production of Double Hyperfragments

4.1. THE MECHANISM OF THE PRODUCTION

The production of double hyperfragments can occur in two ways. One is the high energy K^- absorption, the other is the Ξ^- absorption by complex nuclei. Dalitz [6]) has discussed the reaction $\Xi^- + {}^6\mathrm{Li} \to {}^6\mathrm{He}_{\Lambda\Lambda} + \mathrm{n}$ and the qualitative properties of ${}^6\mathrm{He}_{\Lambda\Lambda}$. The direct production of double hyperfragments can be obtained from K^- absorption by two nucleons in the nucleus:

$$K^- + 2N \to 2\Lambda + K. \tag{7}$$

One can consider $\Lambda\Sigma$ and $\Sigma\Sigma$ as the intermediate steps for process (7). Another possibility is the production of a Ξ particle as an intermediate step:

$$K^- + N \to \Xi + K. \tag{8}$$

The Ξ will be absorbed by a nucleon in the nucleus and form two hyperons and a pion. The absorption of the cascade particle by complex nuclei is essentially the same as above. Finally, the two Λ hyperons produced will form a double hyperfragment and be emitted from the nucleus.

It is interesting to consider the double hyperfragments with $A = 4$ such as $\mathrm{nn}\Lambda\Lambda$, ${}^4\mathrm{H}_{\Lambda\Lambda}$ and ${}^4\mathrm{He}_{\Lambda\Lambda}$ because these would determine not only the relative parity of Λ—Σ to be even, but also K^+ parity from the process

$$K^- + {}^4\mathrm{He} \to \mathrm{nn}\Lambda\Lambda + K^+, \tag{9}$$

since the spins of the particles related to this process are all zero. Another interesting problem is the production of bound states of hyperons and nucleons, such as $\mathrm{n}\Xi^-$, $\mathrm{p}\Xi^0$, $\mathrm{nn}\Xi^-$ etc., which would prove that the $\Xi\Xi\,\pi$-interaction has the same strength as $NN\pi$-interaction under global symmetry.

4.2. EVAPORATION OF DOUBLE HYPERFRAGMENTS

The theory of evaporation of particles from the highly excited nucleus was first developed by Weisskopf and investigated in detail by several authors [7]. We use their results to estimate the probability of the evaporation of double hyperfragments from the heavy nucleus in its excited states. For this purpose we introduce the following quantities: the excitation energy X, the quantity $K = \hbar^2/2m_N r_0^2 \approx 10$ MeV, the weight factor for the spin $g = 2S+1$ ($g = 2$ for a nucleon and $g =$ for an alpha-particle), the temperature T of the excited nucleus in MeV (Boltzmann's constant $k = 1$), the height V of Coulomb potential barrier for the proton and the orbital angular momentum l of an evaporating particle.

For a degenerate Fermi gas, we have approximately

$$X = \tfrac{1}{10} A T^2,$$

where A is the mass number. The condition of applicability of the evaporation model is about $T \lesssim 9$ MeV according to Fujimoto and Yamaguchi [7]. We compare the probability of the evaporation of ${}^{6}\mathrm{He}_{\Lambda\Lambda}$ relative to ${}^{4}\mathrm{He}$ as a typical example. If we do not restrict the orbital angular momentum l of the evaporating particle we have

$$\Gamma_\alpha(X) \approx \frac{g_\alpha}{2\pi} \frac{4A^{\frac{2}{3}}T^2}{K} \exp\left(-\frac{E_\alpha + 2V}{T}\right), \tag{10.a}$$

$$\Gamma_{{}^{6}\mathrm{He}_{\Lambda\Lambda}}(X) \approx \frac{g_{{}^{6}\mathrm{He}_{\Lambda\Lambda}}}{2\pi} \frac{6A^{\frac{2}{3}}T^2}{K} \exp\left(-\frac{E_{{}^{6}\mathrm{He}_{\Lambda\Lambda}} + 2V}{T}\right). \tag{10.b}$$

On the other hand, if we confine $l \lesssim 1$, we obtain

$$\Gamma_\alpha(X) \approx \frac{g_\alpha}{2\pi} T \exp\left(-\frac{E_\alpha + 2V}{T}\right), \tag{11.a}$$

$$\Gamma_{{}^{6}\mathrm{He}_{\Lambda\Lambda}}(X) \approx \frac{g_{{}^{6}\mathrm{He}_{\Lambda\Lambda}}}{2\pi} T \exp\left(-\frac{E_{{}^{6}\mathrm{He}_{\Lambda\Lambda}} + 2V}{T}\right). \tag{11.b}$$

The branching ratio of the evaporation of ${}^{6}\mathrm{He}_{\Lambda\Lambda}$ relative to the alpha-particle is given by

$$\tfrac{3}{2} \exp\left(-\frac{E_{{}^{6}\mathrm{He}_{\Lambda\Lambda}} - E_\alpha}{T}\right), \qquad \exp\left(-\frac{E_{{}^{6}\mathrm{He}_{\Lambda\Lambda}} - E_\alpha}{T}\right)$$

for (10) and (11) respectively. If we assume the binding energy difference is of the order of T, we have 56 % and 37 %, respectively.

5. The Ξ-Hyperfragments

The binding energies of Ξ hyperfragments can be calculated in the same way as that of Λ hyperfragments. We give here the expectation value of the N—Ξ interaction for $A = +2$ and 3 system, assuming two-body N—Ξ forces. In the former cases, the N—Ξ interaction is either $S_{j-\frac{1}{2}}$ or $S_{j+\frac{1}{2}}$, depending upon the spin state of N—Ξ forces where j is the spin of the Ξ hyperon. We have the following form of the matrix elements of two-body forces for both $nn\Xi^-$ and ${}^3He_{\Xi}$:

$$2jS_{j-\frac{1}{2}}/(2j+1)+2(j+1)S_{j+\frac{1}{2}}/(2j+1). \tag{12}$$

One sees that the sum of the coefficients of the two-body matrix elements is always equal to the number of possible pairs of interactions.

The decay schemes for $nn\Xi^-$ and ${}^3H_{e\Xi^0}$ are $n+n+\Lambda+\pi^-$ and $p+p+\Lambda+\pi^0$ or $p+p+\Lambda$, since there are no bound states of $nn\Lambda$ and ${}^3He_{\Lambda}$, both theoretically [1]) and experimentally [2]). The Q values of these decays are about 80 MeV and 220 MeV, which are not large enough compared to baryon masses, hence two neutrons and two protons in the final states will be in singlet S states.

6. Discussion

As discussed in this paper, the various double hyperfragments can form bound states by the known N—Λ forces. The main point of this paper is the determination of the sign and the size of the Λ—Λ interaction parameter in the singlet S state, which will give us information about the relative parity of the Λ and Σ hyperons. We did not consider three-pion contributions, two-K contributions or higher terms. These should be taken into account if a more detailed investigation turned out to be necessary.

In the derivation of potentials (4) and (5), we used an E/ω expansion, where E and ω are the total energy less twice the rest mass of the Λ hyperon, and the pion kinetic energy, respectively. Therefore, these potentials are valid for $V < \mu$, and hence for r larger than some cut off radius.

According to our preliminary analysis, in which we assume the global symmetry and $\frac{3}{2}-\frac{3}{2}$ resonance of pion and nucleon, the branching ratios of Λ and Σ^0 in the two processes $K^-+p \to Y+2\pi$ and $K^-+d \to Y+\pi+p$ are consistent with the experimental rates but not with that of $K^-+{}^4He \to Y+\pi+{}^3H$ (or ${}^3He$) (see ref. [8])), although experimental data are still poor. It must also be remarked that the theoretical rate does not take a simple expression except for the last two processes.

The author expresses his thanks to Professor Richard Arnowitt and Professor Asim Barut for their critical comments and discussions in the course of this work and in the writing of the paper.

Appendix

GLOBAL SYMMETRY AND Λ—Λ POTENTIAL

According to the global symmetry hypothesis, the Λ wave function in charge space can be written as

$$\Lambda = 1/\sqrt{2}\ (Z^0+Y^0),$$

where Z^0 and Y^0 correspond to the proton and neutron, respectively. The product wave function for two Λ-hyperons can be separated into eigenstates of the isobaric spin $I = 0$ and 1 ($I_3 = 1,\ 0,\ -1$) with the weight factors $\frac{1}{2}$ and $\frac{1}{2}$ (for each charge state of $I = 1$), respectively. Hence, the potential is given by the sum of $\frac{1}{4}$ of the $I = 0$ state and $\frac{3}{4}$ of the $I = 1$ state of the N-N potential. The simple treatment of the text is quite adequate but for more complicated cases we have to treat the conservation of i-spin and ω-spin explicitly as an additional requirement to the charge independence. Vector addition of i-spin and ω-spin gives the total isobaric spin of baryons and these are assigned $\frac{1}{2}$ and $\frac{1}{2}$ for Λ and Σ by the introduction of the Z and Y fields. The i-spins of N and Ξ are equivalent to their isobaric spins, hence these have no ω-spins [9]). We can work on the isobaric spin eigenfunctions belonging to a definite charge state of the heavy unstable particles after decomposing them into i-spin and ω-spin separately, for which decoupling of many angular momenta the Racah algebra is more convenient. We do not want to describe details here, but the latter method gives exactly the same answer as that obtained above.

References

1) S. Iwao and E. C. G. Sudarshan, Phys. Rev. Letters **4** (1960) 140;
S. Iwao, Nuovo Cim. **17** (1960) 491;
E. C. G. Sudarshan and S. Iwao, Proc. Indian Acad. Sci. **52** (1960) 27
2) R. Ammar, R. Levi Setti, W. E. Slater, S. Limentani, F. E. Schlein and P. H. Steinberg, Nuovo Cim. **15** (1960) 181
3) G. C. Wick, Rev. Mod. Phys. **27** (1955) 339
4) M. Gell-Mann, Phys. Rev. **106** (1957) 1296
5) K. Nishijima, Prog. Theor. Phys. **6** (1951) 815; **6** (1951) 911;
M. Taketani, S. Machida and S. Onuma, Prog. Theor. Phys. **7** (1952) 45
6) R. H. Dalitz and B. W. Downs, Phys. Rev. **111** (1958) 967
7) V. Weisskopf, Phys. Rev. **52** (1937) 295;
Y. Fujimoto and Y. Yamaguchi, Prog. Theor. Phys. **4** (1949) 468
8) S. Iwao, unpublished
9) Y. Yamaguchi, lecture notes CERN 59—35, Nov. 10, 1959

1.E.1:
2.B

Nuclear Physics **26** (1961) 10—34; © *North-Holland Publishing Co., Amsterdam*
Not to be reproduced by photoprint or microfilm without written permission from the publisher

CIRCULAR POLARIZATION OF γ-RAYS FOLLOWING THE CAPTURE OF POLARIZED NEUTRONS

J. VERVIER †

Physics Division, Atomic Energy of Canada Limited, Chalk River, Ontario

Received 6 February 1961

Abstract: The circular polarization of γ-rays following the capture of polarized neutrons has been measured for some high intensity transitions in S^{33}, Ti^{49}, Fe^{57}, Ni^{59}, Y^{90}, Al^{28}, Cu^{64} and N^{15}. The results are consistent with spin $\frac{1}{2}$ for the 0.46 MeV level in Ni^{59} and spin 2 for the 0.277 MeV level in Cu^{64}. The following spins are confirmed: $\frac{3}{2}$ for the 3.22 MeV level in S^{33}; $\frac{3}{2}$ and $\frac{1}{2}$ for the 1.38 and 1.72 MeV levels in Ti^{49}; 2 for the 0.777 MeV level in Y^{90}. In N^{15} $(25\pm18)\%$ of captures are found to occur in a state with spin $\frac{1}{2}$. In Fe^{57}, $(49\pm19)\%$ of the intensity of the 7.64 MeV doublet γ-ray is found to belong to the ground state transition. In Al^{28}, information is obtained relating the mixture of spins in the capturing state and multipole mixtures and relative intensities of the components of the 7.72 MeV doublet. The results are compared with the predictions of nuclear models and theories of thermal neutron capture.

1. Introduction

It has been predicted theoretically by Biedenharn *et al.* [1]) and verified experimentally by Trumpy [2, 3]) (see also ref. [4])) that the γ-rays following the capture of polarized neutrons are circularly polarized. The γ-ray circular polarization P_γ is given by

$$P_\gamma = P_n R \cos\theta, \tag{1}$$

where P_n is the neutron polarization, θ is the angle between the neutron spin and the γ-ray direction and R is a coefficient which depends only on the multipolarity of the γ-ray (and on its mixture parameter, if any) and on the spins of the target nucleus (J_1), the compound nucleus capturing state (J_c) and the level of the compound nucleus excited by the γ-transition (J_f). The value of R for pure and mixed transitions is given by Trumpy [2]). Trumpy measured P_n and P_γ in order to get R and so was able to obtain information on the γ-ray multipolarity and on the various spins involved in the reaction, for a few high energy, high intensity capture γ-rays in various nuclei. We have carried out similar experiments at the Chalk River NRU reactor using the polarized thermal neutron beam provided by the experimental arrangement of Clark and Robson [5]).

2. Experimental Method

2.1. POLARIZED NEUTRON BEAM

Fig. 1 shows the general experimental arrangement. A collimated thermal neutron beam from the NRU reactor is Bragg diffracted by the (200) planes of

† On leave from C.E.N., Mol (Belgium).

a magnetized Co-Fe crystal A. It then passes through various collimators and guide fields, through a radiofrequency coil C, where the neutron spin can be flipped by magnetic resonance, through the apparatus D used by Clark and Robson to study the decay of polarized neutrons [6]), through a fission counter F used as a neutron monitor and through the present experiment E. It is finally diffracted into a boron counter by a second magnetized Co-Fe crystal B. The

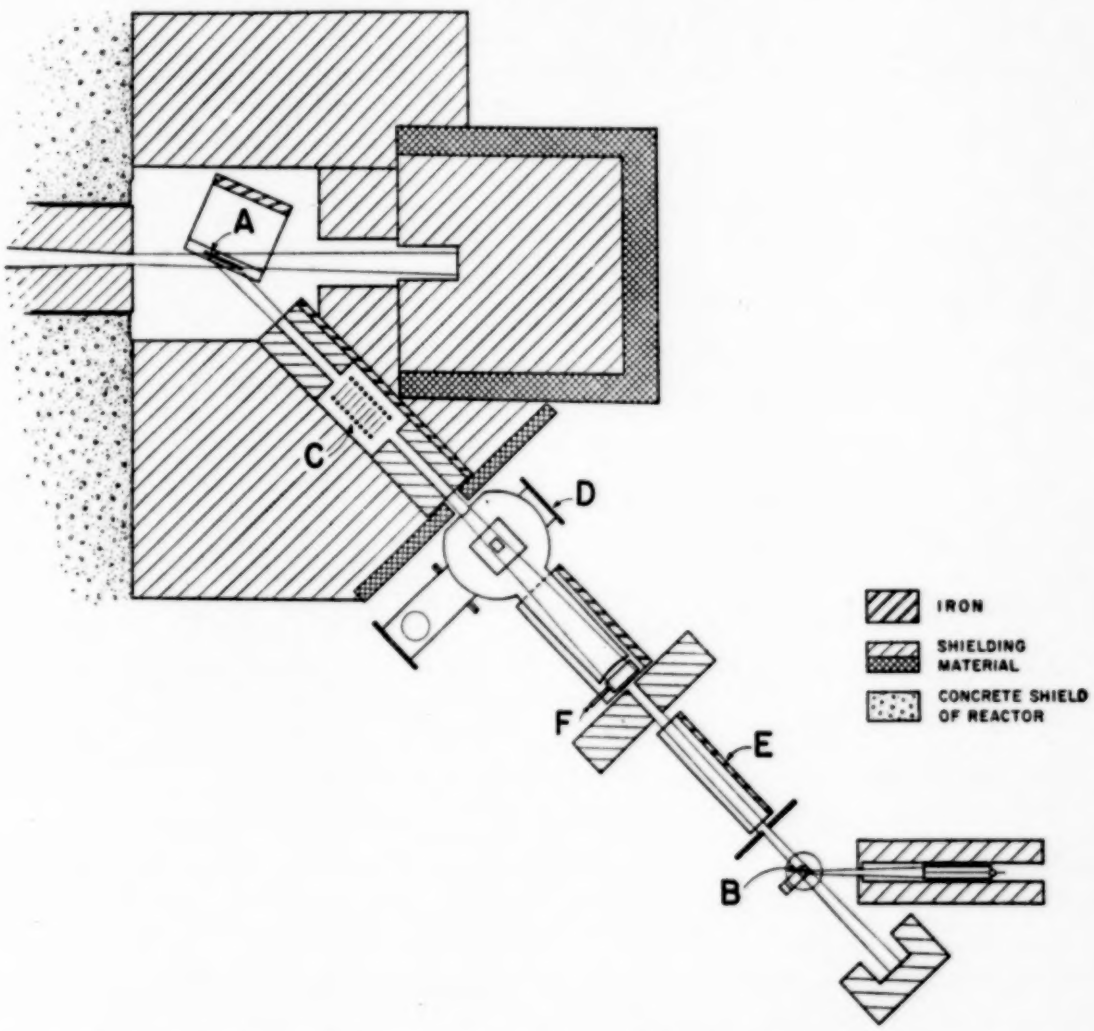

Fig. 1. General experimental arrangement for the production and use of the polarized neutron beam at the Chalk River NRU reactor. Further details are given in ref. [5]).

latter arrangement is used to check continuously the neutron polarization and the flipping probability of the radiofrequency coil C. The effective neutron polarization, taking into account the first and second order diffracted neutrons, the diffuse scattered neutrons and the flipping probability has been measured [5]) to be

$$P_n = 0.895 \pm 0.06. \qquad (2)$$

Further details of the production of the polarized neutron beam are given elsewhere [5]).

2.2. MEASUREMENT OF THE γ-RAY CIRCULAR POLARIZATION

Fig. 2 shows the experimental arrangement used to measure the circular polarization of the capture γ-rays. Polarized neutrons are captured in the cylindrical sample of dimensions 3.81 cm $\times$ 3.81 cm. Cylinders of the sample material alone are used for metallic samples, while for powders a thin wall (0.015 cm) aluminium can was used to contain the sample. The capture γ-rays are detected in a 5.08 cm diameter by 7.62 cm thickness NaI crystal, shielded

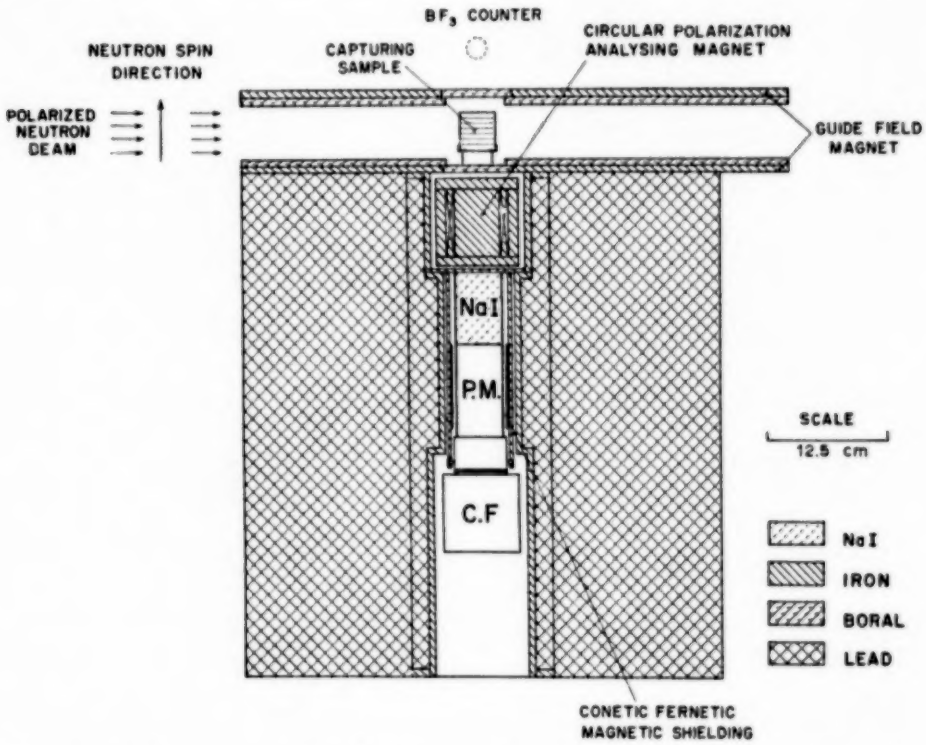

Fig. 2. Experimental arrangement used to measure the circular polarization of the capture γ-rays.

by 20 cm of lead. Magnetic shielding of the photomultiplier (RCA 6342) is ensured by Conetic-Fernetic sheets. After amplification the pulses from the photomultiplier are analyzed in a 100-channel pulse-height analyzer. The background counting rate produced by neutrons scattered from the beam by the sample and captured in surrounding materials is reduced by boral plates which line the beam tube. The iron plates placed above and below the capturing sample are part of the guide field magnet ($\approx$ 25 Oe) used to maintain the vertical direction of the spin vectors of the neutrons during their traversal of the apparatus.

The circular polarization of the capture γ-ray P_γ is measured by transmission [7]) through a magnetized Armco iron core, 5.08 cm diameter and 8.89 cm thick. The effective thickness L of the core, taking into account the inhomoge-

neities of the magnetic induction B in the end plates, has been estimated, and liberal limits were attributed to its uncertainty, giving

$$LB/B_s = 6.68 \pm 0.40, \tag{3}$$

where B_s is the saturation flux and L is measured in cm.

The spectrum detected by the NaI crystal contains, in addition to the capture γ-ray of interest, various backgrounds, namely: (1) the general γ-ray background including γ-rays from the sample container; (2) capture γ-rays from surrounding materials due to neutrons scattered by the sample; (3) capture γ-rays from the sample scattered into the NaI crystal by the circular polarization analyzing magnet. Finally, the capture γ-rays transmitted through the iron core and detected in the NaI crystal generally contain several lines which partially obscure the γ-ray of interest in the detected spectrum.

The relative proportions of the various background contributions in the total spectrum were determined by experiments performed with an empty sample container, with a graphite sample which does not give rise to capture γ-rays to a significant extent and with the circular polarization analyzing magnet removed. The ratio of the neutrons scattered by the sample and by the graphite was measured with a small BF_3 counter placed above the sample (fig. 2) with part of the boral shielding removed.

When these various background contributions were subtracted, the resultant transmitted capture γ-ray spectrum was analyzed into its various components using the known intensities of the capture γ-rays [8]) and line shapes determined with the following well-isolated γ-rays: Po-Be, 4.43 MeV; $Y^{89}(n, \gamma)Y^{90}$, 6.07 MeV; $Al^{27}(n, \gamma)Al^{28}$, 7.72 MeV; $N^{14}(n, \gamma)N^{15}$, 10.83 MeV. The errors involved in the determination of the various background contributions and in the decomposition of the γ-ray spectrum are estimated to be of the order of a few per cent, which is smaller than other sources of error mentioned below.

2.3. THEORETICAL RELATIONS

We denote by δ the asymmetry of the counting rate in a selected energy interval of the total spectrum recorded in the NaI crystal, while flipping the neutron spin with the radiofrequency coil; we have

$$\delta = \frac{N_+ - N_-}{\frac{1}{2}(N_+ + N_-)}, \tag{4}$$

where $N_+(N_-)$ is the counting rate when the neutron spin is down (up), i.e. when the radiofrequency flipping current is off (on). Let α_1, α_2, α_3 and α_γ be the relative contributions to the counting rate in the energy interval selected of the three background sources and the transmitted capture γ-rays, respectively,

and let $\delta_1, \delta_2, \delta_3$ and δ_γ be the corresponding asymmetries. Then we have

$$\delta = \sum_{i=1}^{3} \alpha_i \delta_i + \alpha_\gamma \delta_\gamma . \tag{5}$$

The asymmetries δ_1 and δ_2 were determined by separate measurements in most cases; when they were not determined, liberal limits (± 5 %) were attributed to them. The asymmetry δ_3 cannot be measured and is difficult to calculate in view of the large thickness of the circular polarization analyzing magnet; a safe upper limit [7]) for its absolute value, in the γ-ray energy range considered here, is 5 % and its sign is opposite to δ_γ. The quantity δ_γ was calculated from relation (5) using the measured values of $\alpha_1, \alpha_2, \alpha_3, \alpha_\delta, \delta, \delta_1$ and δ_2. The limits attributed to δ_3, and eventually to δ_1 and δ_2, were taken into account in the calculation of the error of δ_γ.

The relation between δ_γ and R can be obtained by inserting, in the expression giving the efficiency of the transmission method for the measurement of the γ-ray circular polarization [7]), the values of P_γ for $\cos\theta = \pm 1$ (eq. (1)) as well as our value of P_n (eq. (2)) and LB/B_s (eq. (3)). This gives

$$\bar{R} = \frac{\delta_\gamma}{\nu \sigma_c(E_\gamma)} (1 \pm 0.09), \tag{6}$$

where $\nu\sigma_c(E_\gamma)$ (in 10^{-24} cm^2) is the part of the atomic cross-section of iron for γ-ray of energy E_γ which depends on the γ-ray circular polarization; $\nu = 2.06$ is the number of oriented electrons per iron atom in the analyzing magnet at saturation; $\sigma_c(E_\gamma)$ is the polarization dependent part of the cross section of the free electron for γ-rays. The quantity $\nu\sigma_c(E_\gamma)$ is given by Trumpy [2]) and Schopper [7]). The 9 % uncertainty in the coefficient of $\delta/\nu\sigma_c(E_\gamma)$ in eq. (6) is the combination of the uncertainties in P_n (eq. (2)) and LB/B_s (eq. (3)) and is generally smaller than the statistical error in the measurement of δ_γ. As pointed out earlier, it is often impossible to completely isolate the γ-ray of interest with the resolution available. Under these conditions, $\bar{R}$ represents the mean of the coefficients R_n for the various capture γ-ray lines which contribute to the counting rate in the energy interval selected in the NaI crystal spectrum; we have

$$\bar{R} = \sum_n \beta_n R_n . \tag{7}$$

The β_n are the relative contributions of the lines, determined as explained above. The contribution β_1 of the γ-ray of interest is generally predominant and one wants to determine the coefficient R_1 for the corresponding line. The other R_n are generally unknown but their absolute magnitudes are smaller [2]) than 1, so that at worst

$$R_1 = \frac{1}{\beta_1} \left[\bar{R} \pm \sum_{n \neq 1} \beta_n \right] . \tag{8}$$

The final error in R_1 is the combination of the error in δ_γ, calculated as explained above, of the 9 % uncertainty in the coefficient of $\delta/\nu\sigma_c(E_\gamma)$ and of the uncertainty in the $R_n(n \neq 1)$.

2.4. PROCEDURE

The experiment runs automatically. At the end of a preselected counting period, the 100-channel pulse-height analyzer spectrum, the number of counts in the fission monitor and in the boron counter are recorded on typewriter paper and on punch tape; the flipping condition is changed, the pulse-height analyzer and all scalers are re-set and the counting is re-started.

It is to be noted that the γ-ray circular polarization is measured without changing any static magnetic field so that possible asymmetries arising from the effect on the photomultiplier of such changes are avoided. In particular, the influence of the magnetic field of the circular polarization analyzing magnet is of no importance here, since it remains constant.

The data are processed using two programs on the Chalk River Datatron Computer. The first program adds separately the runs with neutron spin "up" and "down". The second program normalizes the two spectra so obtained to the same number of fission monitor counts and computes, for each channel, the sum $N_+ + N_-$, the difference $N_+ - N_-$, the error in the difference $\sqrt{N_+ + N_-}$ and finally δ and its error. The results from the first program are used for calculating δ for a selected energy interval in the detector spectrum.

2.5. DETECTOR STABILITY AND INSTRUMENTAL ASYMMETRY

The detector stability was tested by repeating the measurements and by comparing the asymmetries obtained with various cycling periods. The results of such experiments are given in table 1. They show that the asymmetries of the various experiments sometimes differ by more than the statistical error but that their means for the two cycling periods generally agree well. In view of this result the cycling period of one hour was chosen. The scattering of the results of the various individual measurements was taken into account in the calculation of the error in their mean.

Measurements were also carried out to check any possible instrumental asymmetry by experiments performed with an unpolarized neutron beam. The beam was de-polarized in the usual way by inserting in the beam, after the polarizer crystal A (fig. 1) a thin unmagnetized iron shim. Due to the rapid variations of the magnetic field in the shim, the neutron polarization is reduced to a negligible amount. The results of these experiments are given in table 2. They show that the instrumental asymmetry for a wide interval in the detected spectrum is smaller than 0.15 %. As shown by table 1, this is of the same order of magnitude as the error in δ obtained with a polarized beam. In only one

case, Ti^{48}, the asymmetry measured with an unpolarized beam was significantly different from zero. As explained below, this effect is believed to be due to a detector instability and is indeed of the same order of magnitude as the scattering of the results of the various runs given in table 1.

TABLE 1

Test of the detector stability

Target nucleus	γ-ray energy (MeV)	Cycling period	δ(%)
S^{32}	5.44	1h	-0.67 ± 0.11 -1.47 ± 0.21 -1.43 ± 0.21 -0.80 ± 0.17 -1.17 ± 0.11 -0.33 ± 0.11 -1.42 ± 0.17 Mean -0.82 ± 0.37
		15m	-0.88 ± 0.25 -0.94 ± 0.44 -0.51 ± 0.35 -1.00 ± 0.43 -2.05 ± 0.42 Mean -0.99 ± 0.16
		Mean	-0.96 ± 0.15
Fe^{56}	7.64	1h	0.24 ± 0.20 0.45 ± 0.11 0.48 ± 0.11 0.76 ± 0.11 0.30 ± 0.11 Mean 0.48 ± 0.17
		15 m	0.83 ± 0.30 0.33 ± 0.23 0.74 ± 0.33 Mean 0.56 ± 0.16
		Mean	0.52 ± 0.12
Y^{89}	6.07	1h	-0.51 ± 0.12 -0.71 ± 0.11 -0.78 ± 0.10 -0.62 ± 0.05 Mean -0.64 ± 0.06
		15m	-0.89 ± 0.19 -1.33 ± 0.28 Mean -1.04 ± 0.16
		Mean	-0.69 ± 0.19
Al^{27}	7.72	1h	1.49 ± 0.20 1.27 ± 0.10 Mean 1.31 ± 0.09

The asymmetries δ (eq. (4)) obtained for various runs and for two different cycling periods are given in the fourth column; the energy intervals in the NaI spectrum selected for the calculation of δ are indicated by arrows on figs. 3, 6, 8 and 10.

2.6. CORRECTIONS

The solid angle corrections due to the finite dimensions of the capturing sample and γ-ray detector have been estimated, for our experimental arrangement, to be of the order of 1 % of δ and are neglected.

The correction for the de-polarization of neutrons scattered in the capturing sample before being absorbed has been calculated by Trumpy [2]). It vanishes for spin 0 target nuclei as for most of the samples studied in the present experi-

TABLE 2

Instrumental asymmetry experiments

Target nucleus	γ-ray energy (MeV)	Cycling period	δ(%)
Fe^{56}	7.64	1h	-0.09 ± 0.22
		15m	0.21 ± 0.31 $\quad -0.23\pm0.29$ Mean -0.03 ± 0.21
		Mean	-0.06 ± 0.15
Y^{89}	6.07	15m	0.24 ± 0.48 $\quad 0.06\pm0.47$ -0.67 ± 0.47 $\quad -0.25\pm0.23$ 0.08 ± 0.25 Mean -0.11 ± 0.14
Ti^{48}	6.75+6.41	1h	-0.09 ± 0.03

See caption of table 1. δ is measured with an unpolarized beam. The energy intervals are indicated on figs. 6, 8 and 5.

ment. In other cases, it depends on the incoherent scattering cross section due to spin effects only, which is generally small except for hydrogen. For non-hydrogenous materials the de-polarization correction is of the order [2, 4]) of a few per cent of δ and has been neglected. Hydrogenous sample materials were avoided.

3. Experimental Results

For even target nuclei the spin J_c of the compound nucleus capturing state is $\frac{1}{2}$ with positive parity. The capture γ-rays studied in the present experiment have high relative intensities and, with the exception of the 7.72 MeV γ-ray in Al^{28}, may be assumed to be E1 transitions [9]): for all the even target nuclei studied in the present experiment, the parity of the final level for the γ-ray whose polarization was measured is known to be negative by (d, p) stripping measurements. It is assumed that the relative intensity of M2 radiation is negligible as compared to E1 and therefore we are not concerned with quadrupole mixing in the γ-rays studied. The spin J_f of the level excited by the γ-ray transition is then $\frac{1}{2}$ or $\frac{3}{2}$ with negative parity; the corresponding values of R are 1 or $-\frac{1}{2}$, hence the knowledge of the sign of R is sufficient to distinguish between the two possible values of J_f. For other types of target nuclei, the difference between the values of R for the various possible spins is not so definite as a

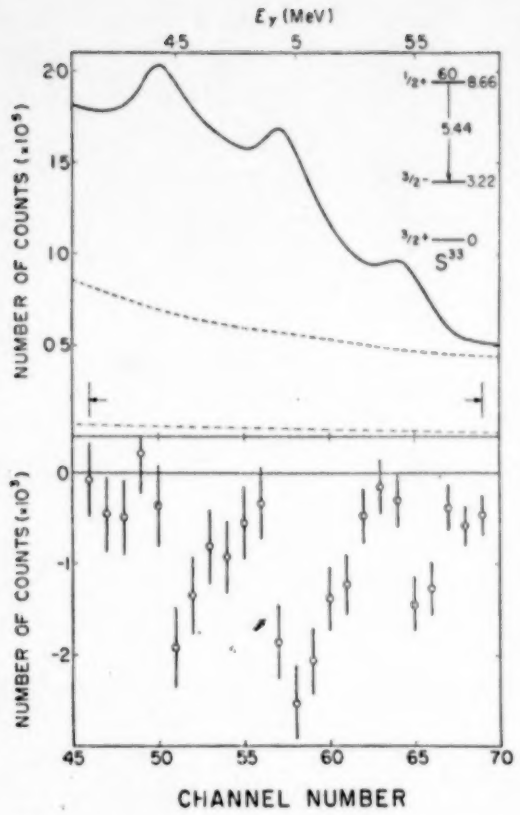

Fig. 3. Experimental result obtained with a sulphur target. The heavy solid curve in the upper part of the figure represents the sum of the spectra recorded in the NaI crystal for neutron spin "down" and "up"; the various points with their error in the lower part of the figure represent the difference between the two kinds of spectra normalized to the same neutron flux on the target. The dashed curve represents the contribution to the sum spectrum of the general background, the dashed-dotted curve, the contribution of the γ-rays due to neutrons scattered by the sample and captured in surrounding materials. The γ-ray energy scale is given at the top of the figure. The part of the compound nucleus decay scheme relevant to the experiment is shown in the upper right hand corner; the energies are expressed in MeV, and the intensity of the capture γ-ray is indicated above the transition, in numbers of photons per 100 radiative neutron captures. The arrows in the sum spectrum indicate the energy interval selected for the calculation of δ (eq. 4)) and R (eqs. (5) and (6)) as outlined in table 3.

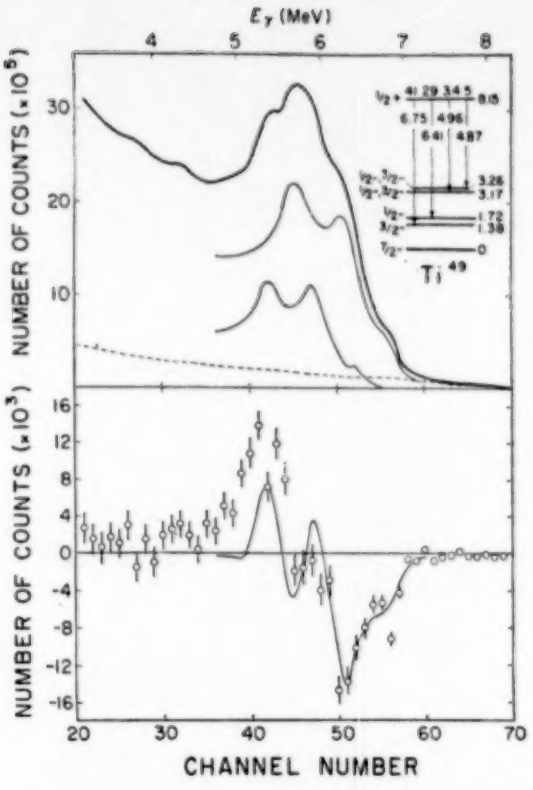

Fig. 4. Experimental result obtained with a titanium target. See the caption of fig. 3. The light solid curves in the upper part of the figure represent the contributions, to the sum spectrum, of the most intense capture γ-ray lines. The light solid curve in the lower part of the figure is the theoretical difference spectrum calculated using the decomposition of the sum spectrum and taking $R = 1$ and $-\frac{1}{2}$ for the 6.41 and 6.75 MeV γ-rays, respectively.

sign change (except for very favourable cases, such as Y^{90}, see below). Since, moreover, the relative admixtures of the two possible spin states $J_c = J_1 \pm \frac{1}{2}$ in

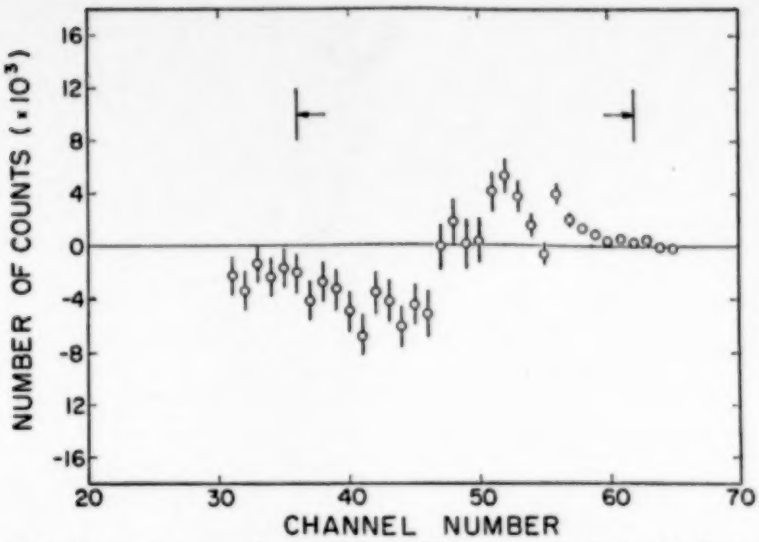

Fig. 5. Instrumental asymmetry experiment with Ti. The various points with their errors represent the difference spectrum, normalized to the same sum spectrum as in fig. 4, obtained with an unpolarized beam. The arrows indicate the energy interval selected for the calculation of δ as recorded in table 2.

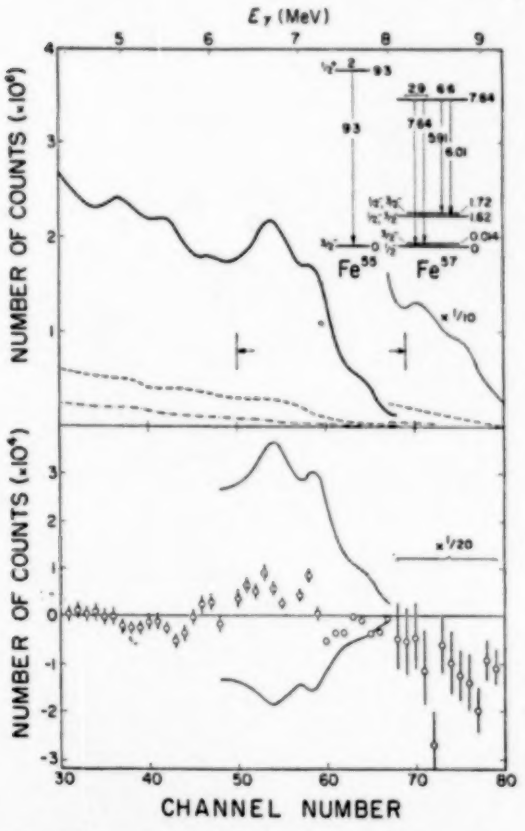

Fig. 6. Experimental result obtained with a Fe_2O_3 target. See the captions of figs. 3 and 4. The ordinate scale is enlarged above channel 68 where the 9.3 MeV capture γ-ray manifests itself. The light solid lines in the lower part of the figure represent the theoretical difference spectra calculated under the assumption that the 7.64 MeV line represents a pure transition to the ground state of Fe^{57} (upper curve) or to the first excited state (lower curve).

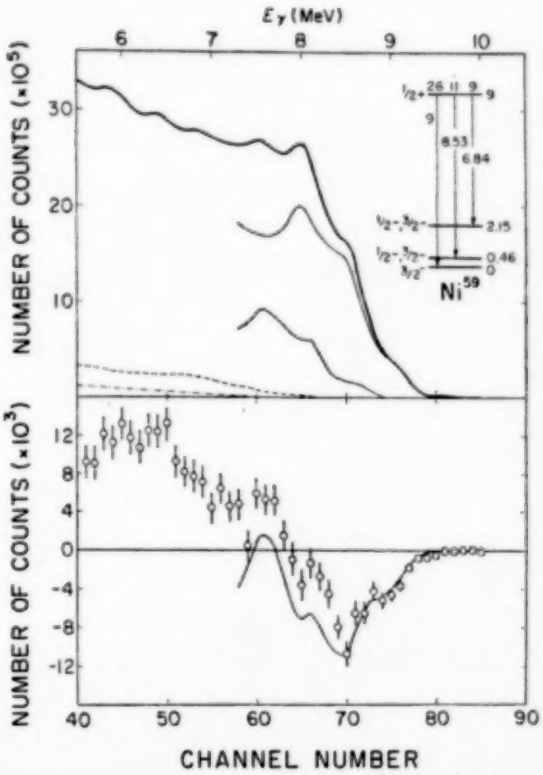

Fig. 7. Experimental result obtained with a NiO target. See the captions of figs. 3 and 4. The theoretical difference spectrum is calculated with the assumption that $R = 1$ and $-\frac{1}{2}$ for the 8.53 and 9 MeV γ-rays, respectively.

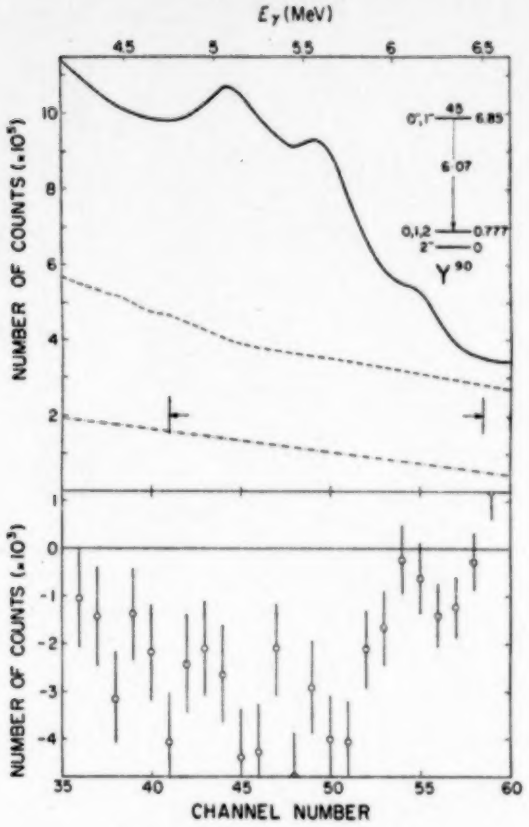

Fig. 8. Experimental result obtained with a Y_2O_3 target. See the caption of fig. 3.

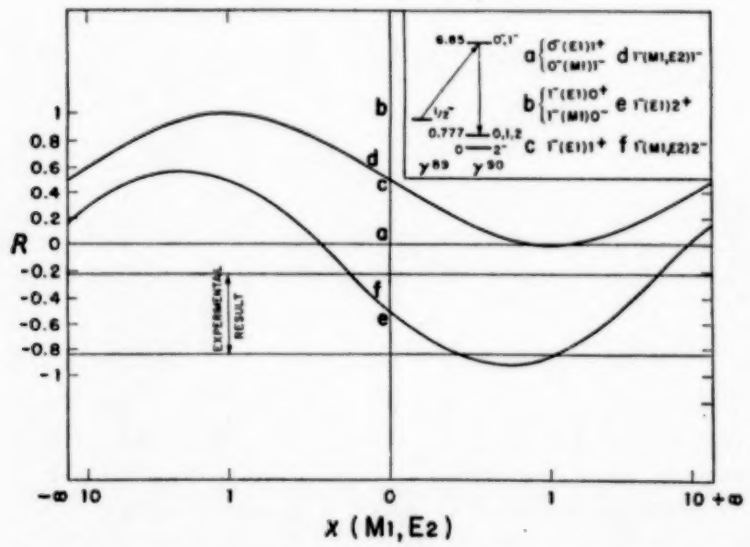

Fig. 9. Comparison of the experimental result obtained for the 6.07 MeV γ-ray in Y^{90} with the theoretical values of R for the various possible combinations of the spins of the capturing state and of the 0.777 MeV level in Y^{90} (points a, b, c and e, curves d and f). x(M1, E2) is the ratio of the amplitudes of the quadrupole and dipole radiation in the 6.07 MeV γ-ray.

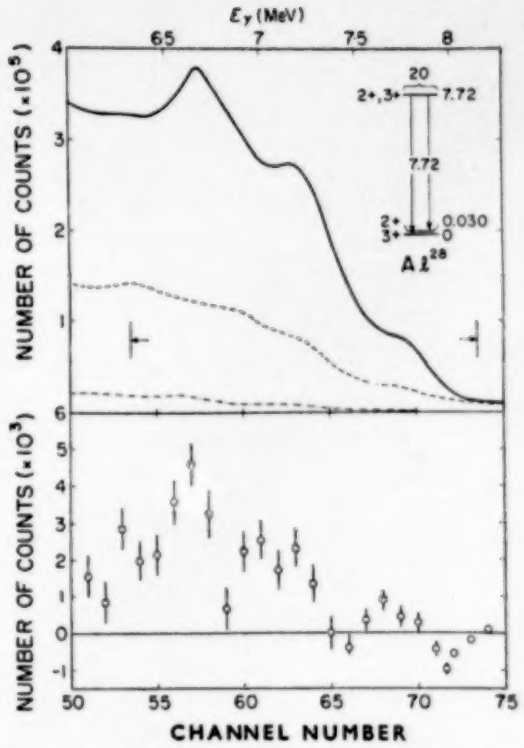

Fig. 10. Experimental result obtained with an aluminium target. See the caption of fig. 3.

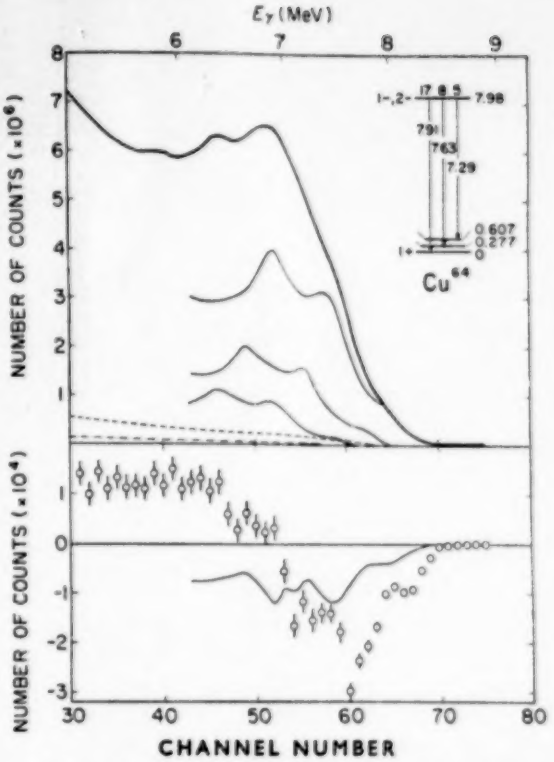

Fig. 11. Experimental results obtained with a copper target. See the captions of figs. 3 and 4. The theoretical difference spectrum is calculated with the assumption that $R = -\frac{1}{4}$ and $\frac{1}{4}$ for the 7.91 and 7.63 MeV γ-ray respectively.

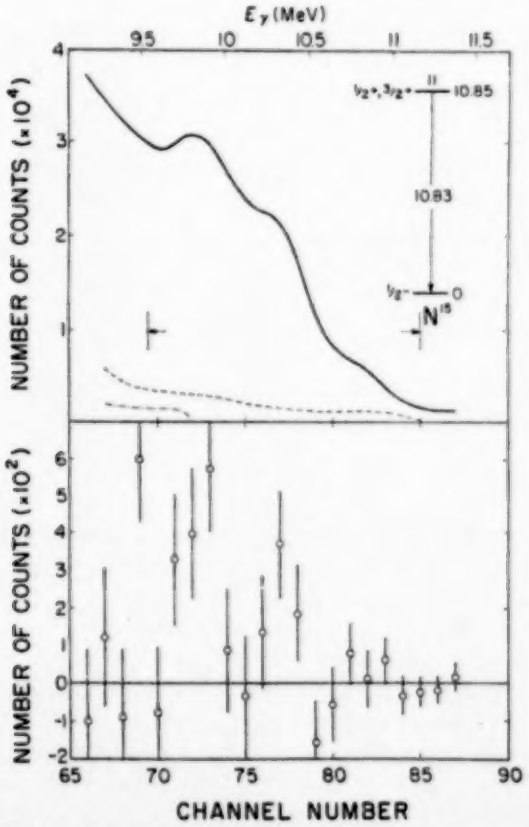

Fig. 12. Experimental result for nitrogen obtained with a $NaNO_3$ target. See the caption of fig. 3.

TABLE 3

Experimental results obtained with a polarized neutron beam

Target nucleus	γ-ray energy (MeV)	Component i	α_i	δ_i(%)	$\alpha_i\delta_i$(%)
S^{32}	5.44	Total	1	-0.96 ± 0.15	-0.96 ± 0.15
		(1)	0.43	0.36 ± 0.31	0.15 ± 0.13
		(2)	0.03	0.09 ± 0.73	0.00 ± 0.02
		(3)	0.02	$2.5\ \pm2.5$	0.05 ± 0.05
		(γ)	0.52	-2.23 ± 0.40	-1.16 ± 0.21
			$\bar{R} = -0.50\pm0.14 = 0.90\ R_1\pm0.10$		
			$R_1 = -0.56\pm0.27$		
Fe^{56}	7.64	Total	1	0.58 ± 0.20	0.58 ± 0.20
		(1)	0.14	0.30 ± 0.30	0.04 ± 0.04
		(2)	0.03	$0\ \pm5$	0.00 ± 0.15
		(3)	0.05	$-2.5\ \pm2.5$	-0.13 ± 0.13
		(γ)	0.78	0.86 ± 0.36	0.67 ± 0.28
			$\bar{R} = 0.21\pm0.11 = 0.87\ R_1\pm0.13$		
			$R_1 = 0.24\pm0.28,\ \beta_{GS} = 0.49\pm0.19$		
Y^{89}	6.07	Total	1	-0.58 ± 0.24	-0.58 ± 0.24
		(1)	0.44	0.70 ± 0.39	0.31 ± 0.17
		(2)	0.13	-0.64 ± 0.83	-0.08 ± 0.11
		(3)	0.02	$2.5\ \pm2.5$	0.05 ± 0.05
		(γ)	0.41	-2.10 ± 0.76	-0.86 ± 0.31
			$\bar{R} = -0.48\pm0.22 = 0.93\ R_1\pm0.07$		
			$R_1 = -0.52\pm0.31,\ -0.2 < x(\mathrm{M1, E2}) < 0.3$ or $1 < x(\mathrm{M1, E2}) < 4$		
Al^{27}	7.72	Total	1	1.37 ± 0.17	1.37 ± 0.17
		(1)	0.36	0.18 ± 0.22	0.06 ± 0.08
		(2)	0.04	-0.22 ± 0.86	-0.01 ± 0.04
		(3)	0.04	$-2.5\ \pm2.5$	-0.10 ± 0.10
		(γ)	0.56	2.54 ± 0.39	1.42 ± 0.22
			$\bar{R} = 0.63\pm0.15,\ \beta_{GS} \leqq 34\ \%$		
N^{14}	10.83	Total	1	1.38 ± 0.36	1.38 ± 0.36
		(1)	0.11	0.97 ± 1.46	0.11 ± 0.16
		(2)	0.03	-4.95 ± 6.57	-0.15 ± 0.19
		(3)	0.05	$-2.5\ \pm2.5$	-0.13 ± 0.13
		(γ)	0.81	1.91 ± 0.57	1.55 ± 0.46
			$\bar{R} = 0.54\pm0.21 = R_1,\ \beta_{\frac{1}{2}} = 0.25\pm0.18$		

The components i of the NaI spectrum referred to in column 3 are: total — the total spectrum; (1) — the general γ-ray background including capture γ-rays from the sample container; (2) — capture γ-rays from surrounding materials due to neutrons scattered by the sample; (3) — capture γ-rays from the sample scattered into the NaI crystal by the circular polarization analyzing magnet; (γ) — capture γ-ray from the sample transmitted through this magnet. The α_i are the relative contributions of these components to the counting rate in a selected energy interval of the detected spectrum, indicated by arrows in figs. 3, 6, 8, 10 and 12; the δ_i are the asymmetries (eq. (4)) of the various components while flipping the neutron spin with the radiofrequency coil. The calculation of $\bar{R}$ uses eqs. (5) and (6), that of R_1 uses eq. (8). The β's are the relative contributions of γ-ray lines to the capture γ-ray spectrum transmitted through the circular polarization analyzing magnet and detected in the NaI crystal. x(M1, E2) represents the ratio of the amplitudes of the quadrupole to the dipole radiations in the 6.07 MeV capture γ-ray in Y^{90}.

the capturing state are generally not known, the conclusions which can be drawn from the present type of experiment for $J_c \neq \frac{1}{2}$ are generally less definite than for even targets.

The results obtained during the present experiment are shown in figs. 3 to 12 and in table 3.

The cycling period for the data shown in the figures was one hour. The heavy solid curve in the upper part of the figures represents the sum of the spectra recorded in the NaI crystal for neutron spin "down" and "up", i.e. $N_+ + N_-$ (eq. (4)); the various points with their errors in the lower part of the figure represent the difference between the two kinds of spectra normalized to the same neutron flux on the target, i.e. $N_+ - N_-$ for each channel. The quantity $\bar{R}$ is proportional to the ratio of the difference to the sum (eqs. (4) and (6)) and has the same sign as the difference. We have also shown in the upper part of the figures the contributions, to the sum spectrum, of the general background (contribution (1) above, dashed curve) and of the γ-rays due to scattered neutrons (contribution (2) above, dashed dotted curve). The de-composition of the capture γ-ray component of the sum spectrum into its various lines is indicated by light solid curves, in the rather complicated capture γ-ray spectra of Ti, Ni and Cu. The γ-ray energy scale is given at the top of each figure. We have also shown the relevant part of the compound nucleus decay scheme in the upper right hand corner of each figure. The contribution of the various capture γ-ray lines indicated in these decay schemes can be found in the sum spectra. The energies (in MeV) and relative intensities (in photons per 100 radiative neutron captures) are taken from the compilation of Bartholomew and Higgs [8]).

The sum spectra for essentially mono-energetic γ-rays (i.e. S^{32}, fig. 3; Fe^{56}, fig. 6; Y^{89}, fig. 8; Al^{27}, fig. 10; N^{14}, fig. 12) show the usual features: full energy, first and second escape peaks. The difference spectra generally show maxima around the channels where these three peaks appear in the sum spectra providing further evidence on the stability of the detector. The same remark holds for the more complicated spectra of Ti (fig. 4), Ni (fig. 9) and Cu (fig. 11). The various maxima generally look more prominent in the difference than in the sum because the various background contributions mentioned earlier show little asymmetry and their effect is largely subtracted out in the difference spectrum.

The calculation of R_1 as outlined in table 3 is carried out as explained above, for the energy interval in the detector spectra indicated by arrows in the upper part of the figures. The measured value of δ was corrected for any possible instrumental asymmetry, using the results of table 1, for Fe^{56} and Y^{89} where measurements with an unpolarized beam were available. The same correction as for Fe^{56} was applied to the Al^{27} result, in view of the proximity of the γ-ray energies.

The Ti, Al and Cu samples were metals of high purity (99. 9% for Al). For the sulphur experiment powder precipitated sulphur (99. 5 % purity) was used. Yttrium was studied in the form of Y_2O_2 powder (extracted from the sample used in the experiment reported by Bartholomew *et al.* [18]), i.e. with impurities concentrations of less than a few parts per million). The commonly used [22]) urea sample for the study of nitrogen was replaced by $NaNO_2$ in order to avoid hydrogenous compounds as explained above. It is necessary to study Fe and Ni as non-ferromagnetic compounds. In the present experiment Fe_2O_3 and NiO were used. We have measured the neutron polarization after passage of the beam through these two samples: no difference, within 2 %, was noticed compared to the value obtained with the samples removed. Trumpy [2]) found a significant de-polarization in his iron and nickel samples, an effect which possibly reflects the difference in purity of the samples used in the two experiments.

3.1. EVEN TARGET NUCLEI

S^{32} (fig. 3)

The very prominent 5.44 MeV capture γ-ray in S^{33} emitted by the capturing state and exciting a level at 3.22 MeV [11]), is shown by our result (fig. 3) to have a negative value of R; this by itself indicates that the 3.22 MeV level has a spin of $\frac{3}{2}$ as pointed out earlier. The more detailed calculations given in table 3 confirm this conclusion by showing that the experimental value of R for this γ-ray is consistent with the theoretical value $-\frac{1}{2}$ for this spin assignment. This experiment served as a check of the apparatus and of the evaluation of its efficiency (i.e. of the coefficient of $\delta/\nu\sigma(E_\gamma)$ in eq. (6)) since the negative parity of this 3.22 MeV level has been determined by (d, p) stripping measurements [10]) and its spin has been shown to be $\frac{3}{2}$ by capture γ-ray angular correlation experiments [11]). The present result agrees with Trumpy's previous measurement [2, 3]) using the same method.

Ti^{48} (fig. 4)

The capture γ-ray spectrum in Ti^{49} shows [12]) two prominent lines at 6.75 and 6.41 MeV emitted by the capturing state and exciting levels at 1.38 and 1.72 MeV. The negative parity of both levels has been determined by (d, p) reactions [13, 14]) and their spins have been shown to be respectively $\frac{3}{2}$ and $\frac{1}{2}$ by capture γ-ray circular polarization [2, 3]) and angular correlation [12]) experiments. Some doubt has recently been cast [14, 15]) on the $\frac{1}{2}$ assignment for the spin of the 1.72 MeV level on the basis of the systematics of the (d, p) reaction in the region of Ti and for this excitation energy. The present experiment was undertaken to check this point.

Starting from the high energy end and decreasing in energy, the difference spectrum we have obtained (fig. 4) is first negative with maxima or plateaus at the position of the full energy and first escape peak of the 6.75 MeV γ-ray. It

then approaches 0 when the first escape peak of the 6.41 MeV line interferes with the second escape peak of the 6.75 MeV line, and finally becomes positive, with a maximum at the position of the second escape peak of the 6.41 MeV γ-ray. This confirms the previous spin assignments [2,3,12]) of $\frac{3}{2}$ and $\frac{1}{2}$ for the 1.38 and 1.72 MeV levels in Ti^{49} and does not agree with the $\frac{3}{2}$ assignment for the spin of the 1.72 MeV level proposed from the systematics of the stripping reaction [14,15]).

A more detailed study of the results has been made by calculating the theoretical difference spectrum using the de-composition of the sum spectrum shown in fig. 4 and taking $R = 1$ and $-\frac{1}{2}$ for the 6.41 and 6.75 MeV γ-rays; the background contributions (1) to (3) (see above) were assumed to be symmetric. The result is shown by the light solid line in the lower part of fig. 4. The experimental points for the difference fit fairly well the theoretical curve down to channel 45. Below this point, the general form of the curve is well reproduced experimentally, but deviations occurred as to the absolute magnitude of the effect. This may be explained by inaccuracies in the de-composition of the sum spectrum in the two γ-ray lines, by asymmetries in the general background contribution (i.e. contribution (1) above; the influence of scattered neutrons, background contribution (2), is negligible for this sample) and, more likely, by the asymmetry of the γ-rays Compton scattered by the circular polarization analyzing magnet: the contribution of the scattered γ-rays from the 6.75 MeV line increases with decreasing energy and its asymmetry is opposite to that of the transmitted γ-ray, i.e. positive; this reinforces the positive asymmetry of the difference spectrum below channel 45 due to the 6.41 MeV line.

An experiment for measuring the instrumental asymmetry was performed with the iron shim as described above. The difference spectrum so obtained, normalized to the same sum spectrum as in fig. 4, is shown in fig. 5. The asymmetry for the spectrum interval indicated by the arrows is (-0.09 ± 0.03) % as recorded in table 2; the individual points in the difference spectrum show asymmetries outside the statistical errors of the order of $\frac{1}{3}$ of the ones observed with the polarized beam (fig. 4), and systematically positive for the high energy side of the Ti peak and negative for the low energy side. These asymmetries are probably due to a gain shift in the NaI detector, the spectra with the neutron spin down having, on the mean, a gain slightly higher than the ones with spin up (of the order of $\frac{1}{10}$ of a channel around the Ti peak). Whether this effect is systematic, due for instance to some influence of the radiofrequency flipping current on the photomultiplier, or is to be attributed to erratic fluctuations of the detector gain for this particular run has not been determined with certainty, although fig. 5 represents the combined results of two experiments giving asymmetries in the same direction. If the effect is systematic, it reinforces the results obtained with the polarized beam since it is in the opposite direction; the same is true for most of the results obtained during the present experiment.

If, on the other hand, the effect is not of systematic origin but is erratic, the fact that the experimental points in the difference spectrum of fig. 4 are in good agreement with the theoretical curve at the high energy end indicates that the runs whose results are summarized in fig. 4 were probably performed with a good overall gain stability. The order of magnitude of the asymmetries of the individual points in fig. 5 shows that, in analyzing complex spectra in the manner used for fig. 4 (e.g. the analysis of the Ni and Cu results, fig. 7 and 11, see below), the sign and the order of magnitude of the effect can be obtained, but quantitative values of R for various interfering lines are subject to considerable uncertainties. This does not affect the analysis of essentially mono-energetic γ-rays using a large energy interval in the detector spectrum as it is performed in table 3: the overall asymmetry of the Ti spectrum is much smaller than that of the individual points and is of the same order of magnitude as the results of the other instrumental asymmetry experiments, as listed in table 2.

Fe^{56} (fig. 6)

The weak 9.3 MeV capture γ-ray in iron is believed [16]) to be the transition to the $\frac{3}{2}^-$ ground state of Fe^{55}; the difference spectrum of fig. 6 above channel 68 supports qualitatively this assignment.

The prominent 7.64 MeV capture γ-ray observed in Fe^{57} is produced by transitions between the capturing state and the $\frac{1}{2}^-$ ground state, or the $\frac{3}{2}^-$ first excited state, 14 keV above the ground state, or both. The two light solid lines in the lower part of fig. 6 represent the theoretical difference spectra calculated under the assumption that the 7.64 MeV line represents a pure transition to the ground state (upper curve) or to the first excited state (lower curve), no asymmetry being assumed for the various background contributions. The experimental points do not agree with either curve and lie between the two curves. A more detailed analysis reported in table 3 confirms this fact: the experimental value of R for the 7.64 MeV γ-ray does not agree with the theoretical values $+1$ or $-\frac{1}{2}$ for a pure transition. This shows that the 7.64 MeV capture γ-ray in Fe^{57} is composed of two unresolved transitions starting from the capturing state, with (49 ± 19) % of the intensity leading to the $\frac{1}{2}^-$ ground state and the remainder to the $\frac{3}{2}^-$ first excited state.

The present result disagrees with Trumpy's previous measurement [2, 3]) using the same method. The contribution of the 6.74 MeV line to the γ-ray spectrum in the NaI crystal was the same for the two experiments (87 %) and Trumpy obtained $\bar{R} = 0.78 \pm 0.14$, whereas our result is $\bar{R} = 0.21 \pm 0.11$. Trumpy concluded from his measurement that the 7.64 MeV line is mainly the ground state transition in Fe^{57}. The disagreement between the two experimental results is so far unexplained.

Ni^{58} (fig. 7)

The high energy part of the neutron capture γ-ray spectrum in nickel shows [16])

a 9 MeV line which is the ground state transition in Ni^{59}, an 8.53 MeV γ-ray which may be the ground state transition in Ni^{61} or (ref. [16])) a transition to the 0.46 MeV level in Ni^{59} (refs. [16,17])), a 6.84 MeV line which is probably † a transition to the 2.15 MeV level in Ni^{59} (ref. [16])) as well as other lower intensity γ-rays. The 0.46 and 2.15 MeV levels are known to have a negative parity from (d, p) reactions [17]).

The difference spectrum we have obtained (fig. 7) can be analyzed in the same way as the Ti results, see above. The high energy part is consistent with the known $\frac{3}{2}^-$ character of the Ni^{59} ground state and shows that the 8.53 MeV γ-ray leads to a spin $\frac{1}{2}$ level. Since the ground state of Ni^{61} is known to be $\frac{3}{2}^-$, this result indicates that the 8.53 MeV line mainly consists of a transition to the 0.46 MeV level in Ni^{59} and that this level has a spin of $\frac{1}{2}$. The experimental points agree fairly well with the theoretical difference spectrum (light solid curve at the lower part of fig. 7) calculated with $R = 1$ and $-\frac{1}{2}$ for the 8.53 and 9 MeV γ-rays, down to channel 70. Below this point, the general form of the curve is well reproduced, and the deviations of the absolute magnitude of the effect may be explained, as in the case of Ti, by the influence of 9 MeV γ-rays Compton scattered by the circular polarization analyzing magnet. The reason why the effect of the scattered γ-rays seems to appear at higher energies in the spectrum of Ni than in Ti, may be found, at least qualitatively, in the difference of the γ-rays energies: the forward peaking of the Compton scattering process is known to increase with increasing energy.

In view of the influence of these scattered γ-rays as well as of the possible fluctuations noticed in the case of Ti (fig. 5), no definite conclusion can be drawn about the spin of the final level for the 6.84 MeV γ-ray. The fact that the difference spectrum becomes rather strongly positive in the region where this γ-ray manifests itself (from channel 55 down) suggests that this spin is $\frac{1}{2}$.

As in the case of Ti, the good agreement between the experimental points and the theoretical difference spectrum in the region of predominance of the 9 MeV γ-ray, for which the spin of the final level is known, is an indication of the good overall gain stability for the experiments whose results are summarized in fig. 7.

The present result on the 9 MeV γ-ray agrees with Trumpy's previous measurement [2,3]) using the same method. Trumpy did not study the circular polarization of the 8.53 and 6.84 MeV γ-rays.

3.2. ODD-PROTON TARGET NUCLEI

Y^{89} (fig. 8)

The very prominent 6.07 MeV capture γ-ray in Y^{90}, emitted by the 0^- or 1^- capturing state and exciting a level at 0.777 MeV [18]) can be assumed to be a dipole transition in view ot its high intensity (45 % per neutron capture) [9,18])

† See *note added in proof* at the end of this paper.

so that the spin of the 0.777 MeV level may be 0, 1 or 2 with either parity. The difference spectrum (fig. 8) shows that the 6.07 MeV γ-ray has a negative polarization and a more detailed analysis outlined in table 3 gives for this γ-ray $R = -0.52 \pm 0.31$. This result is compared in fig. 9 with the theoretical value of R for the various possible combinations of the spins of the capturing state and of the 0.777 MeV level. If the latter has a positive parity, the 6.07 MeV transition may be assumed to be a pure E1 and the corresponding values of R are indicated by the points a, b, c and e on the R axis of fig. 9; if it has a negative parity, the 6.07 MeV transition may be an (M1, E2) mixture and, in that case, R depends on the (M1, E2) mixing parameter X(M1, E2) according to the curves d and f of fig. 9. The experimental result is only consistent with the 6.07 MeV line being a $1 \rightarrow 2$ transition; this shows that the spin of the 0.777 MeV level in Y^{90} is 2 and that at least 45 % of the thermal neutron capture in Y^{89} proceeds by a spin 1 capturing state. If the 0.777 MeV level has a negative parity, rather wide limits can be attributed, from the present measurement, to the (M1, E2) mixing parameter of the 6.07 MeV transition as indicated in table 3.

The present result agrees with previous capture γ-ray angular correlation measurements [18]). The additional information from the present experiment is that the spin assignment we propose is independent of any mixture in the 6.07 MeV transition which may occur if the 0.777 MeV level has a negative parity; in the angular correlation experiment however, one has to deal with possible, although improbable mixtures in the two members of the $\gamma-\gamma$ cascades studied, which may allow other spin combinations to be consistent with the experimental data.

Al^{27} (fig. 10)

The prominent 7.72 MeV capture γ-ray in Al^{28} is emitted from the 2^+ or 3^+ capturing state and excites the 3^+ ground state or the 2^+ first excited state, 30 keV above the ground state, or represents two unresolved transitions leading to these two levels. The difference spectrum (fig. 10) shows that its polarization is negative and a more detailed analysis (table 3) gives for this γ-ray $R = -0.63 \pm 0.15$. The theoretical values of R for the various combinations of J_c and J_f and for pure M1 transitions are [2]): $2 \rightarrow 2$: $R = -\frac{1}{6}$; $2 \rightarrow 3$: $R = \frac{1}{3}$; $3 \rightarrow 2$: $R = \frac{2}{3}$; $3 \rightarrow 3$: $R = \frac{1}{6}$. Our experimental result is consistent with a pure $3 \rightarrow 2$ transition and does not agree with pure $2 \rightarrow 2$, $3 \rightarrow 2$ and $3 \rightarrow 3$ transitions. The 7.72 MeV line may consist of a mixture of the four possible transitions and all four may contain E2 admixtures, so that what our result truly provides is a relation between the relative intensities and the (M1, E2) mixing parameters of these transitions, i.e. between 8 quantities.

The relative amounts of the two possible spin states in the capturing state has not been determined by neutron resonance experiments. The interaction

of slow neutrons with Al has been shown [20]) to be dominated by two resonances at 35 keV and −23 keV; both are mainly scattering resonances and have probably a spin 3. If one then assumes that the capturing state in Al^{28} is a pure spin 3 state and that the transitions to the ground state and first excited state are pure M1, one can deduce from our result that the relative intensity of the ground state $3 \rightarrow 3$ transition in the mixture $3 \rightarrow 3$ and $3 \rightarrow 2$ is smaller than 34 %.

Cu^{63} (fig. 11)

The high energy part of the neutron capture γ-ray spectrum in copper shows [21]) a 7.91 MeV line which is the ground state transition in Cu^{64} as well as 7.63 and 7.30 MeV γ-rays which are probably transitions to the 0.277 and 0.607 MeV levels in Cu^{64} (refs. [2, 22])). The difference spectrum (fig. 11) shows that the 7.91 MeV line has a negative polarization whereas the 7.63 MeV γ-ray has a positive one.

The capturing state in Cu^{64} may be 1^- or 2^- and the ground state is known to be 1^+; the theoretical values of R for the two possible ground state transitions are: $1^- \rightarrow 1^+$: $R = -\frac{1}{4}$; $2^- \rightarrow 1^+$: $R = \frac{3}{4}$. The sign of the polarization of the 7.91 MeV line thus shows that the capturing state is mainly 1^-. If the relative amounts of the two possible spin states in the capturing state are the same for the ground state transition and for the 7.63 MeV line and if the latter is a pure dipole, the spin of the 0.277 MeV level is 0, 1 or 2, in which case $R = -\frac{1}{2}$, $-\frac{1}{4}$ or $\frac{1}{4}$; the sign of the polarization of the 7.63 MeV line then shows that the 0.277 MeV level has a spin of 2.

The light solid curve in the lower part of fig. 11 is the theoretical difference spectrum calculated with $R = -\frac{1}{4}$ and $\frac{1}{4}$ for the 7.91 and 7.63 MeV γ-rays; no asymmetry was assumed for the 7.30 MeV line in absence of any indications of its sign and magnitude. Unlike the ones of Ti and Ni, the Cu experimental difference spectrum does not agree with the theoretical curve in its high energy part and seems to indicate a larger value of $|R|$ for the 7.91 MeV line, close to $\frac{1}{2}$; this disagreement is not considered to be very serious in view of the difficulties mentioned earlier of getting quantitative values for $|R|$ in the case of complicated capture γ-ray spectra. The present spin assignments only depend on the sign of R for the 7.91 and 7.63 MeV γ-rays. In view of these uncertainties, no conclusion can be drawn concerning the circular polarization of the 7.30 MeV transition.

The present result disagrees with Trumpy's previous measurement using the same method, the signs of R he obtained for the 7.91 and 7.63 MeV lines being the reverse of the one we have obtained. The assignment of a spin 2 for the 0.277 MeV level is in agreement with capture γ-ray angular correlation experiments [22]).

3.3. ODD TARGET NUCLEI

N^{14} (fig. 12)

The 10.83 MeV capture γ-ray in N^{15} (ref. [23])) starts from the $\frac{1}{2}^+$ or $\frac{3}{2}^+$ capturing

state and leads to the $\frac{1}{2}^-$ ground state; in view of its high energy, it can be detected in the NaI crystal with a low background (fig. 12) in spite of the small thermal neutron capture cross section of N^{14} (80 mb). The results obtained after a two-week-long experiment show (fig. 12) that the 10.83 MeV γ-rays has a positive polarization and a more detailed analysis (table 3) gives, for this γ-ray, $R = 0.54 \pm 0.21$. The theoretical values of R for the two possible spins of the capturing state are: $R = -\frac{1}{3}$ for $\frac{1}{2}$; $R = \frac{5}{6}$ for $\frac{3}{2}$. Our result thus shows that the relative amount of spin $\frac{1}{2}$ in the capturing state is (25 ± 18) %.

4. Discussion

4.1. EVEN TARGET NUCLEI

For even target nuclei the E1 capture γ-rays of higher relative intensity excite levels in the odd-neutron compound nucleus where the odd neutron is in a p-orbit [9]), i.e. $p_{\frac{3}{2}}$ or $p_{\frac{1}{2}}$. This is the case for the 3.22 MeV level in S^{33}, the 1.38 MeV level in Ti^{49} and the ground state of Ni^{59}, all $p_{\frac{3}{2}}$ levels, as pointed out previously [9, 11, 12]). For the two transitions in Fe^{57} exciting with comparable intensities, the $\frac{1}{2}^-$ ground state and $\frac{3}{2}^-$ first excited state, the same kind of interpretation has been attempted in the framework of Nilsson's model as described elsewhere [24]).

The positions of the energy levels of Ni^{59} have been calculated by Kisslinger

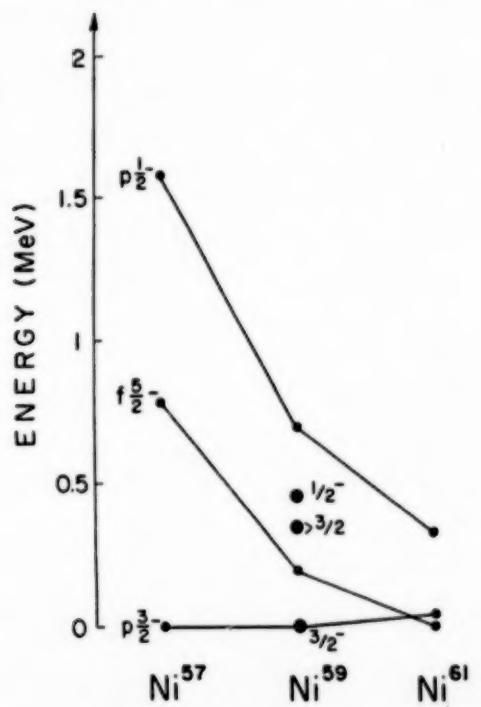

Fig. 13. Energy levels of Ni^{57}, Ni^{59} and Ni^{61} as calculated by Kisslinger and Sorensen [25]). The theoretical points are indicated by small dots; the shell model single particle levels are indicated for Ni^{57}. The levels of Ni^{59} whose spins have been confirmed or determined during the present experiment are indicated by large dots.

and Sorensen [25]) assuming a pairing short range interaction and a $P_2(\cos\theta)$ long range force between the three neutrons of Ni^{59} outside the 28 closed shell; their result is shown in fig. 13. The ground state of Ni^{59} is a $p_{\frac{3}{2}}$ level in agreement with their calculation. It is seen that the level at 0.46 MeV, for which we have assigned a spin of $\frac{1}{2}$, may be identified with the $p_{\frac{1}{2}}$ quasi-particle level whose separation from the $p_{\frac{3}{2}}$ level is considerably modified, compared to the ordinary shell model predictions, by the introduction of the abovementioned interactions. This identification of the 0.46 MeV level as having the odd neutron in a p orbit is further supported by the high relative intensity of the primary capture γ-ray leading to this level. Since no intense primary γ-ray feeding the 0.34 MeV level in Ni^{59} has been detected, its spin is very likely higher than $\frac{3}{2}$ so that it could be identified with the $f_{\frac{5}{2}}$ level predicted, in the neighbourhood of this energy, by Kisslinger and Sorensen. The slight disagreement between theory and experiment as to the absolute value of the energy of the $p_{\frac{1}{2}}$ and $f_{\frac{5}{2}}$ levels may be explained as follows: the energies of the shell model single particle levels in Ni^{57}, which is a doubly magic nucleus plus a neutron, are not known and Kisslinger and Sorensen had to use indirect methods to estimate them in order to conduct their calculations. The discrepancy just mentioned may reflect the approximations in this estimate.

The $\frac{1}{2}^-$ level at 1.72 MeV in Ti^{49} is difficult to interpret. If it mainly contains the $p_{\frac{1}{2}}$ single particle level, the energy difference between the $p_{\frac{3}{2}}$ and $p_{\frac{1}{2}}$ levels in Ti^{49} is small compared to nuclei of lower mass [12]) although this could perhaps be explained by the introduction of the pairing plus long range interaction as in Ni^{59}. However there are also some objections from stripping systematics against the identification of this level as mainly containing the $p_{\frac{1}{2}}$ single particle level [14,15]). If Ti^{49} is a deformed nucleus and if Nilsson's model can be applied to it as for Fe^{57} (ref. [24])), the 1.38 and 1.72 MeV levels could be considered as belonging to the $\Omega = \frac{3}{2}^-$ and $\Omega = \frac{1}{2}^-$ orbits from the $p_{\frac{3}{2}}$ shell model level. The present experiment is not able to give indications for a choice between these and other possible explanations.

4.2. ODD-PROTON TARGET NUCLEI

In the case of an odd-proton target nucleus, the levels of the odd compound nucleus form multiplets [26, 27]), i.e. groups of levels for which the odd proton and odd neutron orbits are the same, with spins and parities j_p^{π} and j_n^{π}, but whose total spins are different. The relative intensities of the primary capture γ-rays exciting the levels of such a multiplet have been calculated by Varshalovich [26]) under the assumption that in the compound nucleus capturing state and in the levels of the multiplet, the proton remains in the same j_p^{π} orbit as in the odd-proton target nucleus. The predictions of Varshalovich depend on the spin of the compound nucleus capturing state. As for even target nuclei the most

intense primary γ-rays excite levels where the odd neutron is in a $p_{\frac{3}{2}}$ or $p_{\frac{1}{2}}$ orbit [27]).

For $_{29}Cu^{63}_{34}$, we have $j_p{}^{\pi} = \frac{3}{2}^-$ (ref. [28])). In the 1^+ ground state of $_{29}Cu^{64}_{35}$, the odd neutron is very likely in a p-orbit in view of the high relative intensity of the primary capture γ-ray leading to this level. That it is a $p_{\frac{3}{2}}$ and not a $p_{\frac{1}{2}}$ orbit is suggested by the following remarks: (1) the ground states of the odd-proton isotopes of bromine having 35 protons are $\frac{3}{2}^-$; (2) although the ground states of the odd-neutron isotopes having 35 neutrons are $\frac{5}{2}$ (except perhaps for Ni^{63} where it may be [28]) $\frac{3}{2}$), there is a low-lying $p_{\frac{3}{2}}$ excited state in $_{30}Zn^{65}_{35}$ (at 0.05 Mev); (3) the ground state spins of $_{31}Ga^{65}_{34}$ and $_{31}Ga^{66}_{35}$ are respectively $\frac{3}{2}^-$ and 0^+ indicating that the odd neutron in Ga^{66} has $j_n \geqq \frac{3}{2}$. Using the result of Varshalovich [26]), one predicts: for a 1^- capturing state, the primary capture γ-ray to the 1^+ member of a $(j_p{}^{\pi} = \frac{3}{2}, j_n{}^{\pi} = \frac{3}{2}^-)$ multiplet has the highest reduced intensity; for a 2^- capturing state, it has only 0.07 times the reduced intensity of the most prominent capture γ-ray to a member of this multiplet. This is in agreement with the facts that the ground state capture γ-ray transition in Cu^{64} is the most intense line of the capture spectrum and that it starts from a 1^- capturing state as shown during the present experiment.

The same kind of consideration cannot be applied to the 6.07 MeV line in Y^{90} since a plausible configuration for the 0.777 MeV level is $j_p{}^{\pi} = \frac{9}{2}^+$, $j_n{}^{\pi} = \frac{1}{2}^+$ (ref. [18])), whereas $j_p{}^{\pi} = \frac{1}{2}^-$ for Y^{89}. Our result on Al [28] is not specific enough to be compared with the theory of Varshalovich.

Concerning the indications obtained during the present experiment on the relative admixture of the two possible spin states in the compound nucleus capturing state of Cu^{64} and Y^{90}, no comparison can be made with other kinds of experiments since the resonances responsible for the capture of thermal neutrons in Cu^{63} and Y^{89} have not been identified [9, 18]). The case of Al^{28} has already been considered.

4.3. ODD TARGET NUCLEI

The levels responsible for the radiative capture of thermal neutrons in N^{14} are believed[29]) to be mainly the 10.806 and 9.84 MeV levels below the neutron binding energy in N^{15}: the 10.806 MeV level should be $\frac{3}{2}^+$ and should account for most of the ground state transition, the 9.84 MeV level should be a $\frac{1}{2}^+$ and contribute most of the cascade radiations in the de-excitation of the neutron capturing state in N^{15}. The result of the present experiment which indicates that the initial level for the ground state transition in N^{15} is mainly $\frac{3}{2}^+$ is in agreement with this interpretation. It provides further support for a $\frac{3}{2}^+$ assignment to the 10.806 MeV level in N^{15}; the $\frac{3}{2}$ spin is in agreement with studies of the $C^{14}(p, \gamma)N^{15}$ reaction [30]) and, although the latter measurements favour a negative parity, they do not exclude a positive parity [23]).

5. Conclusion

We have measured the circular polarization of γ-rays following the capture of polarized neutrons for 13 transitions in 8 nuclei. For even targets, the sign of the γ-ray circular polarization P_γ relative to the neutron polarization P_n is sufficient to determine the spin J_f of the level of the compound nucleus where the higher intensity γ-rays lead, i.e. to distinguish between the two possible values $\frac{1}{2}$ and $\frac{3}{2}$; because of this, the determination of this spin has been possible, not only for relatively isolated capture γ-ray lines as in S^{33} and Fe^{57}, but also for rather complicated capture γ-ray spectra as in Ti^{49} and Ni^{59}. In the case of other target nuclei, the uncertainty about the relative admixture of the two possible spin states J_c in the compound nucleus capturing state generally introduces serious difficulties in the interpretation of the result. For the favourable case of Y^{90}, the sign of P_γ relative to P_n is different for one combination of J_c and J_f than for all the others and, as the experiment gave this relative sign, we have been able to determine uniquely J_c and J_f for one transition. In the case of Al^{28}, Cu^{64} and N^{15}, indications are obtained on the relative admixture of the two possible spin states in the capturing state.

Two levels in Ni^{59}, whose spins have been confirmed or determined during the present experiment, may be identified with levels predicted by the pairing plus long-range force calculation of Kisslinger and Sorensen. The interpretation of our results on Fe^{57} in the framework of Nilsson's model is given elsewhere [24]). For the odd nucleus Cu^{64}, agreement is found between our result and the theory of Varshalovich which predicts the relative intensity of the primary capture γ-rays leading to the levels of a multiplet. Our result on N^{15} supports a recent interpretation of the capture of thermal neutrons by N^{14} as due to two levels below the neutron binding energy.

We are very grateful to Mr. J. M. Robson and Dr. M. A. Clark for giving us the opportunity of using the polarized neutron beam which they have set up at the Chalk River NRU reactor and for their constant help during the course of the present experiment. We are also very grateful to Dr. G. A. Bartholomew for many helpful discussions and for the loan of some high purity samples used in this experiment. We thank Atomic Energy of Canada Limited for the hospitality in the Chalk River Laboratories and the Centre d'Études de l'Énergie Nucléaire for its financial assistance during our stay in Chalk River.

Note added in proof: We are indebted to G. A. Bartholomew for pointing out to us that mass measurements by Quisenberry *et al.* [31]) suggest that the 6.84 MeV. γ-ray is the ground state transition in Ni^{63}.

References

1) L. C. Biedenharn, M. E. Rose and G. B. Arfken, Phys. Rev. **83** (1951) 683
2) G. Trumpy, JENER Publications, No. **13** (1957)
3) G. Trumpy, Nuclear Physics **2** (1957) 664
4) B. Grimeland, C. R. du Congrès Intern. de Physique Nucléaire (Dunod, Paris, 1958) p. 454
5) M. A. Clark and J. M. Robson, Can. J. Phys. **39** (1961) 1
6) M. A. Clark and J. M. Robson, Can. J. Phys. **39** (1961) 13
7) H. Schopper, Nuclear Instruments **3** (1958) 158
8) G. A. Bartholomew and L. A. Higgs, Atomic Energy of Canada Limited, Chalk River, Report AECL-669 (1958) (unpublished)
9) B. B. Kinsey and G. A. Bartholomew, Phys. Rev. **93** (1954) 1260;
G. A. Bartholomew, P. J. Campion, J. W. Knowles and G. Manning, Proc. Intern. Conf. on Neutron Interactions with the Nucleus (Columbia University Press, 1957)
10) J. R. Holt and T. N. Marsham, Proc. Phys. Soc. London A**66** (1958) 467
11) G. Manning and G. A. Bartholomew, Phys. Rev. **115** (1959) 401
12) J. W. Knowles, G. Manning, G. A. Bartholomew and P. J. Campion, Phys. Rev. **114** (1959) 1065
13) Bretscher, Alderman, Elwyn and Shull, Phys. Rev. **96** (1954) 103
14) L. H. Rietjens, O. M. Dilaniuk and M. H. Macfarlane, Phys. Rev. **120** (1960) 527
15) M. H. Macfarlane and J. B. French, Rev. Mod. Phys. **32** (1960) 567
16) B. B. Kinsey and G. A. Bartholomew, Phys. Rev. **89** (1953) 375
17) V. P. Adyasevich, L. V. Groshev, A. M. Demidov and B. N. Lutsenko, J. Nucl. Energy II, **3** (1956) 325
18) G. A. Bartholomew, P. J. Campion, J. W. Knowles and G. Manning, Nuclear Physics **10** (1959) 590
19) B. B. Kinsey, G. A. Bartholomew and W. H. Walker, Phys. Rev. **83** (1951) 519
20) C. T. Hibdon, Phys. Rev. **114** (1959) 179
21) G. A. Bartholomew and B. B. Kinsey, Phys. Rev. **89** (1953) 386
22) G. A. Bartholomew and J. Vervier, to be published
23) G. A. Bartholomew and P. J. Campion, Can. J. Phys. **35** (1957) 1347
24) J. Vervier and G. A. Bartholomew, Proc. Kingston Conf. on Nuclear Structure (North-Holland Publishing Co., Amsterdam, 1960) p. 650 (and to be published)
25) L. S. Kisslinger and R. A. Sorensen, Mat. Fys. Medd. Dans. Vid. Sels. **21** No. 9 (1960) 22
26) D. A. Varshalovich, Soviet Physics JETP (English translation)**11** (1960) 125
27) L. V. Groshev and A. M. Demidov, J. Nucl. Engergy II, **8** (1958) 103
28) K. Way *et al.*, Nuclear Data Sheets, National Academy of Sciences, National Research Council, Washington, U.S.A.
29) D. F. Hebbard and D. N. F. Dunbar, Phys. Rev. **115** (1959) 624
30) G. A. Bartholomew, F. Brown, H. E. Gove, A. E. Litherland and E. B. Paul, Can. J. Phys. **33** (1955) 441
31) Quisenberry *et al.*, Phys. Rev. **104** (1961) 461

9.A

Nuclear Physics **26** (1961) 35—51; © *North-Holland Publishing Co., Amsterdam*

Not to be reproduced by photoprint or microfilm without written permission from the publisher

CHARACTERISTICS OF HIGH-ENERGY NUCLEAR INTERACTIONS AT AND ABOVE 10^{14} eV

A. UEDA † and C. B. A. McCUSKER

Daily Telegraph Theoretical and Falkiner Nuclear Departments, School of Physics, The University of Sydney, Sydney, Australia ††

Received 24 January 1961

Abstract: An attempt has been made to explain a) the changes in slope of the γ ray energy spectrum around γ energies of 1000 GeV at 220 gm/cm² and 740 g/cm² from the top of the atmosphere, b) the change in slope of the extensive air shower density spectrum at sea level at densities of about 1000 particles/m², c) the double change in slope of the energy spectrum of γ rays from local nuclear interactions at 220 g/cm², d) the absence of such a change at sea level, and e) the μ-meson spectrum at sea level. The cascade theory developed by Fukuda, Ogita and Ueda has been used together with the following basic hypotheses: (i) in a nucleon-nucleon collision the maximum pion energy in the CMS is about 25 GeV, (ii) the fractional energy going into the pion component decreases with increasing primary energy (from 30 % at 500 GeV to 5 % at 5×10^7 GeV), (iii) at very high energies a large fraction of the energy goes into a few heavier particles and thence some of this, via the Σ^0, into the electromagnetic cascade. Good agreement between theoretical predictions and experimental results has been obtained.

1. Introduction

Recently a number of very interesting observations on 'jets', extensive air showers and high energy μ-mesons have been made. The Japanese [1]) and Bristol [2]) groups working with mixed stacks of lead and nuclear emulsion have shown that both at 220 g/cm² and 740 g/cm² from the top of the atmosphere, there is a rather sharp change in the slope of the energy spectrum of γ rays incident upon the stacks at an energy of about 1000 GeV. Working on extensive air showers at sea level the Sydney group [3]) has shown that the density spectrum undergoes a similar change in slope at densities of about 1000 particles/m². The energy of the primary particles producing these showers must be higher by a factor of at least 100 than that of the particles producing the γ rays seen in the emulsion work. In addition to these experiments the Bristol group has measured the energy spectrum of the γ rays from nuclear interactions inside the stack at the 220 g/cm² level while Russian [4]) workers have carried

† On leave of absence from the Research Institute for Fundamental Physics, Kyoto University, Kyoto, Japan.

†† This work has been supported by the Nuclear Research Foundation within the University of Sydney and by the Office of Scientific Research of the Air Research and Development Command of the U.S.A.F. under Contract AF 49(638)—842.

out a somewhat similar measurement (but using their ionisation 'calorimeter') at sea level. The spectrum of the Bristol group not only shows a change in slope at about 1000 GeV similar to that of their γ-ray spectrum, but also indicates a second change (resulting in a flattening of the spectrum) at an energy about five times higher. The Russian spectrum, on the other hand, shows no change of slope. Finally, the μ meson energy spectrum has been measured up to energies of about 10^{13} eV and shows no sudden change in slope [5,21]).

Any one of these results, taken by itself, can be explained by making a suitable assumption about the primary cosmic ray energy spectrum. If all are considered, however, this is not possible. One is therefore driven to examine the hypothesis that all are due to the characteristics of nuclear interactions at high energies and the manner in which these change with energy. It is well known that the transverse momentum component of pions produced in high energy interactions has a value close to 0.4 GeV/c. The γ-ray energy spectra and the sea level density spectrum suggest that, in the centre-of-mass system (CMS) of a nucleon-nucleon collision there is also a maximum possible value for the longitudinal momentum component of pions. This might be due to a limitation of the velocity of the "fireball" in the "fireball" model as suggested by Hayakawa and Ogita [6]), or to the preferred production of mesons at right angles to the line of flight, or to a sudden increase in the average number of mesons produced at some given primary energy or some other possibility.

One of the main purposes of this paper is to examine these possibilities. It will be seen that good agreement with all the experiments mentioned can be obtained if we use a cascade model of the type developed by Fukuda, Ogita and Ueda together with the following basic hypotheses:

a) In the CMS of two colliding nucleons the maximum energy of a pion is about 25 GeV.

b) The total number of secondary particles is $2E_0^{\frac{1}{4}}$, where E_0 is the primary energy [8]).

c) The fraction of the incident energy going into the pion component decreases with increasing energy, going from 0.3 at 5×10^2 GeV to 0.05 at 5×10^7 GeV.

d) At high energies a large proportion of the incident energy goes into particles heavier than pions; in particular the Σ^0 hyperon makes a significant contribution to the electromagnetic cascade.

These hypotheses are set out in detail in the next section.

2. The Model of the High-Energy Nuclear Interaction

2.1. BASIC ASSUMPTIONS

We introduce the following assumptions in our model which is an improved version of that proposed by Fukuda *et al.* [7]):

1) The interaction cross section with an air nucleus is independent of the energy of the incident particle and also independent of the nature of the particle.

2) The number of secondary particles produced by a particle of energy † E_0 in the laboratory system (L.S.) in a nucleon-air nucleus collision is given by

$$n = 2E_0^{\frac{1}{4}}. \tag{2.1}$$

One half of them are emitted in the forward direction and the other half in the backward direction in the C.M.S. Among them $f_\pi n$ are pions and $f_X n$ are X particles ($f_\pi + f_X = 1$).

3) A fraction $\eta\varepsilon_0$ of the incident energy ε_0 in the C.M.S. is transferred to the secondary particles, $g_\pi \eta\varepsilon_0$ to pions and $g_X \eta\varepsilon_0$ to X-particles ($g_\pi + g_X = 1$). The remaining energy $(1-\eta)\,\varepsilon_0$ is carried away by the incident particle. The inelasticity of the interaction is represented by η ††. The quantities η, f_π and g_π are dependent on the incident energy, the dependencies being of the form of a step function, i.e. η is constant for $10^n < E_0 \leqq 10^{n+1}$ with $n = 1,2, \ldots$ and can be different for different n.

4) X-particles are classified according to the following properties; whether they decay or not, and if they decay, whether their decay products contribute to the soft component or to the nucleonic component or muons.

(a) $X^{(1)}$ particles. These decay into charged pions, neutral pions or muons. Their decay effect is taken into account in the diffusion equation. The numbers of decay products of an $X^{(1)}$-particle are on average ν_c charged pions, ν_n neutral pions and ν_m muons. The energy of the charged or neutral pions is one half of the parental $X^{(1)}$-particle. Some of hyperons as well as charged K-particles may belong to this category, because their decay constants are of the same order of magnitude.

b) $X^{(2)}$-particles. These contribute to the soft component. Their decay effect is neglected because of their short life times. All the decay products which initiate soft showers are assumed to be neutral pions for simplicity of the calculation. Therefore an $X^{(2)}$-particle is equivalent to a nucleon plus a neutral pion of which the energy is assumed to be $\frac{1}{8}$ of the energy of the parental $X^{(2)}$-particle. To this category Σ^0 (and perhaps K_1^0) may belong.

c) $X^{(3)}$-particles. These are the particles other than $X^{(1)}$- and $X^{(2)}$-particles. They may be nucleons, antinucleons or some hyperons. With f_{X1}, f_{X2} and f_{X3} we indicate the fractions of the numbers of $X^{(1)}$-, $X^{(2)}$- and $X^{(3)}$-particles ($f_{X1} + f_{X2} + f_{X3} = f_X$).

5) The energy distributions of secondary pions and X-particles in the

† Energy is measured in units of the nucleon rest mass energy, if not specially mentioned.

†† In much previous work only the energy going into the pion component has been considered in determining the inelasticity.

CMS are represented by power functions of energy. The maximum energy of the produced pions is limited below a certain value ε_c, which will be regarded as a parameter. It plays an important role in the present model. X-particles have no such limitation on their energies. The details are given in the next subsection.

2.2. THE ENERGY DISTRIBUTIONS OF SECONDARY PARTICLES

From the assumption (5), the energy distributions of secondary pions or X-particles in the forward (or backward) direction in the CMS are represented by

$$\frac{\mathrm{d}n_i}{\mathrm{d}\varepsilon_i} = A_i \varepsilon_i^{-1-\alpha_i} \qquad (\alpha_i \neq 1), \tag{2.2}$$

where $i = \pi$ for pions and X for X-particles. First we shall present the distribution of pions and omit the suffix i for simplicity. We require

$$\begin{aligned} \tfrac{1}{2} nf &= \int_{\varepsilon_{\min}}^{\varepsilon_{\max}} \frac{\mathrm{d}n}{\mathrm{d}\varepsilon}\,\mathrm{d}\varepsilon = \frac{A}{\alpha}\,(\varepsilon_{\min}^{-\alpha} - \varepsilon_{\max}^{-\alpha}), \\ g\eta\varepsilon_0 &= \int_{\varepsilon_{\min}}^{\varepsilon_{\max}} \varepsilon \frac{\mathrm{d}n}{\mathrm{d}\varepsilon}\,\mathrm{d}\varepsilon = \frac{A}{\alpha-1}\,(\varepsilon_{\min}^{1-\alpha} - \varepsilon_{\max}^{1-\alpha}), \end{aligned} \tag{2.3}$$

where ε_0 is the incident energy in the CMS. For given α, f, g, η and $\varepsilon_{\max}$, A and $\varepsilon_{\min}$ are determined. The energy $\varepsilon_{\max}$ is assumed to be

$$\varepsilon_{\max} = \begin{cases} g\eta\varepsilon_0 & \text{for } g\eta\varepsilon_0 \leqq \varepsilon_c, \\ \varepsilon_c & \text{for } g\eta\varepsilon_0 \geqq \varepsilon_c, \end{cases} \tag{2.4}$$

i.e. the maximum pion energy increases with increasing $g\eta\varepsilon_0$ in the region of incident energy smaller than $\varepsilon_c/g\eta$ and above ε_0 it is constant and independent of $g\eta$.

With eq. (2.3), eq. (2.2) turns out to be

$$\frac{\mathrm{d}n}{\mathrm{d}\varepsilon} = \tfrac{1}{2} nf\alpha \frac{1}{\varepsilon} \left(\frac{\varepsilon_{\max}}{\varepsilon}\right)^{\alpha} (R^{\alpha}-1)^{-1}, \tag{2.5}$$

where

$$R = \varepsilon_{\max}/\varepsilon_{\min}. \tag{2.6}$$

The transformation into the L.S. is straightforward. Under the relativistic approximation

$$\left(\frac{\mathrm{d}n}{\mathrm{d}E}\right)_l = \tfrac{1}{2} nf\alpha \frac{1}{E} \left(\frac{E_{\max}}{E}\right)^{\alpha} (R^{\alpha}-1)^{-1} \quad \text{for} \quad E_{\max} \geqq E \geqq E_1 \tag{2.7}$$

corresponds to the distribution in the forward direction and

$$\left(\frac{dn}{dE}\right)_b = \tfrac{1}{2}nf\alpha\frac{1}{E}\left(\frac{E}{E_3}\right)^{\alpha}(R^{\alpha}-1)^{-1} \quad \text{for} \quad E_2 \geqq E \geqq E_3 \tag{2.8}$$

to that in the backward direction in the CMS.
Here we used

$$E_{max} = 2\varepsilon_0\varepsilon_{max}, \qquad E_1 = 2\varepsilon_0\varepsilon_{min} = E_{max}/R, \tag{2.9}$$
$$E_2 = \varepsilon_0 m_\pi{}^2/2\varepsilon_{min} = m_\pi{}^2 RE_0/(2E_{max}), \quad E_3 = \varepsilon_0 m_\pi{}^2/2\varepsilon_{max} = m_\pi{}^2 E_0/(2E_{max}),$$

and m_π is the mass of pions in units of the nucleon rest mass.

The maximum energy of pions in the L.S. is, from eqs. (2.4) and (2.9), given by

$$E_{max} = \begin{cases} g_\pi\eta E_0 & \text{for} \quad E_c \geqq g\eta E_0, \\ (\frac{1}{2}E_0)^{\frac{1}{2}}2\varepsilon_c & \text{for} \quad E_c \leqq g\eta E_0, \end{cases} \tag{2.10}$$

where

$$E_c = 2(\varepsilon_c/g_\pi\eta)^2 \tag{2.11}$$

is the critical incident energy in the L.S. above which the maximum pion energy is limited. It is to be noted that E_{max} is proportional to $E_0{}^{\frac{1}{2}}$ independently of $g_\pi\eta$ above E_c, while to E_0 below E_c for a given $g_\pi\eta$.

A choice of ε_c greater than the primary energy concerned gives no limitation of the maximum pion energy.

In the same way, the expressions for X-particles can be derived except that E_{max} is always given by $g_X\eta\varepsilon_0$.

The detailed treatment of these assumptions and expressions in the diffusion equation of the nucleonic cascade process is given in the appendix.

2.3. SOME ARGUMENTS ON THE MODEL

In terms of the fireball model [9-11]), the limitation of the maximum pion energy corresponds to that of the Lorentz factor $\bar{\gamma}$ of the fireball in the C.M.S. Let the limited $\bar{\gamma}$ be $\bar{\gamma}_c$. Then $\varepsilon_c \approx 2\bar{\gamma}_c\varepsilon^*$, where ε^* denotes the average energy of pions in the rest system of the fireball.

The only difference between the fireball model and ours is as follows: If $\bar{\gamma}_c$ and ε^* are independent of E_0, the ratio $R = \varepsilon_{max}/\varepsilon_{min}$ in the fireball model is also independent of E_0. On the other hand, in the present model, R for a constant $g_\pi\eta$ decreases with increasing E_0 above E_c. In order to keep R independent of E_0, two alternatives may be considered. One is that for a constant $g_\pi\eta$ the multiplicity of pions increases rather rapidly above E_c and the other is that $g_\pi\eta$ has a dependence on E_0 satisfying $g_\pi\eta\varepsilon_0 = \varepsilon_c$ in eq. (2.3). The latter case is approximately treated in our model. The former case seems unlikely since, among other things, it would entail a *decrease* of the maximum pion energy with increasing primary energy.

Fig. 1 shows the relation between E_0 and E_{max} of pions given by eq. (2.10) for various values of $g_\pi\eta$ and ε_c.
Intersections of the solid and dotted lines correspond to the values of E_{max} and E_c satisfying

$$E_{max} = g_\pi\eta E_c = 2\varepsilon_c^2/g_\pi\eta. \tag{2.12}$$

The fact that there is no abrupt change in slope of the muon spectrum up to an energy of at least 10^4 suggests that the limitation of the maximum pion energy should appear at not less than $g_\pi\eta E_c \approx 10^4$, i.e.

$$\varepsilon_c \gtrsim 70\,(g_\pi\eta)^{\frac{1}{2}}. \tag{2.13}$$

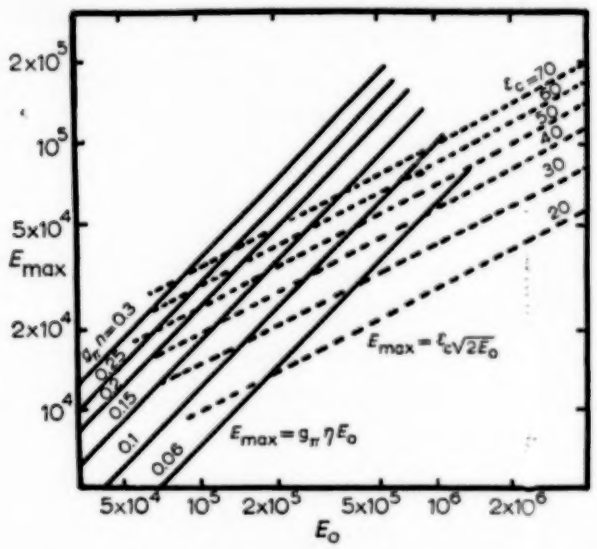

Fig. 1. The incident energy dependence of the maximum pion energy in the L.S. for various values of ε_c and $g_\pi\eta$.

On the other hand the position of the knee at about 10^3 in the γ-ray spectrum suggests intuitively $E_c \lesssim 5\times10^5$, i.e.

$$\varepsilon_c \lesssim 5\times10^2\, g_\pi\eta. \tag{2.14}$$

Thus for $g_\pi\eta \approx 0.1$, one has $20 \lesssim \varepsilon_c \lesssim 50$. This consideration limits to some extent the relation between possible values of ε_c and $g_\pi\eta$.

3. Calculated Results and Comparison with Experiments

Since our model involves a considerable number of parameters, we took the following facts into consideration: If emitted angles of produced particles in the C.M.S. are in one to one correspondence with their energies, the well established constancy of the transverse momenta [14, 18]) of pions together with the observed angular distribution gives [12, 13]) the energy distribution of the pions of the form $\varepsilon_\pi^{-n}\,d\varepsilon_\pi$ with $n \approx 2$. This form is consistent [7]) with the lateral

distribution of high-energy muons observed far underground [15]) and the fire-ball model is compatible with the form [16]). The fraction of incident energy transferred to produced pions decreases with increasing incident energy up to 10^4-10^5 (see ref. [17])).

Throughout the calculations, the integral exponent of the primary spectrum was taken as -1.7 and the integral over the primary energy was carried out from † 3×10^4 to 10^8. All primary particles were assumed to be protons. While this is almost certainly untrue, it should not make much difference to the

TABLE 1

The values of the parameters employed for both the cases A and B

Interaction mean free path	90 g/cm²
Energy distribution	$\alpha_\pi = 0.9, \quad \alpha_X = 0.9$
Limited maximum pion energy	25
Fractions of the number of secondary particles	π: 0.8 $\begin{cases}\pi^{\pm}: \frac{2}{3}\\ \pi^0: \frac{1}{3}\end{cases}$ X: 0.2 $\begin{cases}X^{(1)}: 0.20\\ X^{(2)}: 0.16\\ X^{(3)}: 0.64\end{cases}$ $\nu_e = 0.45, \quad \nu_n = 0.40, \quad \nu_m = 0.60$
Decay constants.	π: 148, $X^{(1)}$: 1100

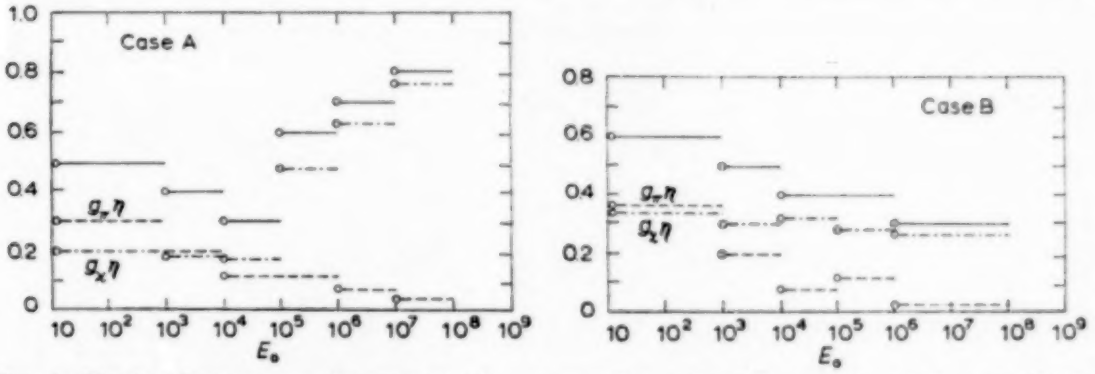

Fig. 2. The incident energy dependence of η, $g_\pi\eta$ and $g_X\eta$ for the cases A and B, respectively. The values at the points are excluded (see the assumption (3) in subsect. 2.1).

results since we are always concerned with energies per nucleon rather than total energies.

Two main cases, called A and B, have been considered. It will be seen that case A gives good agreement with the experiments. In both cases a limitation on pion energy in the C.M.S. is considered, the possibility of the transfer of energy to X-particles is allowed and the fractional energy going into the π-component is made to decrease with increasing energy. But in case A, the

† For the number spectrum the integral was carried out from 10^5 to 10^8.

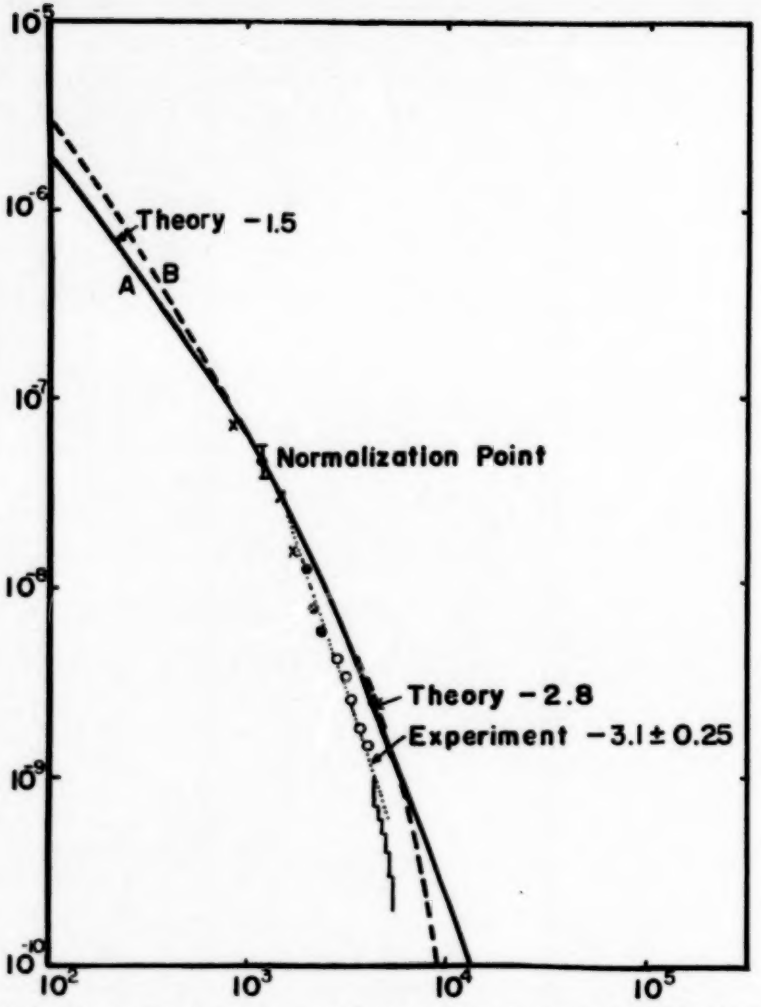

Fig. 3. The integral γ-ray spectrum at a high altitude (220 g/cm^2). The experimental points are cited from ref. [2]). The ordinate gives the absolute intensity in particles per cm^2 per sec per steradian and the abscissa gives energy in units of the proton rest mass. The slope at energies below 5×10^2 is slightly flattened by our low energy cut off in the primary spectrum.

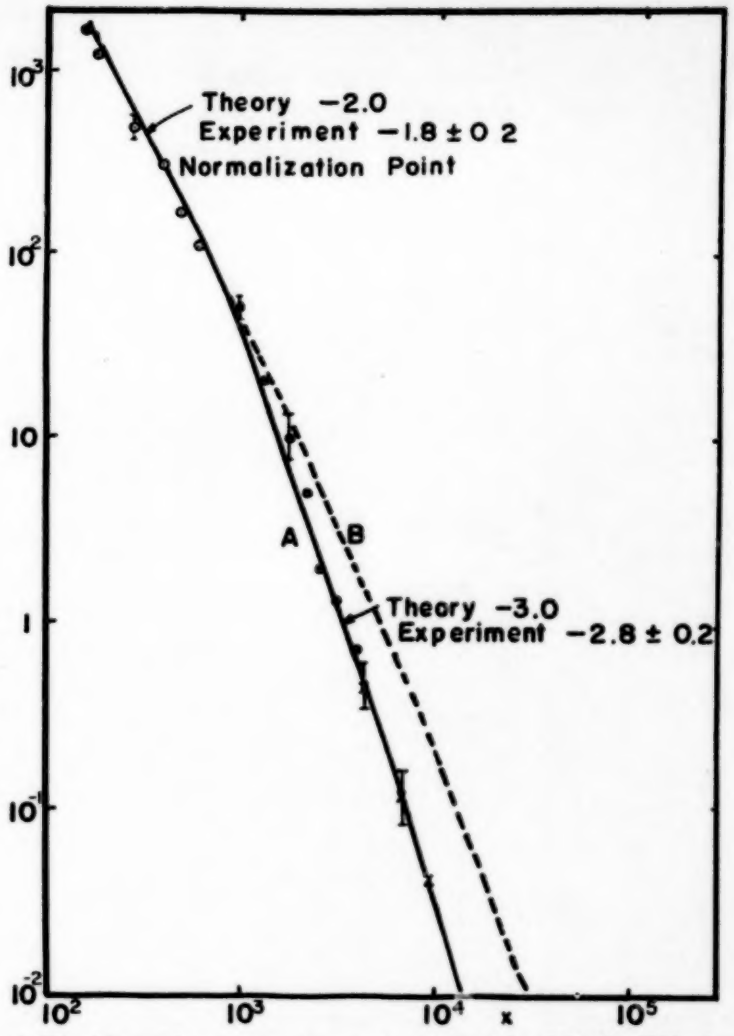

Fig. 4. The integral γ-ray spectrum at a mountain altitude (740 g/cm^2). The experimental points are cited from ref. [1]). The ordinate gives the relative intensity and the abscissa energy in units of the proton rest mass.

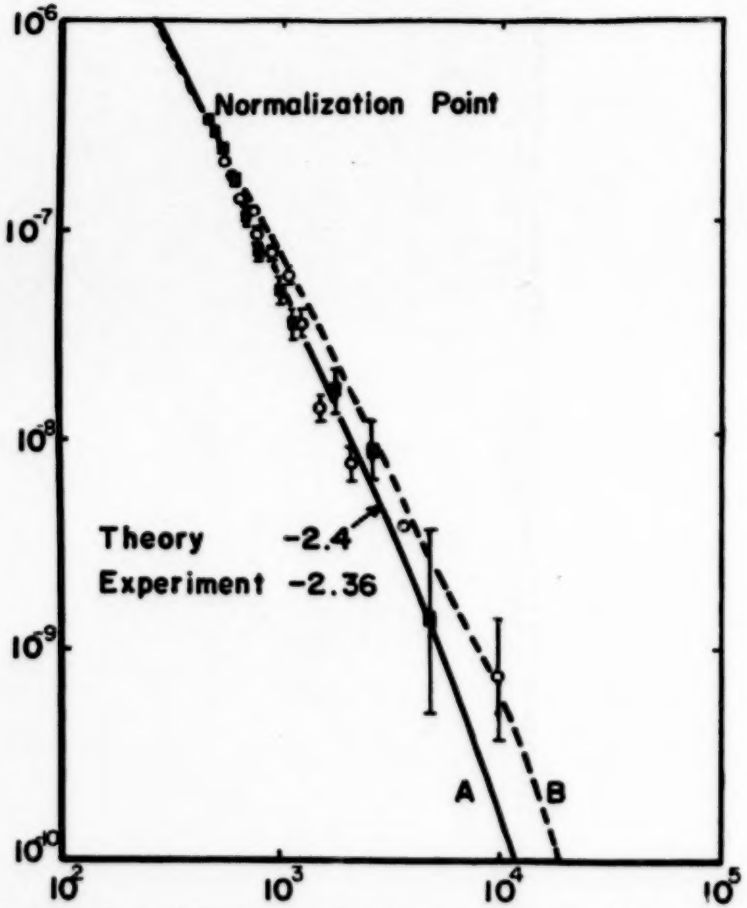

Fig. 5. The integral spectrum of high-energy muons. The experimental points are cited from the ref. [6]) and are for 1840 m.w.e. (○) and 1500 m.w.e. (●). The energies of the calculated spectrum represent those of parental particles (charged pions or $X^{(1)}$-particles) in units of the proton rest mass. The intensity is in particles per cm² per sec per sr.

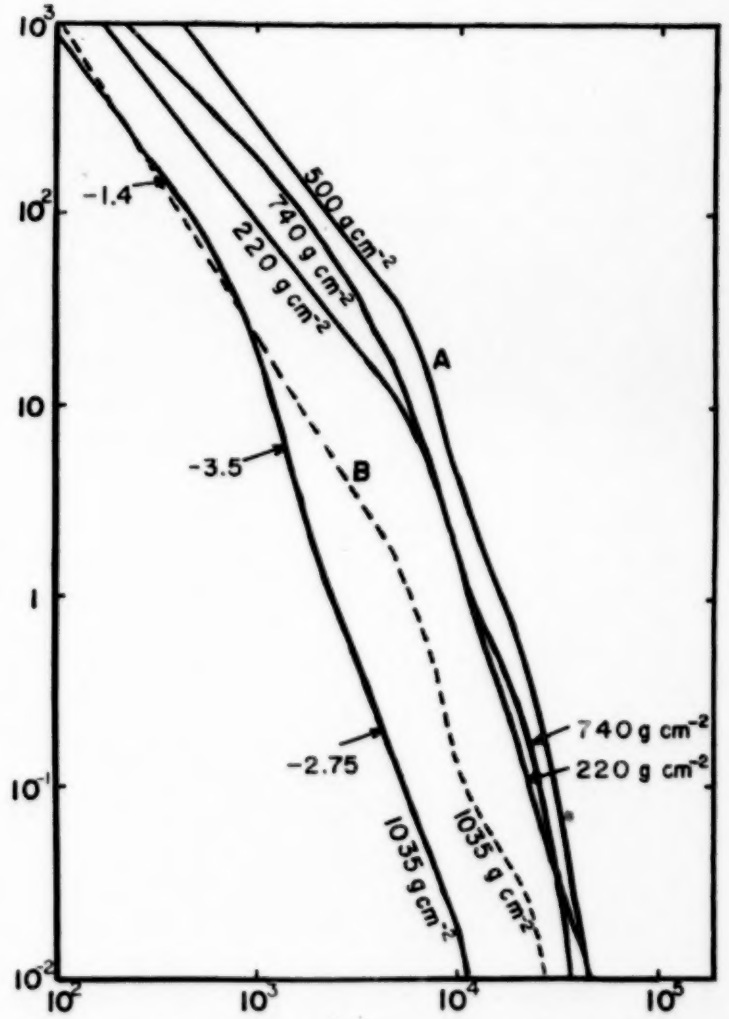

Fig. 6. The integral number of particles produced above an observation level which initiate soft showers and give rise to electrons of greater than n particles at the observation level as a function of n. The ordinates give relative numbers and the abscissa gives n.

total inelasticity is supposed to increase beyond 10^5 while in case B it is supposed to decrease. The details of the two sets of hypotheses are set forth in table 1 and fig. 2.

The results are given in figs. 3 to 7. Figs. 3 and 4 show the predicted and observed γ-ray energy spectra at 220 and 740 g/cm^2, respectively. Fig. 5 gives the μ-meson spectrum at sea level. Fig. 6, which is to be compared with the density spectrum of EAS, shows the total number of particles produced above

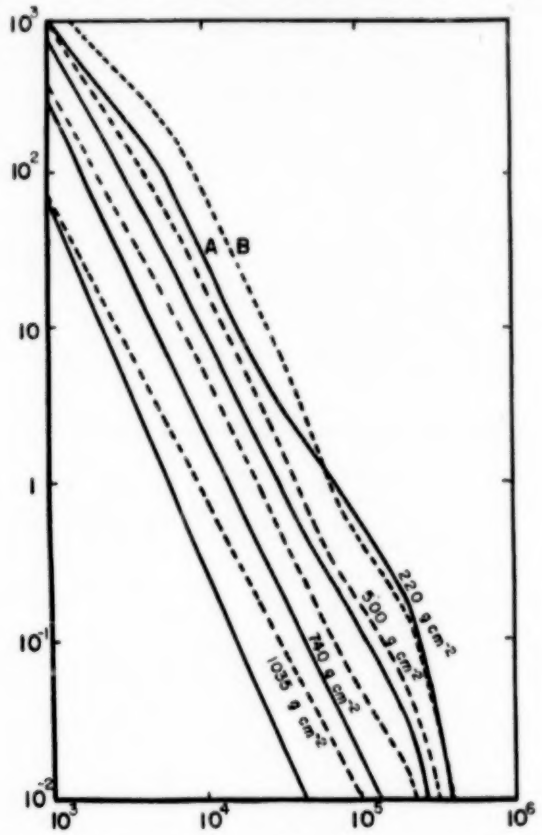

Fig. 7. The integral energy spectrum of the nucleonic component. The ordinates give relative numbers and the abscissa gives the energy in units of the proton rest mass.

a given observation level which give rise to electromagnetic showers of greater than n particles at the observation level as a function of n. This we call the number spectrum. It does not correspond exactly to the density spectrum as observed, by the Sydney group [3]), but the difference will be small providing that overlapping in the area of the cloud chambers of showers initiated by different particles can be disregarded †. Fig. 7 shows the integral nucleonic energy spectrum at 4 different atmospheric levels.

† In the very low density region a density may correspond to that far from a shower axis, where densities of showers initiated by different parental particles will be well smeared out and the overlapping will be appreciable. On the other hand, in the very high density region fluctuations in nuclear interactions during the nucleonic cascade process, from which showers are initiated, may be important and the density observed in a small area will correspond to showers initiated by individual parental particles rather than to a dense part of a *smooth* lateral distribution of an EAS as a whole. This is borne out by examination of the cloud chamber photographs.

It is now worth considering some of the chief ways in which the characteristics of our model affect the various spectra. It was found that the limitation of the maximum pion energy is essentially responsible for the change in slope of the γ-ray spectrum. A value for ε_c of 20 to 30 gives the right position of the knee. A larger value of ε_c makes the slope above the knee less steep as well as shifting the position to a higher energy. Relative slope below and above the knee depends rather essentially on the energy dependences of $g_\pi\eta$ and η in the range of incident energy above $\approx 10^4$ (see fig. 1). Since $g_\pi\eta$ decreases with increasing incident energy up to at least 10^4 to 10^5, in order to reproduce the observed sudden change in slope, it was required that $g_\pi\eta$ still decreases above 10^5. The $g_\pi\eta$ of ≈ 0.1 (see fig. 2) and ε_c of 20 to 30 correspond to the critical incident energy of about 10^5 (see fig. 1) above which the maximum pion energy is limited. The limited value of 20 to 30 is quite consistent with the analyses [9]) based on the fireball model showing that the Lorentz factor of the fireball are almost always less than 20 below $\approx 10^5$. The factor η was definitely required to increase rather suddenly above $\approx 10^5$ even if the decreasing energy dependence of $g_\pi\eta$ was satisfied. The reason is that if η is small neutral pions produced by the survival of a primary particle make the slope above the knee less steep as can be seen in figs. 3, 4 and 6. The contribution of $X^{(2)}$-particles must also be small, since their energies are not limited †.

The change in slope becomes smaller towards lower altitudes. As seen from figs. 3 and 4 the position of the knee is almost independent of altitude, quite different from the case of the number spectrum (see fig. 6). The position of the knee of this is shifted to smaller particle numbers towards lower altitudes, since electrons are produced, through more cascade processes than are high-energy γ-rays. At a higher altitude (<220 g/cm^2) the position is again shifted to smaller numbers, since showers initiated by high-energy neutral pions are not yet fully developed.

An interesting fact is that an inverse knee appears. This is more clearly seen in the spectrum of the nucleonic component as shown in fig. 7. At very high altitudes, say 220 g/cm^2, the first knee at about 6×10^3 is due to the limitation of the maximum pion energy. The second inverse knee arises from the contribution of $X^{(2)}$- and $X^{(3)}$-particles ††. Its position is of course dependent on the values of $g_X\eta$ and f_X and of their energy dependence. Towards lower altitudes both changes in slope are smeared out due to the cascade process. How much they are smeared out with increasing depth depends on how much energy is

† Note that the possibility of the contribution to the soft component from particles other than neutral pions, above incident energy greater than $\approx 10^7$ is not excluded providing the production cross section is not too large. The rapidly decreasing primary intensity makes their contribution to the spectra unimportant.

†† The falling off of the spectrum at 3×10^5 is due to the fact that the integration over the primary spectrum was carried out up to, but not beyond, 10^6 due to machine limitations.

retained by the surviving primary particle, i.e. by the inelasticity. This can be seen by comparing case A with case B in figs. 6 and 7.

Case A gives good agreement with the experiments. At 220 g/cm^2, the calculated slope of the γ-ray spectrum is slightly less steep than that observed. It is, however, to be noted that it is a general consequence of the cascade theory that the energy spectrum becomes softer with increasing thickness through which the cascade develops. In this sense the observed exponent -3.1 ± 0.25 seems little too steep as compared with -2.8 ± 0.2 at 740 g/cm^2.

As mentioned before, the number spectrum shown in fig. 6 does not exactly correspond to the observed density spectrum. However, the observed exponents of the differential spectrum, -2.6 ± 0.2 below 600 particles/m^2 and -3.9 ± 0.5 above 1100 particles/m^2 are in good agreement with those of the integral number spectrum below and above 1000 particles.

The Bristol [2]) and Russian [4]) groups have measured the spectrum of total energy released into soft components at nuclear interactions at a high altitude (220 g/cm^2) and at sea level, respectively. The former group obtained the inverse knee at about 4×10^3 GeV total energy, the exponent changing from -3.0 to -1.9. On the other hand, the latter did not obtain such a change, the slope being represented by a constant exponent of -1.9 ± 0.5 above total energy of 2×10^3 GeV.

The calculated spectrum shown in fig. 7 may explain both the results consistently. If nuclear active particles having such a spectrum transfer 10 to 20 % of their energies into soft components at nuclear interactions, an expected spectrum of the same kind as the observed ones may be obtained by shifting the spectrum in fig. 7 to the left by a factor of $\frac{1}{10}$ to $\frac{1}{5}$. Then the obtained spectrum has the change in slope at higher altitudes and no change at sea level, though the expected slope at higher altitudes is again less steep than the observed one. It is worth emphasizing again that this feature has been realized by the contribution of X-particles, especially X$^{(3)}$-particles.

The energy spectrum of high energy muons has been measured directly by the Durham group [21]) to 3×10^{12} eV and inferred by the Cornell group [5]) to 10^{13} eV.

The former group with a cosmic ray spectrograph obtained the differential exponent of the spectrum -3.2 over the range 10^{11} to 10^{12} eV and the latter the integral exponent -2.36 over the range 10^{12} to 10^{13} eV by changing the thickness of absorber. As argued above the calculated spectrum does not show any sudden change in slope, though of course a gradual change is expected. Our integral exponent is -2.4 between 10^{12} and 10^{13} eV, in good agreement with these experiments.

Poor agreement in the case B can be seen especially in figs. 4 and 6, in spite of the smaller values of $g_\pi\eta$ at higher energies ($>10^6$) than in the case A. The essential fact responsible for the discrepancy is the small inelasticity at the

higher energies. Finally it should be noted that case A gives a nearly constant attenuation length of shower curves near seale vel over a wide range of primary energies. The values are given in table 2.

TABLE 2

The attenuation lengths of shower curves near sea level. A slight irregularity in the values seems due to the discrete energy dependences of η, g_π and g_x (see fig. 2)

Prim. energy	Attenuation length (g/cm^2)	
	Case A	Case B
10^5	241	200
3×10^5	194	188
10^6	189	222
10^7	195	296
10^8	202	290

4. Summary and Discussion

Summarizing the results described in the preceding section, we obtain the following features of the nuclear interactions at high energies:

1) Up to $\approx 10^{14}$eV, the inelasticity as well as the fractional energy transferred to pions decreases with increasing incident energy.

2) The fraction of incident energy transferred to pions is $\approx 10\%$ around 10^{14} eV.

3) Above 10^{14} eV the limitation of the maximum pion energy is effective, the limited values being 20 to 30 GeV in the C.M.S.

4) At the same time the inelasticity increases rather abruptly and the most of the interaction energy above 10^{14} is carried away, not by a single particle, but by a few or several nuclear active particles of the nucleon family. This feature may be correlated with the limitation of the maximum pion energy.

5) The fraction of incident energy transferred to pions continues to decrease with increasing incident energy above 10^{14} eV. The remaining energy will be more and more transferred to X-particles.

From these features the nuclear interaction above 10^{14} eV should be pictured not only as the production of *pion* fireballs but also of nucleon *isobars* from which X-particles decay.

As we have seen, this picture enables us to predict many details of the various spectra observed in air showers and emulsion experiments. It, therefore, seems likely that the gross features of our model are correct. It is also almost certain that in some of the details this model is incorrect. For instance we have assumed that all the primary particles are protons; present evidence suggests very strongly that this is not so and that, in fact, the majority of primaries with a total enegy greater than 10^{15} eV are heavier particles. We have also assumed

that the interaction cross section of high-energy pions is geometric; recent experiments suggest that it is considerably less. There is thus room for considerable improvement in this model and also for extension to other aspects of air shower work. This is in progress and will be treated in a separate paper.

As it stands, the model suggests a number of experiments. In effect these experiments are all aimed at an increase in our understanding of the structure of the nucleon and of nuclear forces.

Firstly, a study of the γ-ray spectrum and of the density spectrum at different altitudes is necessary in order to determine the position of the first knee and the value of the slope on both sides of the knee with greater accuracy. This will enable us to fix the slope and position of the pion cut off energy in the CMS. Secondly, the density spectrum of EAS and the nuclear spectrum at various altitudes, when accurately known, should enable us to determine the production cross section for the various types of X particles at energies in excess of 10^{14} eV. Finally, when once the main characteristics of nuclear interactions at these high energies are known it will be possible to attack the problem of the charge spectrum of the high energy primaries, and the energy spectra of the various components with some hope of success.

The authors would like to express their sincere thanks to Professor H. Messel for the excellent facilities provided and to Dr. D. D. Millar and Dr. K. Nishikawa for valuable discussions. The authors are much indebted to the staff of the Basser Computing Laboratory for their help in carrying out the calculations on the electronic computer SILLIAC.

Appendix

METHOD OF CALCULATION

The diffusion equation of the nucleonic cascade process is solved by the generation method of which details are given elsewhere [19, 20]. We shall therefore present only a part of details related with the present model.

Depth is measured in units of the interaction mean free path.

According to the assumptions given in sect. 2, we denote $N_l(E)$ the differential energy spectrum of nucleons including $X^{(2)}$- and $X^{(3)}$-particles, $\pi_l(E)$ that of charged pions and $K_l(E)$ that of $X^{-(1)}$particles belonging to the l-th generation, respectively.

The recurrence formulae [20] for each generation in the case that the nucleonic cascade is initiated at a given depth, are given by

$$N_l(E) = \int \{S_{NN}(E, E')N_{l-1}(E') + S_{N\pi}(E, E')\pi_{l-1}(E') + S_{NK}(E, E')K_{l-1}(E')\}dE', \quad (A.1)$$

$$\pi_l(E) = \frac{(l-1)E}{(l-1)E+B_\pi}\left[\int\{S_{\pi N}(E, E')N_{l-1}(E')+S_{\pi\pi}(E, E')\pi_{l-1}(E') + S_{\pi K}(E, E')K_{l-1}(E')\}dE' + \int \frac{B_K}{(l-1)E'} D_c(E, E')K_l(E')dE'\right], \quad (A.2)$$

$$K_l(E) = \frac{(l-1)E}{(l-1)E+B_K}\left[\int\{S_{KN}(E, E')N_{l-1}(E') + S_{K\pi}(E, E')\pi_{l-1}(E')+S_{KK}(E, E')K_{l-1}(E')\}dE'\right]. \quad (A.3)$$

The initial conditions are:

$$N_1(E) = S_{NN}(E, E_p), \quad \pi_1(E) = S_{\pi N}(E, E_p), \quad K_1(E) = S_{KN}(E, E_p). \quad (A.4)$$

where E_p is an energy of a primary proton. The quantity $S_{\pi N}(E, E')$ is the production spectrum of charged pions produced by a nucleon (or an $X^{(2)}$- or $X^{(3)}$-particle) of energy E' and so on. They are represented, with the help of eqs. (2.7) and (2.8), by

$$\begin{aligned}
S_{NN}(E, E') &= \delta(E-(1-\eta)E')+(f_{X2}+f_{X3})\left[\left(\frac{dn}{dE}\right)_f+\left(\frac{dn}{dE}\right)_b\right]_X,\\
S_{N\pi}(E, E') &= S_{NK}(E, E') = (f_{X2}+f_{X3})\left[\left(\frac{dn}{dE}\right)_f+\left(\frac{dn}{dE}\right)_b\right]_X,\\
S_{\pi\pi}(E, E') &= \delta(E-(1-\eta)E')+\Delta f_\pi\left[\left(\frac{dn}{dE}\right)_f+\left(\frac{dn}{dE}\right)_b\right]_\pi,\\
S_{\pi N}(E, E') &= S_{\pi K}(E, E') = \Delta f_\pi\left[\left(\frac{dn}{dE}\right)_f+\left(\frac{dn}{dE}\right)_b\right]_\pi,\\
S_{KK}(E, E') &= \delta(E-(1-\eta)E')+f_{X1}\left[\left(\frac{dn}{dE}\right)_f+\left(\frac{dn}{dE}\right)_b\right]_X,\\
S_{KN}(E, E') &= S_{K\pi}(E, E') = f_{X1}\left[\left(\frac{dn}{dE}\right)_f+\left(\frac{dn}{dE}\right)_b\right]_X.
\end{aligned} \quad (A.5)$$

The subscripts f and b in the terms in the square brackets represent the forward and backward directions, and X and π represent X-particles and pions, respectively. Δ is the fraction of charged pions among all pions. The other quantities are defined in the text.

The last term in the right hand side of eq. (A.2) represents the contribution from $X^{(1)}$-particle decay and $D_c(E, E')$ is the energy spectrum of the produced charged pions which is assumed to be

$$D_c(E, E') = \nu_c\,\delta(E-\tfrac{1}{2}E').$$

The energy spectrum of neutral pions of the l-th generation at depth x measured from the depth at which the nucleonic cascade is initiated, is given by

$$\pi_l^0(E,x) = (1-\Delta)\int\{S_{\pi N}N_{l-1}+S_{\pi\pi}\pi_{l-1}+S_{\pi K}K_{l-1}\}\mathrm{d}E'\frac{\mathrm{e}^{-x}x^{l-2}}{(l-2)!}$$
$$+\int\frac{B_K}{lE'}D_{\pi^0}(E,E')K_l(E')\mathrm{d}E'\frac{\mathrm{e}^{-x}x^{l-1}}{(l-1)!} \qquad \text{(A.6)}$$
$$+\int D'_{\pi^0}(E,E')N_l^{(2)}(E')\mathrm{d}E'\frac{\mathrm{e}^{-x}x^{l-1}}{(l-1)!}.$$

The first term in the right hand side represents neutral pions produced directly at the l-th interactions, and the second and third terms those resulting from $X^{(1)}$- and $X^{(2)}$-particle decay. The decay energy spectra are assumed to be

$$D_{\pi^0}(E,E') = \nu_n\delta(E-\tfrac{1}{2}E'),$$
$$D'_{\pi^0}(E,E') = \delta(E-\tfrac{1}{8}E'). \qquad \text{(A.7)}$$

Note that all $X^{(2)}$-particles were assumed to decay into neutral pions.

The energy spectrum of muons resulting from decay of charged pions and $X^{(1)}$-particles of the l-th generation is given by

$$\mu_l(E_\mu,x) = \left(\Delta\frac{B_\pi}{E}\pi_l(E)+\nu_m\frac{B_K}{E}K_l(E)\right)\mathrm{d}E\int_0^x\frac{\mathrm{d}y}{y}\frac{\mathrm{e}^{-y}y^{l-1}}{(l-1)!}. \qquad \text{(A.8)}$$

References

1) Y. Fujimoto, S. Hasegawa, M. Kazuno, J. Nishimura, K. Niu and N. Ogita, Proc. Moscow Conf. **1** (1960) 41
2) J. Duthie, C. M. Fisher, P. H. Fowler, A. Kaddoura, D. H. Perkins and K. Pinkau, Proc. Moscow Conf. **1** (1960) 30
3) R. J. Reid, K. Gopaulsingh, D. E. Page, M. Idnurm, C. B. A. McCusker, J. Malos, D. D. Millar and G. Winterton, Proc. Phys. Soc. (in press)
4) N. L. Grigorov, N. A. Kondratiev, A. I. Savel'eva, V. A. Sobinyakov, A. V. Podgurskaya and V. Ya. Shestoperov, Proc. Moscow Conf. **1** (1960) 130
5) J. Pine, R. J. Davisson and K. Greisen, Proc. Moscow Conf. **1** (1960) 295
6) S. Hayakawa and N. Ogita, Proc. Moscow Conf. **2** (1960) 220
7) H. Fukuda, N. Ogita and A. Ueda, Prog. Theor. Phys. **21** (1959) 29
8) F. C. Roesler and C. B. A. McCusker, Nuovo Cim. **10** (1953) 127
9) K. Niu, Nuovo Cim. **10** (1958) 10
10) G. Cocconi, Phys. Rev. **111** (1958) 1698
11) P. Ciok, T. Coghen, J. Gierula, R. Holynski, A. Jurak, M. Miesowicz, T. Saniewska and J. Pernegr, Nuovo Cim. **10** (1958) 741
12) S. Hasegawa, J. Nishimua and Y. Nishimura, Nuovo Cim, **6** (1957) 979
13) B. Edwards, J. Losty, D. H. Perkins, K. Pinkau and J. Reynolds, Phil. Mag. **3** (1958) 237
14) O. Minakawa, Y. Nishimura, M. Tsuzuki, H. Yamanouchi, H. Aizu, H. Hasegawa, Y. Ishii, S. Tokunaga, Y. Fujimoto, S. Hasegawa, J. Nishimura, K. Niu, K. Nishikawa, K. Imaeda and M. Kazuno, Nuovo Cim. Supp. **11** (1959) 112

15) P. H. Barrett, L. M. Bollinger, G. Cocconi, Y. Eisberg and K. Greisen, Rev. Mod. Phsy. **24** (1952) 133
16) K. Niu, Proc. Moscow Conf. **1** (1960) 234
17) C. F. Powell, P. H. Fowler and D. H. Perkins, The study of elementary particles by the photographic method (Pergamon Press, Oxford) p. 551
18) F. A. Brisbout, C. Gauld, J. Lehane, C. B. A. McCusker, J. Malos, K. Nishikawa and L. G. Van Loon, to be published
19) A. Ueda and N. Ogita, Prog. Theor. Phys. **18** (1957) 269
20) A. Ueda, Prog. Theor. Phys. **24** (1960)
21) F. Ashton, G. Brooke, M. Gardener, P. J. Hayman, D. G. Jones, S. Kisdasamy, L. J. Lloyd, F. E. Taylor, R. H. West and A. W. Wolfendale Nature **185** (1960) 364

8.B

Nuclear Physics **26** (1961) 52—56; © *North-Holland Publishing Co., Amsterdam*

Not to be reproduced by photoprint or microfilm without written permission from the publisher

ON AN ISOBARIC SPIN SCHEME FOR LEPTONS AND THE LEPTONIC DECAYS OF STRANGE PARTICLES

ALLADI RAMAKRISHNAN, A. P. BALACHANDRAN †, N. R. RANGANATHAN ††

University of Madras, Madras, India

and

N. G. DESHPANDE

27 Luz, Mylapore, Madras

Received 7 February 1961

Abstract: An isobaric spin scheme for leptons is discussed using the concept of missing components. A phenomenological set of rules is also suggested to explain the low rates of most of the $|\Delta S| = 1$ decays.

1. Introduction

We wish to consider here an isobaric spin scheme for leptons in which μ^- and e^- are one of the components of isobaric doublets μ and e whose other components are missing and ν is an isosinglet. The consequences of these assumptions are discussed and it is found that the scheme is able to explain many of the features of leptonic interactions in a qualitative way ††.

2. The Isobaric Spin Scheme for Leptons

It is well-known that there is a difficulty in introducing an isobaric spin scheme for the muon and electron in a way analogous to that of baryons and mesons since we find that in nature the neutral counterparts of μ^- and e^- do not exist. At one stage, there were a number of attempts to develop an isobaric spin scheme for these particles by postulating, for instance, the existence of a μ^0 and/or by joining ν and a charged lepton into a doublet [1]). The most natural way of interpreting these particles in the isobaric spin space would, however, be to assume that μ^- and e^- are components of isodoublets μ and e whose neutral counterparts do not exist. This seems plausible since an analogous situation has already arisen for the neutrino field where it is found that only the left-helicity state of ν is realized in nature. As a consequence, we have the γ_5-invariance of the neutrino field,

$$\nu = \gamma_5 \nu. \tag{1}$$

Since the formalism of isobaric spin has been developed in analogy with ordi-

† Atomic Energy Commission Senior Research Fellows.

†† A preliminary version of the ideas presented here is published as an appendix of a paper by Ramakrishnan, *et al.* [8]).

nary spin, we may assume that only the $I_z = -\frac{1}{2}$ state is realized for μ and e. This is equivalent to the imposition of the $-\tau_3$ invariance on μ and e (which is the analogue of the γ_5-invariance of ν),

$$\mu = -\tau_3 \mu, \qquad \mathrm{e} = -\tau_3 e, \tag{2}$$

so that μ and e are of the form

$$\mu = \begin{bmatrix} 0 \\ \mu^- \end{bmatrix}, \qquad \mathrm{e} = \begin{bmatrix} 0 \\ \mathrm{e}^- \end{bmatrix}. \tag{3}$$

It is a well-known consequence of equation (1) that parity is not conserved in all interactions involving the neutrino. The analogue of this for equation (2) would be that interactions involving μ or e necessarily do not conserve isobaric spin.

It may be noticed that we have assumed here that ab initio μ and e are particles with different masses and are not attempting the problem of the μ-e mass difference.

In this scheme, we may take ν and A_μ as isosinglets. It may be noted that as for baryons and mesons, if we assume a relation of the form $Q = I_z + \frac{1}{2}(l+s)$, where l is the lepton number, we may assign $l = +1$ to μ^-, e^- and ν, and $S = -2$ to μ^-, e^- and -1 to ν. For A_μ, of course, we have $I_z = l = S = 0$.

3. Strong Interactions

It will now be shown that with the isobaric spin assignments given above, it is possible to forbid the strong interactions of leptons. This is a consequence of the following assumptions about strong interactions:

a) Strong interactions must conserve the total isobaric spin. It is immediately clear that μ^- and e^- can then have no strong interaction since no isobaric scalar can be formed involving μ or e, as remarked earlier.

b) Strong interactions must conserve parity. Hence, ν also can have no strong interaction since it always occurs in the combination $\frac{1}{2}(1+\gamma_5)\nu$.

In electromagnetic interactions, the combination $\bar{\mu}^- \mu^-$ or $\bar{\mathrm{e}}^- \mathrm{e}^-$ occurs which transforms like a scalar plus the third component of a vector, which is the correct transformation of these interactions in the isobaric spin space for isospinors. The electromagnetic interactions of neutrinos can then be forbidden by assuming, for instance, that these interactions *must* transform as a scalar plus the third component of a vector or as the third component of a vector.

It is interesting to note that only the leptons seem to possess invariance under transformations which eliminate one of their components (γ_5 invariance of ν or $-\tau_3$ invariance of μ and e), while for baryons, such invariances seem to be a property only of some of their interactions and not of the fields themselves.

4. Weak Interactions

Present evidence in weak interactions seems to rule out the existence of neutral lepton currents [2]). We therefore assume that the only leptonic currents relevant for weak interactions are $(\bar{\mu}\,\nu)$ and $(\bar{e}\,\nu)$. These transform as one of the components of an isospinor. We now assume that weak interactions in which baryons are involved obey the rule $|\Delta I| = \frac{1}{2}$ or $\frac{3}{2}$, while weak interactions involving only leptons obey $|\Delta I| = 0$ or 1. Strangeness-changing baryonic currents satisfying $|\Delta s| = 1$ necessarily transform as isospinors corresponding to $I = \frac{1}{2}$ or $\frac{3}{2}$. Therefore an interaction of the form $J_\alpha^{\mathrm{SNC}\,\dagger}\, J_\alpha^{\,l}$ with $|\Delta S| = 1$ will not obey the selection rule $|\Delta I| = \frac{1}{2}$ or $\frac{3}{2}$ and is consequently forbidden. Experimentally, apart from the $\mathrm{K} \to \mu+\nu$ decay, all such decays have low rates. The $\mathrm{K} \to \mu+\nu$ decay is hard to explain. Also in this scheme, if $|\Delta S| = 2$ currents are allowed, we may have decays like $\Xi^- \to \mathrm{n}+\mathrm{e}^-+\bar{\nu}$. The $\mathrm{K_1^0}-\mathrm{K_2^0}$ mass difference however seems to speak against the existence of such currents [3]).

We wish now to suggest an alternative set of phenomenological rules for the $|\Delta S| = 1$ leptonic decays which will allow the $\mathrm{K} \to \mu+\nu$ decay while reducing most of the other strange particle $|\Delta S| = 1$ leptonic decays by at least an order of magnitude. We assume that all the isobaric spin amplitudes are allowed in the final state. However these amplitudes are taken to satisfy the following relations:

$$\alpha_0 \approx \alpha_{\frac{1}{2}} \approx \alpha_1 \approx \alpha_{\frac{3}{2}} \tag{4}$$

up to a sign (α_0, $\alpha_{\frac{1}{2}}$, α_1 and $\alpha_{\frac{3}{2}}$ denote the $I = 0$, $\frac{1}{2}$, 1 and $\frac{3}{2}$ amplitudes). It is now assumed that α_0 and α_1 as well as $\alpha_{\frac{1}{2}}$ and $\alpha_{\frac{3}{2}}$ always interfere destructively. It follows that the decays

$$\Lambda^0 \to \mathrm{p}+\mathrm{L}^-+\bar{\nu}, \qquad \Sigma^+ \to \mathrm{n}+\mathrm{L}^++\nu \tag{5}$$

(where L denotes μ or e) are forbidden, while the decays

$$\begin{aligned}
&\mathrm{K}^+ \to \pi^0+\mathrm{L}^++\nu, && \\
&\mathrm{K}^- \to \pi^0+\mathrm{L}^-+\bar{\nu}, && \Xi^- \to \Sigma^0+\mathrm{L}^-+\bar{\nu}, \\
&\mathrm{K_1^0} \to \pi^++\mathrm{L}^-+\bar{\nu}, && \Xi^0 \to \Sigma^++\mathrm{L}^-+\bar{\nu}, \\
&\mathrm{K_1^0} \to \pi^-+\mathrm{L}^++\nu, && \Xi^0 \to \Sigma^-+\mathrm{L}^++\nu \\
&\mathrm{K_2^0} \to \pi^++\mathrm{L}^-+\bar{\nu}, && \\
&\mathrm{K_2^0} \to \pi^-+\mathrm{L}^++\nu, &&
\end{aligned} \tag{6}$$

are reduced to about $\frac{1}{18}$ of the universal rate if the amplitudes α_i are taken to be of the same order of magnitude as the expected universal decay amplitudes. However, the decays

$$\begin{aligned}
&\mathrm{K}^+ \to \mathrm{L}^++\nu, && \Sigma^- \to \mathrm{n}+\mathrm{L}^-+\bar{\nu}, \\
&\mathrm{K}^- \to \mathrm{L}^-+\bar{\nu}, && \Xi^- \to \Lambda^0+\mathrm{L}^-+\bar{\nu}
\end{aligned} \tag{7}$$

should then have universal rates. Experimentally the $K \to L+\nu$ decay is known to be about as fast as the $\pi \to L+\nu$ decay.

Alternatively we may assume

$$\alpha_0 \approx \alpha_{\frac{1}{2}}, \quad \alpha_1 \approx \tfrac{7}{12}\,\alpha_0, \quad \alpha_{\frac{3}{2}} \approx \tfrac{7}{12}\,\alpha_{\frac{1}{2}}, \tag{8}$$

with destructive interference between α_0 and α_1 as well as between $\alpha_{\frac{1}{2}}$ and $\alpha_{\frac{3}{2}}$. We then find that

$$\begin{aligned} &K^+ \to \pi^0+L^++\nu, \\ &K^- \to \pi^0+L^-+\bar{\nu}, \end{aligned} \qquad \Xi^- \to \Sigma^0+L^-+\bar{\nu} \tag{9}$$

are about $\frac{1}{100}$ times the universal rate. Experimentally, $K^+ \to \pi^0+L^++\nu$ and $K^- \to \pi^0+L^-+\bar{\nu}$ are about 170 times smaller than the universal rate. We also find that the decays

$$\Lambda^0 \to p+L^-+\bar{\nu}, \qquad \Sigma^+ \to n+L^++\nu \tag{10}$$

should be about $\frac{1}{12}$ of the universal rate, while the decays

$$\begin{aligned} &K_1^0 \to \pi^-+L^++\nu, \\ &K_1^0 \to \pi^++L^-+\bar{\nu}, \qquad &&\Xi^0 \to \Sigma^++L^-+\bar{\nu}, \\ &K_2^0 \to \pi^-+L^++\nu, \qquad &&\Xi^0 \to \Sigma^-+L^++\nu \\ &K_2^0 \to \pi^++L^-+\bar{\nu}, \end{aligned} \tag{11}$$

should be about $\frac{1}{4}$ of the universal rate. Experimentally the $|\Delta S| = 1$ leptonic decays of hyperons seem to be an order of magnitude smaller than the universal rate [4]). The decays given by eq. (7) should again be fast.

In this discussion, we have not assumed the $\Delta Q/\Delta S = 1$ rule [5]). Also if $|\Delta S| = 2$ decays are allowed, $\Xi^- \to n+L^-+\bar{\nu}$ should be fast and $\Xi^0 \to p+L^-+\bar{\nu}$ should be about $\frac{1}{12}$ of the universal rate. However, as remarked earlier, the $K_1^0-K_2^0$ mass difference seems to speak against the existence of such currents[3]).

5. Further Possible Extensions

Once we have postulated the existence of doublets with missing components in the isobaric spin space, the idea can be extended to the three-dimensional space whose z-component is given by $U_z = \frac{1}{2}(N+S)$. Such an extension yields a classification of elementary particles which is a modification of the Salam-Polkinghorne scheme [6]). The demand that weak interactions form scalars in the M-space of d'Espagnat, Prentki and Salam [6]), then leads to definite predictions in weak decays. A theory of intermediate vector bosons with charged components only mediating weak decays involving leptons as well as the above theory of weak interactions will be discussed in subsequent papers.

We are grateful to Professor A. Pais and Dr. I. Saavedra for their critical comments. We also wish to thank Mr. K. Venkatesan for the benefit of helptful discussions. Two of us (A.P.B. and N.R.R.) are grateful to the Atomic Energy Commission for providing them with Fellowships.

References

1) R. E. Marshak and E. C. G. Sudharshan, University of Rochester, preprint (1957)
2) T. D. Lee and C. N. Yang, Institute for Advanced Study, Princeton, preprint (1960)
3) L. B. Okun' and B. M. Pontecorvo JETP **34** (1958) 763
4) D. A. Glaser, Intern. Conf. on High Energy Physics, Kiev (1960)
5) R. P. Feynman and M. Gell-Mann, Phys. Rev. **109** (1958) 193
6) A. Salam and J. C. Polkinghorne, Nuovo Cim. **2** (1955) 685
   J. C. Polkinghorne, Nuovo Cim. **6** (1957) 864
7) B. d'Espagnat, J. Prentki and A. Salam, Nuclear Physics **5** (1958) 447
8) Ramakrishnan, Balachandran and Ranganathan, Proc. Ind. Acad. Sc. **53** (1961) 1

8.B

Nuclear Physics **26** (1961) 57—67; © *North-Holland Publishing Co., Amsterdam*

Not to be reproduced by photoprint or microfilm without written permission from the publisher

ENERGY LEVEL SHIFTS IN ATOMIC STATES OF STRONGLY-INTERACTING PARTICLES

T. L. TRUEMAN †

Enrico Fermi Institute for Nuclear Studies and Department of Physics, University of Chicago, Chicago, Illinois ††

Received 16 February 1961

Abstract: The energy-level displacements for atomic states of two oppositely-charged nuclear particles due to their strong interactions are related to the parameters of the effective range approximation for the low-energy scattering of these two particles. For s- and p-states, the level shift and width are obtained to third order in A/B (scattering length A divided by Bohr radius B). The results are illustrated by a brief discussion of the level shifts and lifetimes of the K^-—p and K^-—d systems.

1. Introduction

The problem of relating the energy level shifts in π-mesonic atoms to π—N scattering data has been discussed by several authors. Deser *et al.* [1]), using rather general assumptions about the form of the nuclear interaction, have shown that the shift ΔE_n of the s-state energy levels is given by

$$\frac{\Delta E_n}{E_n} = -\frac{4}{n}\frac{A_0}{B}, \tag{1.1}$$

where E_n denotes the energy of the Coulomb bound state (principal quantum number n), neglecting the nuclear interaction of the pion; B denotes the Bohr radius of the mesonic atom and A_0 denotes the scattering length defined in the absence of the Coulomb field. Bethe and de Hoffmann [2]) have obtained the same result by treating the nuclear interaction in first Born approximation. Byers [3]) has discussed the relation between bound state energies and the low energy scattering data, using a boundary condition method similar to that employed by Landau and Smorodinsky [4]) in their discussion of the non-existence of a bound two-proton system. In the approximation in which the nuclear scattering length A (defined in the presence of a Coulomb field; cf. eqs. (3.4b) and (5.1) below) can be replaced by A_0, Byers' result for s-states agrees with eq. (1.1).

Although these authors give arguments which justify the use of eq. (1.1) for π-mesonic atoms, their calculations do not make clear how accurate an approx-

† National Science Foundation pre-doctoral fellow.

†† This work was supported in part by the U. S. Atomic Energy Commission.

imation this result would be for the K^-—p atom, for example. In this paper, we obtain a quantitative criterion for the validity of eq. (1.1) as well as higher order correction terms.

The present calculations are based on the effective range approximation in the complex k (wave number) plane. In sects. 3 and 4, expressions for the energy level shifts for s- and p-states are obtained as expansions in the dimensionless parameter A/B. The Coulomb interaction is taken fully into account in the definition of A. Since A is, in general, a complex number, these results give both the change in binding energy and the decay rate of the bound state due to nuclear absorption processes. In sect. 5 a brief discussion is given of the relation of these results to those of Byers and of Deser *et al.* For the purpose of illustration, a brief discussion of the K^-—p and K^-—d atoms is given in sect. 6.

2. General Relations

The nuclear interaction is assumed to be short-ranged; only low-energy processes are considered. It is convenient for the discussion to introduce a radius R such that if r, the distance between the two particles, is greater than R, the nuclear interaction may be neglected; however, the precise value of R plays no role in our calculations. Then for $r > R$, the Schrödinger equation with an attractive Coulomb potential describes the dynamics of the system. The radial solution of this Schrödinger equation may be written as

$$\Psi(r) = \Psi_{\text{in}}(r)+S(k)\Psi_{\text{out}}(r); \tag{2.1}$$

$\Psi_{\text{in}}(r)$ and $\Psi_{\text{out}}(r)$ denote the ingoing and outgoing Coulomb wave functions, respectively. For large r and for $\operatorname{Im} k > 0$, these wave functions have the asymptotic form

$$\begin{aligned} \Psi_{\text{in}}(r) &\sim \frac{1}{kr}\, e^{-i\left[kr+\frac{1}{kB}\ln 2kr+X_l\right]}, \\ \Psi_{\text{out}}(r) &\sim \frac{1}{kr}\, e^{i\left[kr+\frac{1}{kB}\ln 2kr+X_l\right]}; \end{aligned} \tag{2.2}$$

X_l denotes the Coulomb phase shift for orbital angular momentum l and is defined by

$$e^{2iX_l} = \frac{\Gamma(1+l-i/kB)}{\Gamma(1+l+i/kB)}. \tag{2.3}$$

The wave functions of bound states of this system must be proportional to $\Psi_{\text{out}}(r)$; this is a consequence of eq. (2.2) and the requirement that bound state wave functions vanish as r becomes infinite. Thus, in order for a bound state to

exist at a point k in the upper half plane, it is necessary that $S(k)$ have a pole at that point †.

These bound states may be divided into essentially the following two classes:

(a) The nuclear bound states, whose existence is determined by the nature of the nuclear interaction. The location of these will be slightly affected by the Coulomb field (which is not essential for their existence); to a good first approximation, they can be treated in the usual way, by neglecting the Coulomb field. These bound states will not be discussed further here.

(b) The Coulomb bound states; i.e. those states which reduce to hydrogen-like states when the nuclear interaction goes to zero. It is these states with which we are concerned here. The effective range theory is an extremely good approximation in the energy range which includes the binding energies of these states. Thus, the effective range approximation provides a well justified way of determining the relevant poles of $S(k)$.

We start from the radial Schrödinger equation in the form

$$\frac{\mathrm{d}^2\Psi}{\mathrm{d}r^2}+\frac{2}{r}\frac{\mathrm{d}\Psi}{\mathrm{d}r}+\frac{2\mu}{\hbar^2}\left(E+\frac{e^2}{r}-\frac{\hbar^2 l(l+1)}{2\mu r^2}\right)\Psi=0; \tag{2.4}$$

μ denotes the reduced mass of the system. Two independent solutions [5]) of this equation are

$$F_l(r)=\frac{C_l(\eta)\mathrm{e}^{-\frac{1}{2}\pi i l}}{\Gamma(2l+2)}\,(2ikr)^l\mathrm{e}^{-ikr}F(l+1+i\eta|2l+2|2ikr), \tag{2.4a}$$

$$G_l(r)=\frac{C_l(\eta)\mathrm{e}^{-\frac{1}{2}\pi i l}}{\Gamma(2l+2)}\,(2ikr)^l\mathrm{e}^{-ikr}G(l+1+i\eta|2l+2|2ikr). \tag{2.4b}$$

In these expressions, $F(a|c|z)$ and $G(a|c|z)$ denote the confluent hypergeometric functions of the first and second kind, respectively, and the following notation has been used:

$$\eta=\frac{1}{kB},\quad C(\eta)=|\Gamma(l+1+i\eta)|\mathrm{e}^{\frac{1}{2}\pi\eta}. \tag{2.5}$$

The normalization of $F_l(r)$ and $G_l(r)$ is such that

$$F_l(r)\underset{r\to\infty}{\to}\frac{\sin\,(kr+\eta\ln 2kr-\frac{1}{2}\pi l+X_l)}{kr}, \tag{2.6a}$$

$$G_l(r)\underset{r\to\infty}{\to}\frac{\cos\,(Kr+\eta\ln 2kr-\frac{1}{2}\pi l+X_l)}{kr}. \tag{2.6b}$$

† Although this is a necessary condition, it is not sufficient. Jost and Kohn [12]) discuss sufficient conditions for cases when there is no Coulomb field. This point is clearly not critical in our calculations, for we can appeal to continuity considerations: as the strength of the nuclear interaction goes to zero, the poles of interest move continuously to points in the k plane corresponding to unperturbed Coulomb bound states.

The series expansions of $F_l(r)$ and $G_l(r)$ can be determined † from

$$F(a|c|z) = 1 + \frac{a}{c}z + \frac{a(a+1)}{2!c(c+1)}z^2 + \ldots, \tag{2.7a}$$

$$G(a|c|z) = \frac{e^{2\pi i a}-1}{2\pi i}\left\{[2\ln z + \pi\cot(\pi a) - \pi i]F(a|c|z)\right.$$
$$\left. -2\sum_{m=0}^{\infty}[\Psi(m+1)+\Psi(c+m)-\Psi(a+m)]\frac{\Gamma(a+m)\Gamma(c)}{m!\Gamma(a)\Gamma(c+m)}z^m\right\} \tag{2.7b}$$
$$-2e^{i\pi a}\frac{\Gamma(c)}{\Gamma(a)}\sum_{r=1}^{c-1}\frac{\Gamma(r)z^{-r}}{\Gamma(c-r)\Gamma(r-a+1)},$$

$$\Psi(x) = \frac{d}{dx}(\ln\Gamma(x)). \tag{2.7c}$$

The general solution of this Schrödinger equation may be written

$$\Psi(r) = -2ie^{i\delta_l}(\sin\delta_l G_l(r) + \cos\delta_l F_l(r)), \tag{2.8}$$

where δ_l is an arbitrary complex constant. The asymptotic form of this function, following from eqs. (2.6), is

$$\Psi(r) \underset{r\to\infty}{\to} \frac{1}{kr}(e^{-i[kr+\eta\ln 2kr+X_l]} - e^{2i\delta_l}e^{i[kr+\eta\ln 2kr+X_l]}). \tag{2.9}$$

Eq. (2.9) has the form of eq. (2.1) with $S(k) = e^{2i\delta_l}$. At the points where $S(k)$ has a pole, $\cot\delta_l = i(S(k)+1)/(S(k)-1)$ takes the value $+i$.

It should be noted that, unlike the cases where the Coulomb field is repulsive or is absent, the phase shifts δ_l do not go to zero at zero energy in the present case. This may readily be illustrated for a weak nuclear potential $V(r)$, where δ_l is given in first Born approximation by

$$\delta_l = -\frac{2\mu k}{\hbar^2}\int_0^{\infty} F_l^2(r)V(r)r^2dr. \tag{2.10a}$$

Using eqs. (2.4a) and (2.7a) leads to

$$\lim_{k\to 0}\delta_l = -\frac{\mu\pi}{\hbar^2}\frac{2^{2l+2}}{[(2l+1)!]^2}\int_0^{\infty}\left(\frac{r}{B}\right)^{2l+1}V(r)rdr. \tag{2.10b}$$

This conclusion may be reached in a more general way which will be more useful for later comparison with the boundary condition method. Define the

† The series expansion given in ref. [5]) for $G(a|c|z)$ is incorrect; the first series in eq. (2.7b) begins with $m = 0$ rather than $m = 1$ as given in their eq. (5.3.62) and in the summary at the end of the chapter.

quantity ε_l by the equation

$$\varepsilon_l = R\left(\frac{1}{\Psi(r)}\frac{\mathrm{d}\Psi(r)}{\mathrm{d}r} - \frac{1}{F_l(r)}\frac{\mathrm{d}F_l(r)}{\mathrm{d}r}\right)_{r=R}. \tag{2.11}$$

The term $(\mathrm{d}\Psi(r)/\mathrm{d}r)/\Psi(r)$ is determined mainly by the nuclear interaction and, in general, will not be equal to $(\mathrm{d}F_l(r)/\mathrm{d}r)/F_l(r)$. On substituting eq. (2.8) into eq. (2.11), we obtain the relation between the zero energy phase shift and ε_l,

$$\lim_{k\to 0}\delta_l = -\frac{2\pi\varepsilon_l}{2l+1+\varepsilon_l}\left(\frac{R}{B}\right)^{2l+1}\frac{2^{2l}}{(2l!)\,(2l+1)!}. \tag{2.12}$$

This should be compared with the analogous expression for the case where there is no Coulomb field,

$$\delta_l \underset{k\to 0}{\to} -\frac{\varepsilon_l}{2l+1+\varepsilon_l}(kR)^{2l+1}\frac{2^{2l}(l!)^2}{(2l+1)!\,(2l!)}. \tag{2.13}$$

3. Energy Level Shifts of S-states

The effective range formula for attractive Coulomb interactions can be derived by the method used by Bethe [6]) for the case of repulsive Coulomb interactions. Following Bethe's discussion, we define

$$\varphi(k,r) = krC_0(\eta)[G_0(r) + \cot\delta_0 F_0(r)], \tag{3.1}$$

and consider the expression

$$\varphi(0,r)\frac{\mathrm{d}\varphi(k,r)}{\mathrm{d}r} - \varphi(k,r)\frac{\mathrm{d}\varphi(0,r)}{\mathrm{d}r}$$
$$= k^2\int_{r\ll R}^{\infty}\mathrm{d}r'\left(\varphi(0,r')\varphi(k,r') - u(0,r')u(k,r')\right). \tag{3.2}$$

The functions $u(k,r)$ denote exact solutions of the Schrödinger equation including the nuclear potential. They are normalized so that $u(k,r) = \varphi(k,r)$ for $r > R$. Using eqs. (2.7) and (3.2), we obtain an expansion in k^2,

$$\frac{1}{B}\frac{C_0^2(\eta)\cot\delta_0}{\eta} - 2h(\eta) = -\frac{1}{A} + \tfrac{1}{2}r_0k^2 + 0(k^4). \tag{3.3}$$

The notation in this equation is defined by

$$h(\eta) = \eta^2\sum_{m=1}\frac{1}{m(m^2+\eta^2)} - \ln\eta - 0.577\ldots,$$
$$\frac{1}{A} = -\frac{2\pi}{B}\cot\delta_0\Big|_{k=0}, \tag{3.4}$$
$$r_0 = 2\int_0^{\infty}\mathrm{d}r(\varphi^2(0,r) - u^2(0,r)).$$

The effective range approximation consists of dropping terms of order k^4 and higher.

In order to obtain an expression giving the location of the bound states, $\cot \delta_0$ is set equal to i in eq. (2.3). Further, we let $K = -ik = -i\sqrt{(2\mu E/\hbar^2)}$. The locations of the poles of $S(k)$ are then given by the equation

$$-\tfrac{1}{2}KB+\Psi\left(-\frac{1}{KB}\right)+\ln KB=\tfrac{1}{2}B\left[\frac{1}{A}+\tfrac{1}{2}K^2r_0\right]. \tag{3.5}$$

A series expansion for the location of the bound states may now be calculated. For the level with principal quantum number n, set $1/KB = n+\lambda$ and assume $|\lambda| \ll 1$. Then we have

$$\frac{\Delta E_n}{E_n}=2\frac{\lambda}{n}-3\left(\frac{\lambda}{n}\right)^2+4\left(\frac{\lambda}{n}\right)^3+\cdots \tag{3.6}$$

For cases of physical interest, it is reasonable to assume $|A/B| \ll 1$ and $|r_0/B| \lesssim 1$. Eq. (3.5) may then be solved for λ by iteration. The result, to third order in (A/B), is

$$\begin{aligned}\frac{\Delta E_n}{E_n}=&-\frac{4}{n}\frac{A}{B}\left\{1-\left(2\Delta_n(r_0)+\frac{3}{n}\right)\left(\frac{A}{B}\right)\right.\\&\left.+4\left(\theta_n(r_0)+\Delta_n{}^2(r_0)+\frac{3\Delta_n(r_0)}{n^2}+\frac{2}{n^3}\right)\left(\frac{A}{B}\right)^2\right\},\end{aligned} \tag{3.7}$$

where

$$\begin{aligned}\Delta_n(r_0)&=\frac{1}{4n^2}\left(\frac{r_0}{B}\right)-\Psi(n)+\ln n-\frac{1}{2n},\\ \theta_n(r_0)&=\frac{1}{2n^3}\left(\frac{r_0}{B}\right)-\frac{1}{2n^2}-\frac{1}{n}-\sum_{q=1}^{n=1}\frac{1}{q^2}-1.645.\end{aligned} \tag{3.8}$$

This result shows clearly that the condition for the validity of the usual expression eq. (1.1) for the energy level shift is that $|A/B| \ll 1$. The dimensionless parameter r_0/B will generally be small for cases of physical interest.

4. Energy Level Shifts of p-States

The effective range formula for p states may be derived in an analogous way. Define the function

$$\varphi_1(k,r)=\frac{C_1(\eta)}{\eta}(kr)[G_1(r)+\cot\delta_1 F_1(r)]. \tag{4.1}$$

The effective range approximation †

$$\varphi_1(0,r)\frac{d\varphi_1(k,r)}{dr}-\varphi_1(k,r)\frac{d\varphi_1(0,r)}{dr}=k^2\int_{r\ll R}dr\left(\varphi_1^2(0,r)-u_1^2(0,r)\right) \quad (4.2)$$

leads to

$$\frac{1}{B}\left[\frac{C_1^2(\eta)\cot\delta_1}{\eta^3}-2h(\eta)\left(\frac{\eta^2+1}{\eta^2}\right)\right]=-\frac{1}{A_1}+\tfrac{1}{2}k^2r_1. \quad (4.3)$$

The notation here is similar to that of eq. (3.3). We shall not give the explicit expression for r_1 as this is considerably more complicated than that for r_0 and we shall not need it here. As in the $l=0$ case, the location of the bound states may be determined by setting $\cot\delta_1=i$ and $k=iK$ in eq. (4.3). The following series expression for the energy level shifts is obtained:

$$\begin{aligned}\frac{\Delta E_n}{E_n}&=-\left(1-\frac{1}{n^2}\right)\left(\frac{4}{n}\right)\left(\frac{A_1}{B}\right)\left\{1-2\left[\alpha_n(r_1)+\left(1-\frac{1}{n^2}\right)\frac{3}{2n}\right]\left(\frac{A_1}{B}\right)\right.\\&\left.+4\left[\alpha_n^2(r_1)+\left(1-\frac{1}{n^2}\right)\beta_n(r_1)+3\left(1-\frac{1}{n^2}\right)\frac{\alpha_n(r_1)}{n^2}+\frac{2}{n^3}\left(1-\frac{1}{n^2}\right)^2\right]\left(\frac{A_1}{B}\right)^2,\right.\end{aligned} \quad (4.4)$$

where

$$\alpha_n(r_1)=\left(1-\frac{1}{n^2}\right)\Delta_n(r_1)-\frac{2}{n^3}+\frac{1}{4n^4}\left(\frac{r_1}{B}\right),$$

$$\beta_n(r_1)=\frac{2}{n^3}\left(-\frac{1}{2n}+\Psi(n)-\ln n\right)-\left(1-\frac{1}{n^2}\right)\left(\frac{1}{2n^2}+\sum_{q=1}^{n-1}\frac{1}{q^2}+\frac{1}{n}+1.645\right)+\frac{1}{2n^3}\left(\frac{r_1}{B}\right).$$

As in the s-state case, the result eq. (4.4) will be a useful approximation if $|A/B|\ll 1$.

5. Discussion

The expressions (3.7) and (4.4) show that the usual result given for the energy level shift is only the lowest order term in an expansion in powers of (A/B). In lowest order, the energy level shift is proportional to A/B and the lifetime width to b/B, where $A=a+ib$ is the (complex) scattering length. In higher approximations, the contributions depend on a, b in a more complicated way.

† In eqs. (3.2) and (4.2), the integrations are not taken to $r=0$ because the irregular Coulomb function is, in general, singular at the origin. In the case $l=0$, the integration may be extended to $r=0$ since the dominant term in $\varphi(k,r)$, for small r, is a constant. For $l=1$, $\varphi_1(k,r)$ has terms diverging as $1/r$ and $\ln r$ for small r, so that the lower limit on the integral must be kept at a finite value. However, it is straightforward to subtract the divergent terms from both sides of eq. (4.2). In the remaining terms r may be set equal to zero.

For example, in the 1s state, the energy level-shift is to second order

$$\frac{R_e(\Delta E)_{1s}}{E_{1s}} = -\frac{4}{n}\left\{\frac{a}{B} - \frac{a^2-b^2}{B^2} \times 3.077 + \ldots\right\}, \tag{5.1}$$

whereas the lifetime width Γ is given by

$$\frac{\Gamma_{1s}}{E_{1s}} = -\frac{4}{n}\frac{b}{B}\left\{1 - \frac{2a}{B} \times 3.077 + \ldots\right\}. \tag{5.2}$$

Even if $a = 0$, there can be an appreciable energy level shift if the ratio b/B is sufficiently large. Owing to the large coefficient of the correction term in (5.2), the lifetime width may be appreciably modified if the elastic scattering is sufficiently strong.

It is worthwhile to discuss the relation of the approximations used here to those used in the previously mentioned papers. The calculations of Deser *et al.* [1]), leading to eq. (1.1), are very general in the handling of the nuclear interaction; no assumption is made that the nuclear interaction may be represented by a potential. However, the Coulomb interaction is disregarded except insofar as it is necessary for the existence of the bound states. Thus, although the form of eq. (1.1) is the same as the first order of eq. (3.6), the scattering lengths A_0 and A, occurring in these two equations are defined differently. A possible way of relating A_0 to A has been given by Chew and Goldberger [7]). They treat the Coulomb field for $r < R$ as a perturbation and show that

$$\frac{1}{A} = \frac{1}{A_0} - \frac{2}{B}\ln\left(\frac{2R}{B}\right) + \frac{1}{B}\left\{\text{series in powers of } \left(\frac{2R}{B}\right)\right\}. \tag{5.3}$$

If we adopt this result, we may replace eq. (3.6) by eq. (1.1) to lowest order. This is a good approximation for π-mesic atoms, as Deser *et al.* point out; however, it is evident from eq. (5.1) that this may involve a substantial error in other cases.

The method followed by Byers [3]) is similar in spirit to the method used here; the Coulomb field is fully accounted for and the displacement of states with $l > 0$ may be calculated. The parameter ε_l, defined in eq. (2.11), is considered as a function of energy:

$$\varepsilon_l(E) = \varepsilon_l(0) + k^2R^2a_l(E), \tag{5.4}$$

where $\varepsilon_l(0)$ and $a_l(E)$ are to be regarded as quantities to be determined by low-energy scattering data. The energy level shifts are then determined by the following equation:

$$\Delta E_n = \frac{\varepsilon_l(0)}{2mR}\left[\int_R^\infty \mathrm{d}r\, \frac{u_K(r)F_n(r)}{u_n(R)F_n(R)}\left(\frac{r}{R}\right)\right]^{-1}. \tag{5.5}$$

In this expression, $u_n(r)/r$ and $F_n(r)$ denote the exact wave function for the bound state of quantum number n and the corresponding Coulomb wave function, respectively. To relate eq. (5.3) to our results, we express $\varepsilon_l(O)$ in terms of the scattering length, defined for general l by

$$\frac{1}{A_l} = -\frac{2\pi}{B}\cot\delta_l\Big|_{E=0}. \tag{5.6}$$

It follows from eq. (2.12) that

$$\frac{A_l}{B} = \frac{\varepsilon_l(O)}{2l+1+\varepsilon_l(O)}\left(\frac{R}{B}\right)^{2l+1}\frac{2^{2l}}{(2l)!(2l+1)!}. \tag{5.7}$$

In the case $|A| \ll R \ll B$, which is valid for the π-mesic atoms considered by Byers, the integral in eq (5.3) may be evaluated approximately to give a result agreeing with the first-order results obtained here †. When this condition does not hold, the criterion for the validity of the first-order result is obscured in complicated integral expressions

6. Illustrative Examples

For the purpose of illustration, in this section eq. (3.7) is used to calculate the s-state energy level shifts for the K^-—p and K^-—d atoms.

6.1. THE K^-—p ATOM

Dalitz and Tuan [8]) have analyzed $\bar{K}N$ scattering data and have shown that there are four sets of s-wave scattering lengths consistent with the data. The K^-—p scattering lengths are given by $A = \frac{1}{2}(A^0+A^1)$, where A^0 and A^1 denote the isobaric spin 0 and 1 scattering lengths. Table 1 gives the best values of A^0 and A^1, as recently revised [9]), and the corresponding changes in binding energy $R_e(\Delta E)$ and the lifetime τ of the atomic states.

TABLE 1

K^-—p energy level shifts

	A^0 (fm)	A^1 (fm)	$n^3 R_e(\Delta E)$ (eV)	$\tau/n^3(10^{-18}$ sec)
$(a+)$	$-0.05-1.15\,i$	$-1.36-0.30\,i$	-280	2.22
$(a-)$	$+0.20-1.65\,i$	$+1.10-0.20\,i$	$+264$	1.63
$(b+)$	$-1.50-2.00\,i$	$-0.58-0.30\,i$	-424	1.39
$(b-)$	$+1.90-1.53\,i$	$+0.37-0.40\,i$	$+464$	1.65

† In order to compare Byers' result with those obtained here, it is necessary to use the following approximate expression for $|F_n(R)|^2$, valid for small R:

$$|F_n(R)|^2 = \left(\frac{2R}{nB}\right)^{2l+2}\frac{(n+l)!}{n^2B[(2l+1)!]^2(n-l-1)!}.$$

The values for the energy level shifts given in table 1 are obtained from the first-order term in eq (3.7). The higher order corrections are quite small; for example, the second-order corrections for the $(b+)$ case are about $(1/n)$ % to the energy level shift and $(8/n)$ % to the lifetime.

6.2. THE K⁻—d ATOM

In a simple model calculation of K⁻-deuterium scattering, using a zero range approximation for the $\bar{K}$—N interaction, Chand [10]) has obtained the following expression for the zero-energy K⁻—d scattering length:

$$A = \tfrac{1}{2}\int_0^\infty \mathrm{d}R\, u_d^2(R)\left(\frac{3A_1+A_0-4A_0A_1/R}{1+(A_1-A_0)/R-A_0A_1/R^2}\right) \tag{6.1}$$

where $(u_d(R)/R)$ denotes the deuteron radial wave function. We have calculated A for each of the four sets $(a\pm)$, $(b\pm)$ using the Hulthén form [11]) of $u_d(R)$ (neglecting d-state contributions):

$$u_d(R) = N[1-\mathrm{e}^{-\beta(x-x_c)}]\mathrm{e}^{-x}, \tag{6.2}$$

where N is the normalization constant, $x = \alpha R$ and the following parameters have been assumed: $\alpha = 0.232$ fm^{-1} and $x_c = 0.10$, $\beta = 7.675$. The resulting scattering lengths and corresponding energy level shifts are given in table 2.

TABLE 2

K⁻—d energy level shifts

	A (fm)	$n^3 R_e \Delta E$ (eV)	τ/n^3 (10^{-18} sec)
$(a+)$	$-1.07-2.40\,i$	-636	0.46
$(a-)$	$1.16-0.35\,i$	$+689$	3.16
$(b+)$	$-1.28-2.12\,i$	-760	0.52
$(b-)$	$1.05-0.99\,i$	$+624$	1.12

The higher order corrections are somewhat larger than in the K⁻—P atom. In the (b+) case, which has the largest corrections, the correction to the energy level shift is about $(10/n)$ % while the correction to the lifetime is about $(15/n)$%.

The author wishes to thank Professor R. H. Dalitz for suggesting this problem and for his constant assistance during the progress of the work.

References

1) S. Deser, M. L. Goldberger, K. Baumann and W. Thirring, Phys. Rev. **96** (1954) 774
2) H. A. Bethe and F. de Hoffmann, Mesons and fields, Vol. 2 (Row, Peterson and Co., Evanston, Illinois, 1955) p. 103 ff.
3) N. Byers, Phys. Rev. **107** (1957) 843

4) L. Landau and Ya. Smorodinsky, J. Phys. (USSR) **8** (1944) 154
5) P. Morse and H. Feshbach, Methods of theoretical physics (McGraw Hill, New York, 1953) p. 604 ff
6) H. Bethe and P. Morrison, Elementary nuclear theory (John Wiley and Son, New York, 1956) p. 90 ff
7) G. F. Chew and M. L. Goldberger, Phys. Rev. **75** (1959) 1637
8) R. H. Dalitz and S. F. Tuan, Ann. Phys. **8** (1949) 100, **3** (1960) 307
9) R. H. Dalitz, private communication
10) R. Chand, report in preparation (1961)
11) L. Hulthén and M. Sugawara, Handbuch der physik, Vol. **34** (Springer-Verlag, Berlin, 1957)
12) R. Jost and W. Kohn, Mat. Fys. Medd. Dan. Vid. Selsk. **26**, No. 9 (1953)

1.C.:
2.A.1

Nuclear Physics **26** (1961) 68—79; © *North-Holland Publishing Co., Amsterdam*
Not to be reproduced by photoprint or microfilm without written permission from the publisher

NUCLEAR REARRANGEMENT AND SIMPLE NUCLEAR REACTIONS

PAUL BENIOFF †

Department of Physics, The Weizmann Institute of Science, Rehovoth, Israel

Received 10 February 1961

Abstract: The effect of nuclear rearrangement on (p, pn) and (p, 2p) reaction cross sections is considered in this work. In general it seems reasonable to require that the rearrangement effect be contained in the overlap of the wave functions of the target and product nuclear states. It is shown that this overlap appears directly in the expression for the (p, pn) and (p, 2p) reaction cross sections. The rearrangement effect is explicitly calculated for two independent particle models and is shown to cause a fractional change of $1/A$ in the reactioncross sections.

1. Introduction

The topic of nuclear rearrangement has geen discussed in recent years by several authors. Much of the work [1–5]) on nuclear rearrangement has dealt with the rearrangement energy contribution to the ground state energy and single particle separation energy of nuclei or nuclear matter. Brueckner [1]) and Thouless [2]) discuss the rearrangement energy in terms of the change in the effective nucleon-nucleon interaction when a nucleon is removed from nuclear matter or a nucleus. Mittelstaedt [4]) defines the rearrangement energy as the energy shift of the remaining nucleons when a nucleon is removed from a nucleus. He concludes, however, that the rearrangement energy does not seem to be a measurable quantity and that it appears as the difference between an experimental and model dependent quantity. Some work [5, 6]) has discussed the rearrangement effect on the (p, 2p) and (p, pn) reaction cross sections. In particular [6]) it was shown that the large values of the (p, pn) reaction cross section in the GeV energy region require that the rearrangement effect allow a large population of the particle stable states of the product nucleus. The change in the population spectrum caused by the rearrangement effect was discussed on the basis of the shell model and rough limits on the energy range of the major part of the spectrum were set.

In this paper we wish to investigate more closely the effect of nuclear rearrangement on simple nuclear reaction cross sections. For the purposes of discussion we shall restrict ourselves to (p, pn) and (p, 2p) reactions, although the results

† Weizmann Fellow 1959—60. Present address: Universitetets Institut for Teoretisk Fysik, Copenhagen, Denmark.

apply to other nuclear reactions as well. In sect. 2 we describe the rearrangement effect, R. Ef. In general it seems sufficient to require that the R. Ef. be contained in the overlap of the eigenfunctions of the target and product nuclear Hamiltonians. The derivation of a general expression for the (p, pn) or (p, 2p) reaction cross section is sketched in sect. 3 in order to demonstrate the explicit appearance and effect on the cross section of this overlap. The use of an approximation such as the direct interaction approximation, impulse approximation, etc., is avoided in order to not leave out any factor which might be essential to the existence of the R. Ef. In sect. 4 the eigenfunction overlap of the target and product Hamiltonians is discussed in further detail. The explicit calculation of the R. Ef. for independent particle models is given in sect. 5. It is shown that for the infinite square well and the harmonic oscillator well the R. Ef. is small, of the order $1/A$ of the observed cross section.

2. The Rearrangement Effect

In a previous paper [6]) we have considered the rearrangement effect on the (p, pn) reaction at high energies as follows. Suppose that the incident proton enters the target nucleus of A nucleons, collides with a neutron and the collision products exit from the nucleus without further interactions with the $A-1$ nucleons remaining behind. Then the product nucleus is left in some sort of "state" in which $A-1$ nucleons occupy the same volume and roughly the same states they had in the target nucleus just before the collision, i.e. there is a "hole" in the target nucleus. Immediately after the reaction the nucleus rearranges itself by slightly decreasing its volume and changing the internucleon spatial correlation to remove the "hole" and ends up in one or another excited product nuclear states l'. The time required for this rearrangement is long compared to the total residence time of the proton and collision products as it is roughly equal to the time required for many crossings of the nuclear diameter by an average kinetic energy nucleon. The total residence time, which is roughly the time during which the proton and collision products are within the nucleus, can be estimated from cloud chamber data [6, 7]) † to be $\leqq 3d/c$ for bombarding energies > 100 MeV. The factors d and c are the nuclear diameter and velocity of light.

Let us assume for the purposes of discussion that real nuclear states are the eigenstates of any one of several different independent particle Hamiltonians. For these models the only rearrangement effect would be due to A-dependent factors in the potential wells and boundary conditions on the Hamiltonians. For any model with the potential well and boundary conditions independent of A, the R. Ef. is zero as the pseudo "state" formed by the snatching out of a target neutron is a real state of the product nucleus. This leads us to attempt

† The author wishes to thank Dr. Holmquist for providing unpublished data.

to define the R. Ef. on the cross section $\Delta\sigma_{l'j'}$ as

$$\Delta\sigma_{l'j'} = \sigma_{l'j}(L_0) - \sigma_{l'j'}(L_1), \tag{1}$$

where $\sigma_{l'j'}(L_0)$ is the total reaction cross section from the target nucleus in its ground state j' to state l' of the product nucleus; L_0 is the product nucleus Hamiltonian in the model considered. The term $\sigma_{l'j'}(L_1)$ is the total cross section from state j' to l' which would be obtained if there were no rearrangement effect in the model considered. The model Hamiltonian of the product nucleus, altered to give no rearrangement effect, is denoted by L_1.

It is easy to see what L_1 would be for any independent particle model for (p, pn) and (p, 2p) reactions. The target and product nuclear Hamiltonians K_0 and L_0 are given by

$$K_0 = \sum_{i=1}^{A} K_i = \sum_{i=1}^{A} [T_i + V(A, \mathbf{r}_i)], \tag{2}$$

$$L_0 = \sum_{i=1}^{A-1} L_i = \sum_{i=1}^{A-1} [T_i + V(A-1, \mathbf{r}_i)], \tag{3}$$

where the A-dependence is explicitly included in the single particle potential. We define L_1 by

$$L_1 = \sum_{i=1}^{A-1} [T_i + V(A, \mathbf{r}_i)], \tag{4}$$

whose eigenfunctions are those of $A-1$ particles moving in a potential well for A particles. If there were no rearrangement effect, L_1 would be identical with L_0.

It also seems that the direct measurement of the R.Ef. is problematic. It is possible to measure $\sigma_{l'j'}(L_0)$ directly[8] †; however, the measurement of $\sigma_{l'j'}(L_1)$ seems impossible as it would require preventing experimentally the rearrangement of the product nucleus. At best it appears that, in agreement with Mittelsteadt [4], the R. Ef. is the difference between a measured and a computed quantity. One would calculate $\Delta\sigma_{l'j'}$ from eq. (1) by calculating $\sigma_{l'j'}(L_0)$ from eq. (3) in a given model. The variable parameters of the model are then adjusted so that the calculated values agree with experiment [6]. The values of the parameters are inserted into eq. (4) and $\sigma_{l'j'}(L_1)$ is calculated.

A consideration of more general types of nuclear models indicates that it is not so easy to give a definition of the R. Ef. in terms of nuclear Hamiltonians. The difficulty is that one does not know what Hamiltonian to choose for L_1 in order to compute $\sigma_{l'j'}(L_1)$. For example, in the ordinary two-body force model we have

$$K_0 = \sum_{i=1}^{A} T_i + \sum_{i>j}^{A} v_{ij}, \tag{5}$$

† In these references differential cross sections are given which can be integrated to obtain $\sigma_{l'j'}(L_0)$.

$$L_0 = \sum_{i=1}^{A-1} T_i + \sum_{i>j}^{A-1} v_{ij}, \tag{6}$$

where the strength of v_{ij} is usually independent of A. There does not seem to be any way to obtain L_1 from eqs. (5) and (6). We do know that there is some sort of R. Ef. in nuclei as there is a definite correlation structure among the nucleons which is disturbed by the sudden removal of a nucleon.

Even though we can not define the R. Ef. in terms of Hamiltonians it seems sufficient to require that the R. Ef. be contained in the overlap of the eigenfunctions $\varphi_{p'}$ and $\theta_{l'}$ of K_0 and L_0 respectively. This is a reasonable requirement as the amount of overlap in the wavefunctions expresses roughly the differences between K_0 and L_0 and consequently the change in the nuclear structure caused by addition of the Ath nucleon. For independent particle models with no R. Ef., the overlap between $\varphi_{p'}$ and $\theta_{l'}$ for a given state p' is zero for all but A eigenstates of L_0. If there is a R. Ef., the overlap deviates from zero for more than A states of L_0 and the magnitude depends on the strength of the internucleon correlation, or nuclear rearrangement.

It should be noted that if the eigenfunctions $\varphi_{p'}$ and $\theta_{l'}$ of more general Hamiltonians (e.g. eqs. (5), (6)) are expanded in terms of a complete set of single particle wave functions, the R. Ef., or original overlap, is contained in the expansion coefficients of $\theta_{l'}$ and $\varphi_{p'}$ (see ref. [5])).

Since the R. Ef. seems to be contained in the overlap of the eigenstates of the initial and final nuclear Hamiltonians, we shall derive in the next section an expression for the (p, pn) or (p, 2p) reaction cross section to show that the overlap enters directly in the cross section.

3. Derivation of the P, PN or P, 2P Reaction Cross Section

The (p, pn) or (p, 2p) reaction cross section can be derived using the techniques of formal scattering theory. Here we shall only sketch the derivation for these reactions as the derivation for the general case has been given previously [9–11]). In this work the incident particle shell be regarded as distinguishable from the rest. This corresponds to neglect of exchange terms which are small at high energies [12]).

Let H be the exact total Hamiltonian describing the scattering process in which protons are incident on a target nucleus of A nucleons. Let K be the Hamiltonian of the free initial state i.e. of the target nucleus and free incident nucleon, and L be the Hamiltonian of a free final state of interest i.e. of the product nucleus plus two free nucleons. The interaction between the incident nucleon and the target nucleus is given by V. The interaction of the incident and exit nucleon with each other and with the product nucleus is given by V'.

We have

$$K = H - V = K_0 + T_0, \tag{7a}$$

$$L = H - V' = L_0 + T_0 + T_A, \tag{7b}$$

where K_0 and L_0 are the target and product nuclear Hamiltonians and T_0 and T_A are the kinetic energy operators of the 0th (incident) particle and A th particle. Let

$$H\Psi_j = E\Psi_j, \tag{8a}$$

$$K\Phi_j = E_j\Phi_j, \tag{8b}$$

$$L\Theta_l = E_l\Theta_l, \tag{8c}$$

where E, E_j and E_l are the total energies of the scattering system, free initial state and free final state respectively; Ψ_j is the exact wavefunction of the whole system. The free initial and final state wavefunctions Φ_j and Θ_l are given by

$$\Phi_j = \varphi_{j'}(\xi_1 \ldots \xi_A)\lambda_m^{\mathrm{a}}(\xi_0), \tag{9a}$$

$$\Theta_l = \theta_{l'}(\xi_1 \ldots \xi_{A-1})\lambda_{m'}^{\mathrm{b}}(\xi_0)\lambda_{m''}^{\mathrm{c}}(\xi_A), \tag{9b}$$

where $\varphi_{j'}$ and $\theta_{l'}$ are the antisymmetric wavefunctions of the target nucleus ground state j' and a product nucleus state l'. The wavefunctions of the free incident and exit particles of momenta $\mathbf{k}_{\mathrm{a}}$ and $\mathbf{k}_{\mathrm{b}}$, $\mathbf{k}_{\mathrm{c}}$ and spin projections m and m', m'' are given by λ_m^{a} and $\lambda_{m'}^{\mathrm{b}}$, $\lambda_{m''}^{\mathrm{c}}$ respectively. We neglect the isobaric spin in order to keep the expressions simpler. However, it can be easily included. Space and spin coordinates are denoted by ξ_i.

The exact wavefunction Ψ_j contains ingoing and outgoing parts. We are interested in only those parts ψ_j^+ and ψ_l^- which correspond to Φ_j and Θ_l respectively at $t = -\infty$ and $t = +\infty$. Following Gell Mann and Goldberger [9]), Hack [10]) and Lippmann [11]) we take (the limit $\varepsilon \to 0^+$ is implied)

$$\psi_j^+ = \Phi_j + \frac{1}{E_j - H + i\varepsilon} V\Phi_j, \tag{10}$$

$$\psi_l^- = -\frac{i\varepsilon\Theta_l}{E_l - K - i\varepsilon} + \frac{1}{E_l - K - i\varepsilon} V\psi_l^-, \tag{11}$$

$$S_{lj} = \langle \psi_l^- | \psi_j^+ \rangle, \tag{12}$$

where S_{lj} is the scattering matrix between the initial state j and the final state l. Substitution of eqs. (10) and (11) into eq. (12) gives after some manipulation

$$S_{lj} = -\frac{i\varepsilon}{E_l - E_j + i\varepsilon}\langle \Theta_l | \Phi_j \rangle - \frac{2i\varepsilon}{(E_l - E_j)^2 + \varepsilon^2}\langle \psi_l^- | V | \Phi_j \rangle. \tag{13}$$

In the limit $\varepsilon \to 0^+$ the first term on the right equals zero unless it has a singularity [10, 11]) at $E_l = E_j$. Eqs. (9a), (9b) show that there is no such singularity,

so that only the second right hand term remains. We get

$$|S_{ij}|^2 = \frac{4\varepsilon^2}{[(E_i-E_j)^2+\varepsilon^2]^2} |\langle \psi_i^- | V | \Phi_j \rangle|^2.$$

Since later on $|S_{ij}|^2$ will be integrated over E_i and the limit $\varepsilon \to 0^+$ taken we can replace the ε-containing factor by its equivalent to obtain [9, 10])

$$|S_{ij}|^2 = \frac{2\pi\delta(E_i-E_j)}{\varepsilon} |\langle \psi_i^- | V | \Phi_j \rangle|^2. \tag{14}$$

The cross section for a transition $j \to l$ is equal to the transition rate divided by the incident flux v_{inc}/L^3, and the density of scatterers L^{-3}.

$$\sigma'_{ij} = \lim_{\substack{\varepsilon \to 0^+ \\ L \to \infty}} \frac{AL^6}{v_{\text{inc}} T} |S_{ij}|^2, \tag{15}$$

where L is the dimension of the normalizing box and T is the lifetime of the perturbation which causes an uncertainty ε in the final state energy E_i. The factor A comes from the fact that the cross section is independent of the coordinate label of the scattered neutron. Since there are A possible equivalent Hamiltonians L for a given Hamiltonian K (eqs. (7a), (7b)) and the perturbation V is symmetric in the coordinates of the scattered nucleon, there are A equal scattering matrices S_{ij} contributing to the cross section. This factor A in eq. (15) is always cancelled by a similar factor A coming from the antisymmetrization normalization of $\varphi_{j'}$ and $\theta_{l'}$ and will be suppressed in the following equations. Similar considerations [12]) hold for the $A+1$ Hamiltonians K.

The cross section per unit volume in $3N$-dimensional momentum space, where N is the number of exit particles (3 for (p, pn) reactions), is

$$\frac{\mathrm{d}\sigma_{l'j'}}{\mathrm{d}\mathbf{k}_b \mathrm{d}\mathbf{k}_c \mathrm{d}\mathbf{K}} = Z \lim_{\substack{\varepsilon \to 0^+ \\ L \to \infty}} \left(\frac{L}{2\pi}\right)^9 \sigma'_{ij}, \tag{16}$$

where Z is an appropriate sum and average over respective final and initial spin states; $\mathbf{K}$ is the C.M. momentum of the product nucleus. To get the differential cross section we substitute eqs. (14), (15) into (16) and set $T = \hbar/\varepsilon$. Let R_{ij} be defined by

$$R_{ij} = \lim_{\substack{\varepsilon \to 0^+ \\ L \to \infty}} \langle \psi_i^- | V | \Phi_j \rangle L^{\frac{15}{2}}, \tag{17}$$

where the $L^{\frac{15}{2}}$ cancels the normalization factors $L^{-\frac{3}{2}}$ for each free particle. (Together ψ_i^- and Φ_j have five such factors when ψ_i^- is expanded later by

iteration of eq. (11)). We finally obtain for the differential cross section [13]) †

$$\frac{\mathrm{d}\sigma_{l'j'}}{\mathrm{d}\Omega_\mathrm{b}\Omega_\mathrm{c}} = Z\frac{1}{(2\pi)^8}\left(\frac{m}{\hbar^2}\right)^2\frac{1}{v_\mathrm{inc}}\int v_\mathrm{b}\delta(E_i-E_j)|R_{ij}|^2\mathrm{d}E_\mathrm{b}k_\mathrm{c}^2\mathrm{d}k_\mathrm{c}\mathrm{d}\mathbf{K}. \tag{18}$$

We have replaced $k_\mathrm{b}^2\mathrm{d}k_\mathrm{b}$ by $m^2v_\mathrm{b}\mathrm{d}E_\mathrm{b}/\hbar^3$. The total cross section to state l' of the product nucleus is

$$\sigma_{l'j'} = \int\frac{\mathrm{d}\sigma_{l'j'}}{\mathrm{d}\Omega_\mathrm{b}\mathrm{d}\Omega_\mathrm{c}}\,\mathrm{d}\Omega_\mathrm{b}\mathrm{d}\Omega_\mathrm{c} \tag{19}$$

and the total (p, pn) or (p, 2p) reaction crosss ection to nucleon stable product states is

$$\sigma_{j'} = \sum_{l'}\sigma_{l'j'}\left(\frac{\Gamma'_\gamma}{\Gamma}\right)_{l'} \approx \sum_{l'}^{\mathrm{st}}\sigma_{l'j'}, \tag{20}$$

where Γ'_γ and Γ are the gamma emission width to particle stable states and the total emission width espectively and the sum is over all product nuclear states l'. The second sum is over particle stable states only and expresses the fact that the width ratio $= 1$ for particle stable states and ≈ 0 for particle unstable states.

Eqs. (18)—(20) show that the reaction cross sections depend on the matrix R_{ij} calculated on the energy shell. Iteration of eq. (11) into eq. (17) gives after rearrangement and removal of the L factors and rearranging

$$R_{ij} = \lim_{\epsilon\to 0^+}\langle\Theta_i\left|\frac{i\varepsilon}{E_i-K+i\varepsilon}V\sum_{\nu=0}^{\infty}\left[\frac{1}{E_i-K+i\varepsilon}V\right]^\nu\right|\Phi_j\rangle. \tag{21}$$

Use of the completeness relation $1 = \sum_p|\Phi_p\rangle\langle\Phi_p|$ (see eq. (8b)), and the fact that

$$\lim_{\epsilon\to 0^+} i\varepsilon[E_i-E_p+i\varepsilon]^{-1} = \delta_{E_i,E_p}$$

gives finally

$$R_{ij} = \lim_{\epsilon\to 0^+}\sum_p\delta_{E_p,E_i}\langle\Theta_i|\Phi_p\rangle\langle\Phi_p|V\sum_{\nu=0}^{\infty}\left[\frac{1}{E_i-K+i\varepsilon}V\right]^\nu|\Phi_j\rangle. \tag{22}$$

In eq. (22) the overlap between eigenfunctions of the initial and final state Hamiltonians appears explicitly as the factor $\langle\Theta_i|\Phi_p\rangle$. We see also that this factor, which contains the rearrangement effect, appears to all orders $\nu+1$ of the perturbation V.

4. Discussion

We will now examine in more detail the overlap of the initial and final

† In this paper an expression for the transition rate has been derived which is equivalent to eq. (18).

states. If we integrate $\langle \Theta_l | \Phi_p \rangle$ over ξ_0 we get

$$\langle \Theta_l | \Phi_p \rangle = (\theta_l \lambda^c_{m''} | \varphi_{p'}) \delta(\mathbf{k}_a - \mathbf{k}_b) \delta_{m'', m'} , \tag{23}$$

where $\mathbf{k}_a$ is the momentum of the incident particle after scattering.

If the nuclear part $(\theta_{l'} \lambda^c | \varphi_{p'})$ of eq. (23) is considered (the spin and spisoin projection quantum numbers are suppressed), one can see that in any independent particle model without any R. Ef., the product nuclear wavefunction $\theta_{l'}$ is orthogonal to the nuclear part of $\varphi_{p'}$. This occurs because the individual particle eigenfunctions in $\varphi_{p'}$ and $\theta_{l'}$ are solutions of the same single particle Hamiltonians i.e. in this case $K_i = L_i$ in eqs. (2), (3). If a model is chosen in which there is a R. Ef. i.e. $K_i \neq L_i$, then the single particle eigenfunctions in $\theta_{l'}$ and $\varphi_{p'}$ are not orthogonal. The overlap expresses the magnitude of the potential well change from K_i to L_i. In these models this change is the nuclear rearrangement.

We see also that we can reformulate the general condition imposed on nuclear rearrangement for simple nuclear reactions [6]) i.e. that the population of particle stable states be > 0. The values of the (p, pn) reaction cross sections calculated by eqs. (18)—(22) are supposed to agree with the experimental values which are large at high energies. The general condition is equivalent to the requirement that

$$\sum_{p'} |(\theta_{l'} \lambda^c | \varphi_{p'})|^2 \delta_{E_{p'}, E_{l'}} \gg 0 \tag{24}$$

for at least one particle stable state of the product nucleus. The Kronecker delta expresses the requirement imposed by the deltas in eqs. (22) and (23) that

$$E_{p'} = E_{l'} + \frac{\hbar^2 k_c^2}{2m}. \tag{25}$$

If eq. (24) were not satisfied all the computed cross sections would be zero in contradiction to experiment.

The description of the R. Ef. given in this work is equivalent in some aspects to that given in other work. Mittelstaedt [4]) considers the separation energy of a particle from a system of $A+1$ particles and defines the rearrangement energy as the energy shift of the remaining A particles. For independent particle models the descriptions seem equivalent because in this case the change in the potential well causes both the energy shift and the R. Ef. on the cross sections.

Brueckner [5]) considers the rearrangement effect to be the population of highly excited product states due to the target neutron being knocked out while it is interacting with another target nucleon. This seems to be the effect described by the non-orthogonality of $(\theta_{l'} \lambda^c | \varphi_{p'})$. Limiting ourselves to the $\nu = 0$ term in eq. (22) we see that the only allowed continuum states $\varphi_{p'}$

are those with one neutron in the continuum. However, the non-orthogonality of $(\theta_{l'}\lambda^{c}|\varphi_{p'})$ may allow the appreciable population of many excited product states l' with a large range of excitation energies.

5. Calculation of the Rearrangement Effect

Since the calculation of the values of $(\theta_{l'}\lambda^{c}|\varphi_{p'})$ for many values of l' for allowed values of p' is a large undertaking, we shall restrict ourselves here to the assumption that nuclei are exactly described by an independent particle model and estimate the R. Ef. The model chosen is

$$H = K+V = K_0+T_0+\sum_{i=1}^{A} V(\mathbf{r}_0-\mathbf{r}_1), \tag{26}$$

with K_0 given by eq. (2); T_0 is the kinetic energy operator of the incident particle. We consider the first order term only of eqs. (21) and (22) by setting $\nu = 0$. Eqs. (22), (23) and (25) give

$$R_{lj} = \sum_{p'} \left(\mathrm{D}[\beta_{l_1}(\xi_1)\ldots\beta_{l_{A-1}}(\xi_{A-1})]\lambda^{c}_{m''}(\xi_A)|\mathrm{D}\alpha_{p_1}(\xi_1)\ldots\alpha_{p_A}(\xi_A)]\right)$$
$$\times\langle \mathrm{D}[\alpha_{p_1}(\xi_1)\ldots\alpha_{p_A}(\xi_A)]\lambda^{b}_{m'''}(\xi_0)|\sum_{n=1}^{A} V(\mathbf{r}_0-\mathbf{r}_n)|\mathrm{D}[\alpha_{j_1}(\xi_1)\ldots\alpha_{j_A}(\xi_A)]\lambda^{a}_{m}(\xi_0)\rangle$$
$$\cdot\,\delta_{E_{p'},E_{l'c}}\delta_{m''',m'}. \tag{27}$$

The single particle solutions to K_0(eq. (2)) and either L_0 (eq. (3)) or L_1 (eq. (4)) are given by $\alpha(\xi_i)$ and $\beta(\xi_i)$ respectively; D is the antisymmetrizing operator. The sum is over all states p' of A single particles. The integration over $\mathbf{k}_q$ has already been performed. The orthogonality of the α's in the V containing matrix element limits the sum over p' to sets in which $p_1 = j_1, \ldots, p_{n-1} = j_{n-1}$, $p_{n+1} = j_{n+1}, \ldots, p_A = j_A$ and $p_n \neq j_n$ and a sum over the subscript n. We see also that R_{lj} is small to second order if $n \neq A$, as the first matrix element in eq. (27) contains the factors

$$\langle\lambda^{c}_{m''}(\xi_A)|\alpha_{j_A}(\xi)\rangle\langle\beta_{l_n}(\xi_n)|\alpha_{p_n}(\xi_n)\rangle,$$

where the delta functions in eq. (27), and the fact that j_A is bound, require that p_n be free and consequently $l_n \neq p_n$. Since β_{l_n} is nearly orthogonal to α_{p_n} and at high energies the projection of $\lambda^{c}_{m''}$ on the bound state j_A is small, we shall neglect all such terms and retain only those with $n = A$. For $n = A$ the first matrix element in eq. (27) gives

$$(\theta_{l'})\lambda^{c}(\xi_A)|\varphi_{p'}) = \frac{1}{\sqrt{A}}\prod_{i=1}^{A-1}\langle\beta_{l_i}(\xi_i)|\alpha_{j_i}(\xi_i)\rangle\langle\lambda^{c}_{m''}(\xi_A)|\alpha_{p_A}(\xi_A)\rangle, \tag{28}$$

where the $A^{-\frac{1}{2}}$ factor comes from the antisymmetrization and normalization. This is the factor which cancels the factor A in eq. (15).

The orthogonality of the eigenfunctions β and α must now be investigated. If the $V(A\mathbf{r}_i)$ in eqs. (2)—(4) are restricted to spin independent and central forces, the matrix elements in eq. (28) are *not* orthogonal with respect to the radial quantum number only. If we put

$$\beta_{l_i}(\xi_i) = \sum_{m_l} C(lsj;\, m_l,\, m_j - m_l) R^{A-1}_{nl_j}(r_i) Y_{lm_l}(\theta_i \varphi_i) \chi_{s,\, m_j - m_l}$$

and

$$\alpha_{j_i}(\xi_i) = \sum_{\mu_{l'}} C(l' sj';\, \mu_{l'},\, \mu_{j'} - \mu_{l'}) R^{A}_{n'l'j'}(r_i) Y_{l'\mu_{l'}}(\theta_i \varphi_i) \chi_{s,\, \mu_{j'} - l'\mu_i},$$

where the factors C are Clebsch Gordan coefficients, we have

$$\langle \beta_{l_i}(\xi_i) | \alpha_{j_i}(\xi_i) \rangle = \int R^{*A-1}_{nl_j}(r_i) R^{A}_{n'l'_{j'}}(r_i) r_i^2 \mathrm{d}r_i \delta_{jj'} \delta_{ll'} \delta_{\mu_{j'} m_{j'}}, \tag{29}$$

where $l_i = n, l, j, m_j$ and $j_i = n', l', j', \mu'_j$. Eq. (29) shows us that the (p, pn) and (p, 2p) reactions populate those product states l' whose configuration is the same as that of the target nucleus minus a nucleon in a given shell. However, there is also a population of product states in which one or more nucleons in the product nucleus are in states with different n but the same l, j, m_j, as in the target nucleus. It is this depopulation of product states with $N = 0$ and populations of states with $N \geqq 1$ which we call the R. Ef. The number of nucleons promoted to states of different n than in the target nucleus is denoted by N. Let

$$\int R^{*A-1}_{nl_j} R^{A}_{n'l_j} r^2 \mathrm{d}r - \begin{cases} 1 - \delta^n_{lj} & \text{if} \quad n' = n, \\ \Delta^{lj}_{nn'} & \text{if} \quad n' \neq n. \end{cases} \tag{30}$$

For $N = 0$ the decrease in the (p, pn) reaction cross section caused by the R. Ef. is found from eqs. (1)—(4), (18), (19) (27)—(30) to be roughly (for $\sigma(L_1)$ we have $\Delta = \delta = 0$)

$$\Delta\sigma_{l'j'} \approx G \int |\sum_{p_A} \langle \lambda^{\mathrm{c}}_{m''} | \alpha_{p_A} \rangle \langle \lambda^{\mathrm{b}}_{m'} \alpha_{p_A} | V | \alpha_{j_A} \lambda^{\mathrm{a}}_{m'} \rangle|^2$$
$$\times [|(1-\delta)^{A-1}|^2 - 1] v_{\mathrm{b}} \delta(E_l - E_j) \delta_{E_{p'},\, E_{l\mathrm{c}}} \mathrm{d}E_{\mathrm{b}} \mathrm{d}\Omega_{\mathrm{b}} \mathrm{d}\mathbf{k}_{\mathrm{c}} \mathrm{d}\mathbf{K}. \tag{31}$$

The factor G contains all the constants and the sum and average over spin states. We have suppressed the dependence of δ on the single nucleon labels n, l and j. The removal of a nucleon from state j_A leaves the remaining nucleons in the same configuration as they have in state l'. If $N \neq 0$ the factor in the brackets in eq. (31) becomes

$$|\Delta^N (1-\delta)^{A-1-N}|^2 \tag{32}$$

which gives a positive $\Delta\, \sigma_{l'j}$. Since $\sigma_{l'j'}(L_1) = 0$ for these product states with

promoted nucleons eq. (1) gives

$$\Delta\sigma_{\nu'\gamma'} = \sigma_{\nu'\gamma'}(L_0),$$

which shows that within this model these states are populated entirely (in the Born approximation) by the R. Ef.

As two specific examples we shall compute the R. Ef. for two simple but physically unrealistic models (no continuum states), the infinite three-dimensional square well and the harmonic oscillator well. For the infinite square well the shift in the radius boundary from $r_0 A^{\frac{1}{3}}$ to $r_0(A-1)^{\frac{1}{3}}$ causes the R. Ef. The evaluation of eq. (30) is straightforward [14]) and gives

$$\delta \approx \frac{1}{8A^2} \quad \text{and} \quad \Delta \approx \frac{1}{A}. \tag{33}$$

For the harmonic oscillator model we set the potential well equal to

$$V(A\mathbf{r}_i) = kA^s r_i^2,$$

where s is a number of order unity. Again the evaluation of eq. (30) is straightforward [15]) and gives

$$1-\delta_l \approx \left(1-\frac{s^2}{32A^2}\right)^{l+\frac{3}{2}}, \tag{34a}$$

$$\Delta^l_{nn'} \approx \left(\frac{n!\Gamma(n+l+\frac{3}{2})}{n'!(n-n')!\Gamma(n'+l+\frac{3}{2})}\right)^{\frac{1}{2}} \left(\frac{s}{4A}\right)^{n-n'}. \tag{34b}$$

For the usual harmonic oscillator model [3]) $\hbar\omega = 41A^{-\frac{1}{3}}$ which gives $s = -\frac{2}{3}$. We see then that for both these models the bracketed factor in eq. (31) is of order $1/A$ for $N = 0$ and is at least of order A^{-2N} for $N \geqq 1$ eq. (32). This means that for these two models and probably for other usual independent particle models the fractional change in the cross section to states with $N = 0$ caused by the R. Ef. is of the order $A^{-1}\sigma_{\nu\gamma}$. Also the cross section for population of product states with promoted nucleons, $N \geqq 1$, is very small as it is of the order $A^{-2N}\sigma_{\nu\gamma}$. Thus if one assumes for the purposes of calculation that nuclei are sufficiently well represented by independent particle models, one may use the eigenfunctions α instead of the eigenfunctions β as final state wavefunctions in computing cross sections. This approximation, which neglects the R. Ef., has been used in other work [6]).

Finally, it should be pointed out that the population of product levels with promoted nucleons is due to the R. Ef. in Born approximation only. All the higher perturbation orders ($\nu \geqq 1$ in eqs. (21), (22)) populate these levels directly and probably swamp the first order rearrangement effect.

6. Conclusion

In this work we have discussed the effect of nuclear rearrangement on simple nuclear reaction cross sections as applied to the (p, pn) and (p, 2p) reactions. From a study of the R. Ef. in independent particle models it is reasonable to assume that, in general, the R. Ef. is contained in the overlap of the wavefunctions of the initial and final states. This overlap was explicitly demonstrated in an expression for the (p, pn) or (p, 2p) reaction cross section. The R. Ef. was explicitly calculated in first order for a couple of independent particle models and was shown to be at most of order $1/A$ of the observed cross section to a given final state.

The author wishes to thank the Weizmann Institute for their hospitality extended during the year. The author is also grateful to Professor A. De-Shalit and Drs. A. Reiner and A. Glick and other staff members and visitors for many helpful discussions and suggestions. Thanks are also extended to Dr. Carl Levinson for reading and criticizing this manuscript.

References

1) K. A. Brueckner and D. T. Goldman, Phys. Rev. **117** (1960) 207;
K. A. Brueckner, J. L. Gammel and J. T. Kubis, Phys. Rev. **118** (1960) 1438
2) D. J. Thouless, Phys. Rev. **112** (1958) 906
3) V. F. Weisskopf, Nuclear Physics **3** (1957) 423
4) P. Mittelstaedt, Nuclear Physics **17** (1960) 499
5) Proc. Int. Conf. on the Nuclear Optical Model, The Florida State University, Tallahassee, Florida, March 1959, pp. 132—144
6) P. Benioff, Phys. Rev. **119** (1960) 324
7) F. Holmquist, Thesis, UCRL-8559, December 1959;
W. B. Fowler, R. P. Shutt, A. M. Thorndike and W. L. Whittemore, Phys. Rev. **95** (1954) 1026;
Wilmont Hess, Revs. Mod. Phys. **30** (1958) 368
8) H. Tyrén, P. Hillman and Th. A. J. Maris, Nuclear Physics **7** (1958) 1, 10;
T. Gooding and H. Pugh, Nuclear Physics **18** (1960) 46;
K. Riley, H. Pugh and T. Gooding, Nuclear Physics **18** (1960) 65
9) M. Gell Mann and M. L. Goldberger, Phys. Rev. **91** (1953) 398
10) M. N. Hack, Phys. Rev. **108** (1957) 1636
11) B. Lippmann, Phys. Rev. **102** (1956) 264
12) G. Takeda and K. M. Watson, Phys. Rev. **97** (1955) 1336;
H. Feshbach, Ann. Revs. Nuclear Sci. **8** (1958) 49
13) E. Gerjuoy, Annals of Phys. **5** (1958) 58
14) P. Morse and H. Feshbach, Methods of Theoretical Physics, (McGraw Hill Book Co., New York, 1953) Vol. II, pp. 1574–1576
15) A. Erdleyi, Bateman Manuscript Project, California Institute of Technology (McGraw Hill Book Co., New York, 1955) Vol. II, p. 56; Vol. IV, p. 175

1.D.2 *Nuclear Physics* **26** (1961) 80—90; © *North-Holland Publishing Co., Amsterdam*
Not to be reproduced by photoprint or microfilm without written permission from the publisher

OCTUPOLE VIBRATIONS OF DEFORMED EVEN NUCLEI

P. O. LIPAS † and J. P. DAVIDSON

Department of Physics, Rensselaer Polytechnic Institute, Troy, New York ††

Received 13 February 1961

Abstract: To explain the systematic occurrence of $K = 0-$ and $K = 2-$ bands in deformed even nuclei, the nuclear surface is assumed to have two octupole degrees of freedom, corresponding to the spherical harmonics Y_{30} and $Y_{3\pm2}$, in addition to the β and γ quadrupole degrees of freedom. An approximate Hamiltonian, valid for small oscillations about a spheroidal equilibrium shape, is constructed with the hydrodynamic moments of inertia. Separation of the Schrödinger equation immediately gives β vibrations ($K = 0+$, $I = 0, 2, 4, \ldots$) and "b vibrations" ($K = 0-$, $I = 1, 3, 5, \ldots$). The remaining equation is solved formally as a degenerate perturbation problem. The result gives rise to two bands with $K = 2$, which are interpreted as the γ vibrational band ($K = 2+$) and a "g vibrational band" ($K = 2-$), both with spin sequence $I = 2, 3, 4, \ldots$ The theory is consistent with experiment in the strongly deformed regions.

1. Introduction

Many odd parity levels with energies below 2 MeV have been observed in deformed even nuclei over the past few years [1–3]). On qualitative grounds these levels are commonly attributed to collective octupole vibrations [4, 5]). Several $K = 0-$, $I = 1, 3, 5, \ldots$ bands are well established, particularly on the low A side of the heavy element region. These are viewed as rotational bands based on axially symmetric octupole vibrations. There is also evidence for $K = 2-$, $I = 2, 3, 4, \ldots$ bands in deformed nuclei [2, 3]).

The aim of the present paper is to account for the observed $K = 0-$ and $K = 2-$ bands in terms of collective octupole vibrations with superimposed rotational motion. An adiabatic approximation is used to solve for small surface oscillations about a spheroidal equilibrium shape, allowing two octupole degrees of freedom in addition to the usual quadrupole degrees of freedom, β and γ.

In sect. 2 we obtain the octupole contributions to the moments of inertia. Then, in sect. 3, we construct the complete Hamiltonian for collective motion and obtain an approximate solution involving the familiar β and γ vibrations of the pure quadrupole case as well as contributions from the octupole degrees of freedom, which we call b and g vibrations. Finally, in sect. 4, we compare the available experimental data with the theory.

† International Atomic Energy Agency fellow 1959—1960. This author will submit this paper in partial fulfilment of the requirements for the degree of Doctor of Philosophy at Rensselaer Polytechnic Institute, Troy, New York.

†† Work supported in part by the National Science Foundation.

2. The Moments of Inertia

We shall use the notation of A. Bohr [6]), in which the nuclear surface in the body-fixed coordinate system is given by

$$R(\theta, \phi) = R_0 \left[1 + \sum_{lm} a_{lm} Y_{lm}(\theta, \phi)\right], \tag{1}$$

while the classical vibrational and rotational kinetic energies are given by

$$T_{\text{vib}} = \tfrac{1}{2} \sum_{lm} B_l \dot{a}_{lm}^2, \tag{2}$$

and

$$T_{\text{rot}} = \tfrac{1}{2} \sum_{l\kappa} q_\kappa^2 \mathcal{I}_\kappa^{(l)}, \tag{3}$$

where we have

$$\mathcal{I}_\kappa^{(l)} = B_l \sum_{mm'} a_{lm} a_{lm'} [(M_\kappa^{(l)})^2]_{mm'}. \tag{4}$$

The q_κ are the components of the angular velocity in the body-fixed system, and the $\mathcal{I}_\kappa = \sum_l \mathcal{I}_\kappa^{(l)}$ are the corresponding moments of inertia. The $M_\kappa^{(l)}$ are the usual angular momentum matrices defined in the body-fixed system by

$$[M_\kappa^{(l)}, M_\lambda^{(l)}] = -i M_{\kappa\times\lambda}^{(l)},$$

and we pick a representation where $M_3^{(l)}$ is diagonal. The total kinetic energy of the system will be just the sum of T_{vib} and T_{rot} (i.e. it will contain no cross term contributions of the form $\dot{a}_{lm}\, a_{lm'}$) if, for each l, the a_{lm} with odd m vanish, or if those with even m vanish. Finally, the reality of $R(\theta, \phi)$ implies that $a_{l,-m} = (-)^m a_{lm}$.

Within the context of the requirement of no vibration-rotation cross terms we can calculate two different octupole contributions to the moments of inertia. Taking on the one hand the coefficients a_{30} and $a_{3\pm2}$ as the only non-vanishing a_{3m}, we find from eq. (4) that

$$\begin{aligned}
\mathcal{I}_1^{(3)} &= B_3(6a_{30}^2 + 2\sqrt{30}a_{30}a_{32} + 8a_{32}^2), \\
\mathcal{I}_2^{(3)} &= B_3(6a_{30}^2 - 2\sqrt{30}a_{30}a_{32} + 8a_{32}^2), \\
\mathcal{I}_3^{(3)} &= 8B_3 a_{32}^2.
\end{aligned} \tag{5a}$$

On the other hand, if we take $a_{3\pm1}$ and $a_{3\pm3}$ as the only non-vanishing a_{3m}, eq. (4) yields

$$\begin{aligned}
\mathcal{I}_1^{(3)} &= B_3(\sqrt{5}a_{31} + \sqrt{3}a_{33})^2, \\
\mathcal{I}_2^{(3)} &= B_3(17a_{31}^2 - 2\sqrt{15}a_{31}a_{33} + 3a_{33}^2), \\
\mathcal{I}_3^{(3)} &= 2B_3(a_{31}^2 + 9a_3^2).
\end{aligned} \tag{5b}$$

Either of these are to be added to the well-known quadrupole moments of inertia

$$\mathcal{I}_\kappa^{(2)} = 4B_2\beta^2 \sin^2(\gamma - \tfrac{2}{3}\pi\kappa),$$

where β and γ were defined in ref. [6]) as $a_{20} = \beta \cos\gamma$, $a_{2\pm2} = (1/\sqrt{2})\beta \sin\gamma$. In what follows we confine our attention to the octupole contribution to the moments of inertia given in eq. (5a), which is based on the *ad hoc* assumption that the a_{30} and $a_{3\pm2}$ expansion coefficients best describe the octupole contribution to the nuclear vibrations for the low-lying negative parity states. Not only is the complete Hamiltonian in this case more tractable than in the other, but the contributions to the shape are more symmetric, a property usually associated with lower energy configurations. These points aside, we again wish to emphasize the *ad hoc* nature of this assumption, recognizing that it can be supported only by direct comparison with experiment.

3. The Approximate Solution of the Vibrational Problem

The classical vibrational kinetic energy is, in this case,

$$T_{\text{vib}} = \tfrac{1}{2}B_2(\dot{\beta}^2 + \beta^2\dot{\gamma}^2) + \tfrac{1}{2}B_3(\dot{a}_{30}^2 + 2\dot{a}_{32}^2).$$

The corresponding quantal operator can be found by the usual methods for curvilinear coordinates [7]). Owing to the fact that the moments of inertia are not expressible in product form, each factor being a function of a single variable, the form of the resulting operator precludes the possibility of exact separation of the Schrödinger equation. The problem can still be solved in the adiabatic approximation. Specifically, we consider the case of small oscillations about a spheroidal equilibrium shape β_0. The adiabatic approximation then consists in replacing β by β_0 (when β appears as a factor) and neglecting the other variables in comparison with β_0. For the moments of inertia this approximation yields

$$\begin{aligned} \mathcal{I}_1 &= \mathcal{I}_2 = 3B_2\beta_0^2 = \mathcal{I}_0, \\ \mathcal{I}_3 &= 4B_2\beta_0^2(\gamma^2 + g^2), \end{aligned} \tag{6}$$

where

$$g^2 = \frac{2B_3}{B_2\beta_0^2}a_{32}^2.$$

The approximate vibrational kinetic energy operator then becomes

$$T_{\text{vib}} = -\tfrac{1}{2}\hbar^2\left\{\frac{1}{B_2}\frac{\partial^2}{\partial\beta^2} + \frac{1}{B_3}\frac{\partial^2}{\partial b^2} + \frac{1}{B_\gamma}\left[\frac{\partial^2}{\partial\gamma^2} + \frac{\gamma}{\gamma^2+g^2}\frac{\partial}{\partial\gamma} + \frac{\partial^2}{\partial g^2} + \frac{g}{\gamma^2+g^2}\frac{\partial}{\partial g}\right]\right\}, \tag{7}$$

where $B_\gamma = B_2\beta_0^2$ and $b = a_{30}$.

Since we are neglecting the difference between $\mathscr{I}_1$ and $\mathscr{I}_2$, K is a good quantum number, and we have

$$T_{\rm rot} = \frac{\hbar^2}{2\mathscr{I}_0}[I(I+1)-K^2]+\frac{\hbar^2}{2}\frac{K^2}{\mathscr{I}_3(\gamma, g)}.$$

Following Birbrair *et al.* [8]), we redefine $T_{\rm vib}$ so as to include the term $\hbar^2K^2/2\mathscr{I}_3$ of $T_{\rm rot}$. Thus

$$T'_{\rm vib} = T_{\rm vib}+\frac{\hbar^2}{2B_\gamma}\frac{\frac{1}{4}K^2}{\gamma^2+g^2}. \tag{8}$$

Then the energy associated with rotation is

$$E_{\rm rot}(I, K) = \frac{\hbar^2}{2\mathscr{I}_0}[I(I+1)-K^2]. \tag{9}$$

For small oscillations about the spheroidal equilibrium shape the potential energy can be written as

$$V = \tfrac{1}{2}C_\beta(\beta-\beta_0)^2+\tfrac{1}{2}C_\gamma\gamma^2+\tfrac{1}{2}C_{\rm b}\hbar^2+\tfrac{1}{2}C_g g^2. \tag{10}$$

Inspection of (7) and (10) shows that β and b separate out from the Schrödinger equation, giving rise to a pair of one-dimensional harmonic oscillator equations. The energy eigenvalues are

$$E(n_\beta) = \hbar\sqrt{\frac{C_\beta}{B_2}}\,(n_\beta+\tfrac{1}{2}), \quad n_\beta = 0, 1, 2, \ldots, \tag{11}$$

$$E(n_{\rm b}) = \hbar\sqrt{\frac{C_{\rm b}}{B_3}}\,(n_{\rm b}+\tfrac{1}{2}), \quad n_{\rm b} = 0, 1, 2, \ldots. \tag{12}$$

Rotational levels are built up on these vibrations. Axial symmetry of the body is preserved, which implies that they have $K = 0$. A β band has even parity; hence the spin sequence $I = 0+, 2+, 4+, \ldots$. The b vibration is the octupole counterpart of the β vibration. Parity is odd for $n_{\rm b} = 1$, which implies the spin sequence † $I = 1-, 3-, 5-, \ldots$.

Let us now consider the γ and g equation

$$\left\{-\frac{\hbar^2}{2B_\gamma}\left[\frac{\partial^2}{\partial\gamma^2}+\frac{\partial^2}{\partial g^2}+\frac{\gamma}{\gamma^2+g^2}\frac{\partial}{\partial\gamma}+\frac{g}{\gamma^2+g^2}\frac{\partial}{\partial g}-\frac{\frac{1}{4}K^2}{\gamma^2+g^2}\right]+\tfrac{1}{2}C_\gamma\gamma^2+\tfrac{1}{2}C_g g^2\right\}\psi(\gamma, g)$$
$$= E_{\gamma, g}\psi(\gamma, g). \tag{13}$$

† The one-phonon octupole vibration in a spherical nucleus has $I = 3-$. However, $I = 1-$ can be obtained by coupling one quadrupole phonon with one octupole phonon. Thus it is plausible that the assumed spheroidal equilibrium shape is equivalent to a spherical nucleus in the one-phonon β vibrational state.

Aside from the difference between C_γ and C_g, eq. (13) is symmetric with respect to γ and g. Further, we observe that in the absence of the g degree of freedom, eq. (13) reduces to the γ equation of ref. [8]).

Now we introduce two new variables

$$\gamma = \Gamma \cos\eta, \qquad g = \Gamma \sin\eta, \tag{14}$$

which are defined on the intervals

$$0 \leqq \Gamma < \infty, \qquad 0 \leqq \eta \leqq 2\pi,$$

and we let

$$C_g = C_\gamma + \delta. \tag{15}$$

With these substitutions eq. (13) becomes

$$\left\{-\frac{\hbar^2}{2B_\gamma}\left[\frac{1}{\Gamma^2}\frac{\partial}{\partial\Gamma}\left(\Gamma^2\frac{\partial}{\partial\Gamma}\right)+\frac{1}{\Gamma^2}\left(\frac{\partial^2}{\partial\eta^2}-\tfrac{1}{4}K^2\right)\right]+\tfrac{1}{2}C_\gamma\Gamma^2+\tfrac{1}{2}\delta\Gamma^2\sin^2\eta\right\}\psi(\Gamma,\eta)$$
$$= E_{\Gamma,\eta}\psi(\Gamma,\eta). \tag{16}$$

Let us now suppose that $|\delta| \ll C_\gamma$. Then

$$H^{(1)} = \tfrac{1}{2}\delta\Gamma^2\sin^2\eta \tag{17}$$

may be regarded as a perturbation on the Hamiltonian obtained by setting $\delta = 0$. The unperturbed solution is

$$\psi^{(0)} = P(\Gamma)Q(\eta),$$

where $P(\Gamma)$ and $Q(\eta)$ satisfy

$$\left\{-\frac{\hbar^2}{2B_\gamma}\left[\frac{1}{\Gamma^2}\frac{\mathrm{d}}{\mathrm{d}\Gamma}\left(\Gamma^2\frac{\mathrm{d}}{\mathrm{d}\Gamma}\right)-\frac{\mu^2+\frac{1}{4}K^2}{\Gamma^2}\right]+\tfrac{1}{2}C_\gamma\Gamma^2\right\}P = E_\Gamma P, \tag{18}$$

$$\frac{\mathrm{d}^2Q}{\mathrm{d}\eta^2}+\mu^2Q = 0. \tag{19}$$

Properly behaved solutions to eq. (19) require μ to be a positive or negative integer or zero. If we set

$$\mu^2+\tfrac{1}{4}K^2 = \lambda(\lambda+1), \tag{20}$$

eq. (18) assumes the form of the radial equation for a three-dimensional harmonic oscillator. In order for $P(\Gamma)$ to be regular in the neighbourhood of the origin, λ must be zero or a positive integer. Making use of these restrictions the following table may be constructed:

λ	0	1	4	8	9	etc.
μ	0	±1	$\pm4, \pm2$	±6	$\pm9, \pm3$	
$\lvert K\rvert$	0	2	4, 8	12	6, 18	

(21)

The energy eigenvalues are given by

$$E(n_\Gamma) = \hbar\sqrt{\frac{C_\gamma}{B_\gamma}}(n_\Gamma+\tfrac{3}{2}), \tag{22}$$

where

$$n_\Gamma = 2k+\lambda, \qquad k = 0, 1, 2, \ldots.$$

For the one-phonon excitation we have $n_\Gamma = 1$, $k = 0$, $\lambda=1$, which requires that $|K|=2$. This state is doubly degenerate with respect to μ : the substates $\mu = +1$ and $\mu = -1$ have the same energy. It is also degenerate with respect to K, but K is a "parametric quantum number" in that it does not label the eigenfunctions. The K degeneracy ($K = \pm 2$) is not removed by the perturbation $H^{(1)}$. Hence $|K|=2$ characterizes the $n_\Gamma = 1$ states, regardless of whether or not they are perturbed by $H^{(1)}$.

For the one-phonon state the μ degeneracy gives rise to a two-by-two perturbation matrix with elements

$$\begin{aligned} H^{(1)}_{\mu\mu'} &= \langle n_\Gamma = 1, \lambda = 1; \mu|H^{(1)}|n_\Gamma = 1, \lambda = 1; \mu'\rangle \\ &= \tfrac{1}{2}\delta\langle 11|\Gamma^2|11\rangle\langle\mu|\sin^2\eta|\mu'\rangle. \end{aligned} \tag{23}$$

The normalization of our "radial" function $P(\Gamma)$ differs from that of the three-dimensional harmonic oscillator. The Γ part of the volume element is taken to be $\Gamma d\Gamma$. The normalized function is then found to be

$$|11\rangle = \sqrt{2}c\Gamma\exp(-\tfrac{1}{2}c\Gamma^2), \tag{24}$$

where

$$c^2 = B_\gamma C_\gamma/\hbar^2.$$

The matrix elements are now calculated by means of simple integrals, and the matrix is readily diagonalized, with the resulting eigenvalues

$$E_1^{(1)} = \frac{\delta}{4c}, \qquad E_2^{(1)} = \frac{3\delta}{4c}. \tag{25}$$

We interpret this result in the following way: The perturbation separates the γ and g vibrations. Both have $|K| = 2$ and $I = 2, 3, 4, \ldots$; the γ band has even parity, the g band odd, owing to their quadrupole and octupole characters. If $\delta > 0$ (i.e. $C_g > C_\gamma$) the g band lies above the γ band; if $\delta < 0$ the opposite is true. The band heads are separated by

$$|\Delta E| = |E_2^{(1)} - E_1^{(1)}| = \frac{|\delta|}{2c}. \tag{26}$$

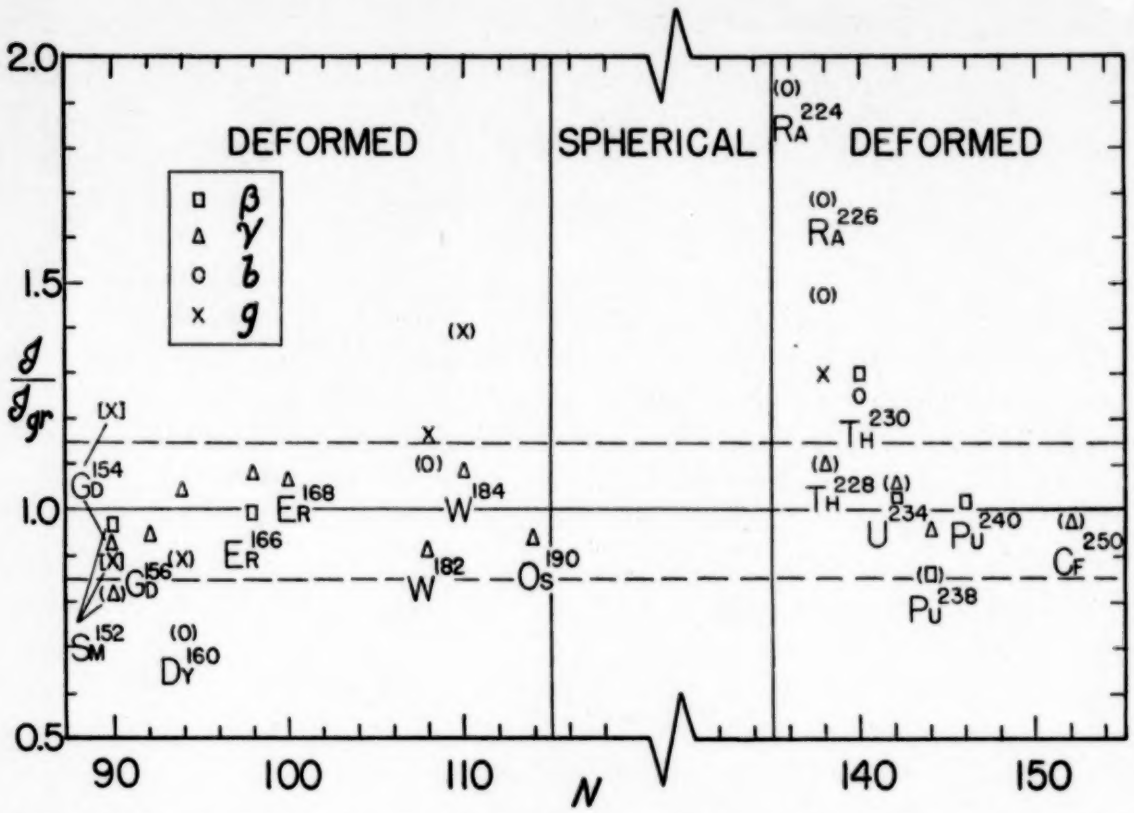

Fig. 1. Ratios of moments of inertia observed in vibrational bands to ground state moments of inertia as a function of neutron number N. Parentheses signify some uncertainty in the assignment of I, K and parity in any of the data used in the calculation of the point; brackets mean that the calculated point is based on spin and parity assignments guessed from level systematics. The moments of inertia are obtained by fitting the first two levels of each band. The experimental data are from the references listed below (ref. [1]) is used generally):

Sm^{152} Cork, Brice, Helmer and Sarason, Phys. Rev. **107** (1957) 1621
Gd^{152} Ref. [3])
Gd^{154} Cork, Brice, Helmer and Sarason, Phys. Rev. **107** (1957) 1621;
K. S. Toth and J. O. Rasmussen, Phys. Rev. **115** (1959) 150;
C. J. Gallagher, Jr. and T. D. Thomas, Nuclear Physics **14** (1959) 1
Gd^{156} Gregers Hansen, Nielsen and Sheline, Nuclear Physics **12** (1959) 389
Dy^{160} Arns, Sund and Wiedenbeck, Nuclear Physics **11** (1959) 411;
M. A. Clark, Can. J. Phys. **38** (1960) 262
Er^{166} Ref. [3])
Er^{168} Jacob, Mihelich, Harmatz and Handley, Phys. Rev. **117** (1960) 1102
W^{182} Ref. [11])
W^{184} Gallagher, Strominger and Unik, Phys. Rev. **110** (1958) 725;
Bodenstedt, Matthias, Körner, Gerdan, Frisius and Hovestadt, Nuclear Physics **15** (1960) 239
Os^{188} W. J. King and M. W. Johns, Can. J. Phys. **37** (1959) 755; Ref. [3])
Os^{190} Kane, Emery, Scharff-Goldhaber and McKeown, Phys. Rev. **119** (1960) 1953
Hg^{200} Gupta, Girgis and van Lieshout, Nuclear Physics **14** (1960) 597
Ra^{226} J. O. Rasmussen, Phys. Rev. **113** (1959) 1593
Th^{228} Ref. [3]) (The points for Th^{230} and the g point for Th^{228} have uncertainties of ± 0.2 due
Th^{230} Ref. [3]) to the fact that the pertinent data were taken from graphs).
U^{234} C. J. Gallagher, Jr. and T. D. Thomas, Nuclear Physics **14** (1959) 1
Pu^{238} Same as above
Pu^{240} Bunker, Dropesky, Knight, Starner and Warren, Phys. Rev. **116** (1959) 143
Cm^{242} Refs. [2, 3])
Cm^{244} Refs. [2, 3])
Cm^{246} Ref. [2])
Cf^{250} Vandenbosch, Diamond, Sjoblom and Fields, Phys. Rev. **115** (1959) 115; Ref. [3])

4 Discussion of Experimental Data

If the mass and stiffness parameters associated with the various degrees of freedom were known, the results of sect. 3 could be used for quantitative predictions of vibrational levels. In the absence of a theory that would provide such knowledge we can still hope to obtain pertinent information from an examination of experimental data. In addition to furnishing a qualitative check on the theory, such an examination may reveal significant trends in the observed quantities.

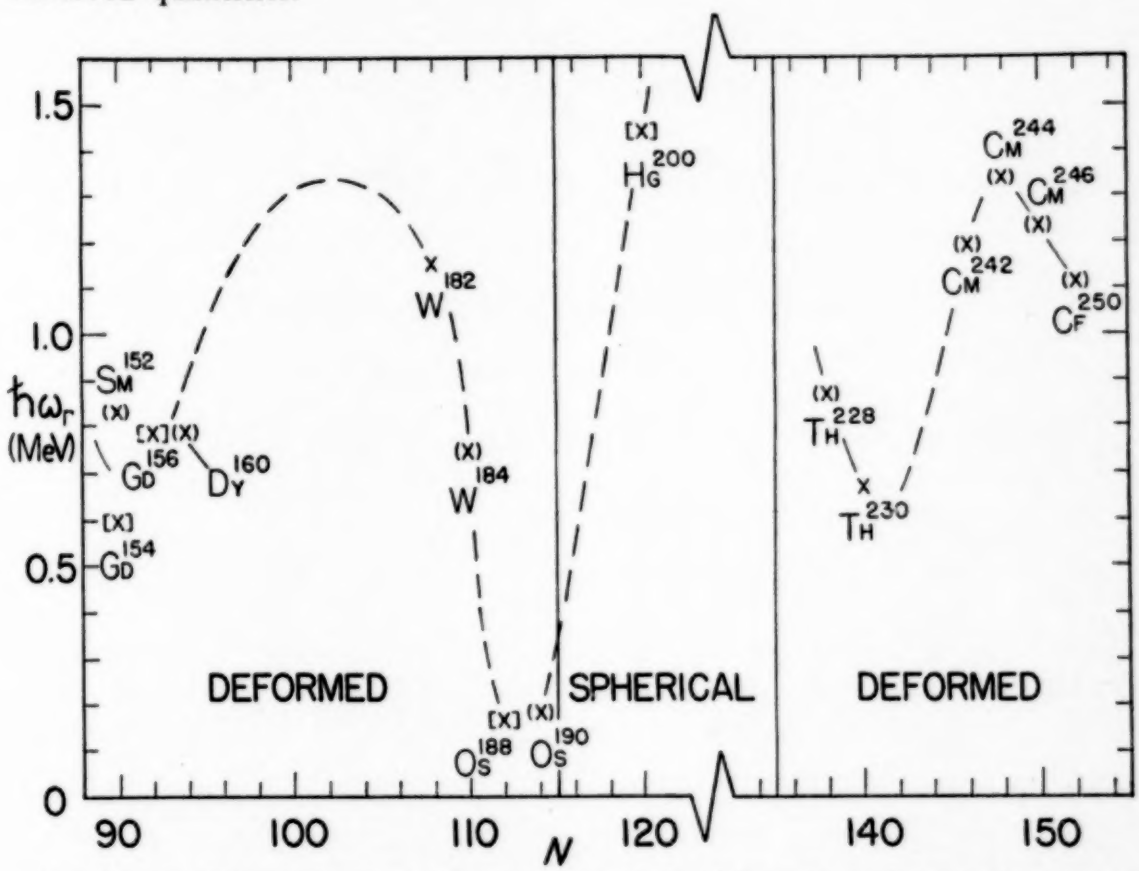

Fig. 2. Energy of "unresolved" γ and g vibrations, calculated from observed γ and g bands, as a function of neutron number. The caption of fig. 1 explains the parentheses and brackets and gives the data references. Curves are drawn through experimental points to indicate trends.

According to our theory, the various bands † of a given spheroidal nucleus should have the same moment of inertia $\mathcal{I} = 3B_2\beta_0^2$. Fig. 1 shows the ratios of the empirical moments of inertia of the various vibrational bands to that of the ground state band as a function of neutron number. Twenty of the thirty-one points lie within 0.15 of unity, indicating that the moment of inertia is indeed approximately constant for a given nucleus. The low A end of the actinides constitutes the only significant and systematic exception: There the b bands have moments

† Corrections due to interactions of bands are neglected. In addition to the "centrifugal stretching" and γ corrections (see e.g. ref. [5])), there is a correction analogous to the latter due to interaction between the b and g bands.

of inertia nearly twice as great as those of the ground state bands. There is no apparent reason for this.

It should be noted that our moments of inertia are calculated from the first two levels of each band. With the exception of the g band of W^{182}, the moments do not change appreciably when the first three levels are fitted † with a correction term proportional to $I^2(I+1)^2$.

Fig. 2 is a plot of $\hbar\omega_\Gamma$, the "unresolved" $|K| = 2$ band head, against the neutron number N. The energy $\hbar\omega_\Gamma$ is calculated from the experimental γ and g band heads by the formula

$$\hbar\omega_\Gamma = E_\gamma(2+) - \tfrac{1}{2}\Delta E - \frac{\hbar^2}{2\mathcal{I}_{gr}}2.$$

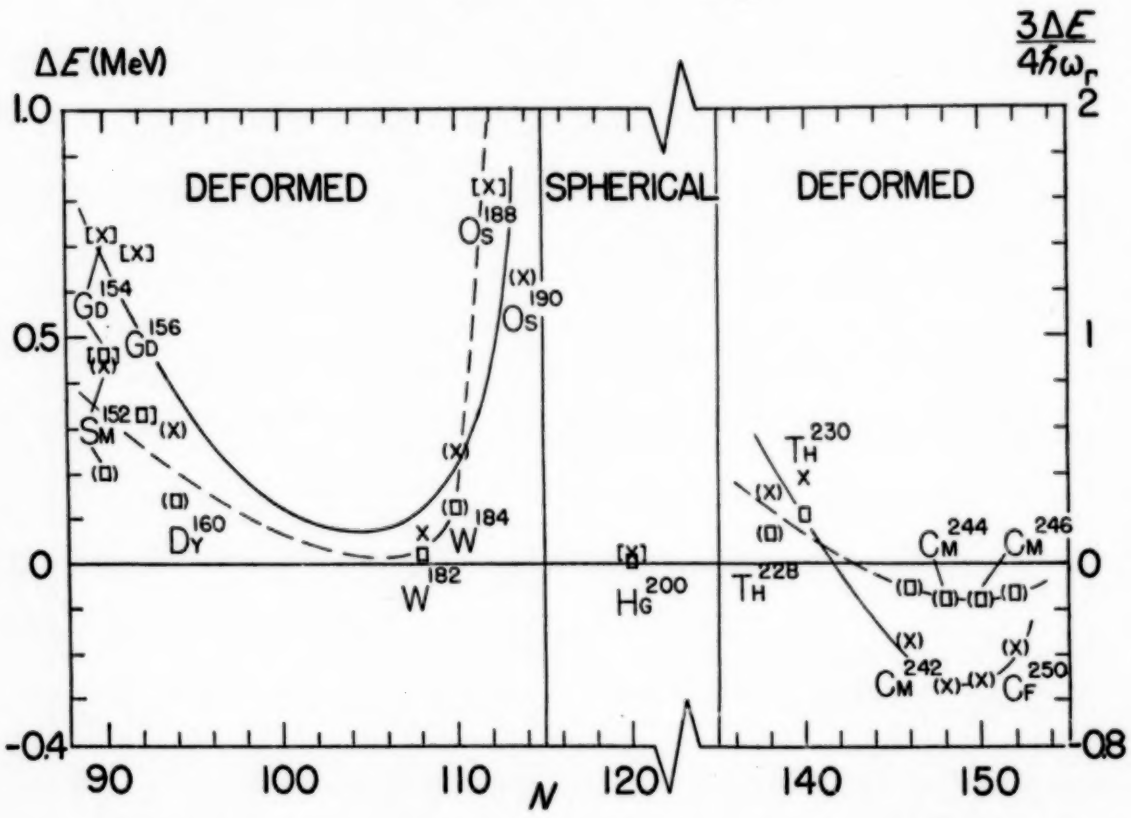

Fig. 3. Separation of observed γ and g band heads (left-hand scale, solid line, crosses), and ratio of maximum energy shift to spacing of unperturbed levels connected by the perturbation operator (right-hand scale, broken line, squares), with neutron number on the horizontal scale. See caption of fig. 1 for meaning of parentheses and brackets and data references. Curves are drawn through experimental points to indicate trends.

Not unexpectedly, the curve has the same general shape as the corresponding curve for $\hbar\omega_\gamma$. It is characterized by a maximum about halfway between closed shells and a minimum in each transition region.

† However, fitting only the first two levels of the g band of W^{182} will give a better over-all fit than fitting the first three with the aid of the correction term.

The energy difference $\Delta E = E_g(I) - E_\gamma(I)$ is depicted in fig. 3, again as a function of N (solid line). The curve has a minimum near the middle of each deformed region and rises sharply as a spherical region is approached. However, the behaviour of ΔE is different in the two deformed regions in that in the heavy element region ΔE becomes negative while it remains positive throughout the rare earth region. We observe that in the middle of the rare earth region g and γ vibrations are nearly degenerate. Similar near degeneracy occurs in the heavy element region, and for $N \gtrapprox 142$ the γ band lies above the g band.

Fig. 3 also includes a plot of the quantity $(\frac{3}{2})\ \Delta E/2\hbar\omega_\Gamma$ versus N (broken line). The quantity $(\frac{3}{2})\ \Delta E$ is the greater of the two energy shifts caused by the perturbation $H^{(1)}$, while $2\hbar\omega_\Gamma$ is the separation between two adjacent unperturbed levels connected by $H^{(1)}$. Thus this graph indicates the validity of our perturbation treatment in the various regions of interest. The perturbation is seen to be small (i.e. n_Γ is approximately a good quantum number) well inside the deformed regions.

Due to the sparsity of well-established data, the graphs presented here must be considered tentative, at least as a basis of quantitative predictions. However, inside the rotational regions experimental evidence supports the qualitative predictions of the theory: the moment of inertia of a given nucleus is nearly the same in all bands, and even and odd parity bands with $K = 0$ and with $|K| = 2$ occur systematically. Further, the observed $|K| = 2$ bands (γ and g) lie sufficiently close to each other to justify our perturbation calculation.

This qualitative agreement between theory and experiment can be construed as a justification for the initial choice of the octupole degrees of freedom, viz. a_{30} and $a_{3\pm2}$. Yet it should be emphasized that *a priori* there is no reason for rejecting $a_{3\pm1}$ and $a_{3\pm3}$.

The general agreement between theory and experiment is not without exceptions. There are a few experimentally observed levels that cannot be assigned to the various bands predicted by our model. For example, Sm^{152} and Th^{230} are reported to have second $1-$ levels at roughly twice the energy of their first $1-$ levels [3]) (note that two-phonon octupole vibrations would have even parity); Wilson and Pool [9, 10]) have recently found even parity rotational bands with $K = 3$ in Yb^{172} and Er^{166}; finally, W^{182} has a complex spectrum [11]) with several levels not explained by our theory.

In spite of these shortcomings, it is hoped that these observations may serve as a step toward a more comprehensive and more quantitative theory of vibrations of spheroidal nuclei.

One of us (P. O. L.) wishes to thank the International Atomic Energy Agency for a fellowship held during the course of this work.

References

1) Strominger, Hollander and Seaborg, Revs. Mod. Phys. **30** (1958) 585
2) R. K. Sheline, Revs. Mod. Phys. **32** (1960) 1
3) Marklund, van Nooijen and Grabowski, Nuclear Physics **15** (1960) 533
4) Alder, Bohr, Huus, Mottelson and Winther, Revs. Mod. Phys. **28** (1956) 432
5) S. A$_f$ Moszkowski in Handbuch der Physik, ed. by S. Flügge (Springer-Verlag, Berlin, 1957) Vol. **39**, p. 411
6) A. Bohr, Mat. Fys. Medd. Dan. Vid. Selsk. **26**, No. 14 (1952)
7) W. Pauli in Handbuch der Physik, ed. by S. Flügge (Springer-Verlag, Berlin, 1958) Vol. 5, Part 1, p. 39
8) Birbrair, Peker and Sliv, JETP **36** (1959) 566
9) R. G. Wilson and M. L. Pool, Phys. Rev. **118** (1960) 1067
10) R. G. Wilson and M. L. Pool, Phys. Rev. **119** (1960) 262
11) C. J. Gallagher, Jr. and J. O. Rasmussen, Phys. Rev. **112** (1958) 1730

8.B

Nuclear Physics **26** (1961) 91—96; © *North-Holland Publishing Co., Amsterdam*

Not to be reproduced by photoprint or microfilm without written permission from the publisher

SOME REMARKS ON GLOBAL SYMMETRY

WOJCIECH KRÓLIKOWSKI †

Institute for Advanced Study, Princeton, New Jersey

Received 6 March 1961

Abstract: According to Gell-Mann's original idea of global symmetry, K-meson interactions violate this symmetry. In the present paper, a speculative argument is described suggesting that all K-meson interactions *must* break down global symmetry and even restricted global symmetry (RGS). There exists, however, a kind of generalized RGS, for which this violation of RGS is more manifest in the real K-meson processes than in the virtual ones. The argument presented connects the problem of RGS and its violation with the question why leptons do not interact strongly with pions and K-mesons.

1. Introduction

Recently, considerable attention was paid again to the problem of global symmetry, because of the possible interpretation of the 1385 MeV resonance in $\pi\Lambda$ interaction as an isobar of the Y-baryon related to the $(\frac{3}{2}, \frac{3}{2})$ isobar of the nucleon [1–3]). Another tentative interpretation of this resonance as a $\bar{K}N$ bound state was, however, also pointed out [4]).

It is well known that even if the restricted global symmetry (RGS) is approximately valid, there must exist some strong interactions or mass-like terms that break down this symmetry [5]). They must lead to the mass differences between Λ and Σ and allow for the observed strong reactions forbidden by RGS.

According to Gell-Mann's original idea of global symmetry, K-meson interactions were those violating this symmetry [6]). In the present paper, a speculative argument is described suggesting that all K-meson interaction *must* break down the RGS. There exists, however, a kind of generalized RGS for which this violation of RGS manifests itself more in the real K-meson processes than in the virtual ones. The argument presented in this paper connects the problem of RGS and its violation with the question why leptons do not interact strongly with pions and K-mesons.

2. Fundamental and Strange Isospins

It was shown in previous papers [7]) that the isospin and charge of baryons can be described by operators

$$\mathbf{T}^{\mathrm{B}} = \int \mathrm{d}_3 x B^*(x)\left(\tfrac{1}{2}\boldsymbol{\tau} + \tfrac{1}{2}\xi_\alpha^* \boldsymbol{\tau}_{\alpha\beta}\xi_\beta\right)B(x) \qquad (1)$$

† On leave from Institute for Nuclear Research, Polish Academy of Sciences, Warsaw and Institute of Theoretical Physics, University of Warsaw.

and that consequently we have

$$Q^{\mathrm{B}} = T_3{}^{\mathrm{B}} + \tfrac{1}{2}(N^{\mathrm{B}} + S^{\mathrm{B}}), \tag{2}$$

where

$$N^{\mathrm{B}} = \int \mathrm{d}_3 x B^*(x) B(x), \qquad S^{\mathrm{B}} = -\int \mathrm{d}_3 x B^*(x) \xi_\alpha{}^* \xi_\alpha B(x) \tag{3}$$

are the number of baryons and the strangeness respectively. In these formulae, $\boldsymbol{\tau} = (\tau_{AB})$ are the ordinary $\frac{1}{2}$ isospin matrices, where the isospin index $A = 1, 2$ corresponds to charges $+e$, 0, and ξ_α ($\alpha = 1, 2$) denotes matrices commuting with τ_i ($i = 1, 2, 3$) and satisfying the anti-commutation relations

$$\{\xi_\alpha, \xi_\beta{}^*\} = \delta_{\alpha\beta}, \qquad \{\xi_\alpha, \xi_\beta\} = 0, \tag{4}$$

where the isospin index $\alpha = 1, 2$ corresponds to charges 0, $-e$; finally, $B(x)$ describes the field of all baryons. Since the field $B(x)$ is acted on by operators τ_i and ξ_α, $\xi_\alpha{}^*$, it can be represented as follows:

$$B(x) = \begin{pmatrix} B_A(x) \\ B_{A\alpha}(x) \\ B_{A\alpha_1\alpha_2}(x) \end{pmatrix}. \tag{5}$$

After the Clebsch-Gordan reduction of components in eq. (5) we get

$$B(x) = \begin{pmatrix} \mathrm{p},\ \mathrm{n} \\ \Lambda \qquad \Sigma^+, \Sigma^0, \Sigma^- \\ \Xi^0, \Xi^- \end{pmatrix}, \tag{6}$$

where

$$\left.\begin{matrix} \mathrm{p} \\ \mathrm{n} \end{matrix}\right\} = B_A, \qquad \Lambda = \frac{B_{12} - B_{21}}{\sqrt{2}},$$

$$\Sigma^+ = B_{11}, \qquad \Sigma^0 = \frac{B_{12} + B_{21}}{\sqrt{2}}, \qquad \Sigma^- = B_{22}, \tag{7}$$

$$\left.\begin{matrix} \Xi^0 \\ \Xi^- \end{matrix}\right\} = \frac{B_{A12} - B_{A21}}{\sqrt{2}}.$$

Notice that $\frac{1}{2}\xi_\alpha{}^* \tau_{\alpha\beta} \xi_\beta$ is the most general operator satisfying the commutation relations for angular momenta and representing

$$\begin{aligned} &0 \text{ isospin vector for N,} \\ &\tfrac{1}{2} \text{ isospin vector for } \Lambda \text{ and } \Sigma, \\ &0 \text{ isospin vector for } \Xi. \end{aligned} \tag{8}$$

This operator was also discussed by Lee and Yang [3]). They denoted it by **M**

and wrote it down explicitly in the doublet representation, in which

$$B(x) = \begin{pmatrix} N_A \\ Y_A \\ Z_A \\ \Xi_A \end{pmatrix}, \tag{9}$$

where, using our notation,

$$N_A = B_A = \begin{cases} \mathrm{p} \\ \mathrm{n} \end{cases},$$

$$Y_A = B_{A1} = \begin{cases} \Sigma^+ \\ \dfrac{\Sigma^0 - \Lambda}{\sqrt{2}} \end{cases}, \quad Z_A = B_{A2} = \begin{cases} \dfrac{\Sigma^0 + \Lambda}{\sqrt{2}} \\ \Sigma^- \end{cases}, \tag{10}$$

$$\Xi_A = \frac{B_{A12} - B_{A21}}{\sqrt{2}} = \begin{cases} \Xi^0 \\ \Xi^- \end{cases}.$$

The operator $\frac{1}{2}\boldsymbol{\tau}$ was denoted in ref. [3]) by $\mathbf{L}$ and the operator $\frac{1}{2}(1-\xi_\alpha^* \xi_\alpha)$ by N_3. The operator $\frac{1}{2}\xi_\alpha^* \boldsymbol{\tau}_{\alpha\beta} \xi_\beta$ when acting on

$$\begin{pmatrix} 0 \\ Y_A \\ Z_A \\ 0 \end{pmatrix}$$

was discussed also by Pais [5]) and denoted by $\boldsymbol{\varrho}$.

Consider now the baryon-pion system. The total isospin of the system is

$$\mathbf{T} = \mathbf{T}_\mathrm{F} + \mathbf{T}_\mathrm{S}, \tag{11}$$

where

$$\mathbf{T}_\mathrm{F} = \int \mathrm{d}_3 x B^* \tfrac{1}{2}\boldsymbol{\tau} B + \text{pion isospin}, \tag{12}$$

$$\mathbf{T}_\mathrm{S} = \int \mathrm{d}_3 x B^* \tfrac{1}{2}\xi_\alpha^* \boldsymbol{\tau}_{\alpha\beta} \xi_\beta B \tag{13}$$

will be called the fundamental and strange isospins respectively. The $\mathbf{T}_\mathrm{F}$ and $\mathbf{T}_\mathrm{S}$ correspond to $\mathbf{I}$ and $\mathbf{K}$ of ref. [5]).

Restricted global symmetry (RGS) or double symmetry can be defined as an invariance under transformations generated by $\mathbf{T}_\mathrm{F}$ and $\mathbf{T}_\mathrm{S}$ *separately* [5]). In the case of RGS, both $\mathbf{T}_\mathrm{F}$ and $\mathbf{T}_\mathrm{S}$ are constants of motion. Each coupling of fundamental and strange isospins leads to a violation of RGS. The general form of the Yukawa pion interaction without derivatives, invariant under RGS, is

$$g_\pi \bar{B} \gamma_5 f_\pi(\xi_\alpha^* \xi_\alpha) \boldsymbol{\tau} B \cdot \boldsymbol{\pi} =$$

$$g_\pi [f_\pi(0) \bar{N} \gamma_5 \boldsymbol{\tau} N + f_\pi(1)(\bar{Y} \gamma_5 \boldsymbol{\tau} Y + \bar{Z} \gamma_5 \boldsymbol{\tau} Z) + f_\pi(2) \bar{\Xi} \gamma_5 \boldsymbol{\tau} \Xi] \cdot \boldsymbol{\pi}, \tag{14}$$

where $f_\pi(\lambda)$ is an arbitrary real function.

The RGS just defined can hold only when strong K-meson interactions are not taken into account. The question arises whether the RGS can be so defined as to be formally possible in the real case of strong K-meson interactions. It seems that there are two possibilities to consider: 1) the K-meson has isospin $\frac{1}{2}$ equal to a strange isospin $\frac{1}{2}$, or 2) the K-meson has isospin $\frac{1}{2}$ resulting from the vector addition of a fundamental isospin 1 and a strange isospin $\frac{1}{2}$.

In the first case, considered by Pais [5]), the K-meson isospin can be added to $\mathbf{T}_S$ and the RGS can hold. In this case the experimentally observed violations of RGS should be provided by couplings of fundamental and strange isospins in some pion and K-meson interactions or in baryon mass-like terms.

In the second case, the K-meson isospin cannot be separated into fundamental and strange parts and added to $\mathbf{T}_F$ and $\mathbf{T}_S$, respectively. Even the formal possibility of RGS now fails. In this case, each K-meson interaction breaks down the RGS, since the K-meson itself couples fundamental and strange isospins.

When speaking about the second case, the following remark may be relevant. If the K-meson field can be derived from a pseudoscalar (or scalar) boson field $M_{i\alpha}$ (isovector $\times$ isospinor, $i = 1, 2, 3$, $\alpha = 1, 2$) by the reduction procedure

$$K_\alpha^{\,G} = \frac{1}{\sqrt{3}}\,\tau_{i\alpha\beta}M_{i\beta}, \qquad \text{where } K^G = \begin{cases} \bar{K}^0 \\ -K^- \end{cases}, \tag{15}$$

then a kind of generalized RGS can hold. This symmetry may be defined in the following way. Separate the isospin of the field $M_{i\alpha}$ into fundamental and strange parts (compare the separation of the isospin of $B_{A\alpha}$) and include these parts into $\mathbf{T}_F$ and $\mathbf{T}_S$, respectively. Then, the invariance under transformations generated by $\mathbf{T}_F$ and $\mathbf{T}_S$ defines the generalized RGS. A Yukawa K-meson interaction consistent with this generalized RGS can be obtained by the following procedure. Write the RGS-invariant Yukawa interaction for the field $M_{i\alpha}$:

$$g_K \bar{B}\gamma_5 f_K(\xi_\beta^*\xi_\beta)\tau_i\xi_\alpha^* BM_{i\alpha}+\text{h.c.}, \tag{16}$$

and separate the K-meson interaction from (16) using the formula

$$(M_{i\alpha}) = \mathbf{M} = \frac{1}{\sqrt{3}}\,\boldsymbol{\tau}K^G+\tfrac{1}{3}(2\mathbf{M}+i\boldsymbol{\tau}\times\mathbf{M}), \qquad \text{where } K^G = \frac{1}{\sqrt{3}}\,\boldsymbol{\tau}\cdot\mathbf{M}. \tag{17}$$

Then, the K-meson interaction takes the form

$$\frac{g_K}{\sqrt{3}}\,\bar{B}\gamma_5 f_K(\xi_\gamma^*\xi_\gamma)\boldsymbol{\tau}\cdot(\xi_\alpha^*\boldsymbol{\tau}_{\alpha\beta}K_\beta^{\,G})B+\text{h.c.}$$

$$= \frac{g_K}{\sqrt{6}}\,[f_K(1)(3\bar{\Lambda}\gamma_5\bar{K}N-\bar{\boldsymbol{\Sigma}}\gamma_5\cdot\bar{K}\boldsymbol{\tau}N)-f_K(2)(3\bar{\Xi}\gamma_5K^G\Lambda-\bar{\Xi}\gamma_5\boldsymbol{\tau}K^G\cdot\boldsymbol{\Sigma})]+\text{h.c.}, \tag{18}$$

where

$$\Sigma_1 = -\frac{\Sigma^+ - \Sigma^-}{\sqrt{2}}, \qquad \Sigma_2 = -i\frac{\Sigma^+ + \Sigma^-}{\sqrt{2}}, \qquad \Sigma_3 = \Sigma^0. \tag{19}$$

The separation of the K-meson interaction from the whole interaction (16) breaks down the generalized RGS of the latter and causes the former interaction to be not RGS-invariant. This violation of RGS would be more manifest in real K-meson processes than in virtual processes, where one would have to sum over all $M_{i\alpha}$ virtual states, making use, therefore, of the full interaction (16). Thus, this generalized RGS would offer a possible answer to the known Pais question [5]).

3. Possible Role of Fundamental Isospin in Strong Interactions

Previously [7]), it was conjectured that leptons have an isospin equal to the strange isospin

$$\mathbf{T}^{\mathrm{L}} = \int \mathrm{d}_3 x L^*(x) \tfrac{1}{2} \xi_\alpha^* \tau_{\alpha\beta} \xi_\beta L(x). \tag{20}$$

This conjecture leads to the charge formula

$$Q^L = T_3^{\mathrm{L}} + \tfrac{1}{2} S^{\mathrm{L}}, \qquad \text{where } S^{\mathrm{L}} = -\int \mathrm{d}_3 x L^*(x) \xi_\alpha^* \xi_\alpha L(x). \tag{21}$$

and to the representation of the lepton field

$$L(x) = \begin{pmatrix} L_0(x) \\ L_\alpha(x) \\ L_{\alpha_1\alpha_2}(x) \end{pmatrix} \quad \text{or} \quad L(x) = \begin{pmatrix} \nu \\ \nu', \mathrm{e}^- \\ \mu^- \end{pmatrix}, \tag{22}$$

where

$$\nu = L_0, \quad \left.\begin{matrix} \nu' \\ \mathrm{e}^- \end{matrix}\right\} = L_\alpha, \quad \mu^- = \frac{L_{12} - L_{21}}{\sqrt{2}} \tag{23}$$

Both (21) and (22) are consistent with the experimental list of leptons, provided there are two types of neutrino, ν and ν'.

We should like to present now an argument in favour of the second possibility for the K-meson isospin. In this case, the K-meson has a fundamental isospin 1 like the π-meson. But in the case of pions it is natural to suspect that just this fundamental isospin 1 causes their strong coupling to pairs of baryons having fundamental isospins $\frac{1}{2}$, whereas any strong coupling of pions to leptons is impossible, since leptons have no fundamental isospin. Assuming that the fundamental isospin is the reason of all strong couplings and the K-meson has a fundamental isospin 1 like the pion, one can understand the presence of strong K-meson baryon interactions and the lack of strong K-meson-lepton interactions. From this point of view a kind of generalized RGS is likely, because then scalars with respect to fundamental isospin indices must occur in strong couplings.

The validity of generalized RGS might be intimately connected with some, so far undiscovered, pseudoscalar (or scalar) bosons, which could be derived from the same boson field $M_{i\alpha}$ as the K-mesons. Indeed, the reduction of $M_{i\alpha}$ leads to four additional single-strange mesons having charges $+e$, 0, $-e$, $-2e$ and to their four antiparticles having charges $-e$, 0, $+e$, $+2e$. From the formal point of view these mesons might as well be excluded as real particles by some constraints.

This single-strange quartet following from $M_{i\alpha}$ would have the same zero spin and the same intrinsic parity as the K-meson doublet. Thus it must not be confused with the possible 878 MeV resonance in $\pi\bar{\mathrm{K}}$ interaction suggested recently by experiment.

If the idea of baryon and lepton classification expressed in formulae (5) and (22) could be extended to mesons, one would write

$$M(x) = \begin{pmatrix} M_i(x) \\ M_{i\alpha}(x) \\ M_{i\alpha_1\ \alpha_2}(x) \end{pmatrix}, \tag{23}$$

where M_i would be the pion triplet π_i and $M_{i\alpha}$ would give both the K-meson doublet and the new quartet just mentioned; finally $M_{i\alpha_1\alpha_2}$ would reduce to a double-strange new triplet $\frac{1}{2}\sqrt{2}\ (M_{i12}-M_{i21})$ corresponding to charges 0, $-e$, $-2e$ (the antiparticles would have charges 0, $+e$, $+2e$). These new mesons either would be real particles (e.g. observable as resonances) or should be cancelled as real particles by some subsidiary conditions. Speculations on these formal possibilities might be attractive, but certainly premature. Notice that the isoscalar meson π_0^0 or ρ, not observed experimentally, does not appear in the scheme (23).

I should like to express my gratitude to Professor R. Oppenheimer for his kind hospitality extended to me at the Institute for Advanced Study in Princeton. Also I am much indebted to Professor A. Pais and to Professor C. N. Yang for stimulating discussions.

References

1) D. Amati, A Stanghellini and B. Vitale, Nuovo Cim. **13** (1959) 1143; Phys. Rev. Lett. **5** (1960) 524
2) Ph. Mayer, J. Prentki and Y. Yamaguchi, Phys. Rev. Lett. **5** (1960) 442
3) T. D. Lee and C. N. Yang, Phys. Rev. (submitted for publication)
4) R. H. Dalitz, UCRL – 9543 (1961)
5) A. Pais, Phys. Rev. **110** (1958) 574, 1480, **112** (1958) 624; Nuovo Ci. **18** (1960) 1003, UCRL–9460 (1960)
6) M. Gell-Mann, Phys. Rev. **106** (1957) 1296
7) W. Królikowski, Nuclear Physics **8** (1958) 461, **17** (1960) 421, **23** (1961) 53

1.B

Nuclear Physics **26** (1961) 97—107; © *North-Holland Publishing Co., Amsterdam*

Not to be reproduced by photoprint or microfilm without written permission from the publisher

A CLUSTER MODEL REPRESENTATION FOR THE 3-BODY GROUND STATE

JAMES E. YOUNG and PAUL R. STEIN

University of California, Los Alamos Scientific Laboratory, Los Alamos, New Mexico †

Received 20 January 1961

Abstract: We have considered the representation of the 3-body ground state as a deuteron plus extra particle. Calculations in this model are done in a very approximate way. In particular, the actual Hamiltonian of the system is not diagonalized in any order. The "model" Hamiltonian containing the chosen nuclear correlations is, of course, utilized properly. We present calculations of the magnetic moment and Coulomb radius for the specific model. The latter result, plus that arising from diagonalization of the "model" Hamiltonian and wave function normalization, furnishes a set of three equations. In the analogous intermediate coupling expansion of the ground state, there are an equal number of admixture coefficients to be determined. Basis wave functions in the deuteron and extra particle are given. These are generated by a separable, non-local potential and are particularly well-suited for eventual diagonalization of the actual Hamiltonian through a variational principle.

1. Introduction

It is often thought useful to represent the structure of an A-particle system as a composite of several sub-systems. For example, the nucleus Li^6 has been represented by several authors as a deuteron plus α-particle. When we follow such a procedure and, indeed, diagonalize the appropriate energy matrix, we are working with the so-called cluster model of the A-particle system.

The use of such models carries a great many ramifications. Indeed, the constituent substructures carry along their own properties: the binding energy, nucleon density and static electric and magnetic moments. In the most modest descriptions the electromagnetic properties are ignored. This neglect possibly furnishes the greatest objection to the cluster models. As the addition of constituent spins is a geometrical problem, the models incorporate this feature without difficulty. In addition, since we employ the cluster model for very light nuclei, generally $A \leqq 10$, and the constituent sub-systems usually have even parity, this aspect gives no trouble.

Perhaps the current interest in cluster models has received new impetus as a result of certain types of direct-reaction data. Unfortunately for our general understanding, these seem insensitive to certain correlations within the nucleus. The result is then a model compatible with a specific cross section determination but otherwise inadequate, or possibly so. A convincing demon-

† Work performed under the auspices of the U. S. Atomic Energy Commission.

stration of general validity would be the quantitative determination of the expectation of several spin moments †. Additionally, one would also like to see angular correlation data discussed and also those dealing with processes such as (n, 2n) and (γ, n).

In the current note, we present a cluster model *representation* of the 3-body ground state. This is *only* a representation, as we have not carried through the problem of diagonalizing the energy matrix. Indeed, the characterization arose out of some work on the reactions D(d, n), T(p, n) and p—T scattering. Our motivation for using the representation was first that of simplicity. Then, too, the representation of Thomas [1]) and the knowledge of the fractional parentage representation suggested that the analogous situation in very light nuclei might be reflected by the representation noted. Finally, we knew that the Brueckner theory, in a vastly modified way, gave the clue as to how one constructed wave functions with certain specific correlations. It was then straightforward to introduce a set of interaction operators to achieve our ends.

The model employed here represents the 3-body system as a "deuteron" plus nucleon. The deuteron wave function is generated by an interaction which acts in the $^1S_0$ and $^3S_1$ states. It is immediate that such a model has intrinsic difficulties. First, a physical deuteron has an r.m.s. radius which exceeds the 2.2 fm Coulomb radius of He^3. Next, the singlet state is virtual and the distance within which the nucleons tend to cluster is fairly large. Moreover, the wave function is that satisfying continuum boundary conditions. Finally, the extra nucleon, which moves with its position correlated with the c.m. of the two-body system, has a spectrum of eigenstates. There is considerable ambiguity in the way in which these are selected.

Nevertheless, we shall proceed to discuss our representation, beset as it is with limitations. In the next section the basic details of the construction of a model are given. This is followed by an enumeration of the correlations which are singled out and the operators which generate these. The wave functions for the deuteron cluster and the extra particle are explicitly constructed. Some consideration is then given to the specification of parameters which appear in the description. The wave functions are then combined, in sect. 3, into an analgous intermediate coupling wave function for the 3-body ground state. This involves definition of an LS-coupling basis and the introduction of relevant admixture parameters. The normalization of the ground state wave function furnishes one relation between these parameters. Determination of the binding energy gives a second relation.

As it turns out here, there are three admixture parameters in our representation. The third relation between these is obtained by computing the magnetic moment of the ground state system. The corresponding computation is carried

† The differential cross section is given by the expectation of a tensor of rank zero. The polarization involves tensors of higher rank.

out in sect. 4. Two methods of evaluation are considered. In the first of these, the magnetic moment operator is decomposed into a sum of terms for the two-particle system and the extra nucleon. The separate operators are then expressed in terms of the spin and orbital operators for the constituent sub-systems. As it is simpler, we perform the required computations for the H^3 system, eventually transforming to a *jj*-coupling representation. The second calculation is in a total angular momentum representation and it serves to check the previous evaluation. It is easy to see from our results that it is not possible to obtain the measured magnetic moment of the 3-body ground state. For H^3 we then adopt a procedure which involves suppressing the neutron contribution to the moment. This procedure provides us with the third of a set of three equations in an equal number of admixture coefficients. It turns out that the set of equations has no physically meaningful solutions. As a result of this, an alternate datum must be sought.

The next physical quantity is available to us only because of an assumption. If we take the charge and matter radii to be equal for the 3-body system, then the Coulomb radius of He^3 is said to be the radius appropriate for the system. Of course the assumption is not correct. However, in the order of approximation in which we choose to work, no serious error is involved. The calculation of the Coulomb radius appears in sect. 5. This provides a consistent set of equations and allows us to determine the admixture coefficients.

In sect. 6 we discuss some of the applications we have made using the cluster model representation. The principal results obtained are summarized and a recapitulation of the restrictive nature of our findings given. It is to be emphasized that this analysis is published as an illustration of the various considerations inherent in the representation.

We do not necessarily believe that such models clarify our understanding of nuclear systems until such time as their connection with the rigorous description is outlined. On the other hand, a serious effort on the part of several workers [2]) has given us some feeling for the surprisingly large scope of the cluster model. We do feel, however, that it is fair to pose several questions. Clustering ought to occur whenever it is energetically favourable for a subsystem to lower its state. Are we entitled to ask that the lifetime of such an entity be consistent with the extrapolated mean-free-path data obtained from the optical model? Clustering, if it exists, is intimately related to the strength with which the exlusion principle operates. In some limit, say at normal nuclear density, the effect will be quenched. Can we put this on a quantitative basis which is reliable? At the very least, clustering is related to some aspect of collective behaviour. In our most elementary conceptual scheme the clusters have a rotational spectrum. This involves a very few quanta of excitation if the system is to stay intact. Many reactions involving α-particles, He^3, etc., devolve upon considerable transfers of angular momentum. Are these data consistent

with the existence of clustering models? Finally, it is not a little disturbing to contemplate a scheme giving at the worst two numbers, nuclear density, and energy per nucleon, and at the best the additional quantity, level separations. This alone is not enough to reject the representation. But, what is to be done in regard to the predictions of β-decays and the electromagnetic moments? Perhaps these are, after all, non-allied questions.

2. Basis Wave Functions for Model

Being given the Hamiltonian

$$H = \sum^{3} T_1 + \sum_{i<j}^{3} v_{ij}$$

for the 3-body system, we ought to minimize the expression

$$J = \int \Psi^* H \Psi \, d\tau \Big/ \int \Psi^* \Psi \, d\tau, \tag{2}$$

using whatever wave function $\Psi(\mathbf{r}, \mathbf{x}_1)$ of the cluster is appropriate. The coordinate designations are $\mathbf{r} = \mathbf{r}_2 - \mathbf{r}_3$ and $\mathbf{x}_1 = \mathbf{r}_1 - \frac{1}{2}(\mathbf{r}_2 + \mathbf{r}_3)$. In giving the form of Ψ we shall have selected the form of the correlations deemed important for the model. The principal utility of the cluster model is the representation of Ψ in the form of an expansion

$$\Psi(\mathbf{r}, \mathbf{x}_1) = \sum c_{\alpha\beta} \psi_\alpha(\mathbf{r}) \psi_\beta(\mathbf{x}_1). \tag{3}$$

We seek to determine here the basis functions which we imagine to satisfy the equations

$$(E_\alpha - T_{\mathbf{r}}) \psi_\alpha(\mathbf{r}) = \int d\mathbf{r}' v(\mathbf{r}, \mathbf{r}') \psi_\alpha(\mathbf{r}'), \tag{4}$$

$$(E_\beta - T_{\mathbf{x}_1}) \psi_\beta(\mathbf{x}_1) = \int d\mathbf{x}'_1 v(\mathbf{x}_1, \mathbf{x}'_1) \psi_\beta(\mathbf{x}'_1). \tag{5}$$

It will often be convenient to use different designations for the energy eigenvalues. Since α and β are generic labels only, this should not cause confusion. In the preceding equations, the energy operators are

$$T_{\mathbf{r}} = -(\hbar^2/M)\nabla_{\mathbf{r}}^2, \quad T_{\mathbf{x}_1} = -(3\hbar^2/4M)\nabla_{\mathbf{x}_1}^2.$$

To solve eq. (4) for the two-body system, we adopt the procedure of Yamaguchi [3]). The Fourier transform is taken, giving

$$(\mathbf{p}^2 + \alpha^2)\Psi(\mathbf{p}) = -\eta \int d\mathbf{p}' (\mathbf{p}|v|\mathbf{p}') \Psi(\mathbf{p}'), \quad \alpha^2 = (ME/\hbar^2), \quad \eta = M/\hbar^2. \tag{6}$$

For an S-wave system the non-local potential is given by

$$(\mathbf{p}|v|\mathbf{p}') = (\lambda/\eta) g(\mathbf{p}) g(\mathbf{p}'), \quad g(\mathbf{p}) = (\beta^2 + p^2)^{-1}. \tag{7}$$

In order to admit both singlet and triplet configurations, both the parameters

β and λ are given the corresponding designations, e.g. β_s and β_t. For the triplet state the binding energy and normalization of the wave function involve two parameters β_t and λ_t. It is straightforward to show that the corresponding wave function is

$$\begin{aligned} \psi_0^{(3)}(\mathbf{r}) &= (\tfrac{1}{2}\pi)^{\frac{1}{2}} N_t(\beta_t^2-\alpha_t^2)^{-1} r^{-1}(e^{-\alpha_t r}-e^{-\beta_t r}), \\ N_t^2 &= \pi^{-2}\alpha_t\beta_t(\alpha_t+\beta_t)^3, \quad \lambda_t^{-1}(\alpha_t) = \pi^2\beta_t^{-1}(\alpha_t+\beta_t)^{-2}. \end{aligned} \tag{8}$$

Here α_t is the binding wave number for a physical deuteron, i.e. $\hbar^2\alpha_t^2/M = 2.23$ MeV, and β_t is determined from effective range theory as $\beta_t = 1.45$ fm^{-1}. The reader should refer to the Yamaguchi papers cited for details.

Now the singlet state wave function can be shown to have the form

$$\psi_0^{(1)}(\mathbf{r}) = A''\left[1-\frac{a_s}{r}(1-e^{-\beta_s r})\right], \tag{9}$$

if it is assumed to "bind at zero energy." The quantities entering here are the singlet scattering length a_s and the parameter $\beta_s = \beta_t$. Evidently, the function as given is non-normalizable. We are led to resort to a device here. One such is to introduce a convergence factor through the replacement

$$A'' \to A' e^{-r/2r_0}. \tag{10}$$

When this is done and r_0 is taken to be of the order of the physical dimensions of the 3-body system, A' is determined by normalizing the wave function over all space. The alternative to this is to determine A'' in expression (9) by cutting off the normalization integral at r_0. Due to the fact that we have many matrix elements to evaluate during the subsequent development, there is considerable advantage in having unrestricted integrals. Another aspect is valuable here for introducing a further approximation. The very large value of $\beta_s a_s$, namely -34.4, means that this product determines the behaviour of expression (9) for small r. The term involving unity is only important for "large" r and we do not care about the error in the wave function beyond ≈ 2.5 fm. We can, in view of the magnitudes involved, use the approximate representation

$$\begin{aligned} \psi_0^{(1)}(\mathbf{r}) &= a_s A(\alpha_2^2-\alpha_1^2)^{-1}(\tfrac{1}{2}\pi)^{\frac{1}{2}} r^{-1}(e^{-\alpha_1 r}-e^{-\alpha_2 r}), \\ a_s^2 A^2 &= \pi^{-2}\alpha_1\alpha_2(\alpha_1+\alpha_2)^3, \quad \alpha_1 = 2/r_0+\beta_s, \quad \alpha_2 = 2/r_0. \end{aligned} \tag{11}$$

We shall use either this form or that implied by the substitution (10) in all of the subsequent computations. Finally, we observe that the deuteron wave functions are completed by appending the spin functions for the singlet and triplet states.

The kinds of functions, i.e. the orbital states, we construct for the extra particle have been determined by the constructions for the deuteron states. In view of the difficulty experienced with the singlet state of the latter, a natural question arises: why consider it at all? Our earlier calculations [4]) of

T(p, n) gave at least one unambiguous result: the scattering of protons from the deuteron core was appreciable in the doublet state. The same result appears to hold true in the analysis of p—T elastic scattering [5]).

The single particle orbital states of even parity which make up the spin one-half state of the 3-body system are $l_p = 0$ and $l_p = 2$. The single particle equation (5) is transformed to give an equation such as (6). The generalization of eq. (7) is, however,

$$(\mathbf{p}'|v|\mathbf{p}) = -\sum (\lambda_l/\eta_1)\, Y_{lm}(\mathbf{p}) Y^*_{lm}(\mathbf{p}') g_l(p) g_l(p'). \tag{12}$$

It is found that the relevant wave function is given by

$$\begin{aligned}
&\Psi_{lm}(\mathbf{x}_1) = N_l \sqrt{8\pi} i^l Y_{lm}(\mathbf{x}_1) f_l(\alpha_l, \beta_l; x_1), \\
&\qquad N_l^2 = \pi^{-2}\alpha_l\beta_l(\alpha_l+\beta_l)^3, \quad \lambda_l^{-1}(\alpha_l) = \beta_l^{-1}\pi^2(\alpha_l+\beta_l)^{-2}, \quad \eta_1 = 4M/3\hbar^2, \\
&f_l(\alpha_l, \beta_l; x_1) = \left\{ \frac{\alpha_l}{\beta_l^2-\alpha_l^2} F_l(\alpha_l x_1) - \frac{\beta_l}{\beta_l^2-\alpha_l^2} F_l(\beta_l x_1) \right\}, \\
&\qquad F_l(\lambda r) = \int_0^1 \mathrm{d}z e^{-\lambda r z} P_l(z).
\end{aligned} \tag{13}$$

The quantity α_l^2 is defined as $|E_l|\eta_1$ and we find it convenient to denote the energy eigenvalues $|E_l|$ as E_D, $l = 0$, and E_Q, $l = 2$. Corresponding labels α_D and α_Q are introduced and the designations imply that the extra particle is in the doublet and quartet states of total angular momentum. These single particle states are non-degenerate and we would like to estimate their positions and separations. To do this we make the assumption that the doublet state is bound by 8 MeV, i.e. $E_D = 8$ MeV. This is not a critical specification; however, it is possible to show from the energy equation which we eventually derive that a value as small as 4 MeV is unacceptable. The variational principle applied to expression (2) would render the sort of estimate made here superfluous. However, from the point of view of the present semi-quantitative analysis, no profoundly large errors appear because of our assumptions. Next, the spacing of the quartet and doublet levels is fixed by considering the corresponding interval in an equivalent spherical square well. This well is chosen such that it just binds the 2s-state at zero energy. The (1d/1s)-ratio is then approximately 0.25 and we have $E_Q = 2$ MeV. Both of the binding energies E_D and E_Q are fairly large and are probably 15 % larger than they should be.

A final word is appropriate regarding the single particle functions. Two range parameters β_0 and β_2 enter the descriptions of the states. These are taken to be equal to each other. An analysis of the T(p, n) problem [4]) gave $\lambda_0 = 0.6$ fm^{-3}, and this value, together with eq. (11), allows us to determine β_0 as 1.42 fm^{-1}, which is very nearly equal to the corresponding n—p parameter of Yamaguchi. An alternate determination of λ_0 is also provided by effective range theory.

3. Analogous Intermediate Coupling Wave Function

Next we should like to combine the wave functions already discussed to form the 3-body ground state. The admixture coefficients introduced in this process carry the total spin designations for both sub-systems: singlet and triplet deuteron, doublet and quartet extra particle. Also, the LS-coupling notation ${}^{2S+1}L_J$ is employed for the configurations making up the wave function. Our result, an analogous intermediate coupling form, is

$$\Psi_{\frac{1}{2}}{}^{M}(\mathbf{r}, \mathbf{x}_1) = a_{D1}{}^{2}S'_{\frac{1}{2}} + a_{D3}{}^{2}S''_{\frac{1}{2}} + a_{Q3}{}^{4}D_{\frac{1}{2}}. \tag{14}$$

The constituent wave functions are

$$\begin{aligned} {}^{2}S'_{\frac{1}{2}} &= \chi_0(23)\chi_{\frac{1}{2}}{}^{M}(1)\psi_0{}^{(1)}(r)\Psi_{00}(x_1), \\ {}^{2}S''_{\frac{1}{2}} &= \sum \begin{bmatrix} 1 & \frac{1}{2} & \frac{1}{2} \\ m_s & n & M \end{bmatrix} \chi_1{}^{m_s}(23)\chi_{\frac{1}{2}}{}^{n}(1)\psi_0{}^{(3)}(r)\Psi_{00}(x_1), \end{aligned} \tag{15}$$

$${}^{4}D_{\frac{1}{2}} = \sum \begin{bmatrix} 2 & \frac{3}{2} & \frac{1}{2} \\ m & M_s & M \end{bmatrix} \Psi_{2m}(\mathbf{x}_1)\psi_0{}^{(3)}(r) \sum \begin{bmatrix} 1 & \frac{1}{2} & \frac{3}{2} \\ m_s & n & M_s \end{bmatrix} \chi_1{}^{m_s}(23)\chi_{\frac{1}{2}}{}^{n}(1). \tag{16}$$

Normalization provides one relation between the admixture coefficients:

$$a_{D1}^2 + a_{D3}^2 + a_{Q3}^2 = 1. \tag{17}$$

A second relation between the admixture coefficients is supplied by the energy statement. This we interpret as meaning that the expectations of the "model" Hamiltonians (4) and (5) †, in particular their sum, gives the binding energy of the 3-body ground state. The particular relation for H^3 is

$$8a_{D1}^2 + 10.23a_{D3}^2 + 4.23a_{Q3}^2 = 8.48. \tag{18}$$

It is again clear that in an approximate diagonalization of the Hamiltonian (1), such a relation would not survive. The variational principle $\delta J = 0$ would provide us with the best values of the admixture parameters. However, due to the discursive nature of the present work, this oversight is left to be corrected in a subsequent note [6]). For the present we seek a third relation to supplement the relations (17) and (18). This is the subject of the next two sections.

4. Magnetic Moment Determinations

A calculation of the magnetic moment on the basis of the model under discussion is known a priori to be poor. The role played by two-body exchange forces in the real 3-body system is of such a nature as to profoundly affect the magnetic moment. This expression of Siegert's theorem makes any computation we might do completely academic. It is, nevertheless, interesting to see what a crude evaluation gives.

† The corresponding Hamiltonians are implied by the integral statements of these equations.

Starting from the ususal definition of the magnetic moment operator with proton (p) and neutron (n) designations,

$$\boldsymbol{\mu} = \mu_0[\sum_i \mathbf{l}_p(i) + \mu_p \sum_i \boldsymbol{\sigma}_p(i) + \mu_n \sum_j \boldsymbol{\sigma}_n(j)],$$

$$\mu_0 = e\hbar/2Mc,\ \mu_p = \tfrac{1}{2}g_p = 2.79255,\quad \mu_n = \tfrac{1}{2}g_n = -1.91280,$$

we decompose the operator into two parts. The resulting contributions arising from the nucleon and the two-particle cluster for H^3 are respectively,

$$^1\boldsymbol{\mu} = 2\mu_0\mu_n \mathbf{s}_n(1), \tag{19}$$

$$^2\boldsymbol{\mu} = \mu_0[(\mu_p+\mu_n)\mathbf{S} + (\mu_p-\mu_n)[\mathbf{s}_p(2)-\mathbf{s}_n(3)] + \tfrac{1}{2}\mathbf{L}]. \tag{20}$$

The expectations of these operators in eq. (14) for the state $M = \frac{1}{2}$ are straightforward to compute. In anticipation of some later work, we have found it convenient to transform to a jj-coupling basis first, and then to use the methods of Racah in evaluating the matrix elements of the tensor operators.

In the notation α_{LS}^{jJ} the transformation coefficients are, in terms of $9j$-symbols,

$$\alpha_{0\frac{1}{2}}^{\frac{1}{2}0} = 2\begin{Bmatrix} 0 & 0 & 0 \\ \frac{1}{2} & 0 & \frac{1}{2} \\ \frac{1}{2} & 0 & \frac{1}{2} \end{Bmatrix},\quad \alpha_{0\frac{1}{2}}^{\frac{1}{2}1} = 2\sqrt{3}\begin{Bmatrix} 0 & 0 & 0 \\ \frac{1}{2} & 1 & \frac{1}{2} \\ \frac{1}{2} & 1 & \frac{1}{2} \end{Bmatrix},\quad \alpha_{2\frac{1}{2}}^{\frac{3}{2}1} = \begin{Bmatrix} 2 & 0 & 2 \\ \frac{1}{2} & 1 & \frac{3}{2} \\ \frac{3}{2} & 1 & \frac{1}{2} \end{Bmatrix}, \tag{21}$$

or each coefficient is equal to unity. After a great deal of tedious manipulation and the carrying out of magnetic sums, we obtain the result

$$\begin{aligned}
&\langle \Psi_{\frac{1}{2}}^{M} | \boldsymbol{\mu} | \Psi_{\frac{1}{2}}^{M} \rangle_{M=\frac{1}{2}} \\
&= 2(\mu_p+\mu_n)[-3a_{D3}^2 W(1\,1\,1\,1;\,0\,1) W(\tfrac{1}{2}\,1\,\tfrac{1}{2}\,1;\,\tfrac{1}{2}\,1) + 3a_{Q3}^2 W(1\,1\,1\,1;\,0\,1) W(\tfrac{1}{2}\,1\,\tfrac{1}{2}\,1;\,\tfrac{3}{2}\,1] \\
&+ 2\mu_n[2a_{D1}^2 W(\tfrac{1}{2}\,\tfrac{1}{2}\,\tfrac{1}{2}\,\tfrac{1}{2};\,0\,1) W(\tfrac{1}{2}\,0\,1\,\tfrac{1}{2};\,\tfrac{1}{2}\,\tfrac{1}{2}) + 2a_{D3}^2 W(\tfrac{1}{2}\,\tfrac{1}{2}\,\tfrac{1}{2}\,\tfrac{1}{2};\,0\,1) W(\tfrac{1}{2}\,1\,1\,\tfrac{1}{2};\,\tfrac{1}{2}\,\tfrac{1}{2}) \\
&- 4a_{Q3}^2 W(\tfrac{3}{2}\,\tfrac{1}{2}\,\tfrac{3}{2}\,\tfrac{1}{2};\,2\,1) W(\tfrac{1}{2}\,1\,1\,\tfrac{3}{2};\,\tfrac{3}{2}\,\tfrac{3}{2})]
\end{aligned}$$

in units of μ_0. The Racah coefficients have been left unevaluated here to facilitate the tracing out of the vector couplings. We shall give an explicit relation for the moment very shortly.

As is well known, it is possible to compute the magnetic moment from the statement

$$\boldsymbol{\mu} = \frac{\boldsymbol{\mu}\cdot\mathbf{J}}{J(J+1)}\mathbf{J},$$

$\mathbf{J}$ being the total angular momentum of the 3-body system. Again, $\boldsymbol{\mu}$ decomposes into two contributions, as previously noted. The angular momentum $\mathbf{L}$ of the deuteron does not contribute to the moment since we consider the system to be in an S-state. In addition, the operator $\mathbf{s}_p(2)-\mathbf{s}_n(3)$ gives no contribution

in the triplet state, and due to the absence of P-states, gives no contribution whatsoever. We find, then, that the magnetic moment is given as the expectation

$$\mu = \frac{1}{(J+1)}\{2\mu_n\langle\tfrac{1}{2}(j_1^2-l_1^2+s_1^2)+\mathbf{s}_1\cdot\mathbf{j}\rangle+(\mu_p+\mu_n)\langle j^2+\mathbf{S}\cdot\mathbf{j}_1\rangle\},$$

where j and S are the total angular momentum and spin of the deuteron, and the subscripted quantities, in standard notation, refer to the extra particle. It is implied that the expectations are to be evaluated for the state of maximum projection. Again, we omit the calculations in detail and simply quote the result † for H^3:

$$\mu_n a_{D1}^2+a_{D3}^2(\tfrac{1}{3}\mu_n+\tfrac{2}{3}\mu_p)-a_{Q3}^2(\tfrac{2}{3}\mu_n+\tfrac{1}{3}\mu_p) = 1.0664\mu_p. \tag{22}$$

Examination of this equation discloses that it is not possible to achieve the measured magnetic moment. One possibility which suggests itself is that we reduce the neutron-moment in order to obtain a value closer to that for a proton. If we set the neutron contribution equal to zero, the following equation results:

$$a_{D1}^2+\tfrac{1}{3}a_{D3}^2-\tfrac{2}{3}a_{Q3}^2 = 0. \tag{23}$$

The system of eqs. (23), (18) and (17) is then seen to provide only a small fraction of the measured magnetic moment, but also to produce a meaningless set of values for the admixture coefficients. This situation also persists when we employ the system consisting of eqs. (22), (18) and (17).

5. Radius of Charge Distribution

It is less frivolous to compute the Coulomb energy and thereby the Coulomb radius of He^3. Here the extra nucleon is a proton and in the two-body cluster, nucleon 2 carries the charge. The equation which we solve here is

$$V_{Coul}/m_e c^2 = r_e\langle\Psi_{\frac{1}{2}}^M|r_{12}^{-1}|\Psi_{\frac{1}{2}}^M\rangle, \tag{24}$$

where $V_{Coul} = 0.76$ MeV, $m_e c^2 = 0.51$ MeV and r_e is the classical electron radius. In addition to the modified wave function of eq. (11) for the cluster, we also introduce the following approximation for the D-state single-particle wave function:

$$\begin{aligned}\Psi_{2\mu}(\mathbf{x}_1) &= (-1)^\mu Y_{2\mu}(\mathbf{n}_{x_1})f_2(\alpha_Q,\beta_2;x_1),\\ f_2(\alpha_Q,\beta_2;x_1) &= C_2(\beta_2^2-\alpha_Q^2)^{-1}[x_1^{-1}(e^{-\beta_2 x_1}-e^{-\alpha_Q x_1})],\quad C_2^2 = 8\pi N_2^2.\end{aligned} \tag{25}$$

The definition of N_l^2 for $l = 2$ is obtained from eq. (13). This approximation is not a serious one as long as the D-state admixture, represented by a_{Q3}, is fairly small in the wave function. What we have achieved by employing this

† This is a result equating the theoretical and experimentally determined moments.

representation and, in addition, that previously noted, is a considerable simplification of the formal work.

Note first that the Green's function r_{12}^{-1} is given by

$$r_{12}^{-1} = \sum_l P_l(\cos\omega)(\tfrac{1}{2}r)^l/x_1^{l+1}, \quad (x_1 > \tfrac{1}{2}r),$$

$$P_l(\cos\omega) = \sum_{m=0} \varepsilon_m \frac{(l-m)!}{(l+m)!} P_l^m(\cos\vartheta_r) P_l^m(\cos\vartheta_{x_1})\cos m(\varphi_r - \varphi_{x_1})$$
$$\equiv \sum \varepsilon_m A_m \cos m\Delta\varphi.$$

The Neumann number ε_m is defined according to $\varepsilon_m = 1$ for $m = 0$ and $\varepsilon_m = 2$ for $m \neq 0$. Then, utilizing the fact that

$$P_l^{-m} = (-1)^m \frac{(l-m)!}{(l+m)!} P_l^m,$$

it is apparent that $A_m = A_{-m}$, whereupon we find

$$\sum_{m=0}^{l} \varepsilon_m A_m \cos m\Delta\varphi = \sum_{-l}^{l} A_m e^{im\Delta\varphi},$$

$$P_l(\cos\omega) = \sum \frac{(l-m)!}{(l+m)!} P_l^m(\cos\vartheta_r) P_l^m(\cos\vartheta_{x_1}) e^{im(\varphi_r - \varphi_{x_1})}$$
$$= \sum \frac{4\pi}{[l]} Y_{lm}(\mathbf{n}_r) Y_{lm}^*(\mathbf{n}_{x_1}) \equiv \sum C_m^{(l)}(\mathbf{n}_r) C_m^{*(l)}(\mathbf{n}_{x_1}).$$

Each of the wave functions is a sum of Yukawa potentials. And it is straightforward to show that in approximation (25) there is no contribution from the D-state to the matrix element (24). We have already observed that the approximate form (11) is in error for large values of r. In this section, we cut off the integrals in which it appears at $R_1 = 2.2$ fm, the Coulomb radius of He^3 calculated on the basis of the so-called uniform model.

We employ the following notation:

$$\psi_0^{(1)}(r) = {}^1C \sum_{k=1}^{2} \varepsilon_k r^{-1} e^{-\alpha_{1k} r}, \quad \Psi_{00}(x_1) = C_D \sum_{p=1}^{2} \varepsilon_p r^{-1} e^{-\alpha_{Dp} x_1},$$

and a similar statement for $\psi_0^{(3)}(r)$. In the preceding expressions, we have, for example, $\alpha_{11} = 2/r_0 + \beta_s$, $\alpha_{12} = 2/r_0$, ${}^1C^2 = (2\pi)^{-1}\alpha_1\alpha_2 \quad (\alpha_1+\alpha_2)(\alpha_2-\alpha_1)^2$, $\alpha_{D1} = \beta_0$, $\alpha_{D2} = \alpha_D$. It may be checked that these results involve only quantities which we have previously defined. A typical calculation using these forms is summarized by the following statement:

$$\langle \psi_0^{(1)}(r)\Psi_{00}(x_1) | r_{12}^{-1} | \psi_0^{(1)}(r)\Psi_{00}(x_1)\rangle$$
$$= {}^1C^2 C_D{}^2 (4\pi)^3 \sum_{kk'\,pp'} ({}^1\mu_{kk'})^{-1} \varepsilon_k \varepsilon_{k'} \varepsilon_p \varepsilon_{p'} [-\mathrm{Ei}(-\nu_{pp'}^D R_1)],$$

which involves the tabulated exponential integral and the quantities

${}^1\mu_{kk'} = \alpha_{1k}+\alpha_{1k'}$, $v^{\mathrm{D}}_{pp'} = \alpha_{\mathrm{D}p}+\alpha_{\mathrm{D}p'}$. After performing the various evaluations indicated by eq. (24), we obtain the equation

$$0.53 = 0.596\, a^2_{\mathrm{D1}}+0.560\, a^2_{\mathrm{D3}}. \tag{26}$$

This expression, together with those given by eqs. (17) and (18), determines the admixture coefficients. Our summarizing results are

$$a_{\mathrm{D1}} = 0.697, \quad a_{\mathrm{D3}} = 0.608, \quad a_{\mathrm{Q3}} = 0.384. \tag{27}$$

6. Discussion and Conclusions

The aim here has been to present a schematic and indeed semi-quantitative discussion of one form of the 3-body cluster model representation. Clearly, the analysis is illustrative and the serious discussion would involve the variational principle. It is expected that the latter would lower the D-state contribution, namely a_{Q3}, considerably. The use of the factorable, non-local potential in eqs. (4) and (5) introduces some simplifications, as we have seen, and several difficulties along with these. In an improved analysis, the effective parameters α_1 and α_2 of the approximate form (11) would also be determined variationally. This removes the serious objection to the way in which the singlet deuteron state has been treated here. The wave functions of eqs. (8), (11) and (13) are especially well-suited for the variational description. However, given the results of such a computation, we confess a certain inability to enunciate the validity and interpretation of the "equivalent" representation. For our part, and subsequent reaction analysis, we prefer to utilize the Yukawa wave functions of Pease-Feshbach [7]), the Gaussian functions of Bransden *et al.* [8]) and the recently-developed functions of Blatt *et al.* [9]). We do share the hope, however, that future studies by other workers will serve to augment the simplicity of the cluster model with a certain reality of its interpretation and necessity for its existence.

We would like to thank Dr. W. M. Visscher for reading the manuscript. Professor L. S. Rodberg made comments to one of us (J. E. Y.) concerning the discussion of sect. 5. Dr. H. E. Wegner furnished some of the reference material.

References

1) R. G. Thomas, Phys. Rev. **100** (1955) 25
2) G. C. Phillips and L. C. Biedenharn, Bull. Am. Phys. Soc. **5** (1960) 44;
V. G. Neudachin, Yu. F. Smirnov and N. P. Yudin, JETP (Soviet Physics) **10** (1960) 1256;
K. Wildermuth and Th. Kanallopoulos, Nuclear Physics **7** (1959) 150;
L. D. Pearlstein, Y. C. Yang and K. Wildermuth, Phys. Rev. **120** (1960) 224
Y. Yamaguchi, Phys. Rev. **95** (1954) 1628, 1635
4) J. E. Young and P. R. Stein, to be published
5) J. E. Young and P. R. Stein, to be published
6) J. E. Young and P. R. Stein, to be published
7) R. L. Pease and H. Feshbach, Phys. Rev. **88** (1952) 945
8) B. H. Bransden, H. H. Robertson and P. Swan, Proc. Phys. Soc. A **69** (1956) 877
9) J. M. Blatt and G. Derrick, Nuclear Physics **8** (1959) 310, 602

2.A.1

Nuclear Physics **26** (1961) 108—112; © *North-Holland Publishing Co., Amsterdam*

Not to be reproduced by photoprint or microfilm without written permission from the publisher

YIELD RATIOS OF THE ISOMERIC PAIR $Ce^{137m/137}$ FORMED BY La^{139}(d, 4n) Ce^{137} REACTION

H. VIGNAU and S. J. NASSIFF

Dto. de Física de la Universidad Nacional de La Plata and Comisión Nacional de Energía Atómica, Buenos Aires †

Received 31 January 1961

Abstract: The variation of the yield ratio between the isomeric pair formed in the reaction La^{139}(d, 4n)$Ce^{137m/137}$ for deuteron energies up to 27 MeV has been measured.

1. Introduction

Nuclear isomers being different states of the same isotope we can expect different relative yields of the isomeric pairs from different nuclear reactions or excitation energies [1–3]). By studying those relationships at variable excitation energies, an indication of the reaction mechanism may be obtained.

The purpose of the present work was to study the cross section ratio of the isomeric states $Ce^{137m}(\frac{11}{2}-)$ and $Ce^{137}(\frac{3}{2}+)$ for the (d, 4n) reaction on La^{139} (99.91 %, $\frac{7}{2}+$), bombarding with deuterons ranging between 18 and 27 MeV.

We have chosen such an isomeric pair and such a nuclear reaction in order to have the same spin difference between the target nucleus and the excited and fundamental levels of the isomeric pair.

2. Experimental

2.1. IRRADIATIONS

The targets for the experience were prepared by using the stacked foils technique. Some La_2O_3 powder was suspended in an nitrocellulose-amyl acetate solution and slurried onto thin copper foils, which were then folded over and stacked together.

The deuteron energy at each sample of the stack was calculated from the range-energy curves of Aaron, Hoffman and Williams [4]).

The irradiations were performed with the internal beam of the 180 cm diameter synchrocyclotron of the C.N.E.A. at the orbit corresponding to 28.1 MeV energy.

The maximum uncertainty in the beam energy was estimated at ± 1.2 MeV for 28.1 MeV.

† This work was partly supported by C.E.F.A.R.

The modification of the curvature radius inside the target was not enough to change the thickness of the absorber traversed by the particles.

Due to the variation of the flux across the different samples of the stack, the excitation functions of the single isomers were not determined.

2.2. CHEMICAL SEPARATIONS

The irradiated sample of La_2O_3 was transferred mechanically into a beaker.

It was dissolved in 10 ml of concentrated HNO_3; Ce^{III} carrier was added, and after oxidyzing to Ce^{IV} with saturated $KBrO_3$ solution, $Ce(IO_3)_4$ was precipitated with KIO_3 (ref. [5]).

The precipitate was dissolved in H_2O_2 with drops of concentrated HNO_3 and afterwards $Ce(OH)_3$ was precipitated with NaOH. The hydroxide was dissolved in HNO_3 and Ce^{IV} reprecipitated as above, adding previously La^{III} as hold-back carrier.

The cycle $Ce(OH)_3$, $Ce(OI_3)_4$ was repeated twice so as to make the La impurity negligible.

2.3. COUNTING METHODS

The decay scheme [6]) is sketched in fig. 1.

Two lines are prominent in the gamma spectrum, one at about 255 keV and one at 445 keV. The first one is attributed to a transition of 34.1 h Ce^{137m}

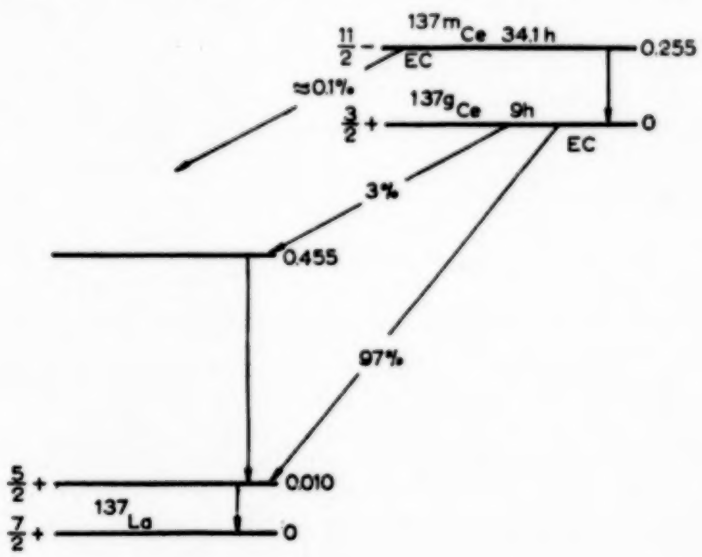

Fig. 1

decaying to Ce^{137}; the 445 keV line arises from the decay of the second excited state of daughter La^{137}.

Measuring the relative intensities of the 255 keV and 445 keV gamma rays the abundances of the 34.1 and 9.0 h levels can be determined.

The radiations of the sample were detected with a 2.54 cm × 2.54 cm sodium

iodide (Tl activated) crystal coupled to a one-channel pulse height analyzer [7]). The same geometry used in the determination of the efficiency curve was maintained during the measurements.

To prevent piling-up effects, the X-ray of the La was absorbed with a Sn foil of 0.581 g/cm² followed by one of Mo of 0.153 g/cm². The low values for the (d, 4n) reaction cross section resulted in low intensities which made the measurements difficult.

Fig. 2 shows as an example the gamma spectrum of the $Ce^{137m/137}$ corresponding to 26.9 MeV deuteron energy, some hours after the end of irradiation.

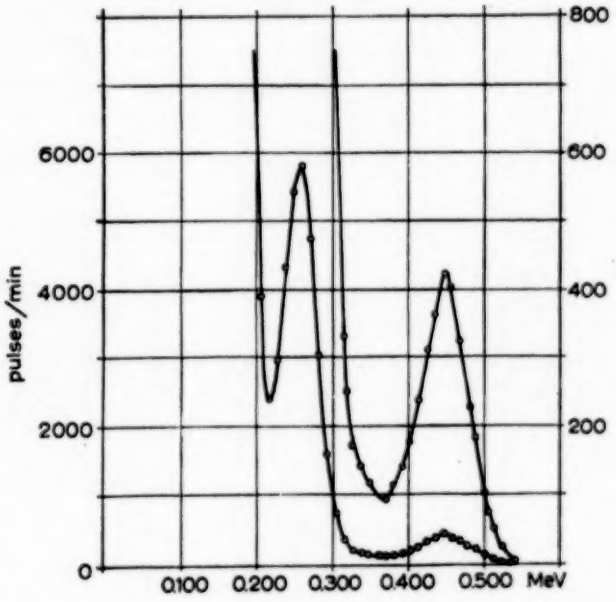

Fig. 2.

The areas under the 255 and 445 keV peaks were graphically integrated. Making the counting corrections and those corresponding to the disintegration scheme, the relative intensities of the 34.1 and 9.0 h levels were calculated for each deuteron energy.

The values of the cross-section ratios (σ_m/σ_g) for the excited and fundamental levels for different deuteron energies are given in table 1. The errors in σ_m/σ_g are of the order of 20 %.

Fig. 3 shows the curves of the variation of σ_m/σ_g, with deuteron energy.

3. Discussion

In the present case, either because the spin of the target nucleus is exactly in the middle between those of Ce^{137m} and Ce^{137}, or because the threshold for the reaction occurs only at 18 MeV, both isomeric states can be equally reached. However, as in other reactions [2, 3, 8, 9, 11]), statistical considerations may indi-

cate that the spin of the compound nucleus increases with energy [12]). Thus, the slope of the curve in fig. 3 can be qualitatively understood.

TABLE 1

Values of the cross-section ratios for the excited and fundamental levels for different deuteron energies

E (MeV)	σ_m σ_g
18.8±0.2	0.03
21.8±0.3	0.09
22.7±0.3	0.15
23.5±0.2	0.34
24.4±0.3	0.38
25.1±0.2	0.59
25.9±0.2	0.46
26.9±0.3	0.76
27.7±0.3	0.67
27.9±0.2	0.68

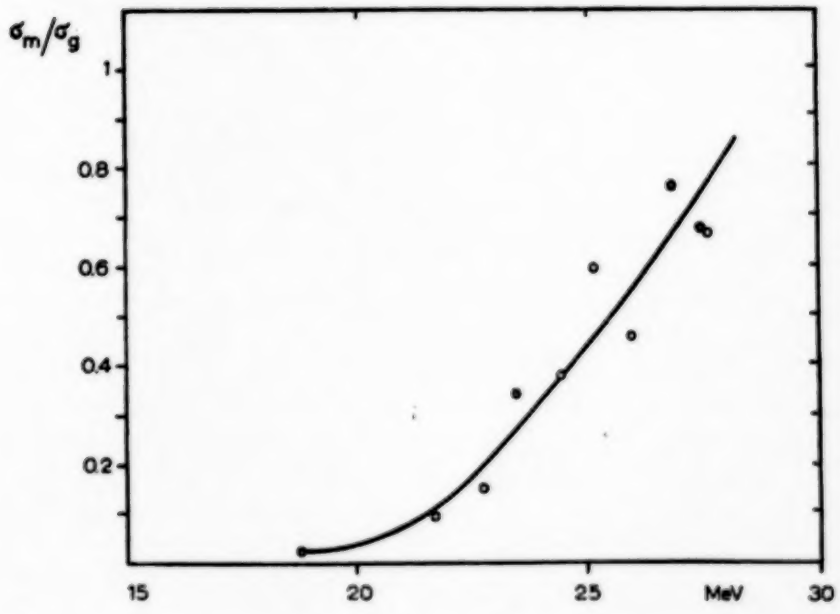

Fig. 3

The available deuteron energies do not allow decision whether there is an asymptotic value of σ_m/σ_g (ref. [13])).

We are grateful to Daniel Bès for his valuable comments and to the Synchrocyclotron group of the C.N.E.A. for the accomplished irradiations.

References

1) R. A. Sharp and A. C. Pappas, J. Inorg. Nucl. Chem. **10** (1959) 173
2) K. I. Zherebtsova, T. P. Makarova, Y. A. Nemilov and B. L. Funstein, Z. Eksp. Teoret. Fiz. **35** (1958) 1355
3) S. Abecasis and S. J. Nassiff, J. Inorg. Nucl. Chem. (in press); Publ. C.N.E.A. (1960) **38**
4) W. A. Aaron, B. L. Hoffman and F. C. Williams, UCRL report A.E.C.U. **663** (1951)
5) J. A. Seiler and L. Winsberg in The fission products, edited by C. D. Coryell and N. Sugarman (McGraw-Hill Book Co. New York 1951)
6) D. Strominger, J. M. Hollander and G. T. Seaborg, Rev. Mod. Phys. **30** (1958) 721
7) K. Franz and S. F. Pinasco, Publ. C.N.E.A. Serie Física, **1** (1957) 13
8) J. K. Meadows, R. M. Diamond and R. A. Sharp, Phys. Rev. **102** (1956) 190
9) B. Linder and R. A. James, Phys. Rev. **114** (1959) 322
10) S. M. Bailey, UCRL Report A.E.C.U. 8710 (1959)
11) J. R. Huizenga and R. Vandenbosch, Phys. Rev. **120** (1960) 1305; **120** (1960) 1313
12) J. M. Blatt and V. F. Weisskopf, Theoretical nuclear physics (John Wiley and Sons, New York, 1952)
13) E. Segrè and A. C. Helmholz, Rev. Mod. Phys. **21** (1949) 271

3.A

Nuclear Physics **26** (1961) 113—116; © *North-Holland Publishing Co., Amsterdam*

Not to be reproduced by photoprint or microfilm without written permission from the publisher

A SEARCH FOR AN ISOMERIC STATE IN Mn^{54}

O. DIETZSCH, R. A. DOUGLAS and VIOLETA GOMES

Laboratório do Acelerador Eletrostático, Universidade de São Paulo, São Paulo, Brasil

Received 19 January 1961

Abstract: An attempt has been made to detect the 2 min isomeric state in Mn^{54} reported by Caldwell and Stoddart and by Elwyn *et al.* A study has been made of activities following the gamma irradiation of Mn^{55} targets and the proton bombardment of a natural chromium target. No activity with half life 2 ± 1.5 min was found which could be attributed to Mn^{54}. From these experiments it is concluded that there is insufficient evidence to establish the existence of the isomeric state in Mn^{54}.

1. Introduction

The suggestion of an isomeric state in Mn^{54} has recently been revived by Elwyn *et al.* [1]). By means of the time-of-flight technique a measurement was made of the energies of neutron groups which resulted from the 3-MeV proton bombardment of a natural chromium target and a group of neutrons with $Q = -2.21\pm0.03$ MeV was observed. Following bombardment of a thick chromium target a 2 min activity was observed by means of a 3.81 cm × 5.08 cm NaI(Tl) crystal. Elwyn *et al.* noted that these data could be explained by assuming an isomeric state in Mn^{54} with 0.061 MeV excitation energy. An isomeric state in Mn^{54} with a 2.1 min half life had previously been proposed by Caldwell and Soddart [2]) to explain an activity produced with different intensities in natural iron and iron enriched in Fe^{54} after bombardment by 10 MeV deuterons or 14 MeV neutrons. According to a private communication to McNeill *et al.* [3]) the observed activity was a negaton decay with a 2 MeV end point energy as measured by absorption. Various unsuccessful attempts [3]) have been made to produce Mn^{54} in this isomeric state. In particular, McNeill *et al.* [3]) failed to produce this state in Mn^{54} through a (γ, n) reaction in Mn^{55}. They could not attribute any negaton or positon activity of 2 min half life to Mn^{54} and did not observe any short lived gamma ray of energy between 100 keV and 3 MeV. As the excitation energy of 61 keV places the possible decay radiation energy below the energy range investigated by McNeill *et al.*, we have attempted to dectect the 61 keV gamma rays associated with the decay of this state. Two methods have been used to produce this state, namely the $Mn^{55}(\gamma, n)Mn^{54}$ and $Cr^{54}(p, n)Mn^{54}$ reactions.

2. The $Mn^{55}(\gamma, n)Mn^{54*}$ Reaction

Samples of 99.9 % pure manganese were irradiated with 20.5 MeV bremsstrahlung from the University of São Paulo betatron. The manganese was surrounded by cadmium and paraffin during irradiation to reduce the neutron flux. Following irradiation, samples were transferred as quickly as possible to the counting apparatus. The gamma ray detector was a NaI(Tl) crystal 25 mm in diameter and 2.5 mm thick. A twenty-channel pulse-height analyser was used to observe the spectral distribution of pulses from the detector. The sample, crystal and phototube were completely surrounded with paraffin to absorb low energy radiation. Lead was used to shield against the cosmic-ray background.

The energy calibration of the apparatus was determined by comparison with standard gamma ray sources of Cs^{137} (32 keV X-ray and 661 keV) and Cd^{109} (87 keV).

The observed spectrum showed no evidence for a peak in the 60 keV region but only the Compton contribution due to higher energy radiations. A strong annihilation line was found which was presumably due to the 2 min positon decay of O^{15} produced by the $O^{16}(\gamma, n)O^{15}$ reaction on the oxygen contamination of the sample. The gamma rays from Mn^{56} produced by $Mn^{55}(n, \gamma)Mn^{56}$ were also observed. As there was no evidence for low energy gammas from Mn^{54} an upper limit on the cross section for the production of Mn^{54} in an excited state by the $Mn^{55}(\gamma, n)Mn^{54*}$ reaction was deduced from the following considerations.

The efficiency of the crystal for low energy quanta was measured with a calibrated source of Cd^{109} (87 keV gamma ray) and from a comparison between the shape of the spectra of the 87 keV gamma ray of Cd^{109} and those of the irradiated samples of manganese, the minimum intensity of a possible 60 keV peak that would be observable was obtained. The cross section was calculated taking into account the geometry, the self-absorption in the sample, the measured efficiency of the crystal and the number of counts under the minimum observable peak. Assuming that the cross-section curve for the production of Mn^{54} is of a giant resonance shape, the maximum cross section of the $Mn^{55}(\gamma, n)Mn^{54*}$ reaction was found to be 0.004 mb, assuming 100 % decay of the state by 60 keV radiation. This may be compared with 100 mb obtained for the $Mn^{55}(\gamma, n)$ Mn^{54} ground state reaction [3]). No search was made for negaton or positon decay of the state as the work of McNeill *et al.* seems to be conclusive in this respect.

3. The $Cr^{54}(p, n)Mn^{54*}$ Reaction

A very thick target of natural chromium † of 99.99 % purity was bombarded by protons from the University of São Paulo electrostatic accelerator. The target was enclosed in a thin walled vacuum chamber and a house consisting of

† Obtained from the Instituto de Pesquisas Tecnológicas da Universidade de S. Paulo.

a 1 cm wall of iron surrounded by 5 cm of lead. The lead reduced the background from cosmic rays while the iron absorbed the lead X-rays.

After four minutes of bombardment with about a 15 μA beam a 3.2×2.5 cm NaI(Tl) crystal was brought up and the activity of the sample observed. A single-channel analyser was used to observe the radiation in particular energy regions of the spectrum. In all cases the decay curve was taken and could be resolved into two activities, one with a half life of about 1 min and the other of about 40 min. The 40 min activity had the spectral distribution of annihilation radiation as determined by comparison with the spectral distribution of a Na^{22} source observed under identical experimental conditions. It was thus identified as due to Mn^{51} from the reaction $Cr^{50}(p, \gamma)Mn^{51}$. The following experiments were performed to identify the 1 min activity:

a) The target was bombarded with 2.75 MeV protons. The spectral distributions of the two activities were similar indicating that the 1 min activity was also annihilation radiation following decay by positon emission.

b) The target was bombarded with protons of 2.2 MeV energy which is below the threshold (2.25 MeV) for the production of the Mn^{54} 0.061 MeV state. The two activities were found to be present in approximately the same intensities as at the higher bombarding energy.

c) The target was cleaned by running a discharge in hydrogen gas to remove a possible oxygen layer on the surface. It was then bombarded with 2.75 MeV protons. The relative intensity of the 1 min activity was reduced by a factor of 3 to 5.

d) A thick aluminium target was bombarded with 2.75 MeV protons. An activity with half life of about 1 min was observed with an intensity comparable to that of the chromium bombardments.

Since no activity of this half life is expected from the proton bombardment of aluminium this activity must be due to the oxygen layer on the aluminium surface. From these experiments it is concluded that the chief source of the 1 min activity is F^{17} from the reaction $O^{16}(p, \gamma)F^{17}$ which is a positon emitter of half life 1.1 min (see ref. [4]).

From these data, an upper limit for the value of the cross section averaged over the energy region from threshold to 2.75 MeV of the $Cr^{54}(p, n)Mn^{54*}$ reaction has been calculated to be 0.02 mb. This appears to be 10^2 or 10^3 times smaller than experimentally determined (p, n) reaction cross sections in neighboring nuclei with this threshold (for example the cross section of the $Cu^{65}(p, n)Zn^{65}$ reaction is 5 mb (see ref. [5])). The energy averaged cross section for the reaction $Cr^{50}(p, \gamma)Mn^{51}$ was calculated to be 0.15 mb which is a reasonable order of magnitude (for example, the cross section of the reaction $Ni^{60}(p, \gamma)Cr^{61}$ is given in ref. [6]) as being 0.1 mb).

4. Conclusion

The evidence for the existence of an isomeric state in Mn^{54} is the following:

a) A 2 min negaton activity with an end point energy of 2 MeV, presumably produced by the reaction $Fe^{54}(n, p)Mn^{54}$.

b) A group of neutrons following the proton bombardment of natural chromium corresponding to a $Q = -2.21 \pm 0.03$ MeV and an activity, not necessarily correlated with this group, of approximately 2 min half life.

It is noted that if the group of neutrons is ascribed to the $Cr^{54}(p, n)Mn^{54*}$ 0.061 MeV reaction the Q for negaton decay calculated using the mass values of Wapstra [7]) is +0.683 MeV while if it is ascribed to the only other energetically possible reaction in chromium, namely $Cr^{53}(p, n)Mn^{53*}$ 0.80 MeV the Q for negaton decay is −3.065 MeV. Hence the items of evidence a) and b) are not consistent.

The reaction $Fe^{54}(n, p)Mn^{54}$ has been studied by McNeill *et al.* [3]) using targets of natural iron (5.9 % Fe^{54}) without finding an activity ascribable to Mn^{54}. They found only the Mn^{57} activity which decays by negaton emission with an end point energy of 2.6 MeV and half life of 1.7 min. The reaction $Mn^{55}(\gamma, n)Mn^{54}$ has been carefully studied by McNeill *et al.* [3]) and ourselves without finding an activity ascribable to Mn^{54} decaying by negaton or position emission or gamma ray emission with energy greater than 30 keV. Activities resulting from the proton bombardment of a natural chromium target have been studied by ourselves without finding an activity attributable to an isomeric state in Mn^{54}. It is concluded that there is insufficient evidence to establish the existence of an isomeric state in Mn^{54} with a half life of 2 ± 1.5 min.

The authors wish to thank Prof. O. Sala for his constant encouragement during the experiment. Financial assistance was received from the Conselho Nacional de Pesquisas (CNPq) and the Rockefeller Foundation. One of us (R. A. D.) received support from the Campanha Nacional de Aperfeiçoamento de Pessoal de Nível Superior (CAPES). We also wish to thank Prof. J. Goldemberg of the Laboratòrio do Betatron and Prof. M. D. Souza Santos of the Instituto de Energia Atômica for the use of their facilities.

References

1) Elwyn, Landon, Oleksa and Glasoe, Phys. Rev. **112** (1958) 1200
2) Caldwell and Stoddart, Phys. Rev. **81** (1951) 660
3) McNeill, Prentice, Katz and Link, Can. J. Phys. **35** (1957) 753
4) Strominger, Hollander and Seaborg, Rev. Mod. Phys. **30** (1958) 585
5) Johnson, Galonsky and Ulrich, Phys. Rev. **109** (1958) 1243
6) Butler and Gassett, Phys. Rev. **108** (1957) 1473
7) A. H. Wapstra, Handbuch der Physik (Springer-Verlag, Berlin, 1958) Vol. **37**, part 1

8.C

Nuclear Physics **26** (1961) 117—125; © *North-Holland Publishing Co., Amsterdam*

Not to be reproduced by photoprint or microfilm without written permission from the publisher

A ONE-DIMENSIONAL FIELD THEORY WITH DEGENERATE VACUUM

K. BAUMANN and R. SEXL

Institute for Theoretical Physics, University of Vienna, Vienna, Austria †

Received 27 January 1961

Abstract: A one-dimensional field theory is considered corresponding to the continuous limit of a spin chain. The vacuum degeneracy of this theory is explored. Besides, it is shown that the theory can equivalently be formulated in terms of an interacting Fermi field or of a Bose field without interaction. Finally, a theory is briefly discussed which can either be treated as an interacting Bose field or as a free Fermi field.

1. Introduction

Within the last few years interest has grown in field theories with a degenerate vacuum. One of the most prominent examples of a theory with a highly degenerate ground state is ferro-magnetism. This theory has the additional advantage of having been solved exactly in one dimension long ago by Bethe [1])††. As we are interested in studying a simple model of a field theory with a vacuum degeneracy, we shall consider the properties of a spin chain in the continuous limit.

The theory we get in this way turns out not only to show up an instructive degeneracy. Besides this we find an interesting ambiguity of statistics, which sheds some light on the well-known controversies concerning the statistics of spin waves. We can formulate the theory either in terms of an interacting Fermi field or of a Bose field without interaction.

2. Discrete Theory

The Hamiltonian has the following form:

$$H = -\tfrac{1}{2}J\sum_{\nu=1}^{N}\boldsymbol{\sigma}_\nu\cdot\boldsymbol{\sigma}_{\nu+1}+\tfrac{1}{2}NJ. \tag{1}$$

The $\boldsymbol{\sigma}_\nu$ are the usual Pauli matrices operating on the spin of the ν-th atom. N is the number of atoms and J is a constant with the dimension of an energy. We impose a periodicity boundary condition such that

$$\boldsymbol{\sigma}_{\nu+N} = \boldsymbol{\sigma}_\nu. \tag{2}$$

† Work supported in part by the United States Government.

†† An approximate solution was given by Bloch [2]).

We can cast the theory into a form more similar to field theory by introducing a new set of matrices

$$\sigma_\nu = \tfrac{1}{2}(\sigma_\nu^x + i\sigma_\nu^y), \quad \sigma_\nu^\dagger = \tfrac{1}{2}(\sigma_\nu^x - i\sigma_\nu^y), \tag{3}$$

whereby

$$\sigma_\nu^z = \sigma_\nu\sigma_\nu^\dagger - \sigma_\nu^\dagger\sigma_\nu = 1 - 2\sigma_\nu^\dagger\sigma_\nu. \tag{4}$$

Thus, after some manipulations, we get

$$H = J\sum(\sigma_{\nu+1}^\dagger - \sigma_\nu^\dagger)(\sigma_{\nu+1} - \sigma_\nu) - 2J\sum\sigma_{\nu+1}^\dagger\sigma_\nu^\dagger\sigma_{\nu+1}\sigma_\nu. \tag{5}$$

The commutation relations are transformed into

$$[\sigma_\nu, \sigma_\nu^\dagger]_+ = 1, \quad [\sigma_\nu, \sigma_\nu]_+ = 0, \quad [\sigma_\nu, \sigma_\mu^\dagger]_- = [\sigma_\nu, \sigma_\mu]_- = 0, \quad \nu \neq \mu. \tag{6}$$

3. Transition to the Continuous Chain

Let us perform a Klein transformation

$$a_\nu = \sigma_\nu \prod_{\mu=1}^{\nu-1} \sigma_\mu^z, \qquad \sigma_\nu = a_\nu \prod_{\mu=1}^{\nu-1} (1 - 2a_\mu^\dagger a_\mu). \tag{7}$$

The new operators a_ν obey pure Fermi commutation relations,

$$[a_\mu, a_\nu^\dagger]_+ = \delta_{\mu\nu}, \qquad [a_\mu, a_\nu]_+ = 0. \tag{8}$$

The Hamiltonian is now

$$H = J\sum(a_{\nu+1}^\dagger - a_\nu^\dagger)(a_{\nu+1} - a_\nu) + 2J\sum a_{\nu+1}^\dagger a_\nu^\dagger a_{\nu+1}a_\nu. \tag{9}$$

The transition to the continuous case can now easily be done. We define

$$a_\nu = \sqrt{\eta}\,a(x_\nu), \quad a_{\nu+1} = \sqrt{\eta}\,a(x_\nu + \eta), \tag{10}$$

and consider the limit $\eta \to 0$, $J \to \infty$, $N \to \infty$, such that $\eta N = L$ and $\eta^2 J = K$ remain finite. In the following we shall put $K = 1$ for simplicity.

Then we have

$$[a(x)a^\dagger(y)]_+ = \delta(x-y), \qquad [a(x)a(y)]_+ = 0, \tag{11}$$

and

$$H = \int \frac{\mathrm{d}a^\dagger(x)}{\mathrm{d}x}\,\frac{\mathrm{d}a(x)}{\mathrm{d}x}\,\mathrm{d}x + \int \mathrm{d}x\mathrm{d}y\,a^\dagger(x)a^\dagger(y)V(x-y)a(x)a(y), \tag{12}$$

with the attractive interaction

$$V(x) = \lim_{\eta\to 0} \frac{\delta(x+\eta) + \delta(x-\eta)}{\eta}. \tag{13}$$

It should be noted that eq. (13) is one of the possibilities of giving a meaning to the product of distributions

$$V(x) = -2\varepsilon(x)\delta'(x). \tag{13a}$$

One is naturally led to $V(x)$ if one tries to set up a Schrödinger equation

$$\varepsilon''(x) = -V(x)\,\varepsilon(x). \tag{14}$$

4. Energy Eigenfunctions

To begin with, we define a vacuum state Ω by

$$a(x)\Omega = 0. \tag{15}$$

Next, consider a one-particle state

$$\int \mathrm{d}x\, \chi(x)\, a^\dagger(x)\Omega.$$

The condition $a(x+L) = a(x)$ implies $\chi(x+L) = \chi(x)$. One easily finds

$$H \int \mathrm{d}x\, \chi(x) a^\dagger(x)\Omega = -\int \mathrm{d}x \chi''(x) a^\dagger(x)\Omega.$$

Thus,

$$|k\rangle = L^{-\frac{1}{2}} \int_0^L \mathrm{d}x\, \mathrm{e}^{ikx} a^\dagger(x)\Omega \qquad (k = 2\pi n/L,\ n = 0, 1, 2, \ldots) \tag{16}$$

is an eigenstate of the Hamiltonian.

Similarly, one can show that the expression

$$\int \mathrm{d}x\mathrm{d}y \chi(x, y) a^\dagger(x) a^\dagger(y)\Omega$$

is a two-particle eigenstate if $\chi(x, y)$ is a solution of the Schrödinger equation

$$(-\nabla^2 - 2V(x-y))\chi(x, y) = E\chi(x, y). \tag{17}$$

We restrict ourselves here to a solution of eq. (17) in the limit $L \to \infty$, where no periodicity boundary condition need be taken into account.

If we observe that the operators in eq. (17) fulfil the identity

$$\nabla^2 \varepsilon(x-y)\phi(x, y) = -2V(x-y)\varepsilon(x-y)\phi(x, y) + \varepsilon(x-y)\nabla^2\phi(x, y) \tag{18}$$

for symmetric functions

$$\phi(x, y) = \phi(y, x), \tag{18a}$$

we find that the solutions of eq. (17) are

$$\chi_{kk'}(x, y) = \varepsilon(x-y)\tfrac{1}{2}[\mathrm{e}^{i(kx+k'y)} + \mathrm{e}^{i(k'x+ky)}], \tag{19}$$

corresponding to an eigenvalue

$$E_{k,k'} = k^2 + k'^2. \tag{20}$$

Finally we consider a general n-particle state

$$\int \mathrm{d}x_1 \ldots \mathrm{d}x_n \chi(x_1 \ldots x_n) a^\dagger(x_1) \ldots a^\dagger(x_n)\Omega.$$

The Schrödinger equation is

$$\{-\nabla_n^2-2\sum_{k<l}^{n}V(x_k-x_l)\}\chi(x_1\ldots x_n)=E\chi(x_1\ldots x_n),\qquad \nabla_n^2=\sum_{j=1}^{n}\partial^2/\partial x_j^2, \tag{21}$$

and has the following solution:

$$\chi_{k_1\ldots k_n}(x_1\ldots x_n)=\prod_{j<l}\varepsilon(x_j-x_l)\frac{1}{n!}\sum_{m}\mathrm{e}^{i\sum_{\mathrm{P}}k_{\mathrm{P}m}x_m}. \tag{22}$$

Here, P means permutation:

$$\mathrm{P}=\begin{pmatrix}1, & 2, \ldots & n\\ \mathrm{P}1, & \mathrm{P}2, \ldots & \mathrm{P}n\end{pmatrix}. \tag{23}$$

The energy corresponding to eq. (22) is

$$E_{k_1\ldots k_n}=\sum_{j=1}^{n}k_j^2. \tag{24}$$

In order to show that eq. (22) solves eq. (21) we calculate $\nabla_n^2\chi_{k_1\ldots k_n}$. The contributions from differentiating $\varepsilon(x_j-x_l)$ twice with respect to x_j and x_l yield $-2V(x_j-x_l)\chi_{k_1\ldots k_n}$ by virtue of eq. (14). The energy term results from differentiating the exponential only. Hence, we have to show that the other contributions vanish. There are two types of terms, namely,

$$\varepsilon(x_j-x_k)\frac{\partial}{\partial x_i}\varepsilon(x_i-x_k)\frac{\partial}{\partial x_i}\varepsilon(x_i-x_j)=4\varepsilon(x_j-x_k)\delta(x_i-x_k)\delta(x_i-x_j)=0$$

and

$$\frac{\partial}{\partial x_j}\varepsilon(x_j-x_k)\frac{\partial}{\partial x_j}\sum_{\mathrm{P}}\mathrm{e}^{i\sum_m k_{\mathrm{P}m}x_m}+\frac{\partial}{\partial x_k}\varepsilon(x_j-x_k)\frac{\partial}{\partial x_k}\sum_{\mathrm{P}}\mathrm{e}^{i\sum_m k_{\mathrm{P}m}x_m}$$

$$=2\delta(x_j-x_k)\left(\frac{\partial}{\partial x_j}-\frac{\partial}{\partial x_k}\right)\sum_{\mathrm{P}}\mathrm{e}^{i\sum_m k_{\mathrm{P}m}x_m}=0.$$

5. Alternative Formulation of the Theory

Let us try to pass to the limit of a continuous spin chain without making a Klein transformation. Analogously to the operators $a(x)$ we put

$$\sigma(x_\nu)=\eta^{-\frac{1}{2}}\sigma_\nu. \tag{25}$$

Then we get a Hamiltonian

$$H=\int\frac{\mathrm{d}\sigma^\dagger(x)}{\mathrm{d}x}\frac{\mathrm{d}\sigma(x)}{\mathrm{d}x}\,\mathrm{d}x-\int\mathrm{d}x\mathrm{d}y\sigma^\dagger(x)\sigma^\dagger(y)V(x-y)\sigma(x)\sigma(y), \tag{26}$$

whereas the commutation relations do not possess a limiting form. Formally

we get

$$[\sigma(x), \sigma(y)]_- = \delta(x-y) \lim_{\eta \to 0} (1-2\eta\sigma^\dagger(x)\sigma(x)). \tag{27}$$

That the factor of the delta function does not generally approach unity is seen from the following example:

$$\lim_{\eta \to 0} (1-2\eta\sigma^\dagger(x_\nu)\sigma(x_\nu))\sigma^\dagger(x_\nu)\Omega = -\sigma^\dagger(x_\nu)\Omega.$$

However, we shall show that in the application of H on an n-particle state the η-term yields a result which is compensated by the potential term.

For simplicity we consider a two-particle state. The kinetic and the potential term of H be denoted by H_0 and H_1. Then

$$\begin{aligned} H_0 \sum \eta^2 \phi(x_\alpha, x_\beta)\sigma^\dagger(x_\alpha)\sigma^\dagger(x_\beta)\Omega \\ = \sum \eta\sigma^\dagger(x_\mu)\sigma(x_\nu)\sigma^\dagger(x_\alpha)\sigma(x_\beta)\Omega\phi(x_\alpha, x_\beta) \\ \cdot \{2\delta(x_\mu, x_\nu)-\delta(x_\mu, x_\nu+\eta)-\delta(x_\mu, x_\nu-\eta)\}, \end{aligned} \tag{28}$$

where $\delta(x, y) = 0$ for $x \neq y$, $= 1$ for $x = y$. If we commute $\sigma(x_\nu)$ to the right we get three contributions,

(i) $\eta^{-1}\delta(x_\nu, x_\alpha)$,

(ii) $\eta^{-1}\delta(x_\nu, x_\beta)$,

(iii) $-2\delta(x_\nu, x_\alpha)\sigma^\dagger(x_\nu)\sigma(x_\nu)$.

(The σ-term from the commutator with $\sigma^\dagger(x_\beta)$ vanishes because it is applied to the vacuum.) The first and second contributions yield the usual second derivatives. Term (iii) yields

$$2 \sum (\delta(x_\mu, x_\nu+\eta)+\delta(x_\mu, x_\nu-\eta))\sigma^\dagger(x_\mu)\sigma^\dagger(x_\nu)\Omega\phi(x_\nu, x_\nu). \tag{29}$$

On the other hand, the application of H_1 on the same state results in

$$-2 \sum \sigma^\dagger(x_\mu+\eta)\sigma^\dagger(x_\mu)\Omega[\phi(x_\mu, x_\mu+\eta)+\phi(x_\mu+\eta, x_\mu)]. \tag{30}$$

Adding expressions (29) and (30) we get

$$\begin{aligned} 2 \sum \sigma^\dagger(x_\nu)\sigma^\dagger(x_\mu)\Omega\delta(x_\mu+\eta, x_\nu)[\phi(x_\mu+\eta, x_\mu+\eta) \\ -\phi(x_\mu, x_\mu+\eta)-\phi(x_\mu+\eta, x_\mu)+\phi(x_\mu, x_\mu)]. \end{aligned} \tag{31}$$

By going to the continuous limit and using the symmetry of $\phi(x, y)$ we can write this as

$$\int dxdy\sigma^\dagger(x)\sigma^\dagger(y)\Omega[\delta(x-y+0)+\delta(x-y-0)]\left[\frac{\partial\phi(x, y)}{\partial x} - \frac{\partial\phi(x, y)}{\partial y}\right] = 0.$$

Therefore, we are left with the Schrödinger equation

$$-\nabla^2\phi(x, y) = E\phi(x, y). \tag{32}$$

We learn from this that we do not change the results if we drop the η term in eq. (27) and the potential term at the same time. Thus, our theory is also correctly described by

$$H = \int \frac{\mathrm{d}s^\dagger(x)}{\mathrm{d}x} \frac{\mathrm{d}s(x)}{\mathrm{d}x} \mathrm{d}x, \tag{33}$$

where $s(x)$ is an ordinary Bose field, with

$$[s(x), s^\dagger(y)]_- = \delta(x-y), \qquad [s(x), s(y)]_- = 0. \tag{34}$$

Hence, we are faced with the strange situation that the same phenomenon can be interpreted as well as a Fermi field *or* as a Bose field †.

If we introduce the Fourier transform

$$s_k = L^{-\frac{1}{2}} \int_0^L s(x) \mathrm{e}^{-ikx} \mathrm{d}x, \tag{35}$$

the energy eigenstates can be expressed in two forms:

$$\prod_{i=1}^{r} (n_i!)^{\frac{1}{2}} |k_1 \ldots k_n\rangle = s_{k_1}^\dagger \ldots s_{k_n}^\dagger \Omega$$
$$= L^{-\frac{1}{2}n} \int \mathrm{d}^n x \chi_{k_1 \ldots k_n}(x_1 \ldots x_n)\, a^\dagger(x_1) \ldots a^\dagger(x_n)\Omega. \tag{36}$$

(The product on the left is the usual Bose normalization factor when not all k's are different.) To prove eq. (36), we formally introduce the continuous limit of the Klein transformation

$$\sigma^\dagger(x) = a^\dagger(x) \exp\left[i\pi \int^x a^\dagger(x')a(x')\mathrm{d}x'\right]. \tag{37}$$

Eq. (37) is equal to $s^\dagger(x)$ whenever the η-term in eq. (27) gives no contribution, as it is the case in constructing the energy eigenstates. By observing that

$$a^\dagger(x) \exp\left[i\pi \int_0^y a^\dagger(z)a(z)\mathrm{d}z\right] = \varepsilon(x-y) \exp\left[i\pi \int_0^y a^\dagger(z)a(z)\mathrm{d}z\right] a^\dagger(x), \tag{38}$$

one easily proves eq. (36).

6. Invariance Properties

The Hamiltonian (1) is invariant with respect to space rotations. The corresponding three conserved quantities are

$$\sum \sigma_\nu^\dagger \sigma_\nu, \qquad \sum (\sigma_\nu^\dagger + \sigma_\nu), \qquad i \sum (\sigma_\nu^\dagger - \sigma_\nu).$$

† Of course we cannot expect this to be possible in a relativistic field theory because of the connection between spin and statistics.

In terms of $s(x)$ these quantities † are

$$N = \int s^\dagger(x)\, s(x)\mathrm{d}x, \qquad T_2 = \int (s^\dagger(x)+s(x))\mathrm{d}x = s_0{}^\dagger+s_0,$$
$$T_3 = i\int (s^\dagger(x)-s(x))\mathrm{d}x = i(s_0{}^\dagger-s_0). \tag{39}$$

Repeated application of

$$\tfrac{1}{2}(T_2-iT_3) = \int s^\dagger(x)\mathrm{d}x = s_0{}^\dagger$$

on the vacuum state Ω creates the states

$$|0\rangle, \quad |0,0\rangle, \quad |0,0,0\rangle, \ldots$$

(up to normalization factors). The energy of all of these orthogonal states is zero. Therefore the vacuum is degenerate. Obviously every eigenstate of the Hamiltonian is degenerate with infinitely many other states, which one gets from it by adding an arbitrary number of zero momentum particles ("spurions").

It should be noted that there are *no* spurions in a relativistic field theory of free mass zero bosons ††. In this case,

$$H = \tfrac{1}{2}\sum (p_k{}^2+k^2 q_k{}^2).$$

Now we can make the usual transformation

$$q_k = (2k)^{-\frac{1}{2}}(a_k+a_k{}^\dagger), \qquad p_k = -i(\tfrac{1}{2}k)^{\frac{1}{2}}(a_k-a_k{}^\dagger)$$

for $k \neq 0$ only and get

$$H = \tfrac{1}{2}p_0{}^2+\sum_{k\neq 0} k(a_k{}^\dagger a_k+\tfrac{1}{2}).$$

Thus there is no degeneracy.

7. An "Inverse" Theory

Consider the Hamiltonian

$$H = \int \mathrm{d}x \frac{\mathrm{d}b^\dagger(x)}{\mathrm{d}x}\frac{\mathrm{d}b(x)}{\mathrm{d}x} + \int \mathrm{d}x\mathrm{d}y b^\dagger(x)b^\dagger(y)V(x-y)b(x)b(y), \tag{40}$$

where $b(x)$ is a Bose field,

$$[b(x), b^\dagger(y)]_- = \delta(x-y), \qquad [b(x), b(y)]_- = 0; \tag{41}$$

$V(x)$ is defined as in eq. (13), and describes a repulsion now.

† Up to factors which provide finiteness in the continuous limit.
†† We have learned this argument from W. Thirring.

In this case one is led to the Schrödinger equation

$$(-\nabla_n^2+2\sum_{k<l}^{n} V(x_k-x_l))\psi(x_1 \ldots x_n) = E\psi(x_1 \ldots x_n), \tag{42}$$

which is solved by

$$\psi_{k_1 \ldots k_n}(x_1 \ldots x_n) = \prod_{j<l} \varepsilon(x_j-x_l) \sum_{\mathrm{P}} (-)^{\mathrm{P}} \mathrm{e}^{i \sum_m k_{\mathrm{P}m} x_m}. \tag{43}$$

We shall prove in detail the case $n = 2$ first. We put

$$\psi(x, y) = \varepsilon(x-y)[\mathrm{e}^{i(kx+py)}-\mathrm{e}^{i(px+ky)}].$$

Then one easily finds

$$\begin{aligned}\left(\frac{\partial^2}{\partial x^2}+\frac{\partial^2}{\partial y^2}+p^2+k^2\right)\psi(x, y) \\ = 4\delta'(x-y)[\mathrm{e}^{i(kx+py)}-\mathrm{e}^{i(px+ky)}]+8i\delta(x-y)[k\mathrm{e}^{i(kx+py)}-p\mathrm{e}^{i(px+ky)}] \\ = 4i\delta(x-y)(k-p)\mathrm{e}^{i(k+p)x}.\end{aligned}$$

In the last step we have used the formula

$$\delta'(x) = \lim_{\eta \to 0} \frac{1}{2\eta} [\delta(x+\eta)-\delta(x-\eta)].$$

On the other hand, we have

$$V(x-y)\psi(x, y) = 2i\delta(x-y)(k-p)\mathrm{e}^{i(k+p)x}.$$

Therefore, we have proved the equation

$$(-\nabla^2+2V(x-y))\psi(x, y) = (k^2+p^2)\psi(x, y).$$

In the general case there are four types of contributions from $\nabla_n^2\psi$:

(i) differentiating two different ε's yields zero,

(ii) differentiating twice the exponential yields $E\psi$,

(iii) differentiating twice one ε yields $-2V\psi$,

(iv) differentiating once an ε and once an exponential yields $4V\psi$. It is clear that the energy spectrum of this kind of Bose field is exactly that of a free Fermi field.

Finally we want to see what kind of spin interaction leads to this theory in the continuous limit. The free Fermi Hamiltonian

$$H = J\sum (a_{\nu+1}^{\dagger}-a_\nu^{\dagger})(a_{\nu+1}-a_\nu) \tag{44}$$

can be subjected to a Klein transformation

$$H = J\sum (\sigma_{\nu+1}^{\dagger}-\sigma_\nu^{\dagger})(\sigma_{\nu+1}-\sigma_\nu). \tag{45}$$

Using eqs. (3) and (4), we can rewrite this as

$$\begin{aligned} H &= -\tfrac{1}{2}J\sum(\sigma_\nu^x\sigma_{\nu+1}^x+\sigma_\nu^y\sigma_{\nu+1}^y)+J\sum\sigma_\nu^z+JN \\ &= -\tfrac{1}{2}J\sum\boldsymbol{\sigma}_\nu\cdot\boldsymbol{\sigma}_{\nu+1}+\tfrac{1}{2}J\sum\sigma_\nu^z\sigma_{\nu+1}^z+J\sum\sigma_\nu^z+JN. \end{aligned} \tag{46}$$

The "inverse" theory thus corresponds to a combination of an isotropic and an Ising interaction. The third term might as well be dropped without changing the Fermion character of the excitations. In this way the Hamiltonian would be replaced by

$$H\to H+2J\sum a_\nu^\dagger a_\nu-JN. \tag{47}$$

The additional mass term then removes the degeneracy of the energy spectrum.

We would like to thank Professor W. Thirring for suggesting this work and for continuing and helpful interest. Our thanks are also due to Dr. J. Wess for many valuable discussions.

References

1) H. A. Bethe, Z. f. Phys. **71** (1931) 205
2) Bloch, Z. f. Phys. **61** (1930) 206

2.L

Nuclear Physics **26** (1961) 126—128; © *North-Holland Publishing Co., Amsterdam*

Not to be reproduced by photoprint or microfilm without written permission from the publisher

ELEMENTARY DERIVATION OF THE MINAMI PHASE SHIFT AMBIGUITY

R. VAN WAGENINGEN

Institute for Theoretical Physics, State University, Groningen

Received 27 February 1961

Abstract: An elementary derivation is presented of the Minami phase shift ambiguity in the analysis of elastic scattering of a spin $\frac{1}{2}$ particle by a spin 0 scattering centre.

1. Introduction

The phase shift analysis of differential cross section and polarization data from the elastic scattering of spin $\frac{1}{2}$ particles by a spin 0 scattering centre is greatly complicated by the well-known Minami-ambiguity [1–3]). Elegant derivations of this symmetry property have been given by Dyson and Nambu (cited by Hayakawa *et al.* [3]) and by Bethe and De Hoffmann [4])), by Ryndin and Smorodinskii [5]), by Ritus [6]), by the author [7, 8]) and others. A generalization with the spin $\frac{1}{2}$ particles initially polarized and several theoretical and experimental implications, were discussed in detail by the author [7, 8]).

It is the purpose of this note a) to show that a simple proof can be given by using solely elementary methods, and b) to rewrite the amplitude operator of the scattering in a form which makes the symmetry property explicitly evident.

2. Derivation

The amplitude operator for the process considered has the form [9]) (the quantities f, 1 and the components of $\boldsymbol{\sigma}$ are 2×2 matrices)

$$f(\vartheta, \varphi, \boldsymbol{\sigma}) = A(\vartheta)1 + B(\vartheta)\boldsymbol{\sigma}\cdot\mathbf{n},$$

where $\boldsymbol{\sigma}$ is the Pauli spin vector operator, and $\mathbf{n}$ is the unit vector normal to the scattering plane, defined by

$$\mathbf{n}\sin\vartheta = \mathbf{n}_i\times\mathbf{n}_f.$$

Here $\mathbf{n}_i$ and $\mathbf{n}_f$ are unit vectors along the direction of incidence and of scattering

respectively. The functions $A(\vartheta)$ and $B(\vartheta)$ are given by

$$A(\vartheta) = k^{-1}\sum_{l=0}^{\infty}\{(l+1)\zeta_l^{+}+l\zeta_l^{-}\}P_l(\cos\vartheta),$$

$$B(\vartheta) = ik^{-1}\sum_{l=0}^{\infty}\{\zeta_l^{+}-\zeta_l^{-}\}\sin\vartheta P'_l\cos\vartheta),$$

where $P_l(\cos\vartheta)$ is the usual Legendre polynomial and $P'_l(\cos\vartheta)$ its derivative with respect to $\cos\vartheta$. The quantities $\zeta_l^{\pm}$ are related to the scattering phase shifts $\delta_l^{\pm} = \delta_l^{j=l\pm\frac{1}{2}}$ by

$$\zeta_l^{\pm} = \sin\delta_l^{\pm}\exp(i\,\delta_l^{\pm}).$$

We now use the relation

$$(\boldsymbol{\sigma}\cdot\mathbf{n}_f)(\boldsymbol{\sigma}\cdot\mathbf{n}_i) = \mathbf{n}_f\cdot\mathbf{n}_i\,1+i\{\boldsymbol{\sigma}\cdot(\mathbf{n}_f\times\mathbf{n}_i)\} = \cos\vartheta 1-i\sin\vartheta\boldsymbol{\sigma}\cdot\mathbf{n},$$

to transform the factor $i\sin\vartheta\,\boldsymbol{\sigma}\cdot\mathbf{n}$ occurring in the second term of $f(\vartheta,\varphi,\boldsymbol{\sigma})$. Furthermore we apply the well-known relations

$$(l+1)P_l(\cos\vartheta)+\cos\vartheta\,P'_l(\cos\vartheta) = P'_{l+1}(\cos\vartheta),$$

$$lP_l(\cos\vartheta)-\cos\vartheta\,P'_l(\cos\vartheta) = -P'_{l-1}(\cos\vartheta).$$

As a result, f takes the following form:

$$f(\vartheta,\varphi,\boldsymbol{\sigma}) = A'(\vartheta)1+B'(\vartheta)(\boldsymbol{\sigma}\cdot\mathbf{n}_f)(\boldsymbol{\sigma}\cdot\mathbf{n}_i), \tag{1}$$

with

$$A'(\vartheta) = \sum_{l=0}^{\infty}(\zeta_l^{+}P'_{l+1}-\zeta_l^{-}P'_{l-1}) = \sum_{l=1}^{\infty}(\zeta_{l-1}^{+}-\zeta_{l+1}^{-})P'_l(\cos\vartheta),$$

$$B'(\vartheta) = \sum_{l=1}^{\infty}(\zeta_l^{-}-\zeta_l^{+})P'_l(\cos\vartheta).$$

This form of the amplitude operator clearly shows the Minami symmetry property. For if we rotate the initial spin over 180° around the incident direction and the final spin over 180° around the scattering direction, this means that we operate on the right with $\boldsymbol{\sigma}\cdot\mathbf{n}_i$ and on the left with $\boldsymbol{\sigma}\cdot\mathbf{n}_f$, which gives

$$\boldsymbol{\sigma}\cdot\mathbf{n}_f)f(\boldsymbol{\sigma}\cdot\mathbf{n}_i) = B'(\vartheta)1+A'(\vartheta)(\boldsymbol{\sigma}\cdot\mathbf{n}_f)(\boldsymbol{\sigma}\cdot\mathbf{n}_i),$$

which is of the same form as f itself, with the roles of A' and B' interchanged. The same interchange is, however, obtained by replacing in A' and B' the quantities ζ_l^{-} by ζ_{l-1}^{+} and ζ_l^{+} by ζ_{l+1}^{-} for all l, i.e. by interchanging the phase shifts with the same j but opposite parity. Thus, when performing the two operations simultaneously, the amplitude operator remains the same, all cross section and polarization data are the same, if the appropriate rotations through 180° are performed. This is the desired symmetry property.

3. Discussion

The above considerations do not give any essentially new results. The form (1) for the amplitude operator f has been given before by Gol'fand [10]) and by Macdowell [11]), though it was not obtained by these authors in the above elementary way and was not used to derive the Minami symmetry. Nevertheless it seems worth while to have this derivation, certainly from a didactic point of view. Moreover, a form for the amplitude operator, such as the one derived here, which explicitly shows its inherent symmetry properties, may be useful for other investigations, e.g. in finding symmetries in the scattering of particles with higher spins.

The author gratefully acknowledges the interest of Prof. H. J. Groenewold in this work.

References

1) S. Minami, Progr. Theor. Phys. **11** (1954) 213
2) S. Hayakawa, M. Kawaguchi and S. Minami, Progr. Theor. Phys. **11** (1954) 332
3) S. Hayakawa, M. Kawaguchi and S. Minami, Progr. Theor. Phys. **12** (1954) 335
4) H. A. Bethe and F. De Hoffmann, Mesons and Fields (Row, Peterson and Co., Evanston, 1955) Vol. II
5) R. M. Ryndin and Ia. Smorodinskii, Dokl. Akad. Nauk USSR **103** (1955) 69 (Russian)
6) V. I. Ritus, JETP (USSR) **32** (1957) 1536 [Soviet Physics, JETP **5** (1957) 1249]
7) R. van Wageningen and H. J. Groenewold, Physica **23** (1957) 720
8) R. van Wageningen, Thesis, Groningen, 1957
9) J. V. Lepore, Phys. Rev. **79** (1950) 137
10) Iu. F. Gol'fand, JETP (USSR) **31** (1956) 224 [Soviet Physics, JETP **4** (1957) 103]
11) S. W. Macdowell, Phys. Rev. **116** (1959) 774

1.C

Nuclear Physics **26** (1961) 129—135; © *North-Holland Publishing Co., Amsterdam*

Not to be reproduced by photoprint or microfilm without written permission from the publisher

ON THE TREATMENT OF A PERTURBATION IN A SYSTEM OF PAIRED FERMIONS

AMNON KATZ

Physics Department, The Weizmann Institute of Science, Rehovoth, Israel †

Received 10 February 1961

Abstract: A straightforward variational calculation with BCS wave functions yields expressions formerly obtained by Migdal [5]) and Blatt [6]) by more complicated methods. As was shown by Migdal and Blatt, these expressions lead to a correct rotational moment of inertia of the system at the limit of a large system, to a correct mass in the pushing model and to a gauge invariant description of the Meissner effect.

1. Introduction

In the treatment of superconductivity [1]) and nuclear superfluidity [2]) by the pairing correlation method, difficulties have arisen when additional perturbations were introduced. Invariance principles and general theorems known to be valid for the system under consideration were found not to be satisfied. The treatment of the Meissner effect was not gauge invariant. The calculation of the nuclear mass in the "pushing model" gave an incorrect result [3]). The calculation of nuclear moments of inertia sometimes gave results smaller than the irrotational value.

Although these difficulties have now been resolved by a number of investigators in a number of ways, all the treatments seem to depart considerably from the simplicity of the original BSC theory. The new treatments appear to be much more powerful than the simple BCS theory. However, their relation with the original BCS theory is not evident, because of the additional complications introduced either by collective excitations [4]), Green's functions [5]), or a general formulation using "condensed pairs" [6]).

The purpose of this paper is to show that certain difficulties can be understood within the original framework of the BCS theory. They can be traced to inconsistencies in the treatment of perturbations. Furthermore, some results obtained by the other methods can also be obtained in a simple way within the spirit of the BCS theory.

† The research reported in this document has been sponsored in part by the Air Force Office of Scientific Research of the Air Research and Development Command, U. S. Air Force, through its European Office.

The essential point is the following: Let us assume that the BCS ground state wave function is a good variational wave function for a Hamiltonian having the proper invariance properties. If a perturbation is added, it is inconsistent to do ordinary perturbation theory using BCS wave functions which are not *exact* eigenfunctions of the unperturbed Hamiltonian, but are only variational trial functions. This is equivalent to replacing the unperturbed Hamiltonian by the "quasi-particle" Hamiltonian for which the BCS wave functions are exact eigenfunctions. The quasi-particle Hamiltonian includes very peculiar non-local interactions which do not satisfy the invariance principles.

A more consistent way of treating the problem is as follows: To calculate the Meissner effect at zero temperature or the nuclear mass or moment of inertia, all that is desired is the perturbed ground state wave functions (or single-particle density matrix) to first order in the perturbation. This can be obtained by a variational treatment of the entire perturbed Hamiltonian to first order, using a reasonable set of trial wave functions which give the BCS ground state in zero order. This is done in the remainder of this paper.

Our program is in principle similar to that of Blatt who also determines his perturbed wave function variationally. The difference is that Blatt has set up new elaborate mathematical methods [7]) for the treatment of his class of trial functions, namely wave functions describing Bose condensation of general pairs (not necessarily coupled to zero). We shall see in section 6 that our trial function of independent excitations of pairs of quasiparticles is essentially equivalent to Blatt's. In this respect our work can be viewed as carrying out Blatt's program by expanding the trial function in BCS functions and thus avoiding the need of the new mathematical methods of Blatt.

2. BCS Theory

The BCS theory assumes a ground state wave function of the form

$$\Phi_0 = \prod_{\alpha>0} (U_\alpha + V_\alpha a_\alpha^\dagger a_{-\alpha}^\dagger)|0), \qquad U_\alpha^2 + V_\alpha^2 = 1. \tag{2.1}$$

Excitations of two, four etc. quasiparticles are described by the wave functions

$$\Phi_{\alpha\beta} = a_\alpha^\dagger a_\beta^\dagger \prod_{\substack{\gamma \neq |\alpha|, |\beta| \\ \gamma>0}} (U_\gamma + V_\gamma a_\gamma^\dagger a_{-\gamma}^\dagger)|0), \tag{2.2}$$

$$\Phi_{\alpha\beta\gamma\delta} = a_\alpha^\dagger a_\beta^\dagger a_\gamma^\dagger a_\delta^\dagger \prod_{\substack{\epsilon>0 \\ \epsilon \neq |\alpha|, |\beta|, |\gamma|, |\delta|}} (U_\epsilon + V_\epsilon a_\epsilon^\dagger a_{-\epsilon}^\dagger)|0), \tag{2.3}$$

where $a_\alpha^\dagger$ creates a fermion in state α. To each single particle state α corresponds a unique state $-\alpha$, its conjugate under time reversal. (We assume that in (2.2) and (2.3) none of the excited indices are paired; i.e. $|\alpha| \neq |\beta| \neq |\gamma| \neq |\delta|$. Excitations involving both α and $-\alpha$ have different wave functions which are not needed in the following).

We assume that ground state Φ_0 and the quasiparticle excitations $\Phi_{\alpha\beta}$, $\Phi_{\alpha\beta\gamma\delta}, \ldots$ are eigenstates of the reduced BCS hamiltonian. The reduced hamiltonian includes the kinetic energy, possibly a single particle potential, and those matrix elements of the the interaction K which are of the form $K_{\alpha,-\alpha,\beta,-\beta}$. We denote the reduced hamiltonian by H_0. The full hamiltonian then is

$$H = H_0 + \sum_{\substack{|\alpha|\neq|\beta| \\ |\gamma|\neq|\delta|}} K_{\alpha\beta\gamma\delta} a_\alpha^\dagger a_\beta^\dagger a_\gamma a_\delta = H_0 + H_1. \tag{2.4}$$

The term H_1 is unimportant in determining the best variational U_α and V_α. They are given by the equations

$$\begin{aligned} U_\alpha^2 &= \tfrac{1}{2}\left(1+\frac{\xi_\alpha}{E_\alpha}\right), \qquad U_\alpha V_\alpha = -\frac{\Delta_\alpha}{2E_\alpha}, \\ V_\alpha^2 &= \tfrac{1}{2}\left(1-\frac{\xi_\alpha}{E_\alpha}\right), \qquad E_\alpha \equiv \sqrt{\xi_\alpha^2+\Delta_\alpha^2}, \end{aligned} \tag{2.5}$$

where the ξ_α are the single particle energies minus the chemical potential and Δ_α is determined by an integral equation involving only those matrix elements which appear in the reduced hamiltonian:

$$\Delta_\alpha = -\sum K_{\alpha,-\alpha;\beta,-\beta}\frac{\Delta_\beta}{2E_\beta}. \tag{2.6}$$

Choosing the ground state energy as 0, the energies of the excited states are given by the (approximate †) equations

$$H_0\Phi_0 = 0, \qquad H_0\Phi_{\alpha\beta} = (E_\alpha+E_\beta)\Phi_{\alpha\beta}, \ldots \text{etc.} \tag{2.7}$$

While assuming eq. (2.7) we must remember that the complete hamiltonian H is different from H_0 and that with respect to the full hamiltonian H the states Φ_0, $\Phi_{\alpha\beta}$ etc. are only sucessful trial functions with parameters determined variationally. Therefore when we introduce an extra perturbation into the hamiltonian, as we shall do in the next section, we must again determine the correction to the ground state wave function variationally to the desired order in the perturbation. (We shall determine it to first order.)

3. Useful Expressions

We shall need in the following a few expressions involving the wave functions (2.1)—(2.3), which can be obtained by straightforward calculation:

$$(\Phi_{\mu\nu} a_\alpha^\dagger a_\beta \Phi_0) = \delta_{\mu\alpha}\delta_{\nu,-\beta}U_\alpha V_\beta - \delta_{\mu,-\beta}\delta_{\nu\alpha}V_\alpha U_\beta, \tag{3.1}$$

$$(\Phi_{\mu\nu} a_\alpha^\dagger a_\beta^\dagger \Phi_0) = \delta_{\mu\alpha}\delta_{\nu,\beta}U_\alpha U_\beta - \delta_{\mu\beta}\delta_{\nu\alpha}U_\alpha U_\beta. \tag{3.2}$$

† The BCS wave functions are exact eigenfunctions of the "quasiparticle hamiltonian". The difference between the quasiparticle hamiltonian and the reduced hamiltonian connects the ground state Φ_0 only to states 4Δ above and the excited states $\Phi_{\alpha\beta}$, $\Phi_{\alpha\beta\gamma\delta}$, to states at least 2Δ above. Its effect is therefore small.

When substituting $-\alpha$ for α in an expression of this kind one should put $V_{-\alpha} = -V_\alpha$ and $U_{-\alpha} = U_\alpha$. The matrix elements of a single-particle operator

$$J = \sum J_{\alpha\beta} a_\alpha^\dagger a_\beta \tag{3.3}$$

are

$$(\Phi_{\alpha\beta} J \Phi_0) = J_{\alpha,-\beta} U_\alpha V_\beta + J_{-\alpha,\beta} V_\alpha U_\beta \tag{3.4}$$

and those of a two-particle operator

$$K = \sum K_{\alpha\beta\gamma\delta} a_\alpha^\dagger a_\beta^\dagger a_\gamma a_\delta, \qquad K_{\alpha\beta\gamma\delta} = -K_{\beta\alpha\gamma\delta} = -K_{\alpha\beta\delta\gamma}, \tag{3.5}$$

are

$$\begin{aligned}(\Phi_{\alpha\beta} K \Phi_{\gamma\delta}) = {} & K_{\alpha\beta\gamma\delta} U_\alpha U_\beta U_\gamma U_\delta + K_{-\delta,-\gamma,-\beta,-\alpha} V_\alpha V_\beta V_\gamma V_\delta \\ & + K_{\alpha,-\gamma,-\beta,\delta} U_\alpha V_\beta U_\gamma V_\delta + K_{\alpha,-\delta,\gamma,-\beta} U_\alpha V_\beta V_\gamma U_\delta \\ & + K_{-\gamma,\beta,-\alpha,\delta} V_\alpha U_\beta U_\gamma V_\delta + K_{-\delta,\beta,\gamma,-\alpha} V_\alpha U_\beta V_\gamma U_\delta \\ & (|\alpha|, |\beta|, |\gamma|, |\delta| \text{ all different}),\end{aligned} \tag{3.6}$$

$$\begin{aligned}(\Phi_{\alpha\beta\gamma\delta} K \Phi_0) = {} & K_{\alpha,\beta,-\gamma,-\delta} U_\alpha U_\beta V_\gamma V_\delta + K_{\delta,\gamma,-\beta,-\alpha} V_\alpha V_\beta U_\gamma U_\delta \\ & + K_{\alpha,\delta,-\gamma,-\beta} U_\alpha V_\beta V_\gamma U_\delta + K_{\alpha,\gamma,-\delta,-\beta} U_\alpha V_\beta U_\gamma V_\delta \\ & + K_{\gamma,\beta,-\alpha,-\delta} V_\alpha U_\beta U_\gamma V_\delta + K_{\delta,\beta,-\alpha,-\gamma} V_\alpha U_\beta V_\gamma U_\delta \\ & (|\alpha|, |\beta|, |\gamma|, |\delta| \text{ all different}).\end{aligned} \tag{3.7}$$

4. Behaviour under a Small Perturbation

The effect of a small single particle perturbation V is to create quasiparticle excitations of the form (2.2) via the matrix element (3.4). We therefore choose as our variational trial function for the perturbed ground state

$$\Psi = \exp \sum_{\alpha\beta} \chi'_{\alpha\beta} a_\alpha^\dagger a_\beta^\dagger \Phi_0 = \Phi_0 + \sum_{\alpha\beta} \eta_{\alpha\beta} \Phi_{\alpha\beta} + \tfrac{1}{2} \sum_{\alpha\beta\gamma\delta} \eta_{\alpha\beta}\eta_{\gamma\delta} \Phi_{\alpha\beta\gamma\delta} + \dots \tag{4.1}$$

This choice implies that excitation of "pairs of quasiparticles" appear independently of each other.

Calculating to second order in V (η being of first order) we obtain

$$\begin{aligned}(\Psi, H+V, \Psi) = (\Phi_0 + \sum_{\alpha\beta} \eta^*_{\alpha\beta} \Phi_{\alpha\beta} + \tfrac{1}{2} \sum_{\alpha\beta\gamma\delta} \eta^*_{\alpha\beta}\eta^*_{\gamma\delta} \Phi_{\alpha\beta\gamma\delta}, \\ H_0+V+H_1, \quad \Phi_0 + \sum_{\alpha\beta} \eta_{\alpha\beta} + \tfrac{1}{2} \sum_{\alpha\beta\gamma\delta} \eta_{\alpha\beta}\eta_{\gamma\delta} \Phi_{\alpha\beta\gamma\delta}).\end{aligned} \tag{4.2}$$

Differentiating with respect to $\eta^*_{\mu\nu}$ and keeping first order terms only we obtain

$$(\Phi_{\mu\nu}, H_0+V, \Phi_0 + \sum \eta_{\alpha\beta} \Phi_{\alpha\beta}) + \sum_{\alpha\beta} \eta^*_{\mu\nu} (\Phi_{\mu\nu\alpha\beta} H_1 \Phi_0) = 0, \tag{4.3}$$

or

$$(E_\mu + E_\nu)\eta_{\mu\nu} - (\Phi_{\mu\nu} V \Phi_0) + \sum_{\alpha\beta} (\Phi_{\mu\nu} H_1 \Phi_{\alpha\beta}) \eta_{\alpha\beta} + \sum_{\alpha\beta} (\Phi_{\mu\nu\alpha\beta} H_1 \Phi_0) \eta^*_{\alpha\beta} = 0. \tag{4.4}$$

This can be put in the form

$$\eta_{\mu\nu}=\frac{(\Phi_{\mu\nu}V\Phi_0)+g_{\mu\nu}}{E_\mu+E_\nu}=\frac{V_{\mu,-\nu}(U_\mu V_\nu-U_\nu V_\mu)+g_{\mu\nu}}{E_\mu+E_\nu}, \tag{4.5}$$

assuming V to be odd under time reversal.

Neglecting the $g_{\mu\nu}$ term we would be back with the expression given by formal perturbation theory using the BCS wave functions and energies (see Belyaev [2]). The $g_{\mu\nu}$ represents a correction to this term and is in turn determined by the integral equation

$$\begin{aligned} g_{\mu\nu} &= -\sum_{\alpha\beta}(\Phi_{\mu\nu}H_1\Phi_{\alpha\beta})\eta_{\alpha\beta}-\sum_{\alpha\beta}(\Phi_{\mu\nu\alpha\beta}H_1\Phi_0)\eta^*_{\alpha\beta} \\ &= -U_\mu U_\nu\sum_{\alpha\beta}K_{\mu\nu\alpha\beta}(U_\alpha U_\beta\eta_{\alpha\beta}-V_\alpha V_\beta\eta^*_{-\alpha,-\beta}) \\ &\quad +V_\mu V_\nu\sum_{\alpha\beta}K_{\mu\nu\alpha\beta}(U_\alpha U_\beta\eta^*_{\alpha\beta}-V_\alpha V_\beta\eta_{-\alpha,-\beta}). \end{aligned} \tag{4.6}$$

The first order correction to the density matrix is given by

$$\begin{aligned} \delta\rho_{\beta\alpha} &= (\Phi_0+\textstyle\sum\eta^*_{\gamma\delta}\Phi_{\gamma\delta},\, a_\alpha{}^\dagger a_\beta,\, \Phi_0+\sum\eta_{\gamma\delta}\Phi_{\gamma\delta}) \\ &= \textstyle\sum\eta^*_{\gamma\delta}(\Phi_{\gamma\delta}a_\alpha{}^\dagger a_\beta\Phi_0)+\sum\eta_{\gamma\delta}(\Phi_{\gamma\delta}(\Phi_0 a_\alpha{}^\dagger a_\beta\Phi_{\gamma\delta}) \\ &= \eta^*_{\alpha,-\beta}U_\alpha V_\beta+V_\alpha U_\beta\eta_{-\alpha,\beta} \\ &= \frac{V_{\beta\alpha}(U_\alpha V_\beta-V_\alpha U_\beta)^2+U_\alpha V_\beta g^*_{\alpha,-\beta}+V_\alpha U_\beta g_{-\alpha,\beta}}{E_\alpha+E_\beta}, \end{aligned} \tag{4.7}$$

where the correction g is again to be determined by (4.5) and (4.6). This correction takes into account the matrix elements of the interaction which are excluded from H_0. It can be shown that this correction insures gauge invariance when V is a magnetic field and makes the total mass come out correctly, porvided the total interaction is not velocity dependent. Rather than showing this directly here, we shall simply point out the equivalence of this treatment to those of Blatt and Migdal.

5. Connection with Migdal's treatment

Let us define $\delta\psi_{\alpha\beta}$ as

$$\delta\psi_{\alpha\beta}\equiv(\Psi,\, a_\alpha{}^\dagger a_\beta{}^\dagger\Psi); \tag{5.1}$$

then

$$\delta\psi_{\alpha\beta}=\eta^*_{\alpha,-\beta}U_\alpha U_\beta+V_\alpha V_\beta\eta_{-\alpha,\beta}. \tag{5.2}$$

We now define $\delta\Delta$ and $\delta\Delta^*$ as follows:

$$\begin{aligned} g^*_{\alpha,-\beta} &= U_\alpha U_\beta\delta\Delta_{\alpha,-\beta}+V_\alpha V_\beta\delta\Delta^*_{-\alpha,\beta}, \\ g_{-\alpha,\beta} &= -V_\alpha V_\beta\delta\Delta_{\alpha,-\beta}-U_\alpha U_\beta\delta\Delta^*_{-\alpha,\beta}. \end{aligned} \tag{5.3}$$

The expressions (4.7) and (5.2) for $\delta\rho$ and $\delta\psi$ can now be written as

$$\delta\rho_{\alpha\beta} = \frac{V_{\alpha\beta}(\xi_\alpha\xi_\beta+\Delta_\alpha\Delta_\beta-E_\alpha E_\beta)-\delta\Delta_{\alpha,-\beta}\xi_\alpha\Delta_\beta+\delta\Delta_{-\alpha,\beta}\xi_\beta\Delta_\alpha}{2E_\alpha E_\beta(E_\alpha+E_\beta)}, \tag{5.4}$$

$$-\delta\psi_{\alpha,-\beta} = \frac{V_{\alpha\beta}(\xi_\alpha\Delta_\beta-\xi_\beta\Delta_\alpha)+\delta\Delta_{\alpha,-\beta}(E_\alpha E_\beta+\xi_\alpha\xi_\beta)-\delta\Delta^*_{-\alpha,\beta}\Delta_\alpha\Delta_\beta}{2E_\alpha E_\beta(E_\alpha+E_\beta)}, \tag{5.5}$$

using the identities (2.5). The equations (5.4) and (5.5) are identical with Migdal's equations (15) and (16). Migdal's integral equation for $\delta\Delta$ in the case of general interaction is

$$\delta\Delta_{\alpha\beta} = -\sum_{\gamma\delta} K_{\alpha\beta\gamma\delta}\delta\psi_{\gamma\delta}. \tag{5.6}$$

This is equivalent to our equation (4.6) for $g_{\alpha\beta}$ as can be easily checked by using (5.2) and (5.3). It can be shown that for a δ-function interaction (5.6) can be brought to the form given by Migdal as his final result [8]).

6. Connection with Blatt's treatment

The projection of Φ_0 on the subspace of N pairs is

$$\frac{1}{N!}\prod_\gamma U_\gamma\left(\sum_\alpha \frac{V_\alpha}{U_\alpha}a_\alpha^\dagger a_{-\alpha}^\dagger\right)^N|0).$$

Blatt insists that even when we include the perturbation the wave function is built out of pair wave functions in a similar form, namely

$$\Psi = \frac{1}{N!}\prod_\gamma U_\gamma\left[\sum_{\alpha\beta}\left(\frac{V_\alpha}{U_\alpha}\delta_{\alpha,-\beta}+\delta\chi_{\alpha\beta}\right)a_\alpha^\dagger a_\beta^\dagger\right]^N|0), \qquad \delta\chi_{\alpha\beta} = -\delta\chi_{\beta\alpha}. \tag{6.1}$$

Expanding this we find

$$\Psi = \frac{1}{N!}\prod_\mu U_\mu\left[\sum_{\alpha\beta}\left(\frac{V_\alpha}{U_\alpha}a_\alpha^\dagger a_{-\alpha}^\dagger\right)^N + N\sum_{\alpha\beta}\delta\chi_{\alpha\beta}a_\alpha^\dagger a_\beta^\dagger\left(\sum_\gamma\frac{V_\gamma}{U_\gamma}a_\gamma^\dagger a_{-\gamma}^\dagger\right)^{N-1}\right.$$
$$\left.+\tfrac{1}{2}N(N-1)\sum_{\alpha\beta\gamma\delta}\delta\chi_{\alpha\beta}\delta\chi_{\gamma\delta}a_\alpha^\dagger a_\beta^\dagger a_\gamma^\dagger a_\delta^\dagger\left(\sum_\epsilon\frac{V_\epsilon}{U_\epsilon}a_\epsilon^\dagger a_{-\epsilon}^\dagger\right)^{N-2}+\ldots\right]|0). \tag{6.2}$$

In the spirit of the saddle point treatment of the number of particles we may put

$$\Phi_0 \approx \frac{1}{N!}\prod_\gamma U_\gamma\left(\sum\frac{V_\alpha}{U_\alpha}a_\alpha^\dagger a_{-\alpha}^\dagger\right)^N|0) \approx \frac{1}{(N-1)!}\prod U_\gamma\left(\sum\frac{V_\alpha}{U_\alpha}a_\alpha^\dagger a_{-\alpha}^\dagger\right)^{N-1}|0)$$
$$\approx \frac{1}{(N-2)!}\prod U_\gamma\left(\sum\frac{V_\alpha}{U_\alpha}a_\alpha^\dagger a_{-\alpha}^\dagger\right)^{N-2}|0) \approx \ldots. \tag{6.3}$$

Using this we have

$$\Psi = \Phi_0 + \sum \eta_{\alpha\beta}\Phi_{\alpha\beta} + \tfrac{1}{2}\sum_{\alpha\beta\gamma\delta} \eta_{\alpha\beta}\eta_{\gamma\delta}\Phi_{\alpha\beta\gamma\delta} + \ldots, \tag{6.4}$$

where

$$\eta_{\alpha\beta} = U_\alpha U_\beta \delta\chi_{\alpha\beta}. \tag{6.5}$$

In this way we see that Blatt's trial function is identical with ours within the limitations of the approximation used. Therefore also his results must be identical within the framework of this approximation. It is interesting to note that there is no difference in the first order between insisting on the pair structure (6.1) and between breaking of pairs by the introduction of quasi-particle excitations.

The connection with Blatt's formalism is given by (6.5): using also the notations

$$\frac{V_\alpha}{U_\alpha} = \chi_\alpha = \chi_{\alpha,-\alpha}, \qquad V_\alpha U_\alpha = \psi_\alpha = \psi_{\alpha,-\alpha}, \tag{6.6}$$

it can be verified that the integral equation (4.4) is what we would have obtained from Blatt's eq. (7.8) of ref. [6]) by substracting the equations for $\delta\chi_{mm'}$ and $\delta\chi_{m'm}$. Blatt's definitions of $\delta\chi$, $\delta\psi$ and $\delta\rho$ (denoted δh by Blatt) are identical with ours.

It is a pleasure to thank Prof. H. J. Lipkin for numerous discussions of the contents of this paper as well as for guidance in its presentation. I also wish to thank Prof. J. M. Blatt with whom I had occasion to work on a related subject, thereby becoming acquainted with his own methods. Comments on the preprint by Professors Blatt, Rickayzen, Valatin and Bardeen are gratefully acknowledged.

References

1) Bardeen, Cooper and Schrieffer, Phys. Rev. **108** (1957) 1175
2) Belyaev, Mat. Fys. Medd. Dan. Vid. Selsk. **31**, no. 11
3) Prange, Lectures Int. Spring School of Physics, Naples (1960)
4) Bardeen and Schrieffer, Prog. of Low Temperature Physics, to be published
5) Migdal, Nuclear Physics **13** (1959) 655
6) Blatt, Prog. Theor. Phys. **24** (1960) 851
7) Blatt, Journal of the Australian Math. Soc. **1** (1960) 465
8) Katz and Blatt, Nuclear Physics **23** (1961) 612

1.B

Nuclear Physics **26** (1961) 136—146; © *North-Holland Publishing Co., Amsterdam*

Not to be reproduced by photoprint or microfilm without written permission from the publisher

ELASTIC AND INELASTIC SCATTERING OF NEUTRONS BY DEUTERONS NEAR THE INELASTIC THRESHOLD

L. M. DELVES

Laboratory for Nuclear Science Massachusetts Institute of Technology, Cambridge, Massachusetts

Received 19 December 1960

Abstract: A calculation is made of the neutron-deuteron s-wave elastic and inelastic scattering cross-sections which includes the interaction between these two channels. The scattering matrix given by this method is unitary. Comparison is made with a calculation of the elastic scattering using the same potentials but neglecting the effect of the inelastic channel. Large differences are found, indicating that it is important to include the deuteron distortion in elastic scattering calculations; however, this conclusion may be due at least partly to neglect of charge exchange scattering.

The proton energy spectrum predicted by the model is the phase-space spectrum. This is identical with that of Frank and Gammel except near the upper end of the spectrum, where it agrees better with experiment at the energies considered.

The size of the anomaly in the elastic scattering cross-section at the inelastic threshold is calculated, and found to be rather small.

1. Introduction

Previous calculations of the elastic [1, 2, 3]) and inelastic [4]) scattering of nucleons from deuterons have neglected the interaction between the elastic and inelastic channels. For elastic scattering calculations this corresponds to neglect of deuteron distortion, while it is implied in calculations of inelastic scattering by use of the distorted wave method. The approximation is clearly not valid for the inelastic channel, since the cross-sections resulting from use of it violate the conservation laws [4]). For the elastic channel the situation is less clear; estimates of the effect on the elastic cross-section of neglect of deuteron distortion range from small [5]) to large [6]). A lower limit to the effect is set by the condition that the scattering matrix be unitary; this is reflected in the elastic scattering cross-section by an anomaly at the inelastic threshold (a discontinuity in the value of the second derivative of the elastic cross-section with respect to energy [7])). However, the total disturbance of the elastic cross-section is not related to the size of the anomaly and may be considerably larger. It is thus of interest to have a method of calculation which explicitly includes the interaction

† Present address: Applied Mathematics Department, University of New South Wales, Sydney, Australia. This work was partly carried out at the Clarendon Laboratory, Oxford, and was supported by a Shell Scholarship and partly by funds provided by the U. S. Atomic Energy Commission, the Office of Naval Research and the Airforce Office of Scientific Research.

between the channels; we give here the results of some calculations with simple potentials using such a method. We write the total wave-function as a sum of resonating group functions including both elastic and inelastic parts. The elastic part of the wave-function is expanded in the usual angular momentum representation, while the inelastic part is expanded in the discrete representation given previously (refs. [7,8]), referred to as (I), (II)); in the present calculations only the lowest terms in each series have been kept (that is, s-wave elastic scattering; inelastic scattering only in the channel of channel order $\frac{3}{2}$ in the notation of (II)). The wave-function used is written explicitly below. The resulting coupled integro-differential equations are solved numerically to give the (automatically unitary) scattering matrix.

2. Formalism

We consider, then, a system of three nucleons, obeying the equation

$$\left[\nabla_1^2+\nabla_2^2+\nabla_3^2+\frac{2m}{\hbar^2}(E-V_1-V_2-V_3)\right]\Psi=0, \tag{2.1}$$

where m is the nucleon mass. The potential we assume between two nucleons j, k has the simple form

$$V_i=-V_0\exp[-(r_{jk}/r_0)^2]. \tag{2.2}$$

Particles 1, 2, 3 have position vectors $\mathbf{r}_1$, $\mathbf{r}_2$, $\mathbf{r}_3$; taking out the centre-of-mass coordinate $\frac{1}{3}(\mathbf{r}_1+\mathbf{r}_2+\mathbf{r}_3)$ we can define the two following distinct coordinate frames in the C.M. system:

(1) the frame x, y, θ_x, θ_y, ϕ_x, ϕ_y given by

$$\mathbf{y}=\mathbf{r}_1-\mathbf{r}_2=(y,\theta_y,\phi_y),\quad \mathbf{x}=\tfrac{1}{2}(\mathbf{r}_1+\mathbf{r}_2)-\mathbf{r}_3=(x,\theta_x,\phi_x), \tag{2.3}$$

(2) the frame r, α, θ_x, θ_y, ϕ_x, ϕ_y, where

$$x=\sqrt{\tfrac{3}{2}}\,r\cos\alpha,\quad y=\sqrt{2}\,r\sin\alpha. \tag{2.4}$$

The first set of coordinates is the natural one for describing the scattering of particle 3 from a bound state of particles 1 and 2, while the second set is just that introduced in (II) for the description of 3-particle channels. We shall write the wave-function Ψ as the sum of a scattering wave-function written in terms of coordinates (1), and a disintegration wave-function written in terms of coordinates (2); i.e. we put

$$\Psi=\frac{\phi(y)}{y}\frac{f(x)}{x}+\frac{g(r)}{r^{2.5}}, \tag{2.5}$$

where $\phi(y)/y$ is the bound state deuteron wave-function with the potential

(2.2), normalized to

$$\int_0^\infty \phi^2(y)\mathrm{d}y = 1.$$

In the notation of (II), this wave-function represents elastic scattering in the channel $l_x = 0$ (and $l_y = 0$ since the deuteron is in an s-state) plus three-particle scattering in the channel $l_x = 0$, $l_y = 0$, $\lambda = 0$ (with channel order $\frac{3}{2}$). Such a wave-function neglects, of course, other channels which will be coupled in these two; in particular, charge exchange elastic scattering is neglected, as are inelastic channels of channel order $> \frac{3}{2}$.

The functions f, g have the asymptotic forms

$$\begin{aligned} f(qx) &\sim \left(\frac{2m}{3q}\right)^{\frac{1}{2}} [AF_0(qx)+BG_0(qx)] \quad \text{for} \quad r \to \infty, \\ g(kr) &\sim \left(\frac{m}{k}\right)^{\frac{1}{2}} [CF_{\frac{1}{2}}(kr)+DG_{\frac{1}{2}}(kr)] \quad \text{for} \quad r \to \infty, \end{aligned} \tag{2.6}$$

where $\frac{2}{3}m$ is the reduced mass of the elastic channel and

$$q^2 = \frac{4m}{3\hbar^2}(E-E_\mathrm{d}), \quad k^2 = \frac{2mE}{\hbar^2} \tag{2.7}$$

E_d is the deuteron bound state energy

$$E_\mathrm{d} = -2.226\ \mathrm{MeV}$$

and we measure energies from the inelastic threshold. The quantities $F_l(z)$ and $G_l(z)$ are the regular and irregular solutions of the force-free Schrödinger equation. The reactance matrix S_R is given explicitly by

$$B = S_{\mathrm{R}11}A+S_{\mathrm{R}21}C, \quad D = S_{\mathrm{R}12}A+S_{\mathrm{R}22}C. \tag{2.8}$$

Above the inelastic threshold S_R is real, and can be expanded in powers of k. We diagonalize S_R by putting

$$\begin{aligned} S_\mathrm{R} &= U^\mathrm{T} \tan \delta U, \\ U &= \begin{pmatrix} \cos\varepsilon & \sin\varepsilon \\ -\sin\varepsilon & \cos\varepsilon \end{pmatrix}, \quad \tan\delta = \begin{pmatrix} \tan\delta_1 & 0 \\ 0 & \tan\delta_2 \end{pmatrix} \end{aligned} \tag{2.9}$$

and use the following expansions (see (II)) for U, δ and the reaction matrix R:

$$R = U^\mathrm{T}(1-\mathrm{e}^{2i\delta})U,$$

$$\begin{aligned}
\cot \delta_1 &= \delta_{10}+\delta_{12}k^2+\delta_{14}k^4+\ldots,\\
\tan \varepsilon &= k^2(\varepsilon_0+\varepsilon_2k^2+\varepsilon_4k^4+\ldots),\\
\cot \delta_2 &= k^{-4}(\delta_{20}+\delta_{22}k^2+\delta_{24}k^4+\ldots),\\
R_{11} &= q(R_{110}+R_{112}k^2+R_{114}k^4+\ldots),\\
R_{12} &= k^2(R_{120}+R_{122}k^2+R_{124}k^4+\ldots),\\
R_{22} &= k^4(R_{220}+R_{222}k^2+R_{224}k^4+\ldots),
\end{aligned} \tag{2.10}$$

where the series for R_{11} has been written in a form which takes account of the behaviour of R_{11} at $q = 0$, that is the elastic scattering threshold. Above the inelastic threshold δ_1, δ_2 and ε are real, since S_R is real; R of course is not. Below this threshold (but above the elastic threshold) S_R is not real but has the form just below threshold

$$S_R^{-1}(-) = \begin{pmatrix} E & F \\ F & H+i \end{pmatrix}, \tag{2.11}$$

where E, F and H are real and related to S_R^{-1} just above threshold by

$$E = (S_R^{-1}(+))_{11}, \quad F = (S_R^{-1}(+))_{12}, \quad H = (S_R^{-1}(+))_{22}-1. \tag{2.12}$$

This change of form affects the coefficients in the expansions (2.10) below threshold; we find, below the three-particle threshold but above the two-particle threshold

$$\begin{aligned}
\cot \delta_1 &= \delta_{10}+\delta_{12}k^2+(\delta_{14}-\varepsilon_0^2+i\varepsilon_0^2)k^4+\ldots,\\
\tan \varepsilon &= k^2(\varepsilon_0+\varepsilon_2k^2+\varepsilon_4k^4+\ldots),\\
\cot \delta_2 &= k^{-4}(\delta_{20}+\delta_{22}k^2+(\delta_{24}-1+i)k^4+\ldots),\\
R_{11} &= q\left[R_{110}+R_{112}k^2+\left(R_{114}+\frac{\varepsilon_0^2\{1+2\delta_{10}-\delta_{10}^2+i(1-2\delta_{10}-\delta_{10}^2)\}}{\delta_{10}^2(1+\delta_{10}^2)}\right)k^4+\ldots\right].
\end{aligned} \tag{2.13}$$

The difference in the form of the expansion for R_{11} above and below threshold implies an anomaly in the elastic cross-section at the inelastic threshold of the form discussed in (II); the second derivative of the elastic cross-section with respect to energy has a finite discontinuity at $k = 0$ given by

$$\begin{aligned}
\sigma_{el} &= \frac{\pi|R_{11}|^2}{q^2},\\
\left.\frac{d^2\sigma_{el}}{d(k^2)^2}\right|_{k^2=+0} - \left.\frac{d^2\sigma_{el}}{d(k^2)^2}\right|_{k^2=-0} &= \frac{8\pi\varepsilon_0^2(\delta_{10}-1)^3}{\delta_{10}^2(1+\delta_{10}^2)^2}.
\end{aligned} \tag{2.14}$$

Note that the size of this discontinuity depends only on the threshold value of the scattering matrix; that is, on the first terms in the expansions (2.10) or (2.13). The discontinuity is not given by calculations of the elastic scattering which ignore the inelastic channel.

If we do ignore the inelastic channel (put $g(r) = 0$ in eq. (2.5)), only R_{11} is of interest; S_{R11} can then be written

$$S_{R11} = \tan \delta_0,$$

where δ_0 is a real phaseshift (above the elastic threshold) with expansion

$$\tan \delta = q(\delta_{00} + \delta_{02}k^2 + \delta_{04}k^4 + \ldots). \tag{2.10a}$$

3. Numerical Calculations

Insertion of the form (2.5) for Ψ into (2.1), with the C.M. motion removed, leads to the following equations for $f(x)$ and $g(r)$:

$$\tfrac{3}{2}\frac{d^2f}{dx^2} + q^2 f + \frac{2mV_0 r_0^2 f}{\hbar^2 x}\int_0^\infty G_0(x, y)dy$$
$$+ x\int_0^\infty \left(r^{-\frac{1}{2}}\frac{d^2g}{dr^2} - \tfrac{15}{4}r^{-\frac{9}{2}}g\right)\phi(y)y\,dy + \frac{2mx}{\hbar^2}\int_0^\infty G_1(x, y)g(r)dy = 0, \tag{3.1}$$

$$\frac{16r^{\frac{1}{2}}}{3^{\frac{1}{2}}\pi}\int_0^{\frac{1}{3}\pi}\left(\tfrac{3}{2}\frac{d^2f}{dx^2} + G_2(r, \alpha)f\right)\phi(y)\sin\alpha\cos\alpha\,d\alpha + \frac{d^2g}{dr^2} - \frac{15g}{4r^2}$$
$$+ k^2 g + \frac{2mg}{\hbar^2}\int_0^{\frac{1}{3}\pi} G_3(r, \alpha)\sin^2\alpha\cos^2\alpha\,d\alpha = 0, \tag{3.2}$$

where

$$G_0 = \frac{\phi^2(y)}{y}Q(x, y),$$
$$G_1 = \frac{y\phi(y)}{r^{\frac{9}{2}}}\left[E + V_0 e^{-(y/r_0)^2} + \frac{V_0 r_0^2}{xy}Q(x, y)\right],$$
$$G_2 = \frac{2m}{\hbar^2}\left[E - E_d + \frac{V_0 r_0^2}{xy}Q(x, y)\right], \tag{3.3}$$
$$G_3 = \frac{16V_0}{\pi}\left[\exp(-y^2/r_0^2) + \frac{r_0^2}{xy}Q(x, y)\right],$$
$$Q(x, y) = \exp[-(x^2+y^2)/r_0^2]\left\{\exp\left(\frac{xy}{r_0^2}\right) - \exp\left(\frac{-xy}{r_0^2}\right)\right\}.$$

Eqs. (3.1) and (3.2) are a set of coupled integro-differential equations for $f(x)$ and $g(r)$; they are complicated by the appearance of the two coordinate systems (x, y) and (r, α), which implies that they are essentially two-dimensional. They can nonetheless be treated in a way similar to that of Fox and Goodwin [9]) for one-dimensional integral equations; the method is given in detail elsewhere [10]), and was programmed for the IBM 704 at this Institute by

M. M. Pennell. Calculations were carried out for a well of width $r_0 = 1.332$ fm which for a deuteron binding energy $E_d = -2.226$ MeV implies $V = 86.674$ MeV. The deuteron wave-function $\phi(y)$ and eigenvalue V_0 were calculated on the Oxford Mercury computer, on which also much preliminary work and the analysis of the results was carried out. Solutions of (3.1) and (3.2) were computed at energies of 0, 0.5, 1 and 7 MeV above the inelastic threshold. The initial work of setting up and testing the programme was carried out at zero energy, since the inelastic wave-function then has the simpler asymptotic form

$$g(r) \approx Cr^{2.5} + Dr^{-1.5}.$$

The constants C and D are found numerically by matching the solution at some radius ($r = 5$ fm was taken) to the asymptotic form; the accuracy of numerical solution aimed at of $\approx 3\,\%$ is then not sufficient to define $Dr^{-1.5}$ well in the presence of the large term $Cr^{2.5}$, so that the scattering matrix was not calculated at this energy. For the same reason it was not practicable to solve the equations directly below the inelastic threshold. For the positive energies chosen, the difficulty is minor; however, the accuracy of the scattering matrix found increases with energy.

Two independent solutions of the equations at each energy are necessary to define the scattering matrix; in fact four solutions were calculated and taken in pairs to give S_R, in order to check that the accuracy of solution was sufficient. The matrices thus found agreed between different sets to better than 0.1 %, indicating that the finite difference equations were being solved to sufficient accuracy; however, the overall accuracy, which depends also on the accuracy with which solutions of the finite difference equations represent solutions of the original equations, is much less than this. The results for S_R are given in table 1;

TABLE 1

Calculated values of S_R at various energies

Energy	0.5	1	7
S_{R11}	−0.38918	−0.40769	−0.45977
S_{R12}	0.037684	0.088604	0.64381
S_{R21}	0.056944	0.11849	0.83335
S_{R22}	0.010385	0.043201	0.58911
cot δ_1	−2.545	−2.334	−1.215
cot δ_2	69.25	16.83	1.071
tan ε	−0.1104	−0.2056	−0.5058
tan δ_0	−0.93252	−1.0449	−2.8152

is is seen that S_{R12} and S_{R21} differ by from 50 % at 0.5 MeV to 30 % at 7 MeV, while in fact S_R must be symmetric. These off-diagonal elements are very sensitive to inaccuracies in the numerical wave-functions; a change of 1 % in the wave-function changes S_{R12} by about 10 %, so that symmetry to within 30 % indicates that the overall accuracy of the numerical solutions is about 1.5 %.

This is slightly better than expected for the step-lengths and finite-difference approximations used.

It can be shown [11]) that a variational estimate of S_{R12} with the numerical wave-functions used is

$$S_{R12} = S_{R21} = \tfrac{1}{2}(S_{R12}^{(\text{numerical})} + S_{R21}^{(\text{numerical})},$$

with an accuracy of perhaps 10 % in our case.

The reactance matrix thus found was diagonalized at each energy and the resulting values of cot δ_1, cot δ_2, and tan ε used to give the first three terms in the expansions 2.10. The results are given in table 2. Expansions (2.10) and

TABLE 2

Leading terms in the expansions (2.10) and (2.10a)

Term	First	Second	Third
cot δ_1	−2.7741	9.8842	−15.5997
cot δ_2	0.04257	−0.12336	1.06266
tan ε	−4.90986	13.90	−11.23
R_{11}	0.873+i 2.424	1.032−i 6.345	2.302+i 6.663
R_{12}	−1.234−i 3.062	−2.676−i 16.077	20.277−i 53.485
R_{22}	3.630−i 35.415	144.36 −i 116.50	−387.2 +i 611.6
tan δ_0	−2.960	−8.024	4.360

(2.13) have been used to plot the s-wave elastic scattering and break-up cross-sections against C.M. energy, in fig. 1. Also given in tables 1 and 2 are the results for the elastic phase-shift assuming that the elastic channel is not coupled to

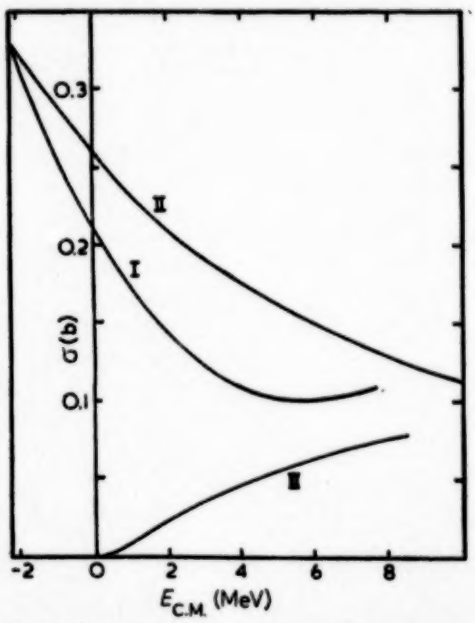

Fig. 1. Elastic scattering and break-up cross-sections as a function of the centre-of-mass energy. Curve I shows σ_{el} as calculated by means of the expansions (2.10) and (2.13). Curve II shows σ_{el} as obtained by solving eq. (3.1) with $g(r) = 0$ (this curve is multiplicated with a factor of 0.367). Curve III shows σ_{inel} as calculated by means of the expansions (2.10) and (2.13)

the inelastic channel; these were obtained by solving (3.1) with $g(r) \equiv 0$. The resulting elastic cross-section is plotted in fig. 1.

4. Discussion

4.1. THE ELASTIC CHANNEL

These results would appear to indicate that the elastic channel is strongly affected by the inelastic channel. Qualitatively the effect of the inelastic channel is to damp out the elastic wave-function inside the range of the forces acting between the incoming neutron and the deuteron. This is illustrated in figs. 2 and 3, which plot the two independent numerical solutions for $f(x)$ and

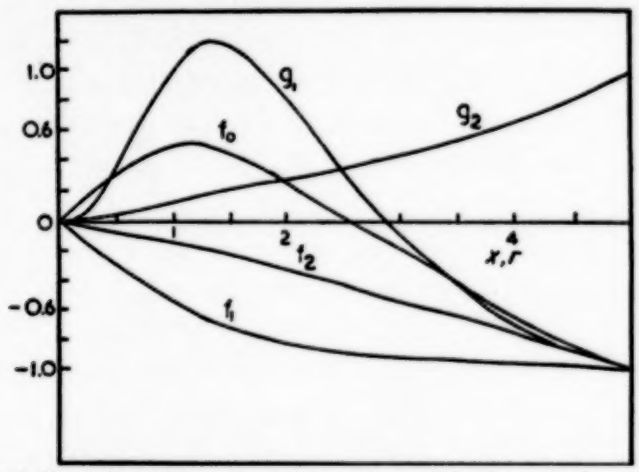

Fig. 2. Numerical solutions for $f(x)$ and $g(r)$ together with the solution f_0 for $f(x)$ obtained by neglecting $g(r)$. The energy is $E = 0$ MeV.

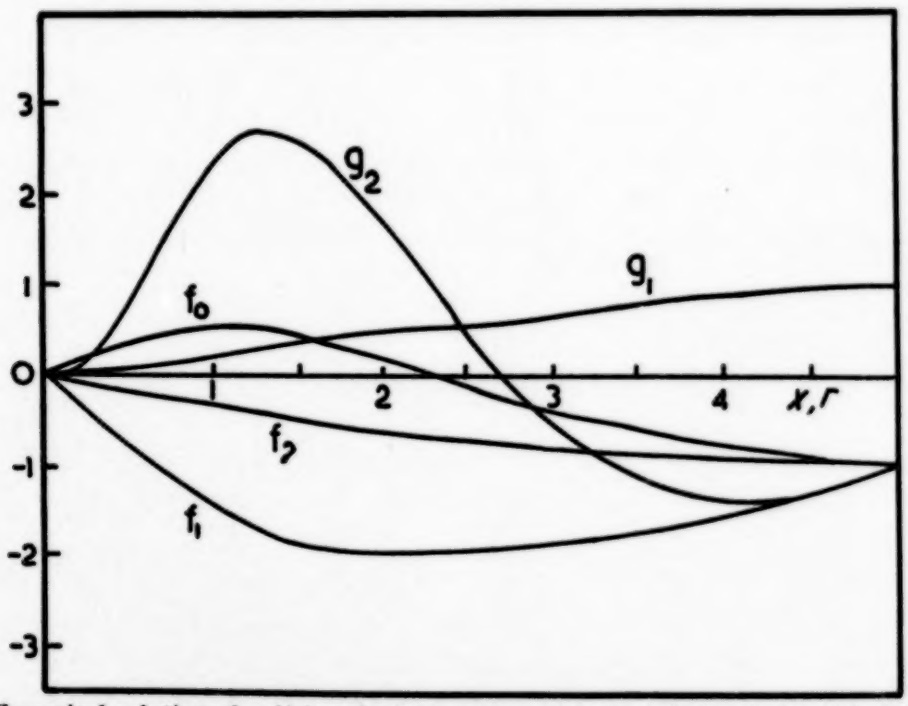

Fig. 3. Numerical solutions for $f(x)$ and $g(r)$ together with the solution f_0 for $f(x)$ obtained by neglecting $g(r)$. The energy is $E = 7$ MeV.

$g(r)$ for $E = 0$ and 7 MeV, together with the corresponding solution f_0 for $f(x)$ neglecting $g(r)$. The degree of damping is striking. The effect of this damping is to reduce the elastic cross-section considerably, by a factor of 0.37 at $E = -2.226$ MeV, that is at the elastic threshold. If these large effects are not dependent on the approximations used, then clearly calculations which ignore the inelastic channel (distortion of the deuteron, in resonating group language) are meaningless, but it is not clear whether this is so. The approximations made are neglect of inelastic channels of channel order greater than $\frac{3}{2}$, and neglect of charge exchange elastic scattering; the first of these is not expected to be too important at low energies, where the $l = \frac{3}{2}$ inelastic channel is dominant kinematically, but the effect of the second approximation is hard to estimate. Previous estimates of the 'distortion' of the deuteron in the elastic scattering channel have been made [5]) which seem to show that a large portion of this distortion is due to the charge exchange channel and not the inelastic channel. It would appear that a good resonating group calculation of elastic scattering should satisfy the following conditions:

(a) Charge exchange scattering should be included. This is the case in most published calculations of n–d scattering.

(b) A good deuteron wave-function should be used. It has been shown by Spruch *et al.* [12]) that certain bounds on the zero energy scattering parameters can even be violated if poor bound-state wave-functions are used. This is so in many resonating-group calculations; see also ref. [5]).

(c) The effects of the inelastic channels should be included.

The present calculation fulfils conditions (b) and (c); those of refs. [1, 3]) fulfil conditions (a) and (b), while the calculations of ref. [2]) fulfil only (a). It would be desirable to have a calculation of this type which satisfied all three, and this seems most easily done not by antisymmetrizing the wave-function used here but by introducing specifically the charge-exchange channel and antisymmetrizing only after solution of the equations.

The elastic scattering anomaly at the inelastic threshold is found from table 2 to be

$$\left.\frac{\mathrm{d}^2\sigma_{\mathrm{el}}}{\mathrm{d}E^2}\right|_{E=+0} - \left.\frac{\mathrm{d}^2\sigma_{\mathrm{el}}}{\mathrm{d}E^2}\right|_{E=-0} = 1.83\ \mathrm{mb/MeV^2}.$$

This is a rather small discontinuity, even though the overall elastic cross-section is modified considerably by inclusion of the inelastic channel.

4.2. THE INELASTIC CHANNEL

Previous calculations of the inelastic processes [43]) have shown that this proceeds almost wholly from the neutron-deuteron s-state; thus within the limitation of the potentials and wave-functions used, the cross-section for deuteron break-up given by the calculation can be compared directly with

experiment. Unfortunately, experiments are somewhat meagre, but estimates [4, 13, 14]) from that of the mirror reaction d(p, n)pp indicate a cross-section some five times that found here. This compares favourably with previous calculations [43]), which gave for energies greater than about 3 MeV a cross-section greater than that allowed by the conservation laws ($\sigma_{\text{inel}} > \pi/k_n^2$). Such a violation is excluded in the present calculation which yields automatically a unitary scattering matrix. The smallness of the calculated inelastic cross-section can be referred back to the behaviour of the proper phase-shifts δ_0 and δ_1 and the mixture parameter ε; the elastic cross-section depends mainly on $\sin^2\delta_1$ over the energy range in question, while the inelastic cross-section is approximately proportional to $\sin^2 2\varepsilon \sin^2\delta_1$. Thus δ_1 as calculated appears to be somewhat small, while ε is of the right order of magnitude.

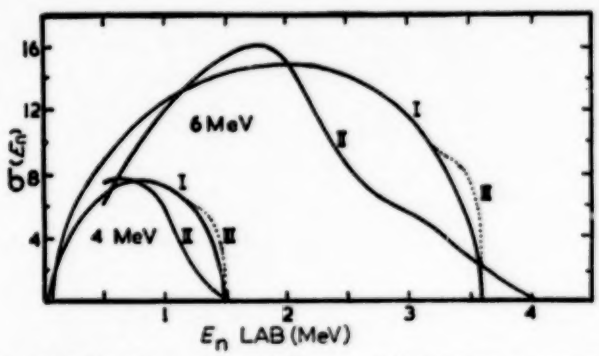

Fig. 4. Neutron spectra at 0° for $E_{\text{lab}} = 4$ and $E_{\text{lab}} = 6$ MeV. The curves I are theoretical spectra calculated from eq. (4.1), the curves II are experimental spectra measured by Cranberg and Smith [15]) and the curves III are theoretical spectra calculated by Frank and Gammel [16]).

The energy spectrum of the emitted particles in the inelastic channel is of interest, and is most easily expressed by giving that of the emitted proton. This is, in the centre-of-mass frame [8]),

$$\mathrm{d}\sigma(E_p/E) \propto \left[\frac{3E_p}{2E}\left(1-\frac{3E_p}{2E}\right)\right]^{\frac{1}{2}} \mathrm{d}E. \tag{4.1}$$

There are no experimental results for this spectrum, but (4.1) can be compared directly with the neutron spectrum from d(p, n)pp (refs. [13–15])). Fig. 4 gives the experimental results of ref. [15]), together with the spectrum of eq. (4.1) and the theoretical spectra of Frank and Gammel [16]), plotted in the lab. system in the forward direction, for $E_{\text{lab}} = 4$ and 6 MeV. We note the following points:

1) The agreement with the overall shape of the spectrum shows that the inelastic state included is the most important one even at $E_{\text{lab}} = 6$ MeV. Agreement is, in fact, closer than would appear from the figure since the finite resolution of the experimental counters has not been folded in [15]).

2) Nonetheless the fit is by no means perfect even at $E_{\text{lab}} = 4$ MeV corresponding to a C.M. energy in the inelastic channel of only 0.44 MeV. Thus, higher inelastic partial waves are not completely negligible even at this energy.

3) The spectrum given by Frank and Gammel is not significantly better at these energies than the "phase space" distribution which our neglect of all except the lowest state gives; in fact, except quite close to the upper end of the spectrum it is indistinguishable from the phase-space distribution, and the changes it does make are such as to worsen the fit to experiment (though at higher energies the bump in the spectrum predicted by Frank and Gammel does appear and becomes indeed an order of magnitude larger than given by their results).

5. Conclusions

We may conclude from these results firstly that the method used would appear to be a practicable one for handling reactions involving three-particle states. Inclusion of higher terms in the three-particle expansion is not difficult, and gives a systematic method for improving the calculated energy spectra, which is not so for the Born approximation method of Frank and Gammel. Moreover the inelastic yield would appear to be given correctly by the approximations used, given a set of potentials which reproduce the elastic scattering adequately. This is certainly not the case with the distorted wave calculations of Bransden and Burhop [4]), which seriously overestimate the inelastic cross-section.

We may also tentatively conclude that approximations neglecting the effect of the inelastic channel upon the elastic channel are poor; however, the large effects found may be due at least partly to the neglect of the change-exchange channels, and calcutions including these may change this result.

Finally, since the scattering matrix is automatically unitary in this calculation the anomaly in the elastic cross-section at the inelastic threshold is reproduced. It is found to be small and probably hard to detect experimentally.

I should like to thank M. M. Pennell for programming this problem for the IBM 704; thanks are also due to Miss E. J. Campbell of the Joint Computing Group and to Dr. R. J. Blin-Stoyle for their constant help and advice.

References

1) Buckingham, Hubbard and Massey, Proc. Roy. Soc. A **211** (1952) 183
2) R. A. Christian and J. L. Gammel, Phys. Rev. **91** (1953) 100
3) A. H. de Borde and H. S. W. Massey, Proc. Phys. Soc. A **68** (1955) 769
4) B. H. Bransden and E. H. S. Burhop, Proc. Phys. Soc. A **53** (1950) 1337
5) L. Sartori and S. I. Rubinow, Phys. Rev. **112** (1958) 214
6) L. M. Delves and D. Brown ,Nuclear Physics **11** (1959) 432
7) L. M. Delves, Nuclear Physics **9** (1959) 391
8) L. M. Delves, Nuclear Physics **20** (1960) 275
9) L. Fox and E. T. Goodwin, Phil. Trans. Roy. Soc. A **245** (1953) 524
10) M. M. Pennell and L. M. Delves, submitted to Mathematics of Computation
11) L. M. Delves, Thesis, Oxford 1960 (unpublished)
12) L. Spruch and L. Rosenberg, Nuclear Physics **17** (1960) 30
13) W. Heckrotte and M. McGregor, Phys. Rev. **111** (1958) 593
14) A. T. G. Ferguson and G. C. Morrison, Nuclear Physics **5** (1958) 41
15) L. Cranberg and R. K. Smith, Phys. Rev., to be published
16) R. M. Frank and J. L. Gammel, Phys. Rev. **93** (1954) 463

1.C

Nuclear Physics **26** (1961) 147—160; © *North-Holland Publishing Co., Amsterdam*

Not to be reproduced by photoprint or microfilm without written permission from the publisher

PAIRING AND QUADRUPOLE FORCES IN A TWO-DIMENSIONAL SOLUBLE MODEL

H. J. LIPKIN

The Weizmann Institute of Science, Department of Physics, Rehovoth, Israel †

Received 20 February 1961

Abstract: The model treated is a system of particles moving in a two-dimensional harmonic oscillator potential with two-body pairing and quadrupole forces mixing states within a single major shell. A simple representation is found in which the Hamiltonian is exactly diagonal. An "energy gap" is obtained in the limit of pure pairing forces and rotational spectra in the limit of pure quadrupole forces. In the intermediate region the spectrum varies from energy gap to rotational as the number of particles is increased. The effective moment of inertia of the rotational band is unaffected by the pairing force, remaining constant at the value for a pure quadrupole force. The model is also treated by replacing the quadrupole force by a self-consistent deformed field and the moment of inertia is calculated using the cranking model. The results agree with the exact solution. Implications of the model for more realistic cases are discussed.

1. Introduction

A simple phenomenological nuclear model has been proposed by the Copenhagen group as one describing many of the observed features of low energy nuclear spectra [1]). This is the j-j coupling shell model, with a residual interaction consisting of a quadrupole force and a pairing force. These two components are not claimed to be the major part of the real residual two-body force. Rather they are pictured as playing a dominant role in low energy spectra, where correlations of the quadrupole or pairing type seem to produce coherent effects which emphasize these particular components of the force.

Although the success of this model in giving qualitative and semi-quantitative predictions of experimental results has been striking, exact calculations using the model have not been made. Such calculations would require the diagonalization of large matrices, since several shell-model configurations are strongly mixed by the pairing force. The approach generally used has been to approximate the quadrupole two-body force by a single particle quadrupole field, to treat the pairing force in the BCS [2]) approximation in which the number of particles is not conserved, and to use the cranking model to treat collective modes [1, 3]). Various heuristic arguments have been presented to justify these

† The research reported in this document has been sponsored in part by the Air Force Office of Scientific Research of the Air Research and Development Command, U.S. Air Force, through its European Office.

approximations. However, none of these are really convincing and one feels the need of finding either a rigorous justification for these approximations or an alternative approach which avoids them. One particular point which requires clarification is the use of the cranking model to calculate nuclear moments of inertia [4]), and the effect of pairing forces on these moments.

Exact calculations can be made for the case of quadrupole or pairing forces alone, leading to the U_3 representation [5]) in one case, with its rotational states, and to the seniority classification [6]) in the other with its "energy gap" [3]). These exact calculations are not helpful in the general case when both types of forces are present. The two forces seem to be so different that it does not appear feasible to treat one exactly and the other as a perturbation.

In this paper a two-dimensional model is presented with quadrupole and pairing forces which can be solved exactly in a very simple way. The solution yields the following features which are similar to those of the Copenhagen three-dimensional model:

(1) In the limit of only quadrupole forces, rotational bands are obtained.

(2) In the limit of only pairing forces, an energy gap spectrum is obtained.

(3) As the number of particles in unfilled shells increases, the quadrupole force becomes more important relative to the pairing force. Thus there exist values of the relative strengths of the forces for which the energy gap spectrum is obtained when the number of particles is small, and rotational bands are obtained when the number of particles is large.

However, when the pairing force is small enough so as not to disturb the rotational spectrum, the moment of inertia is *completely unchanged* by the pairing force. This is in sharp disagreement with the results of cranking model calculations in the three-dimensional case. Another difference is the absence of low-lying vibrational excitations in the two-dimensional model.

The extent to which the results of the two-dimensional model are applicable to three dimensions is questionable, particularly with regard to the moment of inertia. However, the model is so simple that an understanding of its features may give some insight into the more complicated three-dimensional case. In particular, the possibility of finding an analogous representation which diagonalizes both pairing and quadrupole forces at least approximately is an attractive one. The two-dimensional model shows that these very different forces are not so incompatible as one might otherwise think. This point is discussed further at the end of this paper.

The model can also be used to test the cranking approach. It is possible to treat the model by the "deformed-field-cranking method" and to compare the results with the exact solution. In this simple case the results agree very

well. The moment of inertia is given exactly by the cranking model formula, and the ground state energy is given to a good approximation if there are many states in the rotational band.

2. The Model

Let us consider a system of particles moving in a two-dimensional harmonic oscillator well with additional quadrupole and pairing forces described by the Hamiltonian

$$H = H_{\text{osc}} + H_{\text{quad}} + H_{\text{pair}}, \tag{1}$$

where

$$H_{\text{osc}} = \sum_i \left\{ \frac{p_{x_i}^2}{2m} + \frac{p_{y_i}^2}{2m} + \frac{m\omega^2}{2}(x_i^2 + y_i^2) \right\} \tag{2}$$

and H_{quad} and H_{pair} are quadrupole and pairing interactions discussed in detail below. The quantities x_i, y_i, p_{x_i} and p_{y_i} are the coordinates and momenta of the i-th particle, m is the particle mass and ω is the frequency characterizing the oscillator potential.

2.1. THE QUADRUPOLE FORCE AND THE U_2 REPRESENTATION

The two-dimensional model with only quadrupole forces has been treated in detail [7]). We present here the essential features of the U_2 representation.

The usual two-body quadrupole interaction taken in these models is the scalar product of the quadrupole moments of the two particles

$$v_{ij} = -k\{\mathbf{q}_i \cdot \mathbf{q}_j\} \tag{3}$$

where k is a parameter specifying the strength of the force.

The quadrupole moment is a second rank tensor and has two components in two dimensions, proportional to $x_i^2 - y_i^2$ and $2x_i y_i$ respectively.

In standard shell model calculations, one neglects the mixing of configurations in different major shells. This can be achieved analytically in the case of a quadrupole force with harmonic oscillator wave functions by using a quadrupole operator which is a linear combination of the moments in configuration and momentum spaces [7]). We thus define

$$t_{1i} = \frac{m\omega}{4\hbar}\{x_i^2 - y_i^2\} + \frac{1}{4m\omega\hbar}\{p_{x_i}^2 - p_{y_i}^2\}, \tag{4a}$$

$$t_{2i} = \frac{m\omega}{2\hbar} x_i y_i \quad + \frac{1}{2m\omega\hbar} p_{x_i} p_{y_i}. \tag{4b}$$

The quadrupole operators (4) commute with H_{osc} and thus have zero matrix

elements between configurations in major shells. We can therefore write a quadrupole interaction within a major shell as

$$v_{ij} = -k(t_{1i}t_{1j}+t_{2i}t_{2j}). \tag{5}$$

Let us now define the operator

$$t_{0i} = \tfrac{1}{2}(x_i p_{y_i} - y_i p_{x_i}) = \tfrac{1}{2}l_i, \tag{4c}$$

where l_i is the angular momentum of particle i. The three operators t_{1i}, t_{2i} and t_{0i} satisfy commutation rules like angular momenta

$$[t_{1i}, t_{2i}] = it_{0i}, \qquad [t_{2i}, t_{0i}] = it_{1i}, \qquad [t_{0i}, t_{1i}] = it_{2i}. \tag{6}$$

They are just the infinitesimal operators of the U_2 group, analogous to the U_3 group treated by Elliott in the three-dimensional case [5]). Let

$$T_1 = \sum_i t_{1i}, \qquad T_2 = \sum_i t_{2i}, \qquad T_0 = \sum_i t_{0i} = \tfrac{1}{2}L \tag{7a}$$

where L is the total angular momentum of the system,

$$T^2 = T_1^2+T_2^2+T_3^2, \qquad t_i^2 = t_{1i}^2+t_{2i}^2+t_{3i}^2. \tag{7b}$$

The t-operators behave like angular momentum operators in a fictitious three-dimensional space. Since these operators commute with H_{osc}, the states of the two-dimensional oscillator can be characterized by quantum numbers which are the eigenvalues of these operators.

The total quadrupole interaction is obtained by summing eq. (5) over all pairs of particles i and j. It is customary in this model to include also a term for $i = j$, which is equivalent to a slight modification of the single-particle oscillator potential. With the $i = j$ term included, the total quadrupole interaction is expressed very simply in terms of the T operators

$$V_{\text{Q}} = \sum_{ij} v_{ij} = -\tfrac{1}{2}k(T_1^2+T_2^2) = -\tfrac{1}{2}k(T^2-T_0^2). \tag{8}$$

Let us first examine the states of a single particle in a two-dimensional harmonic oscillator well. The two degrees of freedom are separable in both Cartesian and cylindrical coordinates, and either representation can be used to classify the states. In the Cartesian representation the quantum numbers are n_x and n_y, the numbers of oscillator quanta in the two directions. In the cylindrical representation, the quantum numbers are n and m, the total number of oscillator quanta and the angular momentum. In both cases the energy of the oscillator (2) depends only on the total quantum number $n = n_x+n_y$:

$$E_{\text{osc}} = \hbar\omega(n_x+n_y+1) = \hbar\omega(n+1). \tag{9}$$

Each eigenvalue has an $(n+1)$-fold degeneracy, corresponding to the

different possible values of n_x and n_y giving the same n, or to values of $m = n$, $n-2$, $n-4$, . . . $-n$.

The states can also be classified by the eigenvalues of the operators t^2 and t_0. The eigenvalues of the operator t^2 have the form $t(t+1)$ where t is either an integer or half-integer. For each value of t there are $2t+1$ states corresponding to eigenvalues $t_0 = t, t-1, \ldots -t$. This classification turns out to be equivalent to the cylindrical representation, with the quantum numbers (t, t_0) related to the cylindrical quantum numbers (n, m) by the relations

$$t = \tfrac{1}{2}n, \text{ (a)} \qquad t_0 = \tfrac{1}{2}m \text{ (b)}. \tag{10}$$

Eq. (10b) follows directly from (4c). Eq. (10a) can be obtained by explicit substitution of eqs. (4) into the definition (7) of t^2.

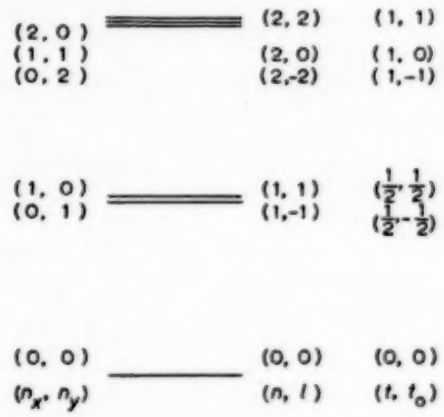

Fig. 1. Energy levels of a single particle in a two-dimensional harmonic oscillator well.

Fig. 1 shows the energy levels of a single particle in a two-dimensional harmonic oscillator well. From fig. 1 and eq. (10), we see that all values of the fictitious angular momentum t appear, both integral and half integral. We note that the quantum number t labels the major shell.

Let us now consider a system of many particles in which the lowest major shells are filled and there are a certain number of particles in one unfilled shell. The particles in the unfilled shell are all in states having the same quantum number t, with different values of the quantum number t_0. This situation is exactly analogous to the j^n configuration in the usual three-dimensional spherically symmetric shell model. There is a degeneracy because of the degeneracy of the different t_0-states. When an additional interaction is added to remove the degeneracy in the spherical shell model, the appropriate eigenfunctions are formed by coupling the angular momenta of the individual particles to give a definite total angular momentum J. In our two-dimensional model, we see that the two-body quadrupole force (8) commutes with the "total fictitious angular momentum" T^2. By analogy with ordinary angular

momentum, we see that we can contruct simultaneous eigenfunctions of the harmonic oscillator hamiltonian and the quadrupole interaction by "coupling the fictitious angular momenta" of the particles to obtain a state which is an eigenfunction of T^2 and T_0.

The interaction energy due to the quadrupole force is given by equation (8) in terms of the eigenvalues of the operators T^2 and T_0. As with ordinary angular momentum, the eigenvalues of T^2 have the form $T(T+1)$, and for each value of T there are $2T+1$ states having eigenvalues of $T_0 = T$, $T-1, \ldots -T$. Eq. (8) shows that a set of states having the same value of T and different valeurs of T_0 are split into a "band" having energy spacings proportional to T_0^2 and therefore, by eq. (7a), to the square of the angular momentum. These are the rotational bands found by Elliott in the three-dimensional U_3 model.

2.2 THE PAIRING FORCE AND THE QUASI-SPIN REPRESENTATION

Pairing forces used in treating finite nuclei have been defined as forces which scatter a pair of particles having equal and opposite angular momenta into another state in which they have equal and opposite angular momenta. These forces are most easily described by using the formalism of "second quantization". Let a_m^* and a_m be creation and annihilation operators for a particle having angular momentum m, disregarding other possible quantum numbers for the moment. Then a pairing force would have the form

$$V_P = -G \sum_{m,m'} s_m s_{m'} a_m^* a_{-m'}^* a_{-m} a_m, \tag{11}$$

where G is a strength parameter and s_m is a coefficient depending upon m. Kisslinger and Sorensen [3]) use a pairing force in which the sum is over all states in a major shell, and with s_m a phase factor of unit amplitude.

In our two-dimensional model, a major oscillator shell consists of all states having a given value of the quantum number n, or t. A pairing force analogous to that used by KS can be written in the t representation as

$$V_P = -\tfrac{1}{4} G \sum_{\sigma,\sigma'} s_\sigma s_{\sigma'} a_{t\sigma}^* a_{t,-\sigma}^* a_{t,-\sigma} a_{t\sigma}, \tag{12}$$

where the quantum number $\sigma = \frac{1}{2}$m specifies the angular momentum by the eigenvalue of the operator t_0.

The pairing force can be described simply by means of the quasispin operators introduced by Kerman [8]). Let us define

$$S_+ = \tfrac{1}{2} \sum_\sigma s_\sigma a_{t\sigma}^* a_{t,-\sigma}^*, \tag{13a}$$

$$S_- = \tfrac{1}{2} \sum_\sigma s_\sigma a_{t\sigma} a_{t,-\sigma}, \tag{13b}$$

$$S_0 = \tfrac{1}{4} \sum_\sigma a_{t\sigma}^* a_{t\sigma} - a_{t\sigma} a_{t\sigma}^* = (\tfrac{1}{2}N - \Omega), \tag{13c}$$

where Ω is the total number of pair states available in the shell (a completely closed shell containing 2Ω particles), and N is the number of particles in the system.

The operator S_+ creates a pair of particles in a "correlated" or "bound" pair state, which is a mixture of all the $(+\sigma, -\sigma)$ states with equal amplitudes. The operator S_- annihilates such a pair. The operator S_0 is simply half the number of particles in the system, measured from the middle of the shell. Thus S_0 can vary from $-\frac{1}{2}\Omega$ to $+\frac{1}{2}\Omega$.

The three "quasispin" operators S_+, S_- and S_0 satisfy commutation rules like angular momenta. One can therefore define a "total quasispin operator"

$$S^2 = \tfrac{1}{2}(S_+S_-+S_-S_+)+S_0^2. \tag{13d}$$

The total quasispin operator has eigenvalues $S(S+1)$ where S can be either integral or half-integral.

The pairing force (12) is expressed very simply in terms of these quasispin operators:

$$V_P = -G(S_+S_-) = -G(S^2-S_0^2+S_0). \tag{14}$$

The pairing force is treated simply by using wave functions which are simultaneous eigenfunctions of S^2 and S_0. The pairing energy is then given simply as a function of the eigenvalues of these operators. These eigenfunctions can be interpreted as describing a state consisting of $(S+S_0)$ correlated pairs and $(\Omega-2S)$ particles which are not in correlated pairs.

3. Solution of the Model

In the preceding section we have presented the well known result that both quadrupole and pairing forces can be described simply in terms of operators which satisfy commutation rules like angular momenta. We shall now see that in our two-dimensional model, the T-operators which describe the quadrupole force and the S-operators which describe the pairing force *commute with one another* if the phase factors s_m in the pairing force are suitably chosen. It will then be possible to diagonalize both the pairing and quadrupole forces simultaneously †).

The operator S_+ creates a pair in a particular correlated state. If we set $s_\sigma = (-1)^\sigma$, this correlated state is an eigenstate of T^2 for the two particles with $T^2 = 0$. The operator S_+ defined in this way therefore commutes with all the T-operators. (This can be verified by direct calculation, or by noting that the T-operators are infinitesimal rotation operators in a fictitious three-dimensional space, and that S_+ creates a pair of particles in a $T^2 = 0$ state

† A similar two-dimensional model has been considered by S. Moszkowski (private communication), with phase factors chosen so that the T and S operators do *not* commute.

which is invariant under rotations in this space.) The operator S_- also commutes with the T-operators, and the operator S_0, which is a constant plus the number of particles, clearly commutes with them as well †.

Our Hamiltonian thus commutes with T^2, T_0, S^2 and S_0. We can therefore find a set of simultaneous eigenfunctions of the Hamiltonian and of all these operators. The energy of such a state is then simply

$$E = E_{\text{osc}}+E_{\text{quad}}+E_{\text{pair}}$$
$$= \hbar\omega \sum_i (2t_i+1)-\tfrac{1}{2}k\{T(T+1)-T_0^2\}-G\{S(S+1)-S_0(S_0-1)\}, \quad (15)$$

using eqs. (9), (10), (8) and (14).

From eq. (15) and the properties of the S and T operators, we can make a number of general observations regarding the energy spectrum of a given system of particles. Let us consider a system in which all the major shells are filled below a certain value of t, and there are an even number of particles in the unfilled t-shell. The quantum numbers t_i are determined by the configuration and S_0 is determined by the number of particles in the unfilled shell. The energy spectrum of the configuration is therefore specified completely by the values of the quantum numbers T, T_0 and S.

The dependence upon the quantum number T_0 is entirely in the term $\frac{1}{2}kT_0^2$. Thus corresponding to any values of the quantum numbers (T, S) which occur, there are $2T+1$ states having values of $T_0 = T, T-1, \ldots -T$. The lowest state in this "band" has $T_0 = 0$, and the others lie above it with energy differences of $\frac{1}{2}kT_0^2 = \frac{1}{8}kL^2$. If T is sufficiently large so that the band has an appreciable number of states, this band can be interpreted as a rotational band †† with an effective moment of inertia

$$\mathcal{I} = \frac{4}{k}. \quad (16)$$

The values of the quantum numbers (T, S) for the ground state band depend upon the relative magnitudes of the pairing and quadrupole forces. If only the

† This is strictly true only for the case in which t is half-integral, when the pairing force is exactly analogous to that in the j^n configuration in ordinary three-dimensional space. If t is integral, a state of two particles with $T^2 = 0$ is *symmetric* with respect to interchange of the particles, and an antisymmetric state does not exist. We can, however, have symmetric states for two particles if we introduce spin into our two-dimensional model. Let there be two spin states for each particle, and let us consider the sums in (12) and (13) as acting over all possible combinations of spin states. Because of the automatic antisymmetrization incorporated in the second-quantized formulation, the operators S_+ and S_- will create and annihilate pairs in anti-symmetrized states having $T^2 = 0$, i.e. states of parallel spin for half-integral values of t and anti-parallel spin for integral values of t.

†† The energy spectrum is not the only reason for referring to these bands as "rotational". The wave-functions have other properties which indicate that the states in the band have a common "intrinsic structure" and differ only by a superimposed collective rotation. These properties are discussed in detail elsewhere [5, 7]).

quadrupole force is present, the lowest state is the one having the maximum possible value of the quantum number T in the given configuration. If only the pairing force is present, the lowest state is the one having the maximum value of the quantum number S. The latter state has all the particles paired in the correlated $T^2 = 0$ state and therefore has $T = 0$. On the other hand, the state of maximum T has no pairs in the correlated $T^2 = 0$ state and therefore has the minimum possible value of S, namely S_0. We thus see that the $(T_{\max}, S_0)$ band is the lowest band if only quadrupole forces are present, but is the *highest* band if only pairing forces are present. Conversely the $(0, S_{\max})$ band is the lowest when only pairing forces are present, and is the *highest* band when only quadrupole forces are present.

If only quadrupole forces are present, the lowest band has $T_{\max}$ energy states, all doubly degenerate except for the $T_0 = 0$ state, and having the proper spacing for a rotational spectrum with an "effective moment of inertia" of $\mathcal{I} = 4/k$. If a small pairing force is added, *this rotational spectrum is unaltered.* The effect of the pairing force is simply to lower the energies of the other bands having lower values of T and higher values of S. The pairing force thus does not affect the moments of inertia of the different rotational bands, it simply moves them with respect to one another.

If only pairing forces are present, the lowest band has $T^2 = 0$ and consists of a single state. It cannot be interpreted as a rotational band. The first excited states have $S = S_{\max} - 1$ and have an excitation energy of $2GS_{\max} = G\Omega$. These excited states have all but two particles in correlated states, with the remaining two particles coupled to any allowed value of T up to $2t$. All these states are degenerate and separated from the ground state by the large "energy gap" $G\Omega$. If a small quadrupole force is added, the effect is to split the large degeneracy of the first excited states according to the different values of T and T_0. However, as long as the quadrupole force is small the characteristic "energy gap" spectrum is preserved.

If both the pairing and quadrupole forces are present the energy spectrum varies with the number of particles. To see the details of the spectrum it is necessary to determine the relation between the quantum numbers S and T; i.e. which values of T occur for a given value of S. It is convenient to introduce the *number of unpaired particles*

$$v = \Omega - 2S. \tag{17}$$

This is just the seniority number introduced by Racah [6]). Rewriting eq. (15) in terms of v instead of S, and omitting the first term and the T_0 and S_0 terms which are independent of T and v, we obtain

$$E(T, v) = -\tfrac{1}{2}kT(T+1) - \tfrac{1}{4}G(\Omega - v)(\Omega - v + 2). \tag{18}$$

For any given value of v, the state of minimum energy is given by the maximum possible value of T for this value of v. The essential qualitative

features of the spectrum can be seen by assuming that t is very large in comparison with v. For this case the maximum value of T is obtained by having the t-vectors of all the v particles oriented parallel in T-space; i.e.

$$T_{\max}(v) \approx vt. \tag{19}$$

Substituting eq. (19) into eq. (7), and neglecting unity in comparison with v, t and Ω, we obtain

$$E_{\min}(v) \approx -\tfrac{1}{2}kt^2v^2-\tfrac{1}{4}G(\Omega-v)^2 = -\tfrac{1}{4}\{(2kt^2+G)v^2-2G\Omega v+G\Omega^2\}. \tag{20}$$

For $v = 0$, $E_{\min}(v) = -\frac{1}{4}G\Omega^2$. As v increases from zero, $E_{\min}(v)$ rises to a maximum and then decreases, passing through the value $-\frac{1}{4}G\Omega^2$ at a value

$$v_0 = 2G\Omega/(2kt^2+G). \tag{21}$$

From eqs. (20) and (21) we see that if the number of particles is less than v_0, the number of unpaired particles v must be less than v_0; the state of lowest energy has $v = 0$, $T = 0$, and an "energy gap" spectrum is obtained. If the number of particles N is greater than v_0, the state of lowest energy has $v = N$, $T = Nt$, and a rotational spectrum is obtained. Thus for small numbers of particles there is an energy gap spectrum, for large numbers of particles there is a rotational spectrum and the cross over occurs at a number of particles v_0 which depends upon the ratio of the pairing force and quadrupole force strengths.

Let us now consider the case when t is half-integral and the particles are spinless. Then $\Omega = t+\frac{1}{2}$ and the exact relations for $T_{\max}(v)$ and $E_{\min}(v)$ are

$$T_{\max}(v) = v(t-\tfrac{1}{2}(v-1)) = v(\Omega-\tfrac{1}{2}v) \tag{22}$$

and

$$\begin{aligned} E_{\min}(v) &= -\tfrac{1}{2}kv(\Omega-\tfrac{1}{2}v)\{v(\Omega-\tfrac{1}{2}v)+1\}-\tfrac{1}{4}G(\Omega-v)(\Omega-v+2) \\ &= -\tfrac{1}{2}[k\{v(\Omega-\tfrac{1}{2}v)\}^2-(G-k)\{v(\Omega-\tfrac{1}{2}v)\}-Gv+\tfrac{1}{2}G\Omega(\Omega+2)]. \end{aligned} \tag{23}$$

Eq. (23) is similar in character to the approximate eq. (20) except that the quantity $v(\Omega-\frac{1}{2}v)$ appears instead of v in eq. (23). Again the energy rises from its value at $v = 0$, goes through a maximum and returns to the value for $v = 0$ at a value v_0 which occurs when the contributions of all the v-dependent terms in (23) add up to zero. If the term Gv is neglected, the critical number of particles at which the cross over occurs is given by

$$N(\Omega-\tfrac{1}{2}N) = (G/k)-1. \tag{24}$$

The parameter $N(\Omega-\frac{1}{2}N)$ is just the product of the number of particles and the number of holes, which has a maximum value of $\frac{1}{2}\Omega^2$ at the middle of the shell where $N = \Omega$. From this and eq. (21) we see that

1) If $G/k > \frac{1}{2}\Omega^2+1$, eq. (24) cannot be satisfied and there is no cross over. There is always an energy gap spectrum.

2) If $G/k < 2\Omega-1$, eq. (24) is satisfied for $N < 2$. Thus there is always a rotational spectrum.

3) If $(2\Omega-1) < G/k < (\frac{1}{2}\Omega^2+1)$, there is a cross over and both types of spectra occur.

4. The Deformed Field and the Cranking Model

In the unified nuclear model and its variations, it is customary to replace the two-body interaction by a "self-consistent deformed field" [8]). Parameters of the collective motion are then calculated using the "cranking model", in which the deformed field is allowed to vary or to rotate as a function of time. The validity of this approach has never been proved rigorously and the cases in which it is used are generally too complicated to allow an exact calculation to be made for comparison.

Since our two-dimensional model has been solved exactly, it is of interest to test the deformed-field-cranking-model approach to see if it gives the correct result.

Let us replace the two-body quadrupole interaction by a deformed well hamiltonian, as has been done by Belyaev [3]) and Kerman [8]):

$$-\tfrac{1}{2}k\{T_1^2+T_2^2\} \rightarrow -k\{\beta_1 T_1+\beta_2 T_2\}, \tag{25}$$

where β_1 and β_2 are parameters which characterize the "equilibrium deformation". The values of β_1 and β_2 are determined by the self-consistency condition,

$$\beta_1 = \langle T_1\rangle, \qquad \beta_2 = \langle T_2\rangle, \tag{26}$$

while the energy of the quadrupole interaction is then

$$E_{\text{quad}} = -\tfrac{1}{2}k\{\beta_1\langle T_1\rangle+\beta_2\langle T_2\rangle\} = -\tfrac{1}{2}k\{\beta_1^2+\beta_2^2\}, \tag{27}$$

with the usual factor $\frac{1}{2}$ common in self-consistent field calculations with two-body forces.

The relative values of β_1 and β_2 determine the orientation of the principal axes of the deformed field. We can without loss of generality set $\beta_2 = \langle T_2\rangle = 0$, and choose wave functions which satisfy this condition; namely the eigenfunctions of T^2, T_1, S and S_0.

Our deformed field hamiltonian is then

$$H_{\text{D}} = H_{\text{osc}}-k\beta_1 T_1-G\{S(S+1)-S_0(S_0-1)\}. \tag{28}$$

If the pairing force strength G is not so great as to destroy the rotational spectrum, the lowest state of H_{D} is the one having the largest possible value of T obtainable in the configuration, and has $T_1 = T$. Therefore, by eq. (26) $\beta_1 = T$. From eq. (27) we see that the energy of the quadrupole interaction given by this approach is

$$E_{\text{quad}} = -\tfrac{1}{2}kT^2. \tag{29}$$

This differs from the exact energy eq. (18) only by the presence of the factor T^2 instead of $T(T+1)$. This is small if $T \approx Nt$ is large. The energy of the pairing force is given exactly by this treatment since our deformed field wave functions are eigenfunctions of S^2 and S_0 with the proper eigenvalues and the pairing part of the deformed hamiltonian H_D is the same as that of the original hamiltonian.

Let us now calculate the moment of inertia using the cranking model. This is given by the Inglis formula [4])

$$\mathscr{I} = 2\sum_i \frac{\langle 0|L|i\rangle\langle i|L|0\rangle}{E_i - E_0} = 8\sum_i \frac{\langle 0|T_0|i\rangle\langle i|T_0|0\rangle}{E_i - E_0}, \tag{30}$$

where the eigenfunctions and eigenvalues used are those of H_D.

The expression (30) is easily evaluated by noting that

$$[H_D, T_2] = -ik\beta_1 T_0,$$

and therefore

$$\frac{\langle 0|T_0|i\rangle}{E_i - E_0} = \frac{\langle 0|T_2|i\rangle}{ik\beta_1}. \tag{31}$$

Substituting eq. (31) into eq. (30) we obtain

$$\mathscr{I} = \frac{4}{ik\beta_1}\langle 0|[T_2, T_0]|0\rangle = \frac{4}{k\beta_1}\langle 0|T_1|0\rangle = \frac{4}{k}, \tag{32}$$

using the self-consistency condition (26). This result (32) is in agreement with the exact result (16).

5. Discussion

5.1. COMPARISON OF RESULTS WITH THE COPENHAGEN MODEL

The simple two-dimensional model has reproduced certain qualitative features of the Copenhagen model, in particular the existence of both rotational and energy gap spectra, with a transition depending upon the number of particles in the manner expected. The treatment using a self-consistent field and the cranking model has given a good approximation to the ground state energy and the exact value of the moment of inertia.

The two following features assumed to be present in the three-dimensional case are absent in the model: 1) the decrease in the moment of inertia of rotational states with increasing strength of pairing force, 2) the existence of low-lying vibrational states in addition to the energy-gap and rotational spectra. The absence of these effects in the simple model should not be surprising. Possible sources of differences between our model and a more realistic one are: 1) the difference between two and three dimensions, (2) the neglect of spin-orbit forces, 3) the simplified quadrupole force which acts only within a major shell.

One essential feature of this oversimplification is found in the deformed field

hamiltonian (28), which is diagonalized exactly by the same eigenfunctions independently of the value of the parameter β_1. If the energy is calculated as a function of the deformation parameter β_1 (without requiring self-consistency) it varies *linearly* with β_1 and there is no minimum and no possibility of vibrations about the point of equilibrium deformation. In order to have these vibrations included in the formulation, a quadratic dependence of the energy on β_1 is required. This can only be achieved if the *eigenfunctions* depend upon β_1; i.e. if the term in the Hamiltonian which is proportional to β_1 *does not commute* with the rest of the hamiltonian. This would not be improved by going to three dimensions in the Elliott model, since a quadrupole force which does not mix major shells automatically commutes with the oscillator hamiltonian. A quadratic term in β_1 can be obtained by including a quadrupole interaction which mixes major shells, such as that which would give an anisotropic harmonic oscillator potential as the deformed field, or by introducing spin-orbit coupling into the central field.

5.2. POSSIBILITIES FOR A SIMPLE REPRESENTATION IN THREE DIMENSIONS.

An attractive feature of the two-dimensional model is the existence of a single simple representation in which both the quadrupole and pairing forces are simultaneously diagonal. This seems paradoxical at first, as one is accustomed to thinking that quadrupole forces and pairing forces are incompatible; the one tending toward strong deformation, the other toward spherical symmetry. However, in the two-dimensional model, these two types of forces are *so* different that they become opposites and are therefore compatible! The state which minimizes the energy of the quadrupole force, maximizes the energy of the pairing force and is therefore an eigenstate of both. Similarly the best state for the pairing force is the worst for the quadrupole force.

The peculiar simplicity of the model lies in the correlated two-particle state which is best for the pairing force and worst for the quadrupole force. The energy of the N-particle state depends upon the number of such pairs, the pairing force preferring the maximum number of correlated pairs, the quadrupole force the minimum. In addition the quadrupole force requires certain configurations of the unpaired particles. However, the states having a definite number of correlated pairs (a definite seniority), are eigenfunctions of both the pairing and quadrupole force.

In three dimensions the situation is more complicated. Let us consider the j^n configuration with pairing and quadrupole forces. In the two-particle system, the total angular momentum quantum numbers (J, M) are sufficient to specify the state. Thus the same representation diagonalizes both the pairing and quadrupole forces for the trivial reason that they are both invariant under rotations. However, the lowest state for both types of forces is the $J = 0$ state. The forces *do not act oppositely at all* in the two-particle system. A single-

particle angular momentum eigenstate, specified by quantum numbers (j, m), has axial symmetry about the z-axis but is definitely deformed in the xz and yz planes which do not exist in the two-dimensional case. The two-particle $J^2 = 0$ state is "spherically symmetric", but has a large "intrinsic quadrupole moment" because of the correlation of the quadrupole moments of the single particle states with respect to one another. Thus this state is best for both pairing and quadrupole forces.

The incompatibility of the two types of forces enters only when there are more particles. The pairing force tries to group the particles into these correlated pairs with large intrinsic quadrupole moments, but with no correlation between the intrinsic moments of different pairs beyond that required by the Pauli principle. The quadrupole force tries to group the particles with all their intrinsic quadrupole moments in the same direction and thus breaks pairs. However, the state with all pairs broken is not the best state for the quadrupole force, as in the two-dimensional model, because the energy of the two-particle configuration is *lowered* by pairing to $J = 0$ instead of being raised.

Thus the three-dimensional problem is more complicated than the two-dimensional one because the two forces do not act in completely opposite directions any more. However, because they are "*almost opposite*" when the number of particles is large, one might hope to find a representation in which both types of forces are nearly diagonal, and in which the off-diagonal parts could be treated as perturbations.

The author would like to express his appreciation to A. K. Kerman and S. A. Moszkowski for stimulating discussions. Dr. Moszkowski has independently considered a similar two-dimensional model.

References

1) B. R. Mottelson, in Proceedings of Kingston Conference on Nuclear Structure (North-Holland Publishing Co., Amsterdam, 1960) p. 525
2) J. Bardeen, L. N. Cooper and J. R. Schrieffer, Phys. Rev. **108** (1957) 1175 (referred to as BCS)
3) S. T. Belyaev, Mat. Fys. Medd. Dan. Vid. Selsk. **31**, No. 1 (1959);
L. S. Kisslinger and R. A. Sorensen, Mat. Fys. Medd. Dan. Vid. Selsk. **32**, No. 9 (1960) (referred to as KS);
B. R. Mottelson, in Cours de l'École d'Été de Physique Théorique des Houches (1958), p. 283
4) D. R. Inglis, Phys. Rev. **96** (1954) 1059, **97** (1955) 701;
A. Bohr and B. R. Mottelson, Mat. Fys. Medd. Dan. Vid. Selsk. **30**, No. 1 (1955)
5) J. P. Elliott. Proc. Roy. Soc. **245** (1958) 128, **245** (1958) 562
6) G. Racah, in Proc. Rehovoth Conf. on Nuclear Structure (North-Holland Publishing Co., Amsterdam, 1958) p. 155
7) S. Moszkowski, Phys. Rev. **110** (1958) 403;
H. J. Lipkin, Nuclear Physics **8** (1958) 421; Annals of Physics **9** (1960) 272
8) A. K. Kerman, Annals of Physics **12** (1961) 300;
P. W. Anderson, Phys. Rev. **112** (1958) 1900

1.D.1:
1.E.7

Nuclear Physics **26** (1961) 161—167; © *North-Holland Publishing Co., Amsterdam*
Not to be reproduced by photoprint or microfilm without written permission from the publisher

ISOBARIC-SPIN RELATIONSHIPS BETWEEN NUCLEAR SPECTRA

J. B. FRENCH

Fysisch Laboratorium der Rijksuniversiteit, Utrecht, The Netherlands

and

Department of Physics and Astronomy, University of Rochester, Rochester, New York, USA †

Received 20 February 1961

Abstract: The simple fact that a one-body energy describes the interaction of a nucleon with a closed neutron subshell is used to establish sets of equations connecting the spectra of nuclei which are related by isobaric-spin when described by means of the nuclear shell model. Certain formal questions about isobaric spin are incidentally considered.

The interaction of a neutron or proton with a closed neutron subshell is representable by a one-body energy. Thus if the nucleons outside closed neutron and proton subshells (which we shall call the "active" nucleons) belong to a single configuration ††, and if a certain neutron subshell is empty we can add neutrons to fill it without changing the relative energy levels. Alternatively we can take away a filled neutron subshell without changing the level structure. However, it will often happen that, if we start with a physically realizable state of definite isobaric spin (we assume charge independence), the state which results from the addition or subtraction of the neutron subshell will not have a definite T. Expanding the resultant wave function in states of definite T we have then

$$\Psi_{JT} \rightarrow \phi_J = \sum_{T'} A_{T'} \phi_{JT'}, \tag{1}$$

where Ψ_{JT} is the initial state and the expansion coefficients $A_{T'}$ of the resultant state ϕ_J may also depend on T, etc. The initial and final *relative* energies are now given by

$$E^{(\mathrm{i})}_{JT} = \sum_{T'} (A_{T'})^2 E^{(\mathrm{f})}_{JT'}, \tag{2}$$

and similar relationships will hold for other quantities.

† Work at the University of Rochester was supported in part by the Atomic Energy Commission. Work at Utrecht was done while the author was Senior Post-Doctoral Fellow of the National Science Foundation on leave during 1959—60 from the University of Rochester.

†† Or more generally for mixed configurations of the active nucleons if a nucleon in the various contributing single-particle orbits has the same interaction energy with the neutron subshell. And of course throughout this paper the words "neutron" and "proton" can be interchanged.

Four cases of interest, involving inequivalent nucleons are illustrated † in figs. 1a . . . 1d. They refer to two subshells of spin j and j', occupied by n and m nucleons, respectively. In fig. 1a and fig. 1b all the configurations are excited ones. Thus the cases $m = 1$, $n = (2j+1)-1 \equiv N-1$, will be most important, the excited states being various kinds of single-particle or single-holes states; besides that these values lead to an eq. (1) in which the sum involves only two

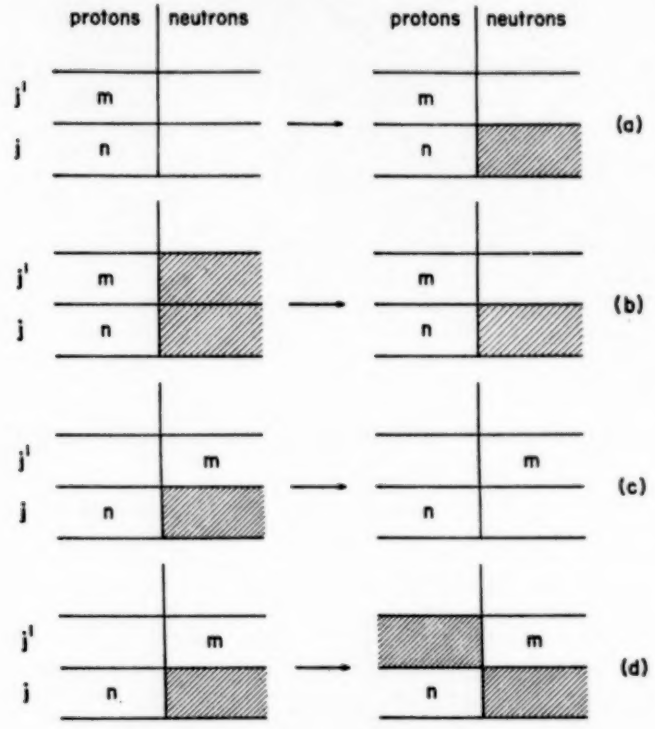

Fig. 1. Each diagram shows the arrangement of neutrons and protons in the two active orbits, all others being empty or completely filled. The cross-hatching denotes filled subshells. Shown on the left are the initial n-p configurations, all with definite $T = |T_z|$, and on the right the n-p configurations, not having definite T, which result when a closed subshell of identical particles is added or taken away.

† If, in the configuration diagrams of fig. 1 it is not possible to transfer a nucleon horizontally (fixed j) in the direction of increasing T_z it follows that T is automatically definite and $T = |T_z|$; for if $T \neq |T_z|$ the states have at least a part with $T > |T_z|$ and this can be produced by starting with a configuration of higher $|T_z|$. Thus T will be definite for an (n-p) configuration with a neutron excess if every orbit which contains protons is filled for neutrons and indeed these $(\text{n-p})_T$ configurations, as we shall call them, are the only ones with a definite T. (If the active neutrons and protons were equivalent, as with a proton and equivalent neutron, certain *states* would automatically have a definite T which would however vary from state to state.) Thus we see that all the initial configurations shown have $T = |T_z|$. Alternatively we see that the number of T values in an (n-p) configuration is equal to the number of different configurations which we can produce by making simultaneous $j \to j'$ (vertical) shifts for protons and $j' \to j$ shifts for neutrons. It is for example because such shifts are possible in the right side of 1a that the closed subshell is *not* inert and the T value not definite. Of course such counting can be replaced by the simple vector coupling of eq. (4).

different T values. In fig. 1c and fig. 1d the initial configuration is a ground-state one and the simplest and physically most interesting cases are $m = 1$ (fig. 1c) and $n = N-1$ (fig. 1d). Our problem now is to compute the expansion coefficients.

If we combine two separate nuclear systems, each with definite T, T_z values, our first reaction is that the resultant function has a T expansion

$$\chi_J = \sum_T C^{T_1 T_2 T}_{T_{z_1} T_{z_2}} \chi_{JT}. \tag{3}$$

This is not generally correct, for the simple vector coupling will not produce wave-functions which are antisymmetrized †.

We therefore must multiply through eq. (3) by the antisymmetrizer $A = \sum (-1)^{P_i} P_i$ and, rewriting it in terms of the normalized antisymmetrized functions, we have

$$\phi_J = \sum_T C^{T_1 T_2 T}_{T_{z_1} T_{z_2}} \frac{d_{JT}}{d_J} \phi_{JT}, \tag{4}$$

where $d_J^2 = \langle \chi_J^* A^2 \chi_J \rangle$ and similarly for d_{JT}. Only in the special case when d_{JT} is independent of T (when obviously $d_{JT} = d_J$) will eq. (4) have the simple Clebsch-Gordan form. The one general circumstance in which this occurs is when the diagonal matrix elements of $A^2 = (n_1+n_2)!\, A$ depend only on n_1 and n_2, the number of particles in each group. This will be satisfied when $\langle \chi^*_{JT} P_i \chi_{JT} \rangle = 0$ for every χ_{JT} and for every P_i which exchanges particles between the groups, and this in turn requires that *every single-particle state for one group be orthogonal to every one for the other group.*

The resultant wave functions in all the cases considered above are of this type; we can take the j-nucleons to form one system with $T = -T_z = \frac{1}{2}n$ in fig. 1c and $T = +T_z = \frac{1}{2}(N-n)$ in the other cases ($t_z = \frac{1}{2}$ for a neutron). Then, *assuming for the moment that taking away or adding the neutron subshell does not disturb the manner in which the nucleons in the separate groups are coupled*, the expansion coefficients all have the form of the obvious Clebsch-Gordan coefficient $C^{T_1 T_2 T}_{T_{z_1} T_{z_2}}$, where T_1, T_2 are the isobaric spins of the separate j, j' groups, and, except in fig. 1c where the signs are reversed, $T_{z_1} = +T_1$ and $T_{z_2} = -T_2$. We are interested in cases in which one of the groups is a single particle or hole and the configurations can be reached from a ground state by excitation of a single particle. These cases are: $m = 1$ or $n = N-1$ in figs. 1a, 1b; $m = 1$ in fig. 1c; and $n = N-1$ in fig. 1d. Then labelling the

† We prefer not to admit the concept of a definite T for a function which is not antisymmetrized. If we did allow such a concept eq. (3) would be correct but not in general pertinent. An illustration of the point involved is that in the coupling of an $s_{\frac{1}{2}}$ neutron to a $J = 0$ pair of $s_{\frac{1}{2}}$ protons the $T = \frac{3}{2}$ state does not exist. Also it is a little simpler to consider the comments which follow eq. (3) in terms of an isobaric-spin formalism and this we temporarily adopt.

isobaric spin of the other group as T_0 ($= T_1$ or T_2) we have

$$(A_{T_<})^2 = \frac{2T_0}{2T_0+1}, \qquad (A_{T_>})^2 = \frac{1}{2T_0+1}. \tag{5}$$

With a new notation we now rewrite the energy equations for the cases of special interest. We use $(j^n|j'^m)$ to denote the configuration j^n for protons and j'^m for neutrons, every other subshell being either empty or fully closed (for neutrons *and* protons); $(j^n|j'^m)$ will be the same but with the j-neutron shell filled and similarly for $(j^n|j'^m)$, etc. In contrast to these (n—p) *configurations*, $(j^nj'^m)$ will denote n j-nucleons and m j'-nucleons *each separately coupled to maximum* T but not necessarily to maximum $|T_z|$. For example the configurations occurring on the left-hand side of figs. 1a, 1b and 1c are respectively $(j^nj'^m|)$, $(j^nj'^m|)$, $(j^n|j'^m)$. The configuration on the right-hand side of fig. 1a is $(j^n\ j'^m|)$; its states do not have a definite T but can be expanded in terms of the states of the configuration $(j^{N+n}\ j'^m)$. The symbols $(j^{-n}|)$ and $(j^{-n}|)$ will indicate n holes in the proton j-shell, the neutron j-shell being respectively empty and filled. The symbol (j^{-n}) will indicate n nucleon holes in the j shell (a very different thing). The equations are now †

$$E_J(j^{-r}j'|) = E_J(j^{-r}j'|) = \frac{r}{r+1}E_{JT_<}(j^{-r}j') + \frac{1}{r+1}E_{JT_>}(j^{-r}j'), \tag{6}$$

$$E_J(j^{-1}j'^r|) = E_J(j^{-1}j'^r|) = \frac{r}{r+1}E_{JT_<}(j^{-1}j'^r) + \frac{1}{r+1}E_{JT_>}(j^{-1}j'^r), \tag{7}$$

$$E_J(j^r|j') = \frac{r}{r+1}E_{JT_<}(j^rj') + \frac{1}{r+1}E_{JT_>}(j^rj'), \tag{8}$$

$$E_J(j^{-1}|j'^{-r}) = \frac{r}{r+1}E_{JT_<}(j^{-1}j'^{-r}) + \frac{1}{r+1}E_{JT_>}(j^{-1}j'^{-r}), \tag{9}$$

where $T_< = \frac{1}{2}(r-1)$and $T_> = \frac{1}{2}(r+1)$. Eqs. (8) and (9) are related by $j \leftrightarrow j'$ together with a (hole $\leftrightarrow$ particle) transformation but since we assume that j' is a higher orbit than j they are physically distinct unless $r = 1$. The right hand sides of eqs. (6) and (8) cannot be related by $r \to -r$ since $r \leqq 2j+1$ and similarly for eqs. (7), (9).

† In these cases we have only two orbits which are neither completely empty nor fully closed (for both neutrons and protons). If we have also on the left-hand side one or more subshells which are filled for neutrons and empty for protons (or vice versa) the energy equations have a slightly different form but still follow immediately from eqs. (2), (5). The equations have an obvious structure in the isobaric-spin formalism. In the n-p formalism consider for example $n = m = 1$ in fig. 1c. The effect of the n-p interaction when the closed subshell is absent is to spread apart the frequencies of the two otherwise-degenerate oscillation modes ($\omega \to \omega \pm \delta$) but the average value is unchanged and has the value ω. On the other hand when the subshell is filled there is only one oscillation mode and this once again has frequency ω. Similarly for the more complicated cases, always provided that the isobaric spin admixture of the r-group can be ignored, as discussed below.

Eqs. (6)—(9), which are formally correct equations connecting certain shell-model diagonal matrix elements, will apply to relative energy levels of nuclei provided that certain conditions are satisfied. An obvious one is that the configuration admixtures in the states should not be too large. Besides this the r-group should be coupled to maximum isobaric spin (in the states on the right-hand side of the equations) and, in the various terms of an equation, should be coupled to the same angular momentum J and seniority or to the same linear combination of these.

For $r = 1$ the latter questions do not of course arise and there are several cases in which we would expect the equations to apply with some precision. In this case eqs. (6) and (7) are equivalent and by using the (hole $\leftrightarrow$ particle) relationship we see that the terms appearing in eqs. (8) and (9) are equal. With $j \equiv d_{\frac{3}{2}}$ and $j' \equiv f_{\frac{7}{2}}$ the $r = 1$ equations then read

$$E_J(S^{36}) = \tfrac{1}{2}\{E_{J,T=0}(Ca^{40}) + E_{J,T=1}(Ca^{40})\} = E_J(Ca^{48}), \tag{10}$$

$$\begin{aligned} E_J(Cl^{38}) &= \tfrac{1}{2}\{E_{J,T=0}(Cl^{34}) + E_{J,T=1}(Cl^{34})\} \\ &= E_J(K^{46}) = \tfrac{1}{2}\{E_{J,T=0}(Co^{54}) + E_{J,T=1}(Co^{54})\}, \end{aligned} \tag{11}$$

where in all cases except Cl^{38} and K^{46} the states involved belong to excited configurations. The $T = 1$ levels of Ca^{40} could be located instead in K^{40} and similarly for the other cases.

For $r \neq 1$ the r-group isobaric-spin and angular-momentum admixtures must be considered. For the T-admixture the question which arises is as follows; if we have an equivalent group of particles coupled to maximum isobaric spin T_0, is then T_0 preserved when we couple an inequivalent particle or hole to the group to form a resultant $T = T_0 - \frac{1}{2}$? The available information is insufficient to answer this question. If $r = 4n+2$, states of different T_0 will in some cases be close together and then large admixtures might occur; this is not necessarily so because the interaction with the added nucleon could in some cases widely separate the states of different T_0. If $r \neq 4n+2$, states of different T_0 should be well separated but, on the other hand, a Majorana interaction in particular may give a large matrix element non-diagonal in T_0. It seems unprofitable to speculate about this at present. The energy equations with $r = 2j$ in eqs. (6), (8) and $r = 2j'$ in the others could inform us about this question; for in these cases, if T_0 is good, there is no possibility of angular-momentum admixtures. An example involving $d_{\frac{3}{2}}$ $f_{\frac{7}{2}}$ interactions is

$$E_J(S^{34}) = \tfrac{3}{4}E_{J,T=1}(A^{38}) + \tfrac{1}{4}E_{J,T=2}(A^{38}). \tag{12}$$

Let us now consider cases in which, though $r \neq 1$, the T_0 admixtures are small enough to be ignored. When we have an excitable odd group of identical particles or holes (r odd $\neq 1, \neq 2j$ or $2j'$) the state of the r-group, in low-lying states of the system, should usually be the seniority one $J = j$ (or j') state

though, since the r-group energy spacings are small, there may be appreciable J-admixtures †. If the admixtures were the same on both sides of an energy equation, the equation would still be valid but we cannot expect this to be so. However, if we construct the energy matrices in a representation which labels the excitation of the r-group we note that the energy equations (6)—(9) apply to the entire matrices (since eq. (2) applies equally to diagonal and off-diagonal elements). The energies are not linear functions of the matrix elements, and therefore we do indeed expect a departure from the energy equations; this will often be small since the $T_>$ matrix will be combined with the $T_<$ matrix with a relative coefficient which is never larger than $\frac{1}{3}$ and often much smaller; it often represents therefore a simple correction to the $T_<$ matrix. In these cases of course the E_J spectrum will be quite similar to the $E_{JT<}$ spectrum. Moreover, since the interaction of a closed subshell with a group of particles may depend on their configuration but does not otherwise depend on their state, we see that the equations may be applied to the complete spectrum arising from a given (n—p) configuration. For example with $(d_{\frac{5}{2}}^2|p_{\frac{3}{2}})$ we have states $(\frac{3}{2})$, $(\frac{1}{2}, \frac{3}{2}, \frac{5}{2}, \frac{7}{2})$, $(\frac{5}{2}, \frac{7}{2}, \frac{9}{2}, \frac{11}{2})$ arising respectively from the $J_0 = 0, 2, 4$ coupling of the $d_{\frac{5}{2}}$ particles. The equations apply separately for the states of fixed J_0 or for the entire spectrum.

Very few data are available to test the above equations. For $A = 14$ reasonable assignments [1]) for the $(p_{\frac{1}{2}}\ s_{\frac{1}{2}})$ levels are 4.91, 5.69, 8.70, 8.06 MeV for $JT = 00, 10, 01, 11$ respectively and these, by eq. (8) with $r = 1$, give 6.80, 6.87 MeV for the $J = 0, 1$ levels of $(\hat{p}_{\frac{1}{2}}|s_{\frac{1}{2}})$. The +70 keV splitting here may be compared with the experimental value +280 keV observed [2]) in N^{16}). For the $(p_{\frac{1}{2}}\ d_{\frac{5}{2}})$ levels we similarly have 5.10, 5.83, 9.50, 8.90 MeV for $JT = 20, 30, 21, 31$ which give 7.30 and 7.36 MeV for the $J = 2,3$ levels of $(\hat{p}_{\frac{1}{2}}|d_{\frac{5}{2}})$, the 60 keV splitting here to be compared with the experimental value 295 keV. In view of the crudity of the jj assumption in $A = 14$ these agreements seem satisfactory but they really tell us nothing new since the $A = 14$, 16 case is quite trivial and has already been considered by many authors in a different manner. We observe incidentally that the binding to the $p_{\frac{1}{2}}$ neutron subshell is about 600 keV larger for a $d_{\frac{5}{2}}$ neutron than for an $s_{\frac{1}{2}}$ neutron. For heavier nuclei there appears to be nowhere enough data for an application of the equations. The $(\hat{d}_{\frac{5}{2}}|f_{\frac{7}{2}})$ levels are known and a study of excited states in that region of the periodic table ($A \approx 40$) would seem worthwhile. Of course the possible complications which arise when we deal with an excitable r-group should be borne in mind and also the fact that "size" effects (and other such effects not easily taken into account in a model) may be significant when we consider together nuclei of quite different atomic number; conversely the energy equations might tell us something about these effects.

† No such admixtures if the admixing interaction is of odd rank. Note however that the n-p interaction which determines the $d_{\frac{5}{2}}\ f_{\frac{7}{2}}$ spectrum of Cl^{38} is predominantly of quadrupole nature.

The energy equations can of course be derived in many other ways † and much more detailed ones can in some cases be given. There are also some cases of interest involving *equivalent* active nucleons outside closed subshells. It is easy to see for example that the excited states of Cl^{38} which arise from a single $d_{\frac{3}{2}} \rightarrow f_{\frac{7}{2}}$ excitation should include a $T = 2$ and a $T = 3$ spectrum, each identical with the even-J $(f_{\frac{7}{2}})^2$ spectrum of Ca^{42}, and a $T = 2$ odd-J spectrum identical with the odd-J $(f_{\frac{7}{2}})^2$ spectrum. However, if the mutual isobaric-spin polarization of an $(f_{\frac{7}{2}})^2$ pair and a closed $d_{\frac{3}{2}}$ neutron subshell were large the $T = 2$ states would be admixed with states in which the $(d_{\frac{3}{2}})^4$ core would involve both neutrons and protons and the $T = 2$ spectrum would corresponding be changed. These effects could be easily calculated if the entire $(d_{\frac{3}{2}}\ f_{\frac{7}{2}})$ two-particle spectrum were known.

Finally if we consider the effects due to a smaller $J = 0$ group than a closed subshell, such as for example a $J = 0$ pair, other results can be derived which might be pertinent to a study of generalized symplectic symmetry in a heavier nucleus; these are particularly simple if the two-body interaction is of odd rank since such an interaction cannot excite a $J = 0$ pair (this is of course the physical reason for the connection between good seniority and odd-rank interactions); but these questions we do not consider here.

† One instructive way is to eliminate the explicit $\mathbf{t}_i \cdot \mathbf{t}_j$ dependence of the two-particle interaction (which may always be written as $A + B\ \mathbf{t}_i \cdot \mathbf{t}_j$) by observing that a configuration such as $(j^n|j^N)$, where $N = (2j+1)$ is the hole $\leftrightarrow$ particle complement of the configuration (j^{N-n}) for identical particles only. In this way one learns that, even with multiply-excited configurations (the sum in eq. (1) having then more than two terms), energy equations involving only two T values are always possible, this coming about because only two tensorial forms are possible for the isobaric-spin dependence of the two body interaction.

References

1) E. K. Warburton and W. T. Pinkston, Phys. Rev. **118** (1960) 733
2) F. Ajzenberg-Selove and T. Lauritsen, Nuclear Physics **11** 1959) 1

1.E.7:
2.E

Nuclear Physics **26** (1961) 168—176; © *North-Holland Publishing Co., Amsterdam*
Not to be reproduced by photoprint or microfilm without written permission from the publisher

ISOBARIC-SPIN SPLITTING OF SINGLE-PARTICLE RESONANCES

J. B. FRENCH

Fysisch Laboratorium der Rijksuniversiteit, Utrecht, The Netherlands
and
Department of Physics and Astronomy, University of Rochester, Rochester, New York, USA

and

M. H. MACFARLANE

Argonne National Laboratory, Argonne, Illinois
and
Department of Physics and Astronomy, University of Rochester, Rochester, New York, USA †

Received 20 February 1961

Abstract: When a single proton is added to, or a single neutron removed from, a definite shell-model orbit in a target nucleus, the total strength can in general be divided into two parts, each part being characterized by a definite value of the isobaric spin T. This separation is pertinent even when the target isobaric spin is a redundant quantum number determined simply by the neutron excess, and probably in many cases when the isobaric spin is not conserved in the individual states which contribute to the strength. General expressions are given for the total strengths and for the strengths of the T-components. The practical problem of observing this effect as a T-splitting of giant resonances is discussed briefly.

1. Introduction

Consider the states produced when a nucleon is added in a definite shell-model orbit j (more completely nlj) to a nucleus with a positive neutron excess †† $(N-Z) = 2M$ and isobaric spin $T_{\text{target}} \equiv T_t$. Since in all cases of practical interest to us here, $T_t = M$, it is clear that addition of a neutron ($m = +\frac{1}{2}$) can lead to only one final isobaric spin $T_t+\frac{1}{2}$. On the other hand, the addition of a proton can excite states with isobaric spin $T_t \pm \frac{1}{2}$. From the preceding paper [1]) it follows that even when a proton is added, states of only one isobaric spin ($T_t-\frac{1}{2}$) exist if the j-neutron shell is filled. In other cases single-particle states of both isobaric spins exist and can be excited by addition of a proton.

If we deal with heavier nuclei or with levels of sufficiently high excitation, these single-particle states can be observed as giant resonances in stripping [2,3]) or in elastic scattering of nucleons [4,5]). The possibility of exciting states of two

† Work supported in part by the U.S. Atomic Energy Commission. Work at Utrecht was done while the first-named author was Senior Post-Doctoral Fellow of the National Science Foundation.

†† The notation M, m is used for the z-components of isobaric spin; M, N and Z refer to the target (in either pick-up or stripping reactions) and m refers to the transferred particle ($m = +\frac{1}{2}$ for a neutron).

different isobaric spins in proton reactions may then lead to a T-splitting of the giant resonances. In this paper we examine the possibility of observing such a splitting and consider also the strengths of the giant resonances and of their isobaric-spin components. A parallel discussion is given of the single-hole states produced in nucleon pick-up reactions. In this case a splitting is expected when a neutron is removed from an orbit which contains some protons.

One might at first object to the idea of T splitting on the ground that the isobaric-spin quantum number may not be good for excited states in heavier nuclei. It seems quite clear that T should be a rather good quantum number for the lowest states of even fairly heavy nuclei (say $A \approx 100$) but the situation for highly excited states is quite obscure. However, the whole question of the goodness of T is probably irrelevant. The essential point would seem to be that, when we add a proton to a shell which is not filled for neutrons, the system so formed has two single-particle modes of oscillation. If we had precise charge-independence these modes would be characterized by T; but if the single-particle components are fairly far apart (say 1 MeV or more) it seems altogether probable that, while the Coulomb effects could make a large change in T, they can scarcely make any major change in the description of the two *single-particle* modes of oscillation. In this case we may as well continue to characterize them by T. The single-particle-level strength is now spread out among neighbouring states to form a giant resonance. It is possible, though not at all obviously true, that the isobaric spin is not preserved in the spreading. In this case the giant resonances (always assuming that the T splitting is large enough) could still be characterized well enough by T even though the major components of some of the contributing states could not.

As discussed earlier [1]) it is difficult at present to estimate the magnitude of the splitting to be expected in various cases. Just as in the energy-level case, the isobaric spin of the *final-state equivalent group* is significant also when we add a nucleon to a nucleus. In principle then one can distinguish four isobaric components of a resonance (two components with $T = T_t + \frac{1}{2}$, two with $T = T_t - \frac{1}{2}$) and splitting could occur in various ways. The final outcome would probably then depend strongly on the number of particles in the equivalent group. In order to be specific we consider in the following the cases in which the splitting is that of the total isobaric spin. More detailed results are included in the Appendix. It should be noted that the question of equivalent-group isobaric-spin conservation does not at all affect the *validity* of the equations given later (unlike the energy-level case) but instead the possibility of testing and using them. To be easily observable the splitting should be larger than the widths of the individual components † which for s-wave resonances near $A = 50$ are about 1—2 MeV.

† Components with a definite T! If the target spin is different from 0, there is also a J-splitting but we do not consider separately the components which arise in this way.

There are not many cases of interest in which we can at present identify a T-splitting. One such involves the $2s_{\frac{1}{2}}$ single-particle levels in N^{14} discussed in the previous paper [1]). And of course, to the extent that they are describable as $d_{\frac{3}{2}}^2$, the low-lying levels of Cl^{34} could be regarded as an example. This and other cases like it are not of much interest in the present context.

2. Resonance Strengths

The strength of a level in a nucleon-transfer reaction is characterized by its "relative reduced width" $\mathscr{S} = \theta^2/\theta_0^2$, the reduced width in units of the single-particle width [6]). Including spin statistical factors and the isobaric-spin coupling factor † $(C)^2$, we define the strength G of a group of of levels as

$$G = \sum \frac{2J_f+1}{2J_i+1} (C)^2 \mathscr{S} \tag{1}$$

for capture reactions (elastic scattering or stripping) and

$$G = \sum (C)^2 \mathscr{S} \tag{2}$$

for pick-up. The summations extend over all levels we wish to consider but must include only one l-value since we have divided out the l-dependent quantity θ_0^2. Except for purely dynamical factors, G characterizes †† the experimental cross section.

We consider the target isobaric spin to be decomposed into two parts

$$\mathbf{T}_t = \mathbf{T}_e + \mathbf{T}_1, \tag{3}$$

where $\mathbf{T}_e$ refers to the entire group of j-nucleons ††† in the target and $\mathbf{T}_1$ to all the others (inequivalent to j); of course T_e, T_1 will not in general be good quantum numbers.

As shown in the Appendix an entirely general expression for the total strength and its separate T components in a stripping or elastic scattering

† See eqs. II.19 and II.21 of ref. [6]).

†† In other words, the 'formal' strength defined by eq. (1) or eq. (2) is a correct measure of the true strength of a resonance. This is obvious in the case of high-resolution experiments. To describe the strength of a single resonance in a low-resolution study, following Schiffer *et al* [2]) we first plot the area under the resonance as a function of angle. If the main contributions are of one l-value, the hybrid angular distribution so obtained can be approximately treated as if it arose from a single resolved level. The 'reduced width' obtained in the usual fashion in then simply $G\theta_0^2(l)$, where G is the formal strength defined above. Of course, it may happen that the composite angular distribution does not uniquely identify a value of l (perhaps because several l-values contribute significantly to the resonance). A better resolution experiment would then be needed to clarify the situation and in any case comparisons of low- and high-resolution experiments with the same target are needed to establish the reliability of the poor-resolution technique.

††† The physical meaning of eq. (3) is obvious but there are some formal complications, discussed in the Appendix.

experiment is

$$\begin{aligned} G_m &= \tfrac{1}{2}\langle\text{holes}\rangle_j - 2mM\langle\mathscr{L}\rangle, \\ G_m(T_>) &= \left(\frac{T_t+2mM+1}{2T_t+1}\right)\{\tfrac{1}{2}\langle\text{holes}\rangle_j - T_t\langle\mathscr{L}\rangle\}, \\ G_m(T_<) &= \left(\frac{T_t-2mM}{2T_t+1}\right)\{\tfrac{1}{2}\langle\text{holes}\rangle_j + (T_t+1)\langle\mathscr{L}\rangle\}, \end{aligned} \tag{4}$$

where $\langle\text{holes}\rangle_j$ is the average number † of holes in the complete j-shell (neutrons *and* protons) and $\langle\mathscr{L}\rangle$ is the average value of the Landé factor

$$\mathscr{L} = \frac{T_t(T_t+1)+T_e(T_e+1)-T_1(T_1+1)}{2T_t(T_t+1)}. \tag{5}$$

In the usual case where $T_t = M$ we have, writing neutron and proton reactions separately,

$$\begin{aligned} G_n = G_n(T_>) &= \{\tfrac{1}{2}\langle\text{holes}\rangle_j - T_t\langle\mathscr{L}\rangle\}, \\ G_p &= \{\tfrac{1}{2}\langle\text{holes}\rangle_j + T_t\langle\mathscr{L}\rangle\}, \\ G_p(T_>) &= \frac{1}{2T_t+1}\{\tfrac{1}{2}\langle\text{holes}\rangle_j - T_t\langle\mathscr{L}\rangle\}, \\ G_p(T_<) &= \frac{2T_t}{2T_t+1}\{\tfrac{1}{2}\langle\text{holes}\rangle_j + (T_t+1)\langle\mathscr{L}\rangle\}. \end{aligned} \tag{6}$$

As shown also in the Appendix these may be written in terms of neutron and proton holes as

$$\begin{aligned} G_n &= \langle\text{neutron holes}\rangle_j, \\ G_p &= \langle\text{proton holes}\rangle_j, \\ G_p(T_<) &= \frac{1}{(N-Z+1)}\langle\text{neutron holes}\rangle_j, \\ G_p(T_>) &= \langle\text{proton holes}\rangle_j - \frac{1}{(N-Z+1)}\langle\text{neutron holes}\rangle_j. \end{aligned} \tag{7}$$

For the pick-up experiments the strengths are given once again by eqs. (4), (6), (7) with the modifications

$$\langle\text{holes}\rangle_j \to \langle\text{particles}\rangle_j, \qquad m \to -m, \qquad n \leftrightarrow p, \tag{8}$$

the Landé factor $\mathscr{L}$ being still given by eq. (5). Eqs. (7) and their pickup analogues are unsymmetrical in neutrons and protons because we assume a ***neutron*** excess in the target.

† If the target wave function is given in the form $\Sigma_k A_k \phi_k$ and if in ϕ_k the number of holes in the j shell is n_k then $\langle\text{holes}\rangle_j = \Sigma_k A_k^2 n_k$. The other averages are defined in the same way.

3. Discussion

We have stressed the obvious, but often ignored, fact that isobaric spin is significant in experiments which add a proton or remove a neutron even when the target quantum number T is redundant, as in the case of heavier nuclei. We have evaluated reaction strengths in a general and compact form.

If we deal with reactions in which all the active nucleons are in the same shell, the present results add little to those which have been given previously [6]). But in other cases, and particularly when we have particle or hole giant resonances, they seem to have considerable value.

It is clear from eqs. (7), (8) that, if the neutron excess is at all large, most of the resonant strength when we add a proton or take away a neutron will belong to the smaller-isobaric-spin component. Thus we shall have a good chance of observing both T-components in a giant resonance only when the target neutron excess is small and hence, say, $A < 70$.

We can always locate the $T_>$ particle resonance by adding a neutron and the $T_<$ resonance by adding a proton to the same target. The position of the $T_>$ resonance in the proton experiment might in some cases be inferred from binding energies and Q values. The same procedure could be followed for hole resonances. Finally, although little is known about the systematics of single-hole states, recent (p, 2p) studies [7]) suggest that single-hole states are rather more widely spaced than single-particle states. If this is indeed the case, it may be easier to detect the T-splitting of hole resonances.

Appendix

The expressions for G given in the text (eqs. (4)—(8)) can be deduced from the sum rules quoted without proof as eqs. (III.140′) and (III.141′) in Appendix 2 of ref. [6]). We derive them here, not by summing explicit expressions for the reduced widths, but by a projection-operator technique which is much simpler and could be used for other sum rules as well.

We consider first the pick-up sum rules (their derivation is simpler) and indicate only the isobaric-spin quantum numbers; it will be understood that all other final-state quantum numbers must be summed over. We expand the target wave function in a representation which specifies the number of j-nucleons and, noting that in a sum rule there is no interference between orthogonal components, we treat each term separately.

A characteristic term has the structure

$$\{T_1 \times T_e\}_{T_t, M},$$

where $\times$ describes vector coupling, $\{\}$ indicates antisymmetry in all nucleons, T_e refers to the j^n group and T_1 to the remaining particles (eq. (3)). We shall

also use the notation

$$(T_1 \times T_e)_{T_t, M}$$

for a state in which the antisymmetry is confined to the separate groups; it will be understood that the nucleons in the T_1 group are numbered $12 \ldots (A-n)$, those of the T_e group having the numbers $(A-n+1) \ldots A$.

By definition (see eq. (2) and section III.7 of ref. [6])), the total strength for given m is

$$G_m = A \sum_{T'_e T_f} (C^{T_f \frac{1}{2} T_t}_{M-m, m})^2 |\langle \{T_1 \times T_e\}_{T_t, M} | (\{T_1 \times T'_e\}_{T_f} \times t(A))_{T_t, M} \rangle|^2, \qquad (9)$$

where m specifies whether the transferred nucleon is neutron or proton and T'_e refers to the group j^{n-1} in the residual nucleus.

Now $\{T_1 \times T_e\}_{T_t, M}$ can be expanded into $A!/n!(A-n)!$ terms differing from $(T_1 \times T_e)_{T_t, M}$ only in the distribution of nucleon numbers $1,2 \ldots A$ between the two groups, and similarly for $(\{T_1 \times T'_e\}_{T_f} \times t(A))$. The overlap integral in (9) is clearly diagonal in distributions of the nucleon numbers $1,2 \ldots A-1$ (A being fixed in the T_1 group). Thus each term in the expansion of $(\{T_1 \times T'_e\}_{T_f} \times t(A))$ gives a non-vanishing contribution to the overlap integral with one and only one term in the expansion of $\{T_1 \times T_e\}$; furthermore, all such contributions are equal. Remembering normalization factors, simple counting yields

$$G_m = n \sum_{T'_e T_f} (C)^2 |\langle (T_1 \times T_e)_{T_t, M} | ((T_1 \times T'_e)_{T_f} \times t(A))_{T_t, M} \rangle|^2. \qquad (10)$$

and summing this over m gives

$$\sum_m G_m = n \sum_{T'_e T_f} |\langle (T_1 \times T_e)_{T_t, M} | ((T_1 \times T'_e)_{T_f} \times t(A))_{T_t, M} \rangle|^2. \qquad (11)$$

A more detailed discussion of the steps leading from (9) to (10) is given in ref. [6]) (p. 608). When applied to the states appearing in (10), the formal significance of the separation $\mathbf{T}_t = \mathbf{T}_1 + \mathbf{T}_e$ (eq. (3)) is immediately clear.

Since the states with the separated particle form a vector space which contains all the states $(T_1 \times T_e)_{T_t M}$ we can use completeness for the sum in (11) and obtain

$$\sum_m G_m = n. \qquad (12)$$

But also by inserting a projection operator

$$P(T_f) \propto \mathbf{T}_f^2 - T'_f(T'_f+1),$$

we can restrict the sum in (11) to states of definite final isobaric spin T_f (T'_f being then the other possible value of final-state isobaric spin). Using $\mathbf{T}_f = \mathbf{T}_t - \mathbf{t}(A)$ and normalizing the P operators we have

$$P(T_f >) = 1 - P(T_f <) = \frac{1}{(2T_t+1)} \{(T_t+1) - 2\mathbf{T}_t \cdot \mathbf{t}(A)\}. \qquad (13)$$

Inserting this in eq. (11) and summing gives then

$$\sum_m G_m(T_f >) = n - \sum_m G_m(T_f <) = \frac{(T_t+1)}{(2T_t+1)}\{n - 2T_t\mathscr{L}\}, \tag{14}$$

where we have used the fact that, in the target state (antisymmetrical in the j-nucleons), $\mathbf{t}(A) \equiv \mathbf{T}_e/n$, rewritten $\mathbf{T}_t \cdot \mathbf{T}_e$ by using eq. (3), and used eq. (5) in writing the final result (14). Note that $\mathbf{T}_t \cdot \mathbf{T}_e \equiv \mathscr{L}\,\mathbf{T}_t^2$ and also that $T_{e,z} \equiv \mathscr{L} T_{t,z}$.

Our real interest of course is in reactions for a transferred neutron *or* proton. But we can undo the sum in (14) by noting that (for fixed m) $(C)^2$ is the same for all terms in any sum in which T_f is specified. Then we have

$$\begin{aligned} G_m(T_f >) &= (C^{T_t+\frac{1}{2},\,\frac{1}{2},\,T_t}_{M-m,\,m})^2 \sum_{m'} G_{m'}(T_f >) \\ &= (C^{T_t\,\frac{1}{2}\,T_t+\frac{1}{2}}_{M,\,-m})^2 \{\tfrac{1}{2}n - T_t\mathscr{L}\}, \\ G_m(T_f <) &= (C^{T_t\,\frac{1}{2}\,T_t-\frac{1}{2}}_{M,\,-m})^2 \{\tfrac{1}{2}n + (T_t+1)\mathscr{L}\}. \end{aligned} \tag{15}$$

Now when we sum over the various components of the target function, $n \to \langle\text{particles}\rangle_j$, $\mathscr{L} \to \langle\mathscr{L}\rangle$ and eqs. (4), (8) follow on inserting explicit forms for the Clebsch-Gordan coefficients.

We have now derived the pick-up sum rules. A formal complication is encountered with the stripping or elastic-scattering sum rules. The same overlap integral enters as in the pickup case but now the states of the final nucleus do not span as large a vector space as do the states with a separated nucleon. We therefore cannot directly use completeness to carry out the summations. This difficulty disappears when we make a j-shell hole $\leftrightarrow$ particle transformation as described several times in ref. [6]) (see section III.10). We need not repeat the arguments here but the results is to produce eq. (8) which relates the pickup and stripping strength functions.

To rewrite our sum rules in terms of neutrons and protons we use

$$\begin{aligned} \langle\text{particles}\rangle_j &= \langle\text{protons}\rangle_j + \langle\text{neutrons}\rangle_j, \\ \langle\text{holes}\rangle_j &= \langle\text{proton holes}\rangle_j + \langle\text{neutron holes}\rangle_j, \\ \langle\mathscr{L}\rangle &= \frac{\langle\text{neutrons}\rangle_j - \langle\text{protons}\rangle_j}{2M} = \frac{\langle\text{proton holes}\rangle_j - \langle\text{neutron holes}\rangle_j}{2M}, \end{aligned} \tag{16}$$

and, for the special case $T_t = M$, eqs. (6), (8) then follow.

If we add the strength functions for (d, p) and (d, t) experiments on the same target we find simply $(2j+1)$. This result, which has an obvious physical significance, could be useful, for example, in indicating that an identification of a group of levels has been wrongly made †. And of course if for any reaction we are unable to separate the two j values for given l a further summation over j can be performed.

† Or in some cases that nucleons may be transferred with two different *principal* quantum numbers but the same (lj).

Finally, as discussed in the text, it may be of interest to derive expressions for the strengths for fixed values of the isobaric spin T'_e of the equivalent group in the residual nucleus. We shall evaluate the four quantities $\sum_m G_m(T'_e, T_f)$ from which the strengths for fixed m follow immediately as in (15). To do this we recognize that the two different values of T_f in a summation for fixed T'_e are weighted in proportion to the square of the Racah coefficient

$$U(T_1 T'_e T_t \tfrac{1}{2} : T_f T_e) \equiv U(T'_e T_f),$$

which carries out the recoupling transformation from a scheme which specifies T'_e to one which specifies T_f (see eq. (9)). In other words, we have for both values of T'_e

$$\frac{\sum_m G_m(T'_e, T_f >)}{U(T'_e, T_f >)^2} = \frac{\sum_m G_m(T'_e, T_f <)}{U(T'_e, T_f <)^2}. \tag{17}$$

We could now solve the four independent linear equations (14) and (17) for $\sum_m G_m(T'_e, T_f)$. However, we obtain an alternative derivation which is much simpler algebraically if we notice that (17) can be rewritten in the form

$$\sum_m G_m(T'_e, T_f) = U(T'_e, T_f)^2 \sum_{T'_f} \{\sum_m G_m(T'_e, T'_f)\}. \tag{18}$$

But the sums on the right side of (18) are simply the strengths for fixed T'_e summed over T_f and can be obtained directly from (11) by inserting the projection operators

$$P(T'_e >) = 1 - P(T'_e <) = \frac{1}{(2T_e+1)} \{(T_e+1) - 2\mathbf{T}_e \cdot \mathbf{t}(A)\}, \tag{19}$$

constructed in obvious analogy to (13). Repetition of the operations which led from (13) to (14) now yields

$$\sum_{T_f} \sum_m G_m(T'_e >, T_f) = n - \sum_{T_f} \sum_m G_m(T'_e <, T_f) = \frac{(T_e+1)}{(2T_e+1)} \{n - 2T_e\}. \tag{20}$$

Substituting from eqs. (20) in eqs. (18), inserting explicit forms for the Racah coefficients, and extracting the strengths for fixed m as in eqs. (15), we have

$$\begin{aligned}
G_m(T'_e>, T_f>) &= \left\{\frac{T_t - 2mM + 1}{2(T_t+1)(2T_t+1)}\right\} \left\{\frac{(T_1+T_e+T_t+2)(-T_1+T_e+T_t+1)}{(2T_e+1)}\right\} \{\tfrac{1}{2}n - T_e\}, \\
G_m(T'_e>, T_f<) &= \left\{\frac{T_t + 2mM}{2T_t(2T_t+1)}\right\} \left\{\frac{(T_1+T_e-T_t+1)(T_1-T_e+T_t)}{(2T_e+1)}\right\} \{\tfrac{1}{2}n - T_e\}, \\
G_m(T'_e<, T_f>) &= \left\{\frac{T_t - 2mM + 1}{2(T_t+1)(2T_t+1)}\right\} \left\{\frac{(T_1-T_e+T_t+1)(T_1+T_e-T_t)}{(2T_e+1)}\right\} \{\tfrac{1}{2}n + (T_e+1)\}, \\
G_m(T'_e<, T_f<) &= \left\{\frac{T_t + 2mM}{(2T_t(2T_t+1)}\right\} \left\{\frac{(T_1+T_e+T_t+1)(-T_1+T_e+T_t)}{(2T_e+1)}\right\} \{\tfrac{1}{2}n + (T_e+1)\}.
\end{aligned} \tag{21}$$

We then obtain the strength equations for pick-up in their most general form by averaging eqs. (21) over the various components in the target wave function; expressions appropriate to stripping and elastic scattering can then be written down by reversing the transformation of eqs. (8).

We take this opportunity to correct an error in the first Appendix of ref. [6]). It was stated there that, in a transition between two $(\mathrm{n}—\mathrm{p})_T$ states, the isobaric-spin coupling factor $(C)^2$ is necessarily unity. But in the exceptional case that a proton is added to (or removed from) a shell filled for neutrons, $(C)^2$ is instead $(2T_0/2T_0+1)$, in the notation of ref. [6]). An example of such a case is in fact discussed on p. 618 of ref. [6]). The reduced widths θ^2 and the relative reduced widths $\mathscr{S}$ can now be quoted in either a T or an n—p formalism and the results will not be the same, but instead $(C)^2\ \mathscr{S}^{(T)} = \mathscr{S}^{(\mathrm{n-p})}$. In these cases $\mathscr{S}^{(\mathrm{n-p})}$ will be a physically simpler quantity than $\mathscr{S}^{(T)}$ but, to avoid confusion, it is still preferable to extract widths using an equation in which the $(C)^2$ factor explicitly enters.

References

1) J. B. French, Nuclear Physics **26** (1961) 161
2) J. P. Schiffer, L. L. Lee, Jr., and B. Zeidman, Phys. Rev. **115** (1959) 427
3) R. A. Peck, Jr., and J. Lowe, Phys. Rev. **114** (1959) 847
4) H. Feshbach, C. E. Porter and V. F. Weisskopf, Phys. Rev. **96** (1954) 448
5) A. M. Lane, R. G. Thomas and E. P. Wigner, Phys. Rev. **98** (1955) 693
6) M. H. Macfarlane and J. B. French, Revs. Mod. Phys. **32** (1960) 567
7) See, e.g., G. Jacob, in Proc. Intern. Conf. on Nuclear Structure, Kingston 1960 (North-Holland Publishing Co., Amsterdam, 1960) p. 429—433

NORTH-HOLLAND BOOKS

Announcing the new series

PROGRESS IN OPTICS

A new international series of review articles devoted to advances in theoretical and applied optics and to related fields

Edited by

EMIL WOLF

Institute of Optics
University of Rochester
Rochester, N.Y., U.S.A.

EDITORIAL ADVISORY BOARD

M. FRANÇON *(Paris)*
A. C. S. VAN HEEL *(Delft)*
E. INGELSTAM *(Stockholm)*
K. S. KRISHNAN *(New Delhi)*
H. KUBOTA *(Tokyo)*
E. L. O'NEILL *(Boston)*
J. PICHT *(Potsdam)*
A. RUBINOWICZ *(Warszawa)*
W. H. STEEL *(Sydney)*
G. TORALDO DI FRANCIA *(Firenze)*
W. T. WELFORD *(London)*
H. WOLTER *(Marburg)*

NORTH-HOLLAND PUBLISHING COMPANY

P.O. BOX 103 — AMSTERDAM

Please turn over

NORTH-HOLLAND BOOKS

PROGRESS IN OPTICS

Edited by

EMIL WOLF

University of Rochester N.Y.

just out
VOLUME I

CONTENTS

R. J. PEGIS *(Rochester, N.Y., U.S.A.)*
The Modern Development of Hamiltonian Optics

K. MIYAMOTO *(Tokyo, Japan)*
Wave Optics and Geometrical Optics in Optical Design

R. BARAKAT *(Boston, Mass., U.S.A.)*
Intensity Distribution and Total Illumination of Aberration-free Diffraction Images

D. GABOR *(London, England)*
Light and Information

H. WOLTER *(Marburg, Germany)*
On Basic Analogies and Principal Differences between Optical and Electronic Information

H. KUBOTA *(Tokyo, Japan)*
Interference Color

A. FIORENTINI *(Arcetri-Firenze, Italy)*
Dynamic Characteristics of Visual Processes

A. C. S. VAN HEEL *(Delft, Netherlands)*
Modern Alignment Devices

6 x 9" XII + 342 pp. 157 ill. Gld. 35.00 (70s.)

Ask your bookseller or

NORTH-HOLLAND PUBLISHING COMPANY

P.O. BOX 103 — AMSTERDAM

Distributor for U.S.A.: Interscience Publishers, Inc. — New York